UNIVERSITAT DE BARCELONA

Decoding the genetic landscape of pediatric and young adult germinal center-derived B-cell non-Hodgkin lymphoma

Juan Enrique Ramis Zaldívar

Decoding the genetic landscape of pediatric and young adult germinal center-derived B-cell non-Hodgkin lymphoma

Doctoral thesis presented by **Juan Enrique Ramis Zaldívar**

UNIVERSITAT DE BARCELONA

Ph. D. Program in Biomedicine

FACULTY OF MEDICINE, UNIVERSITY OF BARCELONA

SALAVERRIA FRIGOLA ITZIAR - 47711254P

Firmado digitalmente por SALAVERRIA FRIGOLA ITZIAR - 47711254P
Fecha: 2021.05.07 12:08:52 +02'00'

Doctoral supervisor: **Dr. Itziar Salaverria**

Tutor: **Prof. Elías Campo**

Molecular Pathology of Lymphoid Neoplasms Program
Molecular Genetics of Pediatric Lymphomas Group
Institut d'Investigacions Biomèdiques August Pi i Sunyer (IDIBAPS)

IDIBAPS
Institut D'Investigacions Biomèdiques August Pi i Sunyer

Barcelona, 2021

This doctoral thesis was supported by a pre-doctoral fellowship FI-2017 grant for the recruitment of novel researchers (2017FI_B_01004) from the Agència de Gestió d'Ajuts Universitaris i de Recerca de Catalunya (AGAUR). A short stay at the group of Prof. Xose S. (Department of Biochemistry and Molecular Biology, University of Oviedo, Spain) and a three-month stay at the group of Dr. Reiner Siebert (Institute of Human Genetics, Ulm University hospital, Ulm, Germany) was conducted thanks to a grant from the Centro de Investigación Biomédica en Red de Cáncer (CIBERONC, Ayudas a la movilidad, 2019 and 2020). The work presented here was founded by Instituto de Salud Carlos III (PI18/00471 and FIS PI15/00580, Principal Investigator: Itziar Salaverria), Asociación Española Contra el Cáncer (AECC) (CICPFI6025SALA AECC Cancer Infantil 2017, Principal Investigator: Itziar Salaverria), Generalitat de Catalunya (2017 SGR 1107, Principal Investigator: Itziar Salaverria; PERIS:SLT002/ 16/00336). This work was mainly developed at the Centre Esther Koplowitz of Barcelona between March 2016 and June 2021.

“No me importaría perecer en el empeño:
la felicidad no consiste en alcanzar un fin,
sino en el camino que debe padecerse,
disfrutarse y recorrerse para lograrlo.”

Enrique Ignacio Zaldívar Lecanda (Ganiya)

TABLE OF CONTENTS

ABSTRACT

B-cell non-Hodgkin lymphoma (B-NHL) of pediatric and young adult population is a diverse group of neoplasms predominantly composed of aggressive B-cell lymphomas from the germinal center (GC). Molecular characterization of pediatric series has allowed the identification of several subtypes that predominantly occur in this subgroup of age. Despite of that, genomic features of these pediatric entities and their relationship to other B-NHL in this group of patients have not been extensively investigated. This thesis has aimed to address this gap of knowledge by performing a genetic and molecular characterization of large series of pediatric and young adult variants of GC-derived B-NHL including the Burkitt-like lymphoma with 11q aberration (BLL-11q) , pediatric type follicular lymphoma (PTFL) and large B-cell lymphomas (LBCL) such as diffuse large B-cell lymphomas (DLBCL) , high grade B-cell lymphomas, not otherwise specified (HGBCL, NOS) and large B-cell lymphoma with *IRF4* rearrangement (LBCL-*IRF4*) entities.

In the **Study 1** we have molecularly characterized a series of 11 BLL-11q observing that BLL-11q differed clinically, morphologically and immunophenotypically from conventional BL and instead showed features more consistent with HGBCL or DLBCL. Genomic profile was also different from that of BL and DLBCL with a mutational landscape characterized by the lack of typical BL mutations in *ID3*, *TCF3*, or *CCND3* genes and recurrent specific *BTG2* and *ETS1* mutations, not present in BL but in germinal center B-cell (GCB) DLBCL subtype. All these observations suggest that BLL-11q is a neoplasm closer to other GC-derived lymphomas rather than BL. In **Study 2**, we expanded our knowledge on the genetic alterations associated to PTFL by verifying the presence of *MAP2K1* and *IRF8* mutations in a previously well characterized series of 43 PTFL. We demonstrate the activating effect of *MAP2K1* mutations by immunohistochemical analysis observing phosphorylation of the *MAP2K1* downstream target extracellular signal-regulated kinase in those mutated cases. Besides, we demonstrate the specificity of *MAP2K1* and *IRF8*-K66R mutations since they are absent in conventional FL or in t(14;18)-negative FL. Finally, in the **Study 3** we characterized a large series of LBCL including DLBCL, HGBCL, NOS and LBCL-*IRF4* through an integrative analysis including targeted next generation sequencing, copy number, and

transcriptome data. Results showed that each subgroup displayed different molecular profiles. LBCL-*IRF4* had frequent mutations in *IRF4* and NF-κB pathway genes (*CARD11*, *CD79B*) whereas DLBCL, NOS was predominantly of GCB-DLBCL subtype and carried gene mutations similar to the adult counterpart (e.g., *SOCS1* and *KMT2D*). A subset of HGBCL, NOS displayed recurrent alterations of BL-related genes such as *MYC*, *ID3*, *CCND3* and *SMARCA4*, whereas other cases were genetically closer to GCB-DLBCL. Interestingly, we could identify age-related differences in pediatric DLBCL since pediatric and young adult cases were mainly of GCB subtype, displayed low genetic complexity and virtually lacked primary aberrations (*BCL2*, *MYC* and *BCL6* rearrangements). Finally, we identify clinical and molecular features related to unfavorable outcome such as age >18 years, high LDH levels, activated B-cell (ABC) DLBCL profile, high genetic complexity, homozygous deletions of 19p13.3/*TNFSF7*/*TNFSF9,* gains of 1q21-q44/*MDM4/MCL1* and *TP53* mutations.

Altogether, we conclude that GC-derived B-NHL of pediatric and young adult population is a heterogeneous group of tumors including different entities with specific molecular profiles and clinical behavior. This thesis has contributed to increase the knowledge of these lymphoma entities identifying biomarkers that might be helpful to improve their diagnosis and to design management strategies more adapted to their particular biological behavior.

INTRODUCTION

1. B-cell Non-Hodgkin lymphomas

Lymphoid malignances comprise a heterogeneous group of B-, T- and NK-cell clonal tumors. The World Health Organization (WHO) Classification of Tumours of Hematopoietic and Lymphoid Tissues, which has become an international standard for clinical practice, stratifies them according to their morphology, immunophenotype, genetic and clinical information available (Swerdlow et al., 2017).

Lymphomas can be subclassified into two major subgroups, Hodgkin and non-Hodgkin lymphomas (NHL). At the same time, NHL comprise a wide spectrum of genetically, phenotypically, and clinically distinct malignancies derived mainly from immature and mature B cells of the germinal center (GC) (Morton *et al.*, 2007). These malignances tend to mimic different stages of normal B-cell differentiation, which explains, in part, the high heterogeneity of this group of malignances and allows their classification based on morphology, immunophenotype, and gene expression profiles (Swerdlow et al., 2017). For that reason, it would be mandatory to bear in mind the basics of the normal B-cell differentiation in order to understand the pathogenesis of B-cell NHL (B-NHL).

1.1 The B-cell development

The biological process from which all blood cells are formed is called hematopoiesis. It occurs during the embryonic development and endures throughout adulthood to produce and replace the blood system. In adults, this multi-step process originates in the bone marrow (BM), where pluripotent hematopoietic stem cells gradually differentiate into committed progenitors that will give rise to myeloid and lymphoid cell lineages (Monroe and Dorshkind, 2007; Rieger and Schroeder, 2012).

B-cell development consists in a series of cellular transitions that culminate in the production of effective B cells and the establishment of a wide repertoire of B-cell antigen receptors (BCR) encoded by rearranged immunoglobulin (IG) genes. (Pieper, Grimbacher and Eibel, 2013) Each different maturation stage of this process is characterized by specific cell-surface and intra-cellular expression markers, the BCR rearrangement status and specific morphological aspects (**Figure 1**).

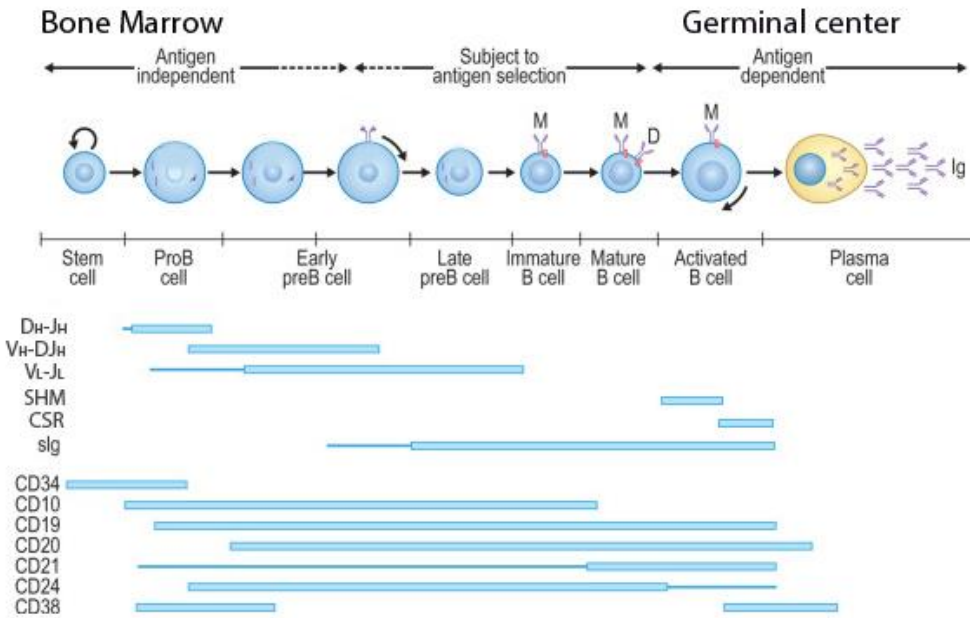

Figure 1. Schematic representation of the different stages in B-cell development. BCR rearrangement status and some cell-surface markers are also shown. SHM: somatic hyper mutation; CSR: class switch recombination; sIg: surface immunoglobulin. Figure modified from (Schroeder, Radbruch and Berek, 2019).

The process starts in the BM where B-cell precursors undergo recombination of the variable (V), diversity (D) and joining (J) segments of the IGH locus to produce the IG heavy-chain (IGH) variable region that is then fused to the constant region of the IG gene. Then, the same occurs in the *Igk* (IGK) and *Igλ* (IGL) loci where the recombination of V and J segments and the constant region produce the IG light-chain (LeBien and Tedder, 2008). This molecular process of recombination involves recombination-activating genes (*RAG1* and *RAG2*) that

induce double-stranded DNA breaks, and the non-homologous end-joined repair apparatus that resolve them (Fugmann *et al.*, 2000). Combination of two IGH and two IGL/K origins the mature and effective BCR (IgM and/or IgD) which is expressed on the surface of naïve B-cells. These naïve B cells leave the BM to the bloodstream where they can visit secondary lymphoid structures in which B-cell activation can occur trigged by antigen recognition through the BCR.

The lymph node is one of the most common places for antigen recognition. B-cell activation sometimes requires additional signals from non-B cells such as T cells. Therefore, T-cell dependent and independent responses can be distinguished (LeBien and Tedder, 2008).

The T-cell dependent B-cell activation mainly occur in the follicles within the cortex of a lymph node known as primary follicles. This activation induces B-cell proliferation and expansion in the central region of the lymphoid follicle region forming transient structures called germinal center. The GC reaction polarizes the follicle into two distinct anatomical areas: the dark zone (DZ) containing large, highly proliferative B cells named centroblasts and the light zone (LZ) containing smaller, nondividing B cells known as centrocytes (Mesin, Ersching and Victora, 2016). These two new compartments are characterized by different transcriptional programs explaining their different functions in the process B-cell development process (Basso and Dalla-Favera, 2015) (**Figure 2**).

In the DZ, activated B cells proliferate rapidly and become centroblasts, which undergo somatic hypermutation (SHM) and affinity maturation processes that contribute to antibody diversity (Kurosaki, Kometani and Ise, 2015). The SHM process consists in the addition of point mutations at the variable regions of the IG genes ($V_HD_HJ_H$ and occasionally V_LJ_L) that increase their binding affinity. As centroblasts, they mature and differentiate further, they become centrocytes which migrate into the LZ.

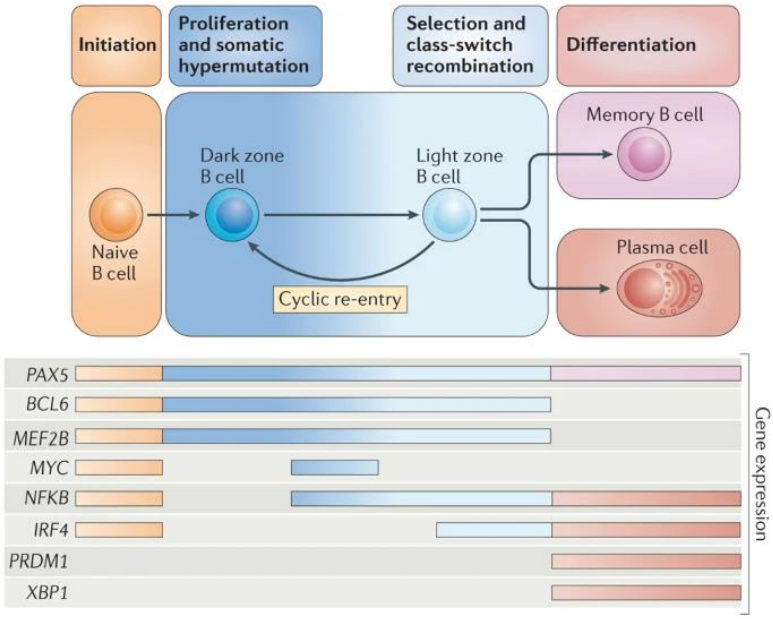

Figure 2. Different transcription factors involved in different stages of germinal center B-cell differentiation. Figure from (Basso and Dalla-Favera, 2015).

In the LZ, centrocytes compete for survival signals derived from follicular dendritic cells. At this point, it takes place the class switch recombination (CSR), a process that increases functional diversity by changing the constant segment of the IG from IgM to other isotypes (IgA, IgE or IgG).

Both SHM and CSR require the activity of an enzyme called activation-induced cytidine deaminase (AID), which is exclusively expressed in GC B cells (Muramatsu *et al.*, 2000). AID is a cytosine deaminase that introduces point mutations by converting cytosine to uracil causing C:G to T:A transitions in the DNA strand after replication. Subsequently, the action of error-prone DNA repair machinery may lead to the introduction of double strand breaks, which are essential for CSR process (Li *et al.*, 2004; Choudhary *et al.*, 2017).

At the end of all these processes, the surviving centrocytes can undergo multiple cycles of re-entry in the DZ before completing their differentiation into plasma cells or memory B

cells. Once differentiated, these plasma B cells will remain in the lymphoid organs, while memory B cells will migrate to bloodstream.

T-cell independent activation may occur in the outermost region of the lymphoid follicle called the marginal zone, where B cells can interact with antigens presented by macrophages. This activation produces a rapid response of the marginal zone B cells that differentiate into extrafollicular plasma cells. In absence of T-cell interaction, SHM and CSR may occur in a less efficiently way than in the GC. Therefore, antibodies generated are mainly IgM of limited diversity (Cerutti, Cols and Puga, 2013).

1.2. Advances in diagnostic techniques for B-cell lymphoma diagnosis

Lymphoma diagnosis has been enormously challenging for clinicians. Over the time it has evolved tremendously thanks to the advances in diagnostic techniques. Initially, lymphoma classification was strictly based on clinics and the appearance down the microscope (morphology) corresponding of normal B-cell stages. Over time, with the appearance of monoclonal antibodies and their adaptation to formalin-fixed paraffin embedded (FFPE) sections, the use of immunophenotype analysis by flow cytometry and immunohistochemistry was integrated as a new tool for the clinician to better diagnose and subclassify lymphomas (Ferry, 2020).

The introduction of conventional cytogenetic methods and new advances in DNA genome-wide techniques allowed the detection of different types of genetic alterations associated with different lymphoma entities. These findings have been determinant for the understanding of lymphoma pathogenesis leading to a more accurate classification and diagnosis of the different lymphoma subtypes.

For these studies, most available samples are the ones preserved in FFPE blocks, which sometimes have some antiquity and then the extensive clinical follow-up information that is

needed for highly powerful retrospective studies. Although, the problem with this kind of samples is the low quality of nucleic acids extracted from these FFPE blocks compared to those obtained from fresh or frozen biospecimens. This occurs because of the formalin-fixation procedure which causes nucleic acids fragmentation, degradation, chemical modification and cross-linking to proteins (Srinivasan, Sedmak and Jewell, 2002). For that reason, the application of molecular genome-wide techniques such as copy number (CN) arrays, sequencing or gene expression techniques are sometimes limited to the use of fresh frozen samples, although its availability is scarcer. Even that, in order to take advantage of this widely available repertory of FFPE samples, new adapted techniques and optimization strategies have been introduced to reduce the low quality results obtained from FFPE samples and minimize sequence artifacts (Do and Dobrovic, 2015).

A brief overview of most used techniques is explained below, and its application, advantages and disadvantages are summarized in **Table 1**.

Table 1. Comparison of genomic molecular techniques

	Cytogenetics	FISH	CGH array	SNP array	MIP-assay	Sanger	NGS
Features							
Resolution	>5 Mb	50 kb	3 kb	10-20 kb	50-100 kb	1bp	1bp
Requires viable cells	Yes	No	No	No	No	No	No
Requires prior knowledge of the DNA sequences	No	Yes	No	No	No	Yes	No
Allows FFPE DNA	No	Yes	Yes*	Yes*	Yes	Yes	Yes*
Identification							
Rearrangement	Yes	Yes	Yes#	Yes#	Yes#	Yes	Yes
CNA	Yes	Yes	Yes	Yes	Yes	No	Yes
CNN-LOH	No	No	No	Yes	Yes	No	Yes
SNV/indels	No	No	No	No	No	Yes	Yes

SNV: single nucleotide variant; CGH: comparative genomic hybridization, SNP: single nucleotide polymorphism; MIP: molecular inversion probe; NGS: next generation sequencing; CNA: copy number alteration; CNN-LOH: copy number neutral loss of heterozygosis.
Can be deduced from some unbalanced rearrangements with CNA associated.
* Generally limited to good quality FFPE-derived DNA.

1.2.1. Conventional cytogenetics and Fluorescence *in situ* hybridization

Conventional cytogenetic analysis has been used to obtain the karyotype of the neoplastic cells. The technique is based on the study of metaphase chromosomes with different banding staining techniques. It provides a view of all chromosomes and allows the detection of large abnormalities including rearrangements and whole chromosomal gains and losses or large portions of them (**Figure 3A**). A significant limitation is its low resolution and the requirement of fresh tissue with growing viable cells.

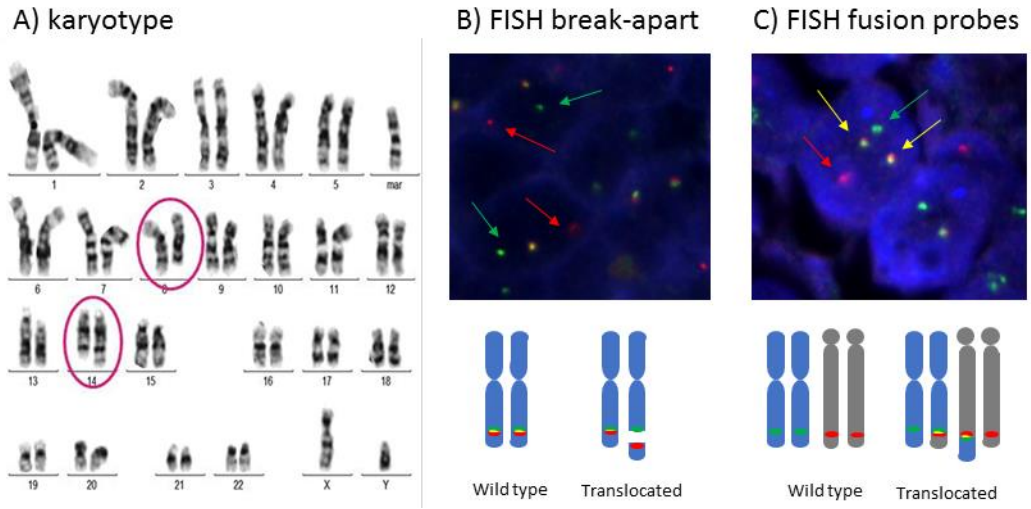

Figure 3. Conventional karyotype and FISH for detection of t(8;14)/IGH-*MYC* rearrangement. A) Karyotype showing the two altered chromosomes involved in the translocation, B) FISH break apart probes and C) FISH dual-color dual-fusion probes. Karyotype from (Angi *et al.*, 2017).

On the other hand, fluorescence *in situ* hybridization (FISH) is a powerful technique for detection of cancer-specific aberrations such as rearrangements and gene CN alterations. It is widely used in routine diagnostics since it can be performed on FFPE sections. This technique is based in the use of probes labelled with specific fluorochromes that allow the visualization of a concrete region of the genome by using a fluorescence microscope. There are two different designs for translocation detection including the break-apart and dual-color dual-fusion probes. Break-apart probes flank either side of a specific loci where the

breakpoint is located. These probes are close to each other but, in the event of a rearrangement, the two signals would split and would be visualized physically separated (**Figure 3B**). The limitation is that with these probes the partner of the translocation remains unknown. On the other hand, dual-color dual-fusion probes usually target the two known regions, usually from the two derivative chromosomes involved in a specific translocation (e.g., t(8;14)/IGH-*MYC)*. When translocation occurs, the juxtaposition of both signals will be observed (**Figure 3C**).

1.2.2. Copy number arrays

The CN arrays are high-resolution techniques for genome-wide CN detection. This technology is based on a chip of synthetic oligonucleotides complementary to human DNA and the hybridization of labelled fragments of DNA samples. Unlike karyotype or FISH techniques, where dividing cells are needed to obtain metaphases, CN arrays only need genomic DNA. Comparative genomic hybridization (CGH) array is a type of CN array that allows detection of CN alterations by comparing the genome from a tumor sample with a reference one, each of them marked with a different fluorochrome. Comparison of the two signals by an image analysis software results in the identification of gains, losses, amplifications and homozygous deletions. Besides, this technique also allows the identification of chromothripsis patterns, which are massive genomic clustered rearrangement of one chromosome in a single catastrophic event, by the detection of at least seven switches of CN states on a single chromosome (Stephens *et al.*, 2011; Edelmann *et al.*, 2012).

The single nucleotide polymorphism (SNP) array is another CN array similar to CGH array but differently the design includes different oligonucleotides containing both alleles of a SNP bind to a solid surface area. This type of array only requires the hybridization of the target samples and allows the identification of not only gains and losses, but also loss of heterozygosity (LOH) and CN neutral-LOH (CNN-LOH) alterations (**Figure 4**).

The application of CN arrays to FFPE-derived DNAs has been controversial since lower success rates and higher number of CN changes including artifacts were reported compared to those from fresh or frozen tissues (Mc Sherry *et al.*, 2007; Tuefferd *et al.*, 2008; Nasri *et al.*, 2010). These genotype discordances between FFPE and frozen samples differ among different platforms but, in the end, raise troubling questions about the reliability of the data generated from poor quality FPPE samples. In order to overcome these problems, some CN array platforms have optimized their protocols for FFPE samples obtaining good results comparable to frozen samples (Lyons-Weiler *et al.*, 2008). Additionally, recent advances in the methodology of CN arrays have allowed the development of different array platforms suitable for low quality FFPE-derived DNA. For instance, Oncoscan platform (Thermofisher inc.) is based on molecular inversion probe (MIP)-assay, a new methodology in which only a small intact target DNA sequence footprint, including a SNP, is required by MIP probes (~40 bp) allowing to work with highly degraded FFPE-derived DNAs (Wang *et al.*, 2009).

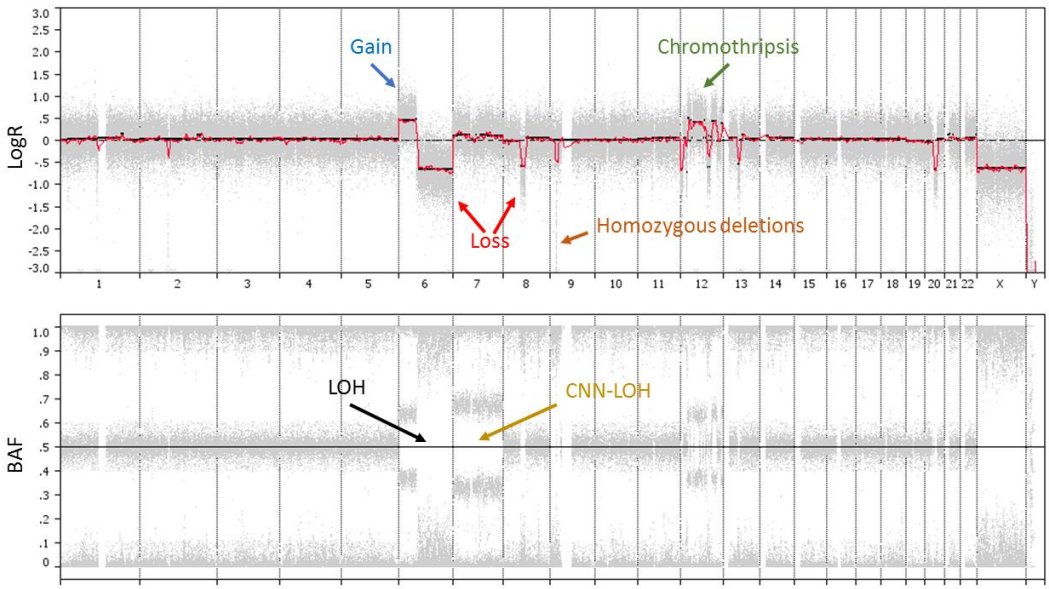

Figure 4. **Oncoscan SNP-array representation.** In the first panel, CN calls are represented, whereas in the second panel, the B-allele frequency (BAF). The profile includes the representation of different CN alteration (gain, loss and homozygous deletion), chromothripsis pattern and LOH and CNN-LOH.

1.2.3. DNA Sequencing approaches

DNA sequencing is the process in which the nucleotide order of a given DNA sequence is determined, allowing the identification of different genetic alterations including single nucleotide mutations, insertions and deletions (indels) and even structural variants (gains, losses, inversions and rearrangements). It englobes different techniques from the conventional Sanger sequencing to the different next generation sequencing (NGS) approaches.

Sanger sequencing was the first technique that allowed DNA sequencing. It is based on the chain termination method which relies on the incorporation of labelled modified nucleotides (dideoxynucleotides, ddNTPs) by a DNA polymerase. This technique only allows the sequencing of a specified target region identifying high frequency mutations (>15% allele frequency). Translocations and indels can be also identified with appropriated primers.

On the other hand, NGS techniques consist in the massive parallel sequencing of millions of small fragments of DNA called reads. These techniques allow the sequence of entire genomes (whole genome sequencing; WGS) or specific regions of interest, including all the exomes from all the 22.000 genes of the genome (whole exome sequencing; WES) or small number of individual genes (targeted sequencing). An advance in NGS approaches has been the introduction of the paired-end sequencing that allows the sequencing of both ends of a fragment. This new methodology produces twice the number of reads, more accurate read alignment and allows detection of small indels, CN alterations and translocations and inversions with the appropriate algorithms (**Figure 5**) (Nakagawa *et al.*, 2015). It is necessary to emphasize that the implementation of these techniques requires the use of bioinformatics tools to assess the massive amount of data generated.

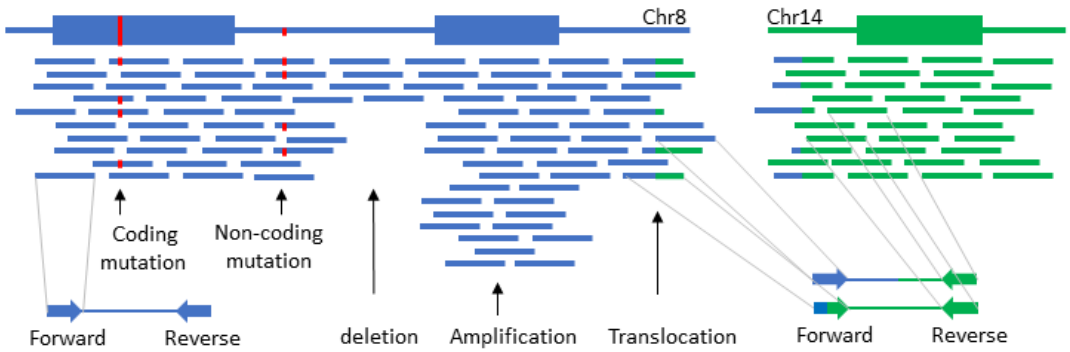

Figure 5. **NGS technology scheme.** Representation of WGS paired-end reads and different genomic alterations including coding and non-coding mutations, copy number alterations and translocations.

NGS techniques cover the sequencing of DNA from both FFPE and frozen samples. Despite of that, there are some concerns with the use of FFPE-derived DNA since high frequency of false-positive artifacts were detected compared to frozen-derived DNA (Gallegos Ruiz *et al.*, 2007; Astolfi *et al.*, 2015). These artifacts are transitional C:G to T:A changes produced from the hydrolytic deamination of cytosine bases to uracil (Do and Dobrovic, 2015). Since these artifacts show very low frequency due to the arbitrariness of the process, they can be filtered out using appropriate pipelines. A second major problem related to FFPE-derived DNA is the high fragmentation of the nucleic acids that significantly reduces the number of amplifiable templates available for PCR amplification (Carrick *et al.*, 2015). Capture-based targeted sequencing approach may be a solution for these highly degraded low-quality DNA from FFPE samples since it is based on DNA capture by hybridization using synthesized oligonucleotide probes, also known as baits, which are shorter than amplicons and can be overlapped, enabling more templates to be captured (Wong *et al.*, 2013; Do and Dobrovic, 2015).

1.3. B-cell Non-Hodgkin Lymphoma pathogenesis

Lymphoma development or pathogenesis is a process in which the accumulation of genetic alterations in normal B cells leads to an activation of oncogenic pathways and impairment of normal cell growth and survival. Akin to other cancers, these genetic alterations include somatic mutations, CN changes and structural gene rearrangements. A single genetic event is not enough to develop a tumor, but rather an accumulation of them. These genetic alterations arise from replication errors or DNA damage (caused by exogenous and endogenous factors) and are accumulated arbitrary in the somatic cells of our body during its lifespan (Martincorena and Campbell, 2015).

Most of the mutations that the cells acquire are harmless and do not affect the phenotype. Unfortunately, on some occasions, a mutation can affect important genes (oncogenes or tumor suppressor genes) or regulatory elements that alter cellular functions of great importance for the cell. These mutations can confer a selective advantage to the cell, leading to a better growth, increased proliferation and survival (Stratton, Campbell and Futreal, 2009). Therefore, mutations can be considered as "drivers" when confer a selective advantage to the cell, or "passengers" if they have no phenotypic or biological effect.

As it was mention before, the process of B-cell development leads to changes in the genome as well as clonal expansion of the B cells that may have some risks associated. Normally, the entire process is tightly regulated by homeostatic controls but sometimes this regulation might be disrupted by different reasons including the acquisition of genetic alterations, viruses and bacterial infections or an immunosuppression by immunosuppressive treatment or baseline immune deficiency disorders (Zhang *et al.*, 2011).

Most of the B-NHL genetic alterations converge in the same biological programs, signaling pathways and regulatory networks that operate during the normal B-cell differentiation in order to sustain growth and cell survival. The mechanisms underlying these alterations are

diverse and still incompletely understood. Even that, two important types of genetic alterations in B-NHL, which are chromosomal translocations and aberrant SHM (aSHM), are known to occur as a consequence of the IG gene remodeling processes malfunctions leaded by AID machinery (Pasqualucci *et al.*, 2008) (**Figure 6**).

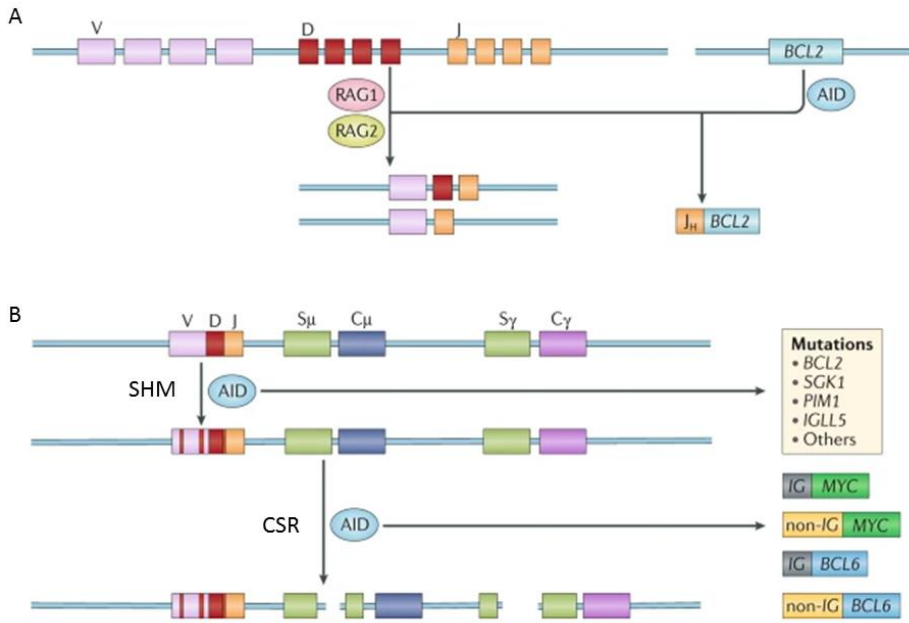

Figure 6. Main genetic alterations in B-NHL. A) In the bone marrow, RAG1 and RAG2, which mediate VDJ recombination, cause breaks in genes encoding immunoglobulins. B) In the germinal center, the AID machinery, which is involved in SHM and CSR processes, causes aSHM of non-IG genes and breaks in immunoglobulin or non-immunoglobulin genes, which promotes the generation of gene translocations. Figure adapted from (Miao *et al.*, 2019).

1.3.1. Chromosomal translocations

IG related chromosomal translocations are supposed to be the first hit in the process of lymphomagenesis. These rearrangements can occur in different steps of the B-cell development involving the malfunction of the IG gene remodeling processes (RAG-mediated VDJ recombination and AID-mediated CSR and SHM) (Küppers and Dalla-Favera, 2001). These translocations mainly cause the juxtaposition of IG regulatory regions with the intact

coding region of another target gene, which is mainly an oncogene, driving its overexpression. These affected oncogenes are usually genes related with the GC B-cell development regulation (e.g., *BCL6*, *PAX5*, *MYC* and *BCL2*). However, these alterations are not sufficient to cause the tumor since they have been detected in healthy individuals in very small clonal population (Lecluse *et al.*, 2009). Therefore, other secondary alterations including single nucleotide variants and CN alterations must be acquired during cancer progression with different implications in the pathogenesis.

1.3.2. Aberrant somatic hypermutation

Another alteration, which is exclusive of GC-derived B-cell lymphomas is the termed aSHM. This mechanism of alteration consists in the deregulation of the physiological SHM mechanism which leads to the extension of the AID mutagenic activity to several non-IG genes causing an hypermutation or kataegis of the locus. In normal GC-derived B cells, this AID mutagenic activity can affect the 5' regulatory sequences of *BCL6* and *TNFRSF6*/*FAS* (Pasqualucci *et al.*, 1998; Müschen *et al.*, 2000). On the other hand, in some GC-derived B-NHL and particularly in diffuse large B-cell lymphoma, aSHM may cause a hypermutated pattern affecting numerous known proto-oncogenes such as *PIM1*, *PAX5, RHOH/TTF* and *MYC* (Pasqualucci *et al.*, 2001). The SHM pattern caused by the AID is characterized by multiple C:G to T:A transitions, mainly affecting WRCY/RGYW hotspot sequences of the firsts 2kb after a transcript start site, which may include intronic or non-translated sequences containing regulatory regions and sometimes exonic regions (Khodabakhshi *et al.*, 2012). The functional consequences of aSHM on non-IG genes may cause a dysregulation in the gene expression or alterations in the protein structure. Nevertheless, a comprehensive characterization of the functional consequences of the aSHM on non-IG genes is still missing. This mechanism has been also described as a driving mechanism for chromosomal translocations in B-NHL since it generates also double-strand DNA breaks that are potentially recombinogenic (Küppers and Dalla-Favera, 2001).

2. Pediatric non-Hodgkin lymphomas

NHL mainly affect adults, with a median age at diagnosis of 67 years old but can also occur in pediatric population (cut-off stablished at 18 years old) (SEER 21 2013–2017). In fact, pediatric NHL is the fifth most common neoplasia occurring in children and adolescent, representing a 6% of all malignances (Downing *et al.*, 2012). These pediatric NHL are mainly aggressive B-cell lymphomas, characterized by age-related differences in terms of clinic presentation, prognosis and biology (Minard-Colin *et al.*, 2015).

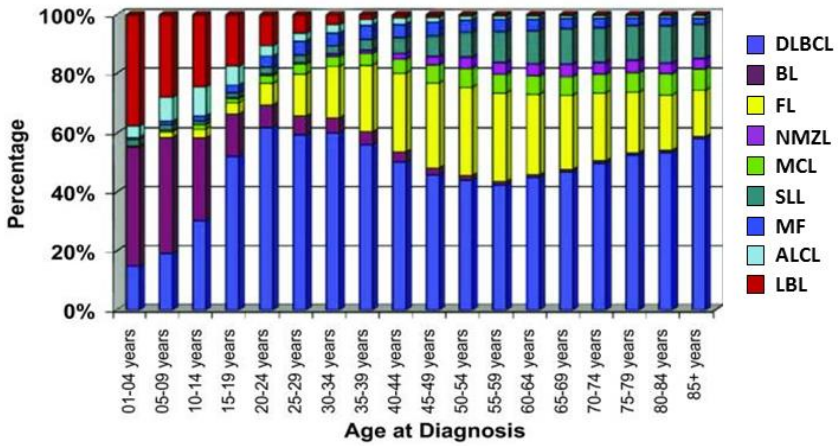

Figure 7. Relative frequency of NHL subtypes according to the age at diagnosis. ALCL, anaplastic large-cell lymphoma; BL, Burkitt lymphoma; DLBCL, diffuse large B-cell lymphoma; FL, follicular lymphoma; LBL, lymphoblastic lymphoma; MCL, mantle cell lymphoma; MF, mycosis fungoides; NMZL, nodal marginal zone lymphoma; SLL, small lymphocytic lymphoma. Figure from (Sandlund and Martin, 2016).

The spectrum of different NHL subtypes varies with the age. In pediatric and young adult population there are more frequent aggressive high-grade tumors comprising Burkitt lymphoma (BL), diffuse large B-cell lymphoma (DLBCL), primary mediastinal B-cell lymphoma (PMBCL), lymphoblastic lymphoma (LBL) and anaplastic large cell lymphoma (ALCL), whereas low-grade lymphomas such as follicular lymphoma (FL) and nodal marginal zone lymphoma (NMZL) are much less common (**Figure 7**) (Sandlund and Martin, 2016).

Sometimes, overlapping immunophenotypic, morphological and clinical features makes difficult the differential diagnosis between some of these pediatric entities. For instance, there is an entity in the WHO termed high grade B-cell lymphoma (HGBCL) for those cases with intermediate features between BL and DLBCL that should not be classified as neither of them (Swerdlow *et al.*, 2017).

2.1 Clinical aspects and therapeutic regimens of pediatric B-NHL

In general, pediatric NHL have better treatment outcome than adults, with an overall survival (OS) rate exceeding 80% (Minard-Colin *et al.*, 2015). This might be explained by age-related differences in terms of the biology of the tumor and the therapeutic approaches. For instance, young patients can receive more intensive therapeutic regimens than adults. Accordingly, pediatric regimens are based of highly intensive chemotherapy whereas in adults, different doses are required depending of the lymphoma entity (Sandlund, 2007). Even that pediatric NHL have an excellent prognosis, there are some concerns regarding the use of these highly intensive poly-therapies since they may produce long-term toxicities and other late complications such as risk of second malignancies, reduced fertility and risk of cardiomyopathy (von der Weid, 2008).

Aggressive B-NHL, including DLBCL and BL, are extremely chemosensitive, achieving excellent results using intensive short cycle multiagent cyclophosphamide-based chemotherapeutic regimens adapted from B-cell acute lymphoblastic leukemia, in addition to central nervous system (CNS) prophylaxis. Some of these regimens and protocols are indicated in the **Table 2** (Reiter *et al.*, 1999; Patte *et al.*, 2001; Lacasce *et al.*, 2004; Thomas *et al.*, 2006; Mead *et al.*, 2008; Dunleavy, Pittaluga, Shovlin, *et al.*, 2013; Minard-Colin *et al.*, 2020). Outcomes improved dramatically as a result of two large clinical trials performed by the French-American-British Lymphomes Malins B (LMB) and the Berlin-Frankfurt-Munster (BFM) groups, in which different chemotherapy protocols were tested (Reiter *et al.*, 1999; Patte *et al.*, 2001). Both protocols rely on similar intensive multiagent chemotherapy and

stratify cases into risk groups according to the degree of surgical resection, stage and serum lactate dehydrogenase (LDH) activity. The use of rituximab, a chimeric monoclonal antibody against the CD20 cell surface antigen, has been demonstrated to improve survival of high-risk patients when combined with LMB/BFM chemotherapy backbones (Goldman *et al.*, 2013; Minard-Colin *et al.*, 2020), suggesting its use independently of the risk group.

Table 2. Front line Treatment Options for ped B-NHL.

Regimen/ protocols	Components	Rituximab	Study patients	Outcomes	Reference
CODOX-M/IVAC	cyclophosphamide, cytarabine, vincristine, doxorubicin and methotrexate in combination with ifosamide, etoposide and cytarabine	No	BL	72% OS 64% EFS 2-years	(Lacasce *et al.* , 2004; Mead *et al.* , 2008)
DA-EPOCH-R	etoposide, prednisone, vincristine, cyclophosphamide, doxorubicin	Yes	BL	>90% CR and PFS	(Dunleavy *et al.* , 2013)
Hyper-CVAD-R	cyclophosphamide, vincristine, doxorubicin and dexamethasone in combination with methotrexate and cytarabine	Yes	BL/B-ALL	89% OS 3-year 80% EFS 3-year	(Thomas *et al.* , 2006)
LMB89 protocol (COPADM)	cyclophosphamide, vincristine, prednisone, doxorubicin and methotrexate	No	pediatric B-NHL	97% CR 92% 5-year EFS/OS	(Patte *et al.* , 2001)
BFM90 protocol	Similar to LMB protocol	No	pediatric B-NHL	89% 6-year EFS	(Reiter et al., 1999)
Inter-B-NHL Ritux	LMB chemotherapy plus rituximab	Yes	pediatric BL/ALL	93.9% 3-year EFS	(Minard-Colin et al., 2020)

OS: Overall survival; CR: complete response; EFS: Event free survival; PFS: progression free survival.

On the other hand, therapeutic options for low-grade indolent lymphomas such as pediatric type FL (PTFL) and pediatric NMZL (PNMZL) include watch and wait strategy after resection or limited chemotherapy approaches, obtaining survival rates exceeding the 95% of the cases (Attarbaschi *et al.*, 2013; Ronceray *et al.*, 2018).

Even that relapses are rare in pediatric B-NHLs, their outcome is dismal with curate rates of less than 30% and no standard of care available (Moleti, Testi and Foa, 2020). Therefore, novel approaches are needed to both reduce toxicities and improve outcomes in those pediatric patients that relapse. There are fewer novel agents that are being tested in

pediatrics in comparison with adults. Despite of that, some clinical trials are evaluating novel approaches including chimeric antigen receptor T-cells (phase 2 clinical trial: NCT03610724) or targeted therapies such as Ibrutinib (phase 3 clinical trial: NCT02703272) (Harker-Murray, Pommert and Barth, 2020).

2.2. Molecular profiling of pediatric B-NHL

Whereas adult B-NHLs have been widely studied, data on molecular profiling of pediatric B-NHLs series are almost lacked except for BL and PMBCL which have been extensively studied with now well-established profiles of genomic alterations (Savage *et al.*, 2003; Love *et al.*, 2012; Richter *et al.*, 2012; Schmitz *et al.*, 2012; Reddy *et al.*, 2017). This occurs because most of the molecular studies did not take into account the age of the patients, diluting in that way the biology of the pediatric variants.

Even that, some genetic studies have been performed only in pediatric patients identifying clear differences with their adult counterparts which has been crucial for the recognition of these pediatric variants as separated pediatric entities in the WHO classification of lymphoid neoplasms such as PTFL and PNMZL (Louissaint *et al.*, 2016; Schmidt *et al.*, 2016). Additionally, these studies of mature B-NHL in children also led to the identification of two new entities such as Burkitt-like lymphoma with 11q aberration (BLL-11q) and large B-cell lymphoma with *IRF4* rearrangement (LBCL-IRF4) which were introduced as provisional entities in the 2017 revision of the WHO classification (Swerdlow *et al.*, 2017). These newly recognized entities have not been yet studied in detail due to the novelty and the rareness of the disease.

Therefore, genome wide studies of pediatric cohorts could significantly help to extend our understanding of lymphoma pathogenesis leading to a more accurate re-definition of the lymphoma subtypes and to better stratify the cases in risk groups in order to reduce toxicities and to identified new targets for novel therapies. From now, we will focus on

pediatric GC-derived B-NHL including BL, BLL-11q, HGBCL, DLBCL, LBCL-IRF4, PMBCL and PTFL subtypes. Therefore, next sections will review in detail all these pediatric entities.

3. Burkitt lymphoma

BL is a highly aggressive B-cell NHL derived from mature GC B cells described for the first time in 1958 by the Irish surgeon Denis Burkitt (BURKITT, 1958). It is the most prevalent B-NHL in pediatric population accounting 40% of all B-NHL in childhood but less than 5% in adults (Dunleavy and Gross, 2018). It is characterized by *MYC* rearrangements, the hallmark of the disease, which causes a constitutive overexpression of the oncogene leading to a rapid cell proliferation (Swerdlow *et al.*, 2017). Of note, it was the first cancer discovered to be pathologically driven by a genetic rearrangement and also the first human tumor related with a virus infection (Casulo and Friedberg, 2018).

According to the WHO classification, three different clinical entities of BL have been identified with similar morphology, immunophenotype, but epidemiologically and clinically distinct. These entities are the endemic, sporadic, and immunodeficiency associated, being the sporadic variant the most prevalent worldwide (Dunleavy, Little and Wilson, 2016; Swerdlow *et al.*, 2017) (**Table 3**).

3.1. Morphological and clinical aspects of BL

Independent of subtype, all BL variants display high proliferation rate and present with a diffuse growth of medium-sized, monomorphic cells with blastic chromatin and multiple small nucleoli. BL is also characterized by the “starry-sky” appearance due to the scattered tingible body macrophages that get stuffed with cellular debris caused by a high fraction of apoptotic neoplastic cells. Immunophenotypically, BL expresses pan-B cell surface markers such as CD19, CD20 and CD79a in addition to the GC markers CD10 and BCL6 but lack BCL2

expression (Casulo and Friedberg, 2018). Strong expression of MYC protein is also seen in most of cells (Grimm and O'Malley, 2019). The marker ki-67 is expressed around 100% of the cells evidencing the high proliferation rate of the cells. Negativity for the GC marker LMO2 is typically seen in BL and has been shown to predict presence of *MYC* translocations (Colomo *et al.*, 2017).

Table 3. Epidemiology and clinical presentation of BL subtypes.

Characteristics	Endemic BL	Sporadic BL	HIV associated BL
Epidemiology	Equatorial belt of Africa and Papua New Guinea	Worldwide	Worldwide
Incidence	5-10/100,000 cases	2-3/1,000,000 cases	6/1000 AIDS cases
NHL (percentage)	90% of PedNHL	30-40% of PedNHL 1-2% of AdultNHL	
Age and gender	Peak incidence: 4-7 y Male:Female 2:1	Median age: 30 y Male:Female 2-3:1	Median age: 44 y
EBV association	100%	10-20%	25-40%
Location	jaw and facial bones	abdomen in 60-80% and head and neck	
CNS involvement	30-40%	15%	high risk
BM involvement	10%	30%	

CNS: central nervous system; BM: bone marrow; Y: year

Clinically, BL presents as a rapidly growing tumor, with affection of extranodal sites including the CNS and the BM. Consequently, almost 70% of the patients have an advanced stage III or IV disease at the diagnosis (Swerdlow *et al.*, 2017). Despite its aggressive behavior, BL is extremely chemosensitive, achieving excellent results using intensive short cycle multiagent chemotherapeutic programs regimens including a combination of multiagent cytotoxic chemotherapies with tumor lysis and CNS prophylaxis management (**see section 2.1**.). Interestingly, adults and pediatric cases are treated with the same regimens with a paucity for older patients. In pediatric population, BL outcome reaches more than 90% of survival rate whereas in adults, recent data reported OS rate exceeding 70% (Saleh *et al.*, 2020).

3.2. Role of infectious agents: Epstein Barr virus

The role of Epstein Barr virus (EBV) infection in BL pathogenesis is quite enigmatic. EBV a is gamma-1 herpesvirus with oncogenic potential since it promotes growth-transforming proliferation to resting B-cells lymphocytes (Mrozek-Gorska *et al.*, 2019). This virus has been associated with distinct lymphoproliferative diseases and tumors including B-cell lymphomas (Shannon-Lowe and Rickinson, 2019). EBV-positive BL, typically display a latency I program which promotes cell survival via microRNAs (e.g. *BART*s and *BHRF1* miRNAs), thereby counteracting the apoptotic signals that entails elevated *MYC* expression (Komano *et al.*, 1999; Seto *et al.*, 2010; Vereide *et al.*, 2014). EBV can also promote genomic instability, dysregulate telomere functions, and induce DNA damage to infected cells (Kamranvar *et al.*, 2007). Despite of that, EBV infection is clearly not sufficient to cause BL since it is not present in all BL cases and is quite prevalent in the normal adult population (90% of the adults).

3.3. Gene expression profiling: molecular BL signature

In comparison with other aggressive B-NHL, BL gene expression profile is close to that of DZ centroblasts of the GC (Victora *et al.*, 2012). Gene expression assays defined the BL gene expression signature which is characterized by overexpression of *MYC* and its target genes, a subgroup of GC B-cell related genes including *BCL6*, and decreased expression of major-histocompatibility-complex class I genes and NF-kB target genes in comparison with other aggressive B-NHL (Dave *et al.*, 2006; Hummel *et al.*, 2006). These gene expression signatures that define “molecular Burkitt lymphoma (mBL)” were not exclusive of conventional BL but could also be identified in atypical BL and some HGBCL and DLBCL cases (**Figure 8**).

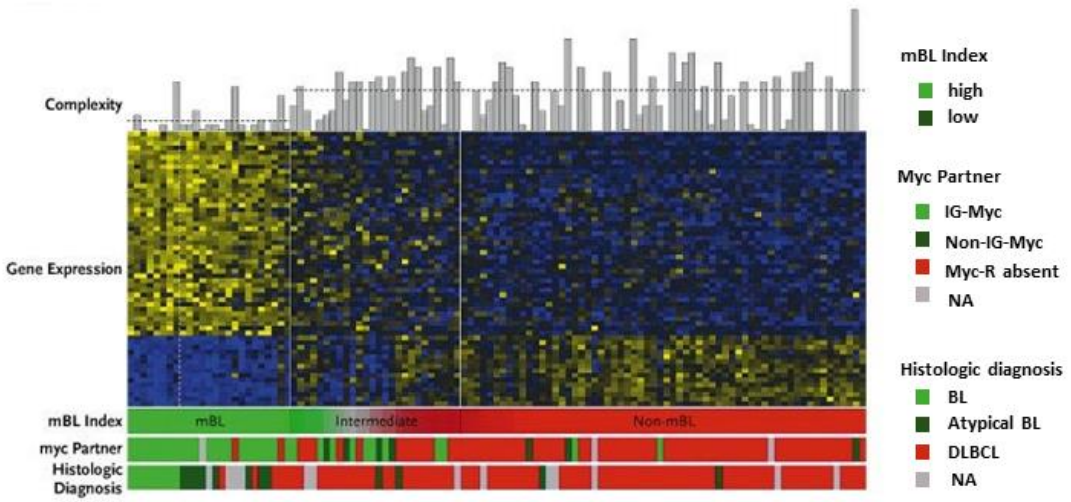

Figure 8. BL gene expression signature prediction of 105 cases. Genomic complexity is described in the bar plots at the top of the panels. Heat map shows the gene-expression levels of the 58 mBL-signature genes, with 1 gene shown per row. Bright blue indicates a low level of expression, bright yellow indicates a high level of expression, and black the average level of expression across all samples. Figure from (Hummel *et al.*, 2006).

3.4. BL genomic landscape and pathogenesis

BL displays a low complex genomic profile characterized by the presence of *MYC* rearrangement and other secondary events including CN alterations and somatic mutations. Several high-resolution genotyping techniques including CGH, CGH-arrays and SNP-arrays have been applied to BL to elucidate its CN landscape (Salaverria *et al.*, 2008; Scholtysik *et al.*, 2010; Schiffman *et al.*, 2011). These studies described simple genomic profiles (around 6 CN alterations per case) characterized with recurrent gains of 1q, 7q, 13q and losses of 17p and 19q13 (**Figure 9**). Additionally, NGS analysis including WGS and transcriptome sequencing identified a mutational profile characterized by a low tumor mutational burden with a mean of 29 coding mutations per case (Lopez *et al.*, 2019).

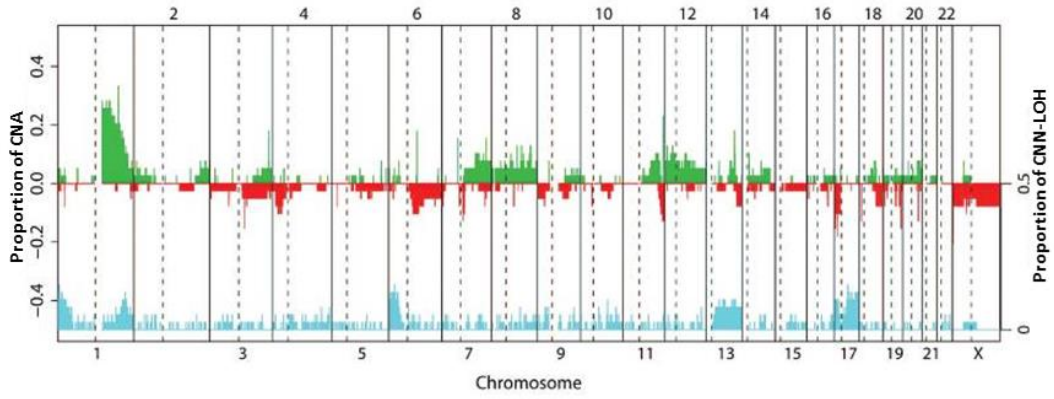

Figure 9. Copy number landscape of BL. Proportion of gains, losses and CNN-LOH along chromosomes. y-axis indicates the proportion of cases with the respective aberration, to the left CN, to the right CNN-LOH; green: gains; red: losses; blue: CNN-LOH; dotted vertical lines depict centromeres. Figure modified from (Scholtysik *et al.*, 2010).

All these genetic alterations identified in the BL genetic landscape converge into the deregulation of *MYC* and the activation of the PI3K signaling pathway, both of which are not characteristic of the physiological program of DZ B cells. Additionally, BL is also characterized by Gα13 pathway inactivation and other genetic alterations affecting apoptosis regulation (**Figure 10**).

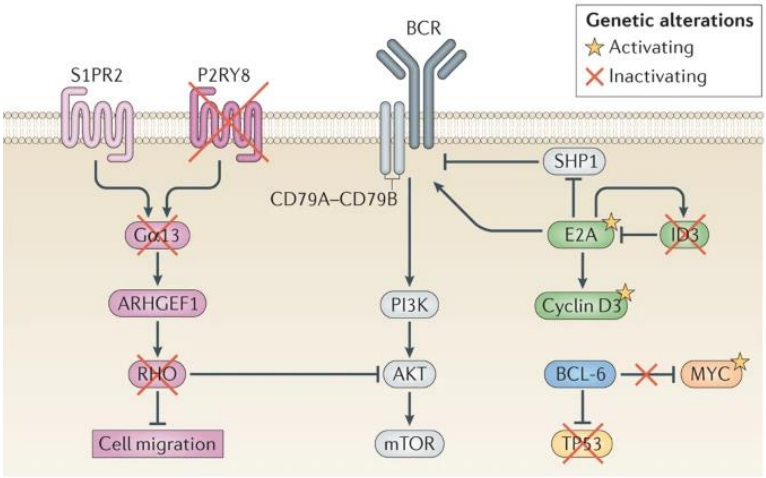

Figure 10. **Schematic representation of the pathways affected during lymphomagenesis in BL.** The different colors that are used in the figure indicate molecules that belong to a specific pathway and/or lead to a specific outcome. Figure from (Basso and Dalla-Favera, 2015).

3.4.1. *MYC* rearrangements and deregulation of *MYC* activity

As said, the most important genetic feature of BL is the presence of a reciprocal, balanced *MYC* rearrangements with IG genes, that was firstly discovered in 1976 using cytogenetic techniques (Zech *et al.*, 1976; Zayac and Olszewski, 2020). Among *MYC* translocation, the t(8;14)(q24;q32) is the most common chromosomal translocation occurring in 80% of BL juxtaposing the *MYC* and the IGH locus. Other less frequent *MYC* rearrangements occur involving the IGK t(2;8) and IGL t(8;22) light chains in 15% and 5% of patients, respectively (Swerdlow *et al.*, 2017; Casulo and Friedberg, 2018). These rearrangements lead to a constitutive *MYC* overexpression due to the juxtaposition of IG regulatory sequences to the *MYC* locus. *MYC* overexpression is a feature present in all BL cases, even in rare cases that are clinically and morphologically evident BL but lack *MYC* rearrangements, suggesting the presence of alternative mechanisms including cryptic rearrangements or miRNA deregulation that lead to *MYC* overexpression (Leucci *et al.*, 2008; Wagener *et al.*, 2019). For instance, gains and amplifications of 13q locus have demonstrated to upregulate the mir-17-92 cluster located within the region, which counteracts MYC-induced apoptosis and drives PI3K activity by reducing *PTEN* expression (Schiffman *et al.*, 2011; Schmitz *et al.*, 2014). There is an ongoing discussion about if BL is without exception defined by the presence of *MYC* rearrangement or whether a small subset of true BL without *MYC* rearrangement exist.

MYC is also known as the most frequently mutated gene in BL (Love *et al.*, 2012; Richter *et al.*, 2012; Schmitz *et al.*, 2012). *MYC* mutations have been described as aSHM patterns induced AID machinery, the same mechanisms that causes the *MYC* rearrangements (Grande *et al.*, 2019). *MYC* mutations are located within the first non-coding exon and first intron which contain negative autoregulatory sequences although can also extended into coding exon 2 (Lopez *et al.*, 2019) (**Figure 11**). Coding mutations occur in the trans activation domain affecting phosphorylation sites that alter either MYC degradation through increased protein stability or MYC-dependent transactivation of BIM and p53 pro-apoptotic proteins (Bahram *et al.*, 2000; Dang, O'donnell and Juopperi, 2005; Hemann *et al.*, 2005).

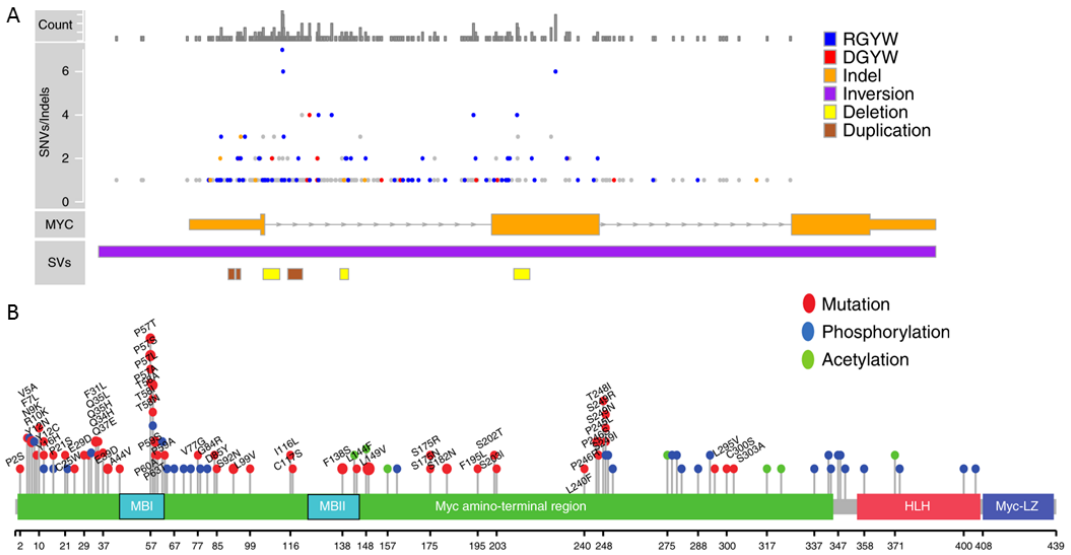

Figure 11. Recurrent *MYC* mutations in BL. A) Distribution of somatic mutations, indels and SVs in MYC. Mutations affecting SHM motifs (RGYW/DGYW) are indicated by blue and red dots; gray dots show mutations outside the motifs. B) Distribution of *MYC* mutations (red lollipops) across the MYC protein, and the location of the post translational modification sites. Figure from (Lopez *et al.*, 2019).

Altogether, *MYC* alterations lead to intensify the *MYC* activity in proliferation, energy metabolism modulation, ribosome and protein biogenesis, telomere maintenance, RNA transcription and DNA replication. In this manner, *MYC* regulates cell growth and proliferation (Meyer and Penn, 2008; Dang, 2013). However, *MYC* translocation alone is not sufficient for BL oncogenesis, as it occurs also in other NHL. Therefore, other factors might play role in the BL pathogenesis (Nguyen, Papenhausen and Shao, 2017).

3.4.2. Constitutive PI3K signaling pathway

High resolution NGS analysis identified activating mutations affecting the transcription factor *TCF3* and inactivating mutations of its inhibitor *ID3* (Love *et al.*, 2012; Richter *et al.*, 2012; Schmitz *et al.*, 2012). These mutations are highly recurrent in the three variants of BL, occuring in 70% of sporadic BL, 67% of immunodeficiency associated BL, and 40% of endemic BL variant. Interestingly, these mutations are exclusives of BL, being absent in other B-NHL

such as DLBCL, suggesting its defining role in BL pathogenesis. (Richter *et al.*, 2012) Constitutive activation of *TCF3*, which is the main regulator of the centroblast program, leads to an enhance proliferation and tonic BCR-PI3K signaling which promotes survival of the BL cells (Schmitz *et al.*, 2014; Rohde *et al.*, 2017). Moreover, *TCF3* also activates *CCND3* which pairs with *CDK6* to form an active kinase in contribute to cell cycle progression (Schmitz *et al.*, 2014). Activating mutations in *CCND3* have been also observed in 38% of sporadic BL but less prevalent among endemic BL cases (3%) (Schmitz *et al.*, 2012).

3.4.3. Additional genetic alterations

TP53 alterations, including mutations and deletions, are present in 35% of BL (present in both sporadic and endemic BL variants) (Richter *et al.*, 2012; Grande *et al.*, 2019). These alterations contribute to decrease the pro-apoptotic function induced by *MYC* overexpression. In absence of *TP53* mutations, inhibition of this pathway can also occur by other mechanisms related to the overexpression of two *TP53* inhibitors, *MDM2* and *MDM4*, which cooperate to degrade *TP53* (Leventaki *et al.*, 2012). The overexpression of these *TP53* inhibitors may be consequence of the recurrent 1q gain/amplifications where *MDM4* is located or the 9p21.3 deletions harboring *CDKN2B* gene, an inhibitor of *MDM2* (Lindstrom and Wiman, 2002; Hullein *et al.*, 2019).

Several additional mutations are also present in the molecular landscape of BL, cooperating with *MYC* and PI3K activation in the pathogenesis of the disease. (Love *et al.*, 2012; Richter *et al.*, 2012; Schmitz *et al.*, 2012). These frequently mutated genes include SWI/SNF chromatin-remodeling complex genes (*ARID1A* and *SMARCA4)*, *FOXO1*, *DDX3X* and *PCBP1*. The Gα13 signaling pathway that is involved in modulating GC B-cell migration and confinement is frequently disrupted by mutations affecting *GNA13*, *RHOA* and *P2RY8* genes (Muppidi *et al.*, 2014).

3.5. Age related differences

BL is quite a homogeneous disease regardless of the age. No significant differences have been observed between pediatric and adult BL in terms of morphology, cytogenetic aberrations or mutations (Onciu *et al.*, 2006; Havelange *et al.*, 2016). Additionally, gene expression and CGH analysis did not also found significant differences between age groups in a series of molecular BL (aggressive B-NHL with BL gene expression signature) (Klapper *et al.*, 2008).

In terms of therapy, adult BL patients are treated with the same regimens used for pediatric BL with some modification in order to decrease toxicities. Very good outcomes, although less favorable than in pediatrics, were observed in adults treated with adapted protocols. Examples include CODOX-IVAC (65% 2-y EFS) (Mead *et al.*, 2002), R-Hyper-CVAD (89% 3-y EFS) (Thomas *et al.*, 2006) and LMB protocols (65% 2-y EFS) (Divine *et al.*, 2005).

4. Burkitt-like lymphoma with 11q aberration

BLL-11q is a provisional entity in the 2017 revised version of the WHO classification (Swerdlow *et al.*, 2017). It represents cases which have morphological, phenotypic, and gene expression profiles resembling those of BL, but lack *MYC* rearrangements according to standard detection methods such as FISH and are characterized by an 11q-arm aberration.

BLL-11q was initially identified in series of gene expression classified molecular BL cases and MYC-negative HGBCL resembling BL (Pienkowska-Grela *et al.*, 2011; Salaverria *et al.*, 2014). BLL-11q cases are mainly of pediatric and young adult population although occasional cases in old patients have been reported (Pienkowska-Grela *et al.*, 2011; Salaverria *et al.*, 2014; Rymkiewicz *et al.*, 2018).

4.1. Morphological and clinical aspects of BLL-11q

BLL-11q may have a diverse morphology, mainly of BL with the typical cytologic features as the "starry-sky" pattern, but sometimes of HGBCL, and sporadically of DLBCL. It can also display a certain degree of cytological pleomorphism, sporadically a follicular pattern (Salaverria *et al.*, 2014; Rymkiewicz *et al.*, 2018). Immunophenotypically, BLL-11q is similar to BL with positive expression of CD19, CD20 in addition to the GC markers CD10 and BCL6 and lack BCL2, but some variations can be observed. It is also characterized by a high proliferation rate (ki-67; >90% of the cells) and negativity for EBV RNA expression. Additionally, the GC marker LMO2, which predict the absence of *MYC* translocations in aggressive B-cell lymphomas, is expressed in 70% of the cases (Rymkiewicz *et al.*, 2018).

Clinically, BLL-11q presents as a rapidly growing tumor, with a higher incidence of nodal presentation in comparison with BL (82% vs 55%). These cases have an excellent survival rate, similar to BL if treated with the same BL regimens (>90% 3-year OS) (Salaverria *et al.*, 2014).

4.2. BLL-11q genomic landscape and pathogenesis

Absence of *MYC* rearrangements is a crucial feature for the recognition of these cases. Nevertheless, caution is warranted to define a true MYC-negative BL, because the wide range of breakpoints in the *MYC* and IG loci along with cryptic insertions of one locus into the other can make *MYC* breaks undetectable by FISH (Lopez *et al.*, 2019; Wagener *et al.*, 2019). Despite of that, it has been demonstrated that these cases have lower *MYC* expression in comparison with BL, proving in that way the negativity of *MYC* rearrangements (Salaverria *et al.*, 2014).

BLL-11q seems to have slightly more complex karyotypes than BL (6-12 CN alterations per case, using different SNP and CGH microarray platforms) characterized by recurrent 11q-

arm aberrations in addition to 6q14-q24 deletions and gains of 7q, 12p, 18q21.1 and 19p (Pienkowska-Grela *et al.*, 2011; Salaverria *et al.*, 2014; Rymkiewicz *et al.*, 2018). The 11q-arm alteration is composed by proximal gains of 11q23.2-q23.3, some of them inverted, and telomeric losses of 11q24.1-qter. Additionally, isolated cases have been recognized with single 11q24-qter losses or 11q23 gain with 11q24 CNN-LOH (Salaverria *et al.*, 2014; Grygalewicz *et al.*, 2017). This 11q alteration is quite heterogeneous among cases since reported 11q-breakpoints between regions of gain and loss are not conserved, suggesting that this alteration is do not lead to a fusion gene product or a conserved rearrangement. (**Figure 12**). Some interesting candidate genes have been identified to be deregulated based of GEP and/or Western Blot experiments in both gain (*PAFAH1B2*) and deleted (*ETS1* and *FLI1*) locus of the 11q-aberration. The *ETS1* gene that is included in the minimal region of loss was also target of a focal homozygous deletion and was shown to be mutated in 4 of 16 investigated cases (Salaverria *et al.*, 2014).

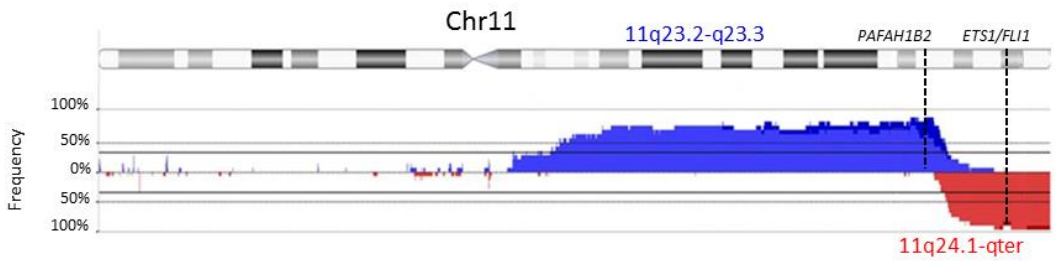

Figure 12. **The 11q alteration of BLL-11q** (n = 14, including SU-DHL-5 and HT cell lines). Chromosomal view of chromosome 11 analyzed by SNP arrays. Gains are depicted in blue whereas losses in red. Figure modified from (Salaverria et al., 2014).

The 11q aberration might not be specific of BLL-11q entity since similar pattern of alteration was observed in a few typical BL and *MYC*-positive HGBCL (Grygalewicz *et al.*, 2017). Additionally, same 11q alterations were observed in adult *MYC*-negative post-transplant molecular BL, although they are best considered to be BLL-11q (Ferreiro *et al.*, 2015; Swerdlow *et al.*, 2017).

Comparative analysis with BL showed that BLL-11q lacks 1q gains, has a different gene expression profile and lacks *ID3* mutations (Salaverria *et al.*, 2014).

4.3. BLL-11q differential diagnosis

The overlapping morphological and immunophenotypic features with BL and other aggressive B-cell lymphomas from the GC such as HGBCL, NOS, makes difficult their recognition. Even that the presence of its characteristic 11q aberration is helpful in the diagnosis, the methodology to identify this alteration still needed to be stablished. Thus, study of larger series will be necessary to better define the morphological, genetic and clinical features of these cases.

5. High grade B-cell lymphoma

HGBCL is a group of aggressive, mature B-cell lymphomas that for biological and clinical reasons should not be classified as DLBCL or BL (Swerdlow et al., 2017). In the 2008 WHO classification, these cases were grouped together into a provisional category called B-cell lymphoma, unclassifiable, with features intermediate between DLBCL and BL. In the 2017 updated classification, this category was renamed by the current HGBCL entity dividing this group into two different categories: HGBCL with *MYC* and *BCL2* and/or *BCL6* rearrangements and HGBCL, not otherwise specified (NOS) (Swerdlow *et al.*, 2016).

5.1 Morphological and clinical aspects of HGBCL

HGBCL with *MYC* and *BCL2* and/or *BCL6* rearrangements, also known as double-hit or triple-hit (DH/TH) lymphomas, is group of aggressive B-cell lymphomas which encompasses all B-cell lymphomas (with the exception of follicular lymphoma and B-lymphoblastic leukemia/lymphoma) that harbor *MYC* rearrangements in combination with *BCL2* and/or

BCL6 rearrangements. HGBCL-DH/TH morphological spectrum includes DLBCL, intermediate between DLBCL and BL and few cases with blastoid appearance (**Figure 13**) (Aukema *et al.*, 2011; Swerdlow *et al.*, 2017).

HGBCL-DH/TH mainly occur in elderly patients, with a median age at diagnosis about 60 years (range 17-87 years) and no cases have been reported in pediatric and young adult population (Klapper *et al.*, 2012; Perry *et al.*, 2013). Most patients present as widespread disease, with advanced stage (stage IV according to Ann Arbor classification), involving more than one extranodal site (30-88%), the BM (59-94%) and even the CNS (45%)(Le Gouill *et al.*, 2007; Li *et al.*, 2012). Immunophenotypically, these lymphomas mainly have a GC B-cell like (GCB) phenotype with CD10 and BCL6 expression, in addition to BCL2 (Swerdlow *et al.*, 2017).

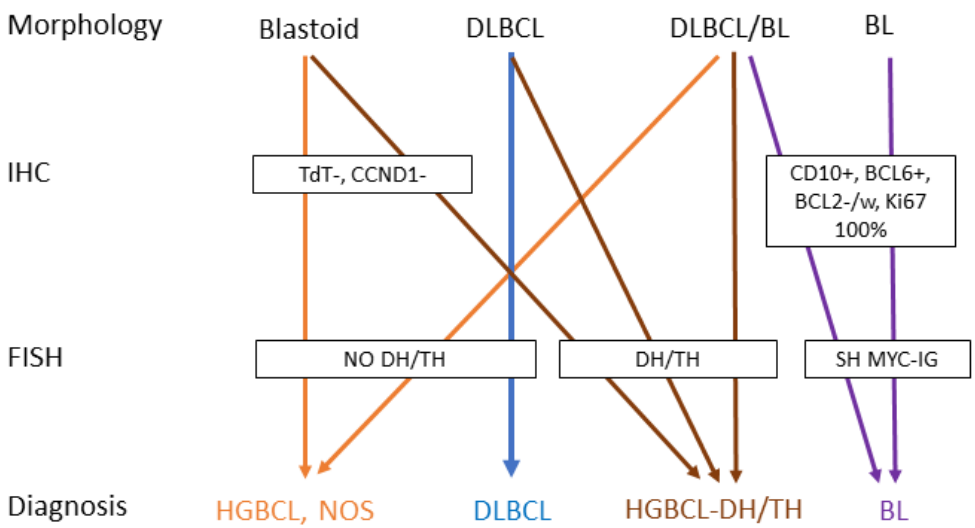

Figure 13. Diagnostic algorithm useful in the differential diagnosis of HGBCL. It includes morphology, immunohistochemistry and FISH analysis. DH/TH: double hit/triple hit; SH: single hit; w: weak. Figure adapted from (Swerdlow *et al.*, 2017).

On the other hand, HGBCL, NOS encompasses a heterogeneous group of mature B-cell lymphomas with a spectrum of morphological appearances from blastoid to cases with intermediate features between BL and DLBCL, characterized by lack of double and triple-hits

events, independently of *MYC* rearrangements (**Figure 13**) (Swerdlow *et al.*, 2017). Studies purely focused on this entity are rare due to the recent recognition of these lymphomas as an independent category from those HGBCL-DH/TH. According to some studies in which few HGBCL, NOS were included, clinical features and immunophenotype were quite similar to HGBCL-DH/TH (Perry *et al.*, 2013; Li *et al.*, 2015).

As with HGBCL-DH/TH, HGBCL, NOS mainly occurs in elderly patients although a few HGBCL, NOS cases may occur in children. Even so the current WHO classification recommends avoiding this terminology and states that these lymphomas should be better classified as BL or DLBCL due to their good prognosis (Swerdlow *et al.*, 2017).

Clinically, both entities have very poor prognosis with a median OS less than two years after standard regimens for DLBCL (Perry *et al.*, 2013; Ok and Medeiros, 2020) since no optimal therapeutic treatment is available for these patients (Snuderl *et al.*, 2010; Perry *et al.*, 2013).

5.2. HGBCL gene expression assays

Two different studies have applied gene expression signatures to identify high-risk patients with DLBCL including HGBCL-DH/TH cases. While *Sha* and colleges used a BL-like signature, (Sha *et al.*, 2019) Ennishi and colleagues used a signature derived from genes differentially expressed between HGBCL-DH and non-DH GCB-DLBCL (Ennishi *et al.*, 2019). Both signatures were able to identify most of the HGBCL-DH, as well as non-DH, which actually accounted half or the majority of the cases positive for the signatures. In other words, none of the signatures were specific of HGBCL-DH/TH or HGBCL, NOS.

5.3. HGBCL genomic landscape and pathogenesis

By definition, HGBCL-DH/TH cases are characterized by the presence of *MYC* rearrangements in combination with *BCL2* and/or *BCL6* rearrangements. The most frequent combination of rearrangements is the concurrent *MYC* and *BCL2* translocation present in 65-70% of HGBCL-DH/TH cases. Concurrent *MYC/BCL6* rearrangements occur in 10-15% while triple-hit events (*MYC*/*BCL2*/*BCL6* concurrent rearrangements) are present in 15-20% of the HGBCL-DH/TH cases (Ok and Medeiros, 2020). On the other hand, HGBCL, NOS cases lack double and triple hit events but, approximately 20-35% of the cases display *MYC* rearrangements (Perry *et al.*, 2013; Swerdlow *et al.*, 2017).

Mutational profile has been poorly studied including both HGBCL-DH/TH and a few HGBCL, NOS. Two different studies observed an intermediate mutational profile between BL (mutations in *MYC, ID3, CCND3*) and GCB-DLBCL (mutations in *BCL2, EZH2, CREBBP, KMT2D, FOXO1* and *SOCS1*), but lack of BL-related *TCF3* mutations (Momose *et al.*, 2015; Evrard *et al.*, 2019).

6. Diffuse large B cell lymphoma

DLBCL is a medium or large B-cell neoplasm with a diffuse growth pattern originated from mature GC B cells. It is a heterogeneous disease that encompasses many different entities with distinct pathological, clinical and biological features **(Table 4)**. Cases that do not belong to any specific subtype, which represents the 80-85% of all the DLBCL, are diagnosed as DLBCL not otherwise specified (hereafter referred as simply DLBCL), although they can still be biologically and genetically heterogeneous.

DLBCL constitutes 25-35% of adult NHL in Western countries and a higher percentage in developing countries (Swerdlow *et al.*, 2017). It is more common in the elderly with a median

age in the seventh decade, but it can also occur in pediatric and young patients accounting only 10-20% of the pediatric NHL (Sandlund and Martin, 2016). It usually arises *de novo* but it can rise from the histologic progression or transformation of more indolent lymphomas such as FL and chronic lymphocytic leukemia (Swerdlow *et al.*, 2017).

Table 4. Large B-cell lymphomas included in the last version of WHO classification.

Diffuse large B-cel lymphomas, NOS
Molecular subtypes
Germinal center B-cell (GCB) subtype
Activated B-cell (ABC) subtype
Other lymphomas of large B cells
T-cell/histiocyte-rich large B-cell lymphoma
Primary diffuse large B-cell lymphoma of the CNS
Primary cutaneous diffuse large B-cell lymphoma, leg type
EBV-positive diffuse large B-cell lymphoma, NOS
Diffuse large B-cell lymphoma associated with chronic inflammation
Lymphoid granulomatosis
Large B-cell lymphoma with IRF4 rearrangement
Primary mediastinal (thymic) large B-cell lymphoma
Intravascular large B-cell lymphoma
ALK-positive large B-cell lymphoma
Plasmablastic lymphoma
HHV8-positive diffuse large B-cell lymphoma
Primary effusion lymphoma
High grade B-cell lymphomas
B-cell lymphoma, unclassified, with features intermediate between DLBCL and classical Hodgkin lymphoma

6.1. Morphological and clinical aspects of DLBCL

Neoplastic cells are large and arranged in a diffuse pattern that totally or partially effaces normal nodal architecture. The morphology of DLBCL findings is diverse, so the disease can be divided into different morphological variants: the centroblastic variant (80% of all DLBCL) predominantly composed of centroblasts, the immunoblastic variant (8-10% DLBCL cases), predominantly composed of immunoblasts and the anaplastic variant (3% DLBCL cases),

characterized by large, pleomorphic and bizarre cells, often resembling Hodgkin/Reed-Sternberg cells (Swerdlow *et al.*, 2017; Li, Young and Medeiros, 2018). Immunophenotypically, DLBCL cells express pan-B cell surface markers CD19, CD20, CD22, CD79a and PAX5, but may lack some of them. The presence of EBV in most of the cells should lead to a diagnosis of EBV-positive DLBCL, not otherwise specified.

Clinically, DLBCL patients present with a rapidly growing tumor mass involving single or multiple lymph nodes with up to 40% of the cases being at least initially confined to extranodal sites. Therefore, almost half of the patients have stage I or II disease. Virtually any extranodal location can be the primary site, being the gastrointestinal tract the most common. Other frequent sites include bone, testis, spleen, Waldeyer ring, salivary gland, thyroid, kidney, and adrenal gland. Besides, BM involvement may occur in 10-20% of the patients.

Prognosis of DLBCL depends on the age of the patient, having much better outcome DLBCL of the pediatric population (Reiter and Klapper, 2008). This might be partially explained by the fact that different therapeutic strategies are followed depending on the age of the patient, with a stablished cut-off arbitrarily settled at the age of 18 years old. Adult patients (>18 years old) are treated with R-CHOP (rituximab with cyclophosphamide, doxorubicin, vincristine, and prednisone) achieving an OS around 60-65%, (Swerdlow *et al.*, 2017; Karube *et al.*, 2018) whereas pediatric patients have better prognosis according to previously mentioned protocols of pediatric NHL study groups (LMB/BFM/Inter-B-NHL protocols; PFS higher than 90%) (Patte *et al.*, 2001; Woessmann *et al.*, 2005; Minard-Colin *et al.*, 2020).

6.2. Cell-of-origin: subtype classification

DLBCL can be classified into two major molecular subgroups defined by gene expression patterns that reflect the cell-of-origin (COO) at different stages of the GC differentiation: the GCB-DLBCL, derived from GC LZ B-cells, and the activated B cell like DLBCL (ABC-DLBCL),

derived from later stage of GC differentiation when B cells are committed to plasmablastic differentiation (Alizadeh *et al.*, 2000; Rosenwald *et al.*, 2002). Nonetheless, a third group of unclassified cases remained. Relative frequencies of GCB and ABC subtypes are typically 60 and 40% of the cases respectively, but it can vary based in the age of the patient population. These two major molecular subgroups predict survival, having GCB-DLBCL a significantly better prognosis than those with ABC-DLBCL after standard protocols with or without rituximab (Rosenwald *et al.*, 2002; Scott *et al.*, 2015). Additionally, these subgroups are not only clinically and phenotypically different but are also associated with different genetic profiles indicating different oncogenic mechanisms (**see next section**).

The original methodology used to define these COO subgroups was based on gene expression microarrays on RNA derived from frozen tissue. Subsequently, different IHC algorithms have been stablished in an attempt to determine COO in standard practice using commonly available FFPE slides such as the Hans algorithm (**Figure 14**) (Hans *et al.*, 2004; Meyer *et al.*, 2011).

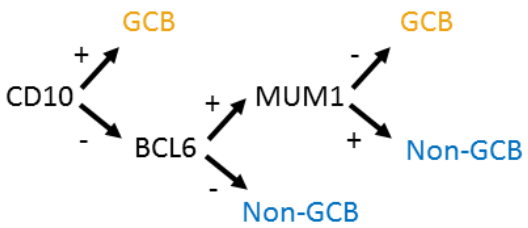

Figure 14. Hans algorithm based on three IHC markers: CD10, BCL6 and MUM1.

In 2014, the Lymphoma/Leukemia Molecular Profiling Project demonstrated the feasibility of the quantitative gene expression Lymph2Cx assay for the COO classification applicable to FFPE samples, a digital gene expression NanoString-based test that interrogates only 20 genes (**Figure 15**) (Scott *et al.*, 2014).

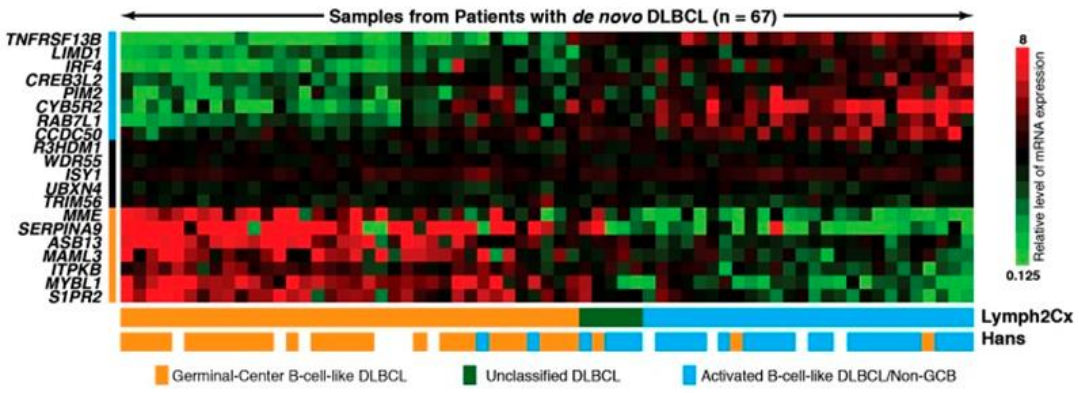

Figure 15. Lymph2Cx gene expression assay. The 20 genes that contribute to the model are shown at the left, with the top 8 genes being overexpressed in ABC, the middle 5 genes being housekeeping genes, and the lower 7 genes being overexpressed in GCB. COO assignments are shown for the assay, and the IHC-based Hans algorithm. Figure modified from (Scott *et al.*, 2014).

6.3. Frequent rearrangements in DLBCL

DLBCL is characterized by recurrent rearrangements involving *BCL6*, *BCL2* and *MYC* genes (**Figure 16**).

Rearrangements in the 3q27 locus involving *BCL6* gene are found in 30% of the DLBCL cases, more frequently in the ABC subtype. These events mostly juxtaposed *BCL6* gene to 14q32 loci involving IGH genes (Offit *et al.*, 1994). Even that, *BCL6* is a promiscuous gene and it is found to be rearranged with many other potential partner loci, which leads to the *BCL6* deregulation by the promoter substitution mechanism (Ye *et al.*, 1995). These rearrangements will prevent physiological *BCL6* downregulation, required for B cells terminal differentiation.

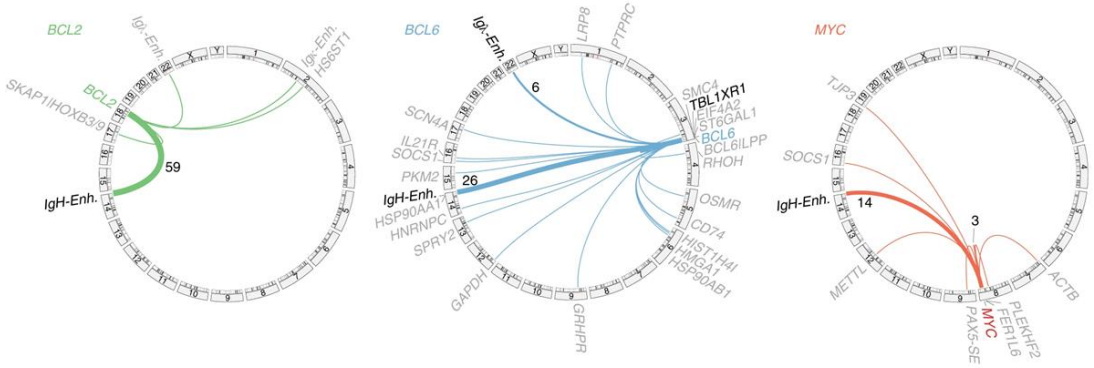

Figure 16. Circos plots of recurrent structural variants involving *BCL2*, *BCL6* and *MYC* genes in DLBCL. Thickness of partner linking lines indicates frequency (numbers indicate frequency > 1). Modified Figure from (Chapuy *et al.*, 2018).

The *BCL2* rearrangements, t(14;18)(q21;q32)/IGH-*BCL2*, are observed in 20–30% of DLBCL cases, more commonly in the GCB subtype, where accounts 40% of the GCB-DLBCL cases. These BCL2 rearrangements lead to BCL2 protein expression. Nevertheless, BCL2 expression does not necessary correlate with *BCL2* translocation since other mechanisms such as *BCL2* amplification may occur in DLBCL (Kramer *et al.*, 1998).

Translocations involving *MYC* at 8q24 also occur in 8-14% of DLBCL cases, evenly distributed between ABC- and GCB-DLBCL subtypes (Barrans *et al.*, 2010). These *MYC* rearrangements are often associated with high-grade morphological features and a complex karyotype. *MYC* locus can be juxtaposed with IGH, IGK, IGL or non-IG loci such as *PAX5*, *BCL6*, *BCL11A*, *IKZF1* and *BTG1* genes. Cases with *MYC* rearrangements that also show a *BCL2* and/or *BCL6* translocation belong to the previous mentioned category of HGBCL-DH/TH.

Other less common translocations in DLBCL include *PDCD1LG1/2* (5%), *TBLXR1* (4%), *TP63* (3%), *CIITA* (3%), and *ETV6* (2%) locus (Scott *et al.*, 2012; Twa *et al.*, 2015; Chapuy *et al.*, 2018).

6.4. DLBCL molecular landscape and pathogenesis

Consistent with its clinical and phenotypical heterogeneity, DLBCL displays a complex genomic profile that includes a wide spectrum of alterations including CN alterations, mutations and structural variants, in addition to primary rearrangements. Since DLBCL is more frequent in adult population and most of the molecular studies did not consider the age of the patients, the biological features that will be explained in this section are representative of the adult variants.

CN studies described a genomic profile characterized by high levels of genomic complexity with 15-21 CN alterations per case (Scholtysik *et al.*, 2015; Sebastián *et al.*, 2016; Karube *et al.*, 2018). The CN landscape includes recurrent gains in 1q, 2p16.1, 6p, 12q15, 18q21.3 and deletions in 1p36.32, 6q, 8p23.3, 15q21-q22, 17p13.1 (**Figure 17**).

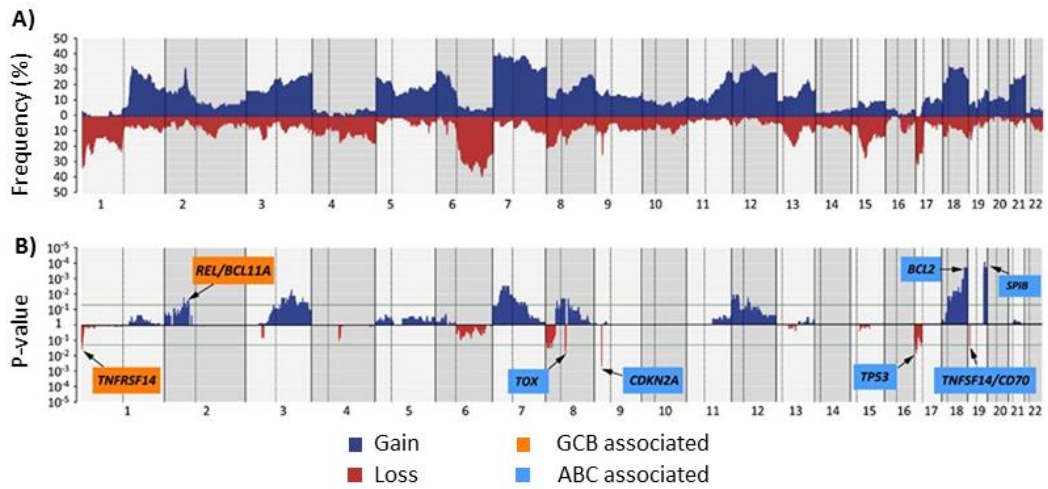

Figure 17. CN landscape of 119 DLBCL. A) Frequency of CNA analyzed by Cytoscan assay. Each probe is aligned from chromosome 1 to 22 and p to q. The vertical axis indicates frequency of the genomic aberration among the analyzed cases. B) Significant patterns of CNAs between DLBCL subtypes are depicted: ABC (light blue boxes) and GCB (orange boxes). The X-axis shows P-value among these two groups and significant threshold is marked with a green line. Figure from (Karube *et al.*, 2018)**.**

DLBCL is also characterized by a high tumor mutational burden accounting 50-100 coding mutations per case (Pasqualucci and Dalla-Favera, 2015; Chalmers *et al.*, 2017). Around 150 driver genes have been found to be mutated in DLBCL, with a median of 17 drivers per case (Reddy *et al.*, 2017; Chapuy *et al.*, 2018). These somatic mutations are caused by multiple mutational processes, each of which generates a specific mutational signature characterized with a unique pattern of mutation types combinations (Alexandrov *et al.*, 2020). This way, mutational signature analysis revealed that somatic mutations in DLBCL may be explained by different mutational processes that include spontaneous deamination of cytosines and consequent switch to thymine (C>T) that is associated to with aging, action of APOBEC enzymes and defects on mismatch or homologous recombination DNA repair (Arthur *et al.*, 2018; Alexandrov *et al.*, 2020; Hübschmann *et al.*, 2021). Additionally, two other mutational signatures related with AID have been identified: one signature, called canonical AID (cAID), characterized by C>T/G mutations at AID hotspots associated with the SHM patterns. The other, called AID2, characterized by A>T/C/G mutations associated with error-prone DNA polymerase eta subsequent to the cytosine deamination produced by the AID machinery (Alexandrov *et al.*, 2013; Chapuy *et al.*, 2018). Interestingly, these mutational processes contribute differently depending on the particular gene (Chapuy *et al.*, 2018; Hübschmann *et al.*, 2021).

All these alterations affect different biological programs including those specific to B-cell lymphomas (e.g. B-cell differentiation and BCR-signaling), as well as those commonly affected in most of cancers (e.g. cell proliferation and apoptosis). Some of these alterations are shared by both COO subtypes reflecting general mechanisms of DLBCL pathogenesis, whereas others are specific of a COO subtype (**see next sections**) (Bea *et al.*, 2005; Basso and Dalla-Favera, 2015; Pasqualucci and Dalla-Favera, 2018).

6.4.1 General oncogenic programs in DLBCL

Nearly 85% of all DLBCL display alterations affecting epigenetic remodeling biological program which include genes encoding for histone or chromatin modifiers (Lohr *et al.*, 2012; Reddy *et al.*, 2017). The most frequently mutated genes are the methyltransferase *KMT2D* (Morin *et al.*, 2011), the acetyltransferases *CREBBP* and *EP300* (Pasqualucci, Dominguez-Sola, *et al.*, 2011), and linker histones *ARID1A* and *TET2*. Although these alterations are shared by both COO subtypes, GCB-DLBCL have preference in acetyltransferases alterations and have specific mutations affecting *EZH2* gene, a polycomb-group methyltransferase oncogene (Morin *et al.*, 2010).

BCL6, the master regulator of the GC reaction, is also a commonly exploited oncogenic in DLBCL (**Figure 18**). In addition to chromosomal rearrangements, up to 75% of DLBCL display multiple somatic mutations affecting the 5' regulatory sequences of the *BCL6* gene, as a physiological SHM mechanisms. Nevertheless, some of these mutations have been specifically recognized in lymphomas, mainly GCB-DLBCL, targeting *BCL6* or *IRF4* DNA binding motifs which will prevent *BCL6* repression by negative auto-regulatory loop or by *IRF4*-mediated repression (Pasqualucci *et al.*, 2003; Saito *et al.*, 2007). Other indirect genetic alterations that contribute to prevent physiological *BCL6* downregulation are the previously mentioned *CREBBP* and *EP300* inactivating mutations (Ying *et al.*, 2013), gain-of-function mutations of the positive *BCL6*-regulator *MEF2B,* and inactivating mutations of *FBXO11* which targets *BCL6* for proteasomal degradation (Duan *et al.*, 2012). Altogether, these *BCL6* alterations lead to an aberrant *BCL6* expression that promotes GC formation and disrupt plasma cell differentiation (Cattoretti *et al.*, 2005).

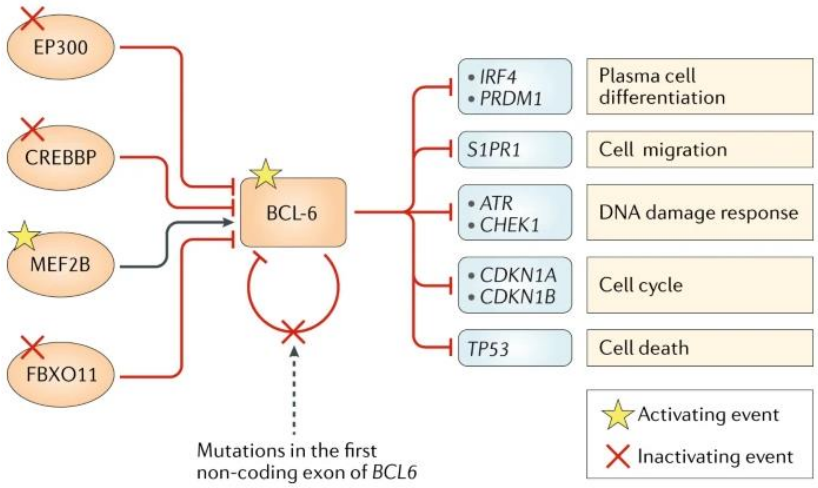

Figure 18. Different mechanisms of BCL6 disruption in DLBCL. Figure from (Miao *et al.*, 2019).

Another oncogenic mechanism commonly exploited by DLBCL is the evasion from immune surveillance. This is achieved by multiple mechanisms that reduce expression of the Major Histocompatibility Complex (MHC) class-I and class-II, which are necessary for cytotoxic T-cell recognition. Genetic mechanisms include the inactivation of MHC-I/II components or regulator genes including *B2M*, *HLA*, *CD58* and *CIITA* by different alterations (Challa-Malladi *et al.*, 2011; Chapuy *et al.*, 2018). Finally, *TP53* pathway is also altered in both ABC and GCB subtypes of DLBCL by recurrent 17p/*TP53* deletions and/or *TP53* inactivating mutations (Karube *et al.*, 2018).

6.4.2 GCB-DLBCL specific oncogenic alterations

In addition to t(14;18)/*BCL2* and t(8;14)/*MYC* translocations, present in 40% and 10% of the cases, GCB-DLBCL subtype is characterized by *EZH2* gain-of-function mutations in 20% of the cases (**Figure 19**). These *EZH2* mutations are located within the catalytic SET domain leading to an increasing methyltransferase activity, which has been involved in transcriptional repression of anti-proliferation CDKN family genes and terminal differentiation-related genes such as *PRDM1* and *IRF4* (Morin *et al.*, 2010; Béguelin *et al.*, 2013).

As in BL, the Gα13 signaling pathway involved in modulating GC B-cell migration, is also frequently disrupted (30% GCB-DLBCL) by mutations affecting *S1PR2, GNA13, ARHGEF1* and *P2RY8* genes (**Figure 19)** (Muppidi *et al.*, 2014). Another characteristic pathway deregulated in GCB-DLBCL, similar to BL, is the PI3K signaling pathway, which is altered by 10q23.3 deletions including *PTEN* gene as well as amplifications of 13q targeting mir-17-19 cluster (Lenz, Wright, *et al.*, 2008).

Finally, 1p36.32 deletions and inactivating mutations of *TNFRSF14*, an immunomodulator receptor, are observed in 40% of the cases. Loss of *TNFRSF14* is thought to induce a tumor-supportive microenvironment characterized by exacerbated lymphoid stroma and increased T follicular helper cells recruitment (Steinberg, Cheung and Ware, 2011).

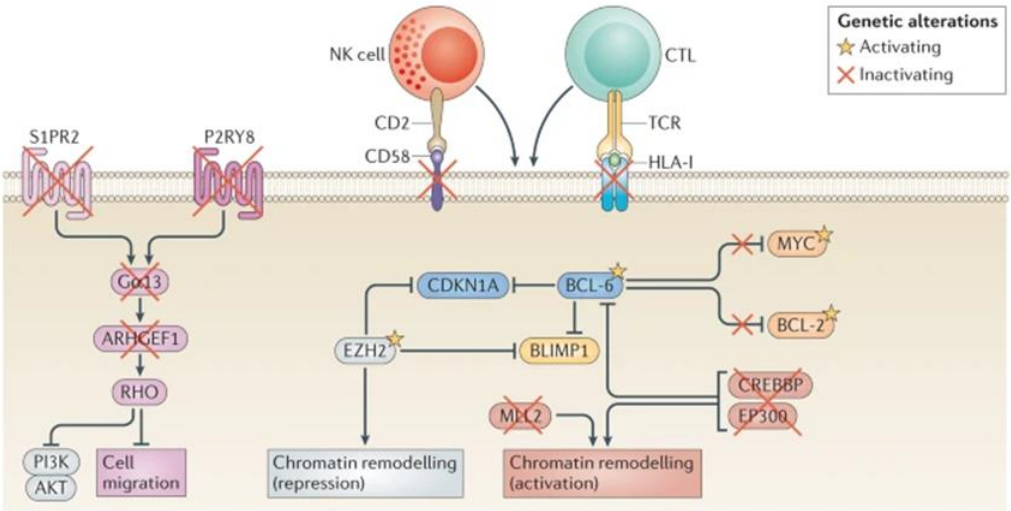

Figure 19. Schematic representation of the pathways affected during lymphomagenesis in GCB-DLBCL. The different colors that are used in the figure indicate molecules that belong to a specific pathway and/or lead to a specific outcome. Figure from (Basso and Dalla-Favera, 2015).

6.4.3. ABC-DLBCL specific oncogenic alterations

On the other hand, the ABC-DLBCL subtype is characterized by a subset of genetic alterations converging in the NF-kB pathway activation, which is crucial for its survival (Davis *et al.*, 2001; Compagno *et al.*, 2009) (**Figure 20**). Among these alterations, gain-of-function mutations targeting *CD79A/B (*20% of the cases), which are components of the BCR complex, contribute to the constitutive BCR signaling (Davis *et al.*, 2010). *MYD88* gene, encoding an adaptor molecule critical for the toll-like receptor and IL1R-mediated NF-kB signaling, is also frequently mutated (around 30% of the cases) by an activating hot spot L265P substitution resulting in downstream activation of NF-kB and JAK-STAT pathways (Karube *et al.*, 2018). Activating mutations of *CARD11,* present in a 10% of the cases, have been described to activate NF-kB signaling independently of upstream signals (Lenz, Davis, *et al.*, 2008). Finally, the *TNFAIP3* gene, encoding the NF-kB inhibitor A20, is inactivated by 6q deletions and/or mutations in 30% of the cases, thus preventing termination of NF-kB responses (Compagno *et al.*, 2009).

In addition to the constitutive activation of NF-kB, ABC-DLBCL are also characterized by the blockage of the B-cell differentiation to plasma cell. This occur due to the biallelic inactivation of *PRDM1* gene, which encodes BLIMP1, by 6q deletions and mutations in 25% of the cases (Pasqualucci *et al.*, 2006). Other indirect mechanisms of *PRDM1* inactivation includes previously mentioned *BCL6* rearrangements, present in 25% of the cases, and 19q gains/amplifications targeting *SPIB*, a transcription factor that also repressed PRDM1, observed in 27% of the cases (Pasqualucci, 2019).

Additional frequent alterations restricted to ABC-DLBCL are 18q21 amplifications targeting *BCL2* and homozygous deletions of 9p21 including *CDKN2A/B* loci.

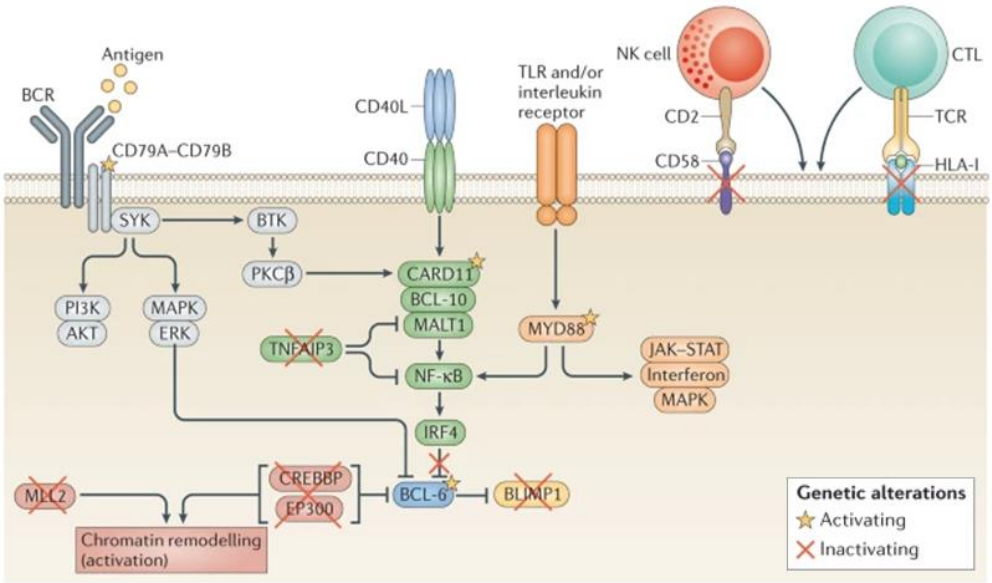

Figure 20. Schematic representation of the pathways affected during lymphomagenesis in ABC-DLBCL. The different colors that are used in the figure indicate molecules that belong to a specific pathway and/or lead to a specific outcome. Figure from (Basso and Dalla-Favera, 2015).

6.4.4 Genetic DLBCL subclassification

Genetic classification of DLBCL represent a major step in understanding this heterogeneous disease. Recently, different multiplatform studies proposed a new framework for DLBCL subclassification based on their genetic alterations integrating mutations, copy number and structural variants (Chapuy *et al.*, 2018; Schmitz *et al.*, 2018; Wright *et al.*, 2020). By implementing different algorithms, these studies have led independently to the identification of at least five genetic subtypes characterized by specific concurrent genetic alterations (**Figure 21**). Interestingly, each subtype has unique clinical outcome. In the ABC subgroup, patients with the MCD/C5 subtype have a poorer prognosis, whereas in GCB subgroup, patients with the EZB/C3 subtype have poorer outcomes. Additional studies would be necessary to confirm these results and to possibly integrate them in a common classification picture. Once more, as it was previously mentioned, since these studies did not consider the age of the patients, results might not be representative of the pediatric population.

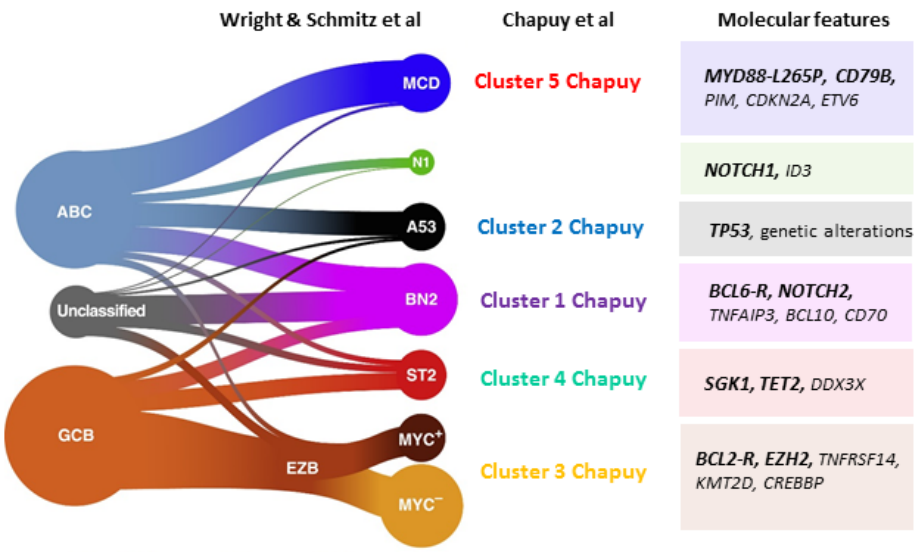

Figure 21. Summary of the relationship between DLBCL COO subgroups and the genetic subtypes from Chapuy et al., 2018; Schmitz et al., 2018 and Wright et al., 2020 studies. Most significant genetic alterations defining the genetic subgroups are indicated at the right boxes. Figure modified from (Wright *et al.*, 2020)

6.5. DLBCL in pediatric patients

DLBCL in the pediatric population have better outcome in comparison with adults, as it was previously mentioned. Although these differences might be in part the result of treatment protocol differences or unknown host factors, evidence suggest also biological differences from their adult counterparts. For instance, pediatric DLBCL are more from the GCB subtype (80%), which have been described to have better prognosis (Oschlies *et al.*, 2006; Miles *et al.*, 2008; Klapper *et al.*, 2012; Szczepanowski *et al.*, 2017). Only a few genetic studies of pediatric DLBCL have been performed identifying low levels of genetic complexity characterized by low number of CN alterations and lack of primary aberrations including *BCL2* and *BCL6* rearrangements in comparison to adults (Oschlies *et al.*, 2006; Klapper *et al.*, 2012). Interestingly, these analysis in pediatric populations identified a subset of cases with *IRF4* rearrangement recently recognized as a different entity termed LBCL-*IRF4* (**see section 8**) (Salaverria *et al.*, 2011; Klapper *et al.*, 2012).

In terms of mutational status, some NGS studies include isolated pediatric and young adult cases but again, it is difficult to dissect the mutational landscape of the pediatric cases and no studies focused specifically in the pediatric disease had been performed at the moment when the present series was initiated.

Overall, it seems that DLBCL in children are more homogeneous and biologically different from adults. Even that, more analysis specific of that range of age need to be done to clarify whether they might be a separate entity different from adult DLBCL.

6.6. Predictive prognostic variables

The International Prognostic Index (IPI), is the main clinical tool used for outcome prediction in patients with DLBCL (International Non-Hodgkin's Lymphoma Prognostic Factors Project, 1993). It assigns 1 point to each of the five negative clinical variables with prognostic factor (**Table 5**) and categorizes patients into 4 risk groups based on the total score: low risk (0-1), low-intermediate risk (2), high-intermediate risk (3) , and high risk (4-5). Since this score was developed in the pre-rituximab era, it has lost some of its stratification power. Therefore, new scores have been developed such as the revised IPI (R-IPI) or the National Comprehensive Cancer Network IPI (NCCN-IPI) (Ruppert *et al.*, 2020).

Table 5. The International Prognostic Index

Risk Factor	0 Point	1 Point
Age	≤ 60 years	> 60 years
Ann Arbor stage	I or II	III or IV
Serum LDH level	Normal	Above normal
Number of extranodal sites	≤ 1	> 1
ECOG performance status	0-1	≥ 2

LDH: serum lactate dehydrogenase; ECOG: Eastern Cooperative Oncology Group.

The IPI score is not used in childhood NHL since different staging method is applied for pediatric patients and because the performance status index does not reflect quality-of-life deterioration. Staging methods currently applied for pediatric patients include the St Jude childhood and adolescent NHL staging system (Murphy, 1980) or the revised international pediatric NHL staging system (IPNHLSS) (Rosolen *et al.*, 2015) which incorporated new histologic entities, extranodal dissemination, improved diagnostic methods, and advanced imaging technology.

As it was previously explained, another important predictive factor is the COO subtype, having the ABC subtype worse prognosis than the GCB subtype (Rosenwald *et al.*, 2002; Scott *et al.*, 2014).

In addition to these clinical prognostic factors included in the clinical IPI and the COO, several studies have identified additional molecular biomarkers for prognosis including dual expression of MYC and BCL2 (Green *et al.*, 2012; Johnson *et al.*, 2012; Valera *et al.*, 2013), *MYC* rearrangements (Savage *et al.*, 2009; Copie-Bergman *et al.*, 2015), *TP53* deletions and/or mutations (Young *et al.*, 2008; Xu-Monette *et al.*, 2012), deletions of *CDKN2A* locus on chromosome 9p21 (Jardin *et al.*, 2010), and *FOXO1* mutations (Trinh *et al.*, 2013). However, all these biomarkers have been established almost exclusively for lymphomas in adults, so the significance in pediatric cases has not been yet verified.

7. Primary mediastinal B-cell lymphoma

PMBCL is a mature aggressive lymphoma derived from thymic B cells that arises in the mediastinum. It is a rare disease that accounts for about 2-3% of NHL that predominantly occurs in adolescents and young female adults (median age around 35 years). Although it was previously considered a subtype od DLBCL, it is now recognized as a distinct entity based on its morphological, clinical and biological differences from DLBCL, closely related to nodular sclerosing Hodgkin lymphoma (Swerdlow *et al.*, 2017).

7.1. Morphological and clinical aspects of PMBCL

PMBCL displays a diffuse growth pattern of medium size to large cells with abundant pale cytoplasm and relatively round or ovoid nuclei. In some cases, cells may have pleomorphic and/or multilobate nuclei resembling Reed-Sternberg cells, which are suspicious of Hodgkin lymphoma (Traverse-Glehen *et al.*, 2005). Immunophenotypically, PMBCL expresses B-cell-related antigens such as CD19, CD20, CD22 and CD79a. They are also characterized by CD30 and IRF4 expression whereas they are mainly EBV negative (Barth *et al.*, 2002).

Clinically, almost all PMBCL present with a localized anterior superior mediastinal mass in the thymic area that might reach adjacent structures such as the lungs, pleura and pericardium (Barth *et al.*, 2002). Dissemination to distant extranodal sites is not common and BM involvement is usually absent (Cazals-Hatem *et al.*, 1996). PMBCL have better survival rate than DLBCL subtypes when treated both pediatric and adults patients with intensive chemotherapy including rituximab (DA-EPOCH-R) with or without radiotherapy (>90% 3-year OS) (Dunleavy, Pittaluga, Maeda, *et al.*, 2013). On the other hand, previously mentioned pediatric protocols (LMB/BFM protocols without Rituximab) have a limited efficacy in the treatment of children with PMBCL (Seidemann *et al.*, 2003; Gerrard *et al.*, 2013).

7.2. PMBCL genomic landscape and pathogenesis

PMBCL virtually lacks *MYC*, *BCL2* or *BCL6* rearrangements (Tsang *et al.*, 1996; Scarpa *et al.*, 1999). On the other hand, PMBCL is characterized by recurrent 16p13.13/*CIITA* rearrangements and mutations (53% of the cases), resulting in reduced MHC class II expression (Mottok *et al.*, 2015). These *CIITA* rearrangements have been described to occur with 9p24.1 locus targeting *PDL1/2* (also called *PDCD1LG1/2*) genes (Twa *et al.*, 2014). In addition to these 9p24.1 rearrangements, gains and amplifications of the same locus

including *JAK2*, *PDL1* and *PDL2* genes have been identified in up to 75% of the cases leading to a PDL1/PDL2 overexpression (Bentz *et al.*, 2001; Wessendorf *et al.*, 2007).

PMBCL is also characterized by recurrent alterations leading to a JAK-STAT and NF-kB pathway activation (**Figure 22**) (Steidl and Gascoyne, 2011). In addition to 9p24.1/*JAK2* amplifications, losses or inactivating mutations of negative regulators *SOCS1* (Melzner *et al.*, 2005) and *PTPN1* (Gunawardana *et al.*, 2014) and activating mutations of *STAT6* (Ritz *et al.*, 2009) and *IL4R* (Vigano *et al.*, 2018) have been reported to result in JAK-STAT constitutive pathway activation. Gains/amplifications of 2p16.1 including REL gene have been described to lead to nuclear accumulation (Joos *et al.*, 1996; Weniger *et al.*, 2007). Besides, deleterious mutations of negative regulator *TNFAIP3* have been described to activate NF-kB pathway (Schmitz *et al.*, 2009).

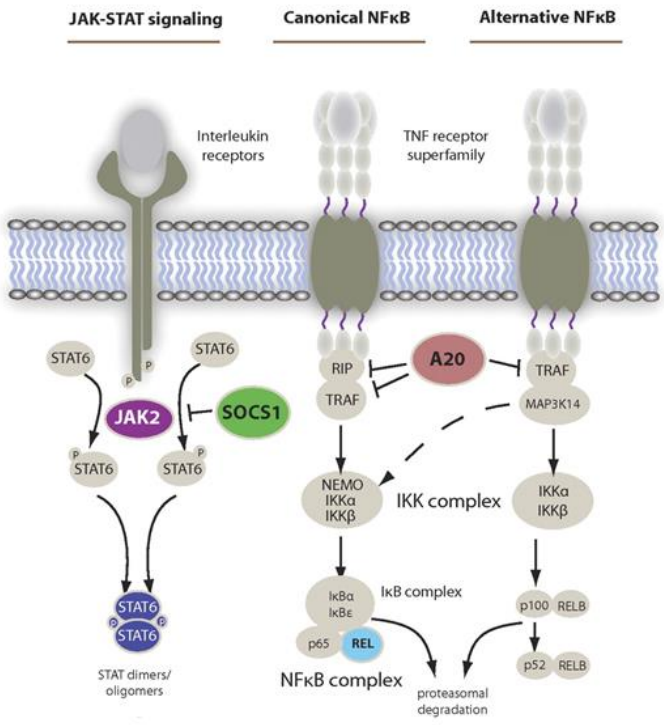

Figure 22. Schematic representation of the pathways affected during lymphomagenesis in PMBCL. The main activation cascades of JAK-STAT and NF-κB signaling are shown leading to altered transcriptional regulation. Known gene alterations in the pathway are highlighted in color. Figure from (Dunleavy, 2017).

7.3. Gene expression profile analysis

PMBCL has a gene expression profile different from other DLBCL subtypes. Contrary, PMBCL profile have similarities with Hodgkin lymphoma, with whom shares the expression of genes that are inducible by interferon/JAK-STAT pathway and targets of the NF-kB pathway (Rosenwald *et al.*, 2003; Savage *et al.*, 2003).

Thanks to these gene expression profile analyses uncommon PMBCL cases at non-mediastinal sites, and without evidence of mediastinal disease, have been identified (Yuan *et al.*, 2015; Chen *et al.*, 2019). The problem with these cases is that they are mainly miss in routine practice. Fortunately, in 2018, it was published a robust and accurate 58-gene expression assay called Lymph3Cx (NanoString, Inc) able to distinguish between PMBCL and the two DLBCL subtypes using FFPE samples, with potential to be used as a routine clinical test (Mottok *et al.*, 2018).

8. Large B-cell lymphoma with *IRF4* translocation

LBCL-*IRF4* is another provisional entity in the 2017 revised version of the WHO classification of lymphoid neoplasms (Swerdlow *et al.*, 2017). It englobes a subset of large B-cell lymphomas from the GC characterized by strong MUM1/*IRF4* expression mostly along with *IRF4* translocations (Salaverria *et al.*, 2011; Chisholm *et al.*, 2019).

This entity was initially identified by the screening of novel IGH translocation partners in pediatric and adult mature B-cell lymphoma in which they identified a novel recurrent chromosomal translocation involving the *IRF4* oncogene associated with young age and a favorable outcome (Salaverria *et al.*, 2011; Klapper *et al.*, 2012). Although, they have been mainly described in pediatric and young adult patients, occasional cases in old patients have also been reported (Salaverria *et al.*, 2011; Chonabayashi *et al.*, 2014; Büyüktaş *et al.*, 2020).

8.1. Morphological and clinical aspects of LBCL-*IRF4*

Morphologically, LBCL-*IRF4* cases may have a follicular, follicular and diffuse, or pure diffuse growth pattern resembling FL grade 3B or DLBCL (Salaverria *et al.*, 2011; Liu *et al.*, 2013). Immunophenotypically, they display strong *IRF4*/MUM1 expression usually along with *BCL6*, negative *PRDM1*/BLIMP1 expression and a high proliferative index (Ki67; >80% of the cells). BCL2 and CD10 are also expressed in more than half of the cases. Despite showing a strong *IRF4*/MUM1 expression, which is a marker of the ABC-DLBCL (Alizadeh *et al.*, 2000), they are mostly GCB-DLBCL (Salaverria *et al.*, 2011).

Clinically, these lymphomas occur as localized disease or low stage, typically in Waldeyer's ring and/or cervical lymph nodes. In terms of survival, an excellent outcome after treated with pediatric NHL intensive chemotherapy protocols (100% 2-y EFS) have been observed (Salaverria *et al.*, 2011; Chisholm *et al.*, 2019).

8.2. LBCL-*IRF4* genomic landscape and pathogenesis

LBCL-*IRF4* is characterized by t(6;14) rearrangements, which juxtapose the *IRF4* gene to the IGH locus in the der(14)t(6;14) in the same transcriptional direction which leads to an overexpression of the *IRF4* translocated allele. Even that, *IRF4* rearrangements can also involve light-chain IG genes (IGK and IGL) (Salaverria *et al.*, 2011). Some cases have been described to present concomitant *BCL6* rearrangements, but they uniformly lack *BCL2* translocations. Cases without a demonstrable *IRF4* rearrangement but with strong *IRF4*/MUM1 expression are also included in the LBCL-*IRF4* category (Swerdlow *et al.*, 2017). Similar *IRF4* rearrangements were previously identified in a small fraction of plasma cell myeloma cases (Yoshida *et al.*, 1999) but rarely in adult DLBCL (Hunt, Hall and Reichard, 2010; Klapper *et al.*, 2012).

The *IRF4* gene is transcriptional factor that shows a biphasic expression pattern in B cells, since it is expressed in immature B cells in BM, and again in a subset of centrocytes of the GC-LZ. In the GC, *IRF4* has important roles in mediating the B-cell plasma cell differentiation by inhibiting *BCL6*, the master regulator of the GC reaction (Shukla and Lu, 2014; De Silva and Klein, 2015). Co-expression of both *IRF4* and *BCL6* genes in these cases suggests as disruption of this regulatory loop by *BCL6* rearrangements and/or mutations in *BCL6* autoregulatory regions (Salaverria *et al.*, 2011).

One study analyzed the genetic landscape of 23 cases by CN arrays. All except one case carried chromosomal imbalances (mean of 6 CN/case), most frequently gains of Xq28, 11q22.3-qter, and 7q32.1-qter and losses of 6q13-q16.1, 15q14-q22., and 17p (**Figure 23**). Interestingly, *TP53* mutations were also detected in three out of six cases with concomitant 17p losses (Salaverria *et al.*, 2013).

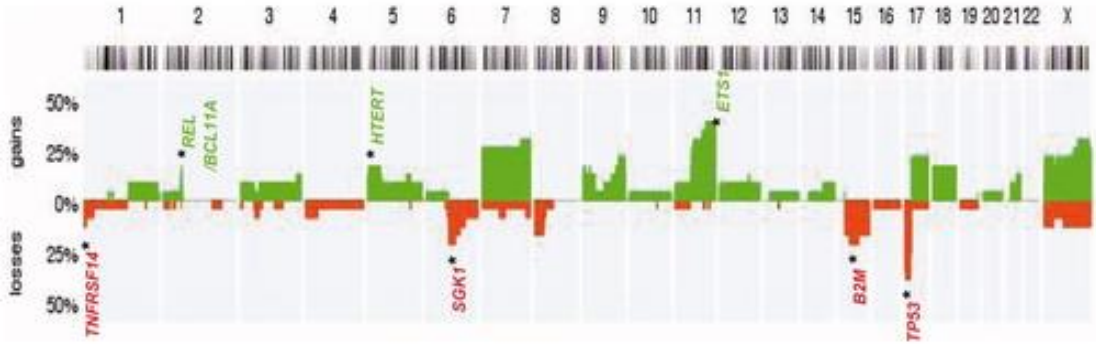

Figure 23. Copy number profiles of 23 LBCL-IRF4. On the x-axis, the chromosomes are represented horizontally from 1 to x. On the y-axis, the percentage of cases showing copy number alterations. Gains are represented in green, whereas losses are represented in red. Candidate genes in regions of gain are displayed in green and in regions of loss in red. Figure from (Salaverria *et al.*, 2013).

8.3. LBCL-*IRF4* differential diagnosis

As it has been mentioned, LBCL-IRF4 presents a wide range of morphology between diffuse and follicular which makes its differential diagnosis with DLBCL and PTFL challenging. The

clarification of the biological nature of this uncommon subtype of lymphoma is clinically relevant since different therapeutic strategies are being applied between DLBCL and PTFL (**see section 3.2**). Therefore, more molecular studies should be performed on larger series of LBCL-*IRF4*.

9. Pediatric type follicular lymphoma

PTFL is an indolent lymphoma occurring predominantly in males of the pediatric and young adult population, which has been recognized by the WHO as a separate entity from its adult counterpart due to its clinical, morphological, immunophenotypic and genetical differences with adult conventional FL (Oschlies *et al.*, 2010; Swerdlow *et al.*, 2017). This new FL variant, in contrast to conventional FL, is characterized by lack of the t(14;18) rearrangement and weak or negative BCL2 expression.

It is a rare disease that mainly affects male children (median age of 14 years old), accounting less than 2% of all NHL of the pediatric population (Woessmann and Quintanilla-Martinez, 2019). Even that, some cases have been observed in young adults and adults patients; therefore, the name "pediatric type" (Louissaint *et al.*, 2012).

9.1. Morphological and clinical aspects of PTFL

Morphologically, neoplastic cells displayed a follicular growth pattern that efface partially or totally the lymph node architecture. These atypical follicles are characterized by a high-grade cytology with medium sized to large blastoid cells (Liu *et al.*, 2013). Immunophenotypically, neoplastic cells express pan-B-cell markers as CD20, CD79a and PAX5 in addition to CD10 and BCL6, that are also strongly expressed. BCL2 is usually absent but it can be weakly expressed in 20% of the cases (Lorsbach *et al.*, 2002; Quintanilla-Martinez *et al.*, 2016).

Moreover, they also present a moderate to high proliferation rate (ki67; >30% of cells) (Louissaint *et al.*, 2012).

Clinically, these lymphomas present typically as isolated adenopathy or low stage disease in the head and neck region with an excellent outcome (>95% survival rates) after complete resection and/or limited chemotherapy (Louissaint *et al.*, 2012; Attarbaschi *et al.*, 2013).

9.2. PTFL molecular landscape and pathogenesis

The main feature that differentiate the pediatric type from conventional FL is the lack of t(14;18) rearrangements involving *BCL2* oncogene, which is present in 80% of the conventional FL (Swerdlow *et al.*, 2017). Additionally, these lymphomas also lack other rearrangements involving *BCL6* and *IRF4* genes.
In 2016 three different molecular studies elucidated the molecular landscape of the PTFL (Louissaint *et al.*, 2016; Ozawa *et al.*, 2016; Schmidt *et al.*, 2016). Overall, PTFL is characterized by a low genomic complex profile (mean, 0.23-0.77 CN/case) and a mutational profile that differs from the conventional FL.

PTFL mutational landscape is characterized by *TNFRSF14* mutations (incidence from 29 to 51%) (Louissaint *et al.*, 2016; Schmidt *et al.*, 2016), which is also frequently mutated in conventional *BCL2* rearranged FL (Okosun *et al.*, 2014; Green *et al.*, 2015). Mutations of that gene have been described to abrogate the interaction between *TNFRSF14* and BTLA receptors (B and T lymphocyte attenuator) disrupting an important tumor suppressor axis that leads to B-cell receptor activation (Boice *et al.*, 2016). Biallelic inactivation of *TNFRS14* by recurrent mutations associated to CNN-LOH or losses of the 1p36 region (12-54% of the cases) indicates a powerful selection against the *TNFRSF14* gene during PTFL development (Schmidt *et al.*, 2016). Activating mutations in the negative regulatory region (exon 2) and the catalytic core domain (exon 3) of *MAP2K1* are also present in 43% of cases (Louissaint *et*

al., 2016). Additionally, *IRF8* mutations at the hotspot p.K66R have been identified in 50 % of the cases (Ozawa *et al.*, 2016).

9.3. Differences between adult FL

As it has been previously mentioned, PTFL is considered a separately entity to its clear differences with conventional FL from the adults (Araf and Fitzgibbon, 2016; Swerdlow *et al.*, 2017) **(Figure 24**).

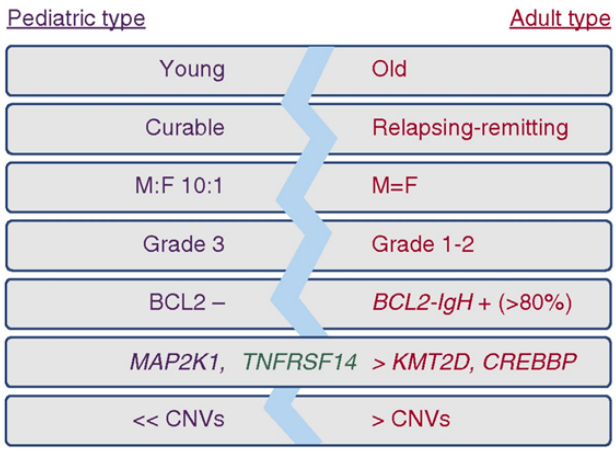

Figure 24. Features of PTFL and typical adult-type FL. CNA, copy number alterations; F, female; M, male. Figure from (Araf and Fitzgibbon, 2016).

In comparison with adult conventional FL, PTFL have less genetic alterations and virtually lack mutations of histone and chromatin-modifying genes (*CREBBP*, *KMT2D*, *EZH2*, *MEF2B* and *EP300*) typical of FL (Louissaint *et al.*, 2016; Schmidt *et al.*, 2016). The same occur when compared with adult FL without *BCL2* rearrangements, which display similar alterations with typical FL with *BCL2* rearrangements (Schmidt *et al.*, 2016; Nann *et al.*, 2020). Besides, *MAP2K1* mutations seem to be specific of PTFL since were not present in adult FL with or without *BCL2* rearrangements (Nann *et al.*, 2020).

Conventional FL is also considered an indolent disease, but contrary to PTFL, is incurable, characterized by recurrent relapses over time (Swerdlow *et al.*, 2017). Survival rates in adult FL are similar to PTFL (>90% 5-yeat OS) with a median survival of more than 12 years after treated with conventional immunochemotherapy (Batlevi *et al.*, 2020).

Since some PTFL occur in young adult and adult patients, it is important to distinguish PTFL from adult typical FL, irrespective of age, in order to appropriately stratify patients to avoid potentially unnecessary treatment.

AIMS AND OBJECTIVES

B-cell non-Hodgkin lymphoma (B-NHL) of pediatric and young adult population is a diverse group of neoplasms predominantly composed of aggressive B-cell lymphomas from the germinal center (GC). Molecular characterization of pediatric series has allowed the identification of several subtypes that predominantly occur in this subgroup of age. Despite of that, genomic features of these pediatric entities and their relationship to other B-NHL in this group of patients are not known. It is still widely unclear whether biological differences exist between pediatric and adult counterparts since most of biological studies have been performed in adult lymphomas.

With the hypothesis that pediatric B-NHL display specific genetic landscapes, different from adult counterparts, the global aim of this thesis is the genetic and molecular characterization of large series of pediatric and young adult GC-derived B-NHL lymphomas in order to shed light to the fuller molecular portrait of pediatric and young adult variants including BLL-11q (**Study 1**), PTFL (**Study 2**) and large B-cell lymphomas (LBCL) including DLBCL, HGBCL, NOS and LBCL-*IRF4* (**Study 3**) entities.

This global aim is in turn divided into the following specific objectives:

1. To gain insights in the molecular pathogenesis of pediatric lymphoma by means of an extensively characterization of different pediatric lymphoma subtypes (**Study 1, 2 and 3**).
2. To improve the differential diagnosis between close pediatric lymphoma entities and identify new targets for novel therapies (**Study 1, 2 and 3**).
3. To identify age-related biological differences through the systematic comparison of the morphological, immunophenotypic and the molecular findings of pediatric and young-adult patients with adult cohorts (**Study 2 and 3**).
4. To identify molecular alterations with clinical implications to improve stratification of the cases into risk groups (**Study 3**).

RESULTS

Study 1:

Burkitt-like lymphoma with 11q aberration: a germinal center-derived lymphoma genetically unrelated to Burkitt lymphoma

Gonzalez-Farre B*, **Ramis-Zaldivar JE***, Salmeron-Villalobos J, Balagué O, Celis V, Verdu J, Nadeu F, Sábado C, Ferrández A, Garrido M, Garcia-Bragado F, de la Maya MD, Vagace JM, Panizo CM, Astigarraga I, Andrés M, Jaffe ES, Campo E, Salaverria I. ***Co-first author.**

Haematologica 2019 Sep;104(9):1822-1829.

Summary

Burkitt-like lymphoma with 11q aberration (BLL-11q) is a provisional entity that represents cases which have morphological, phenotypic, and gene expression profiles resembling those of Burkitt lymphoma (BL), but lack *MYC* rearrangements and are characterized by an 11q-arm aberration. To improve the understanding of this disease, we molecularly characterized a series of 11 BLL-11q observing that this disease differed clinically, morphologically and immunophenotypically from conventional BL and instead showed features more consistent with high grade B-cell lymphoma, not otherwise specified (HGBCL, NOS) or diffuse large B-cell lymphoma (DLBCL). Most patients had localized nodal disease and a favorable outcome after therapy. Histologically, they were HGBCL, NOS (8 cases), DLBCL (2 cases) and only one was considered as atypical BL. All cases had a germinal center B-cell signature and phenotype with frequent LMO2 expression. Genetic landscape was characterized by recurrent 12q12-q21.1 gains, 6q12.1-q21 losses and lack of common BL or DLBCL alterations. BLL-11q mutational profile also differed from that of BL since all cases lacked the typical BL mutations in *ID3*, *TCF3*, *CCND3* or *SMARCA4* genes and had recurrent mutations in *BTG2* and *ETS1* not present in BL. Altogether, these results suggest that Burkitt-like lymphoma with 11q aberration is a germinal center-derived lymphoma closer to HGBCL, NOS or DLBCL than to BL.

Ferrata Storti Foundation

Haematologica 2019
Volume 104(9):1822-1829

Burkitt-like lymphoma with 11q aberration: a germinal center-derived lymphoma genetically unrelated to Burkitt lymphoma

Blanca Gonzalez-Farre,[1,2,3]* Joan Enric Ramis-Zaldivar,[2,3]* Julia Salmeron-Villalobos,[2] Olga Balagué,[1,2,3] Verónica Celis,[4] Jaime Verdu-Amoros,[5] Ferran Nadeu,[2,3] Constantino Sábado,[6] Antonio Ferrández,[7] Marta Garrido,[8] Federico García-Bragado,[9] María Dolores de la Maya,[10] José Manuel Vagace,[10] Carlos Manuel Panizo,[11] Itziar Astigarraga,[12] Mara Andrés,[13] Elaine S. Jaffe,[14] Elias Campo[1,2,3*] and Itziar Salaverria[2,3*]

[1]Hematopathology Unit, Hospital Clínic de Barcelona, University of Barcelona, Barcelona, Spain; [2]Institut d'Investigacions Biomèdiques August Pi i Sunyer (IDIBAPS), Barcelona, Spain; [3]Centro de Investigación Biomédica en Red de Cáncer (CIBERONC), Madrid, Spain; [4]Pediatric Oncology Department, Hospital Sant Joan de Déu, Esplugues de Llobregat, Spain; [5]Pediatric Oncology Department, Hospital Clínico Universitario de Valencia, Valencia, Spain; [6]Pediatric Oncology Department, Hospital Universitari Vall d'Hebron, Barcelona, Spain; [7]Pathology Department, Hospital Clínico de Valencia, Valencia, Spain; [8]Pathology Department, Hospital Universitari Vall d'Hebron, Barcelona, Spain; [9]Pathology Department, Complejo Hospitalario de Navarra, Pamplona, Spain; [10]Pediatric Hematology Department, Hospital Materno Infantil de Badajoz, Badajoz, Spain; [11]Department of Hematology, Clínica Universidad de Navarra and Instituto de Investigación Sanitaria de Navarra (IdiSNA), Pamplona, Spain; [12]Pediatrics Department, Hospital Universitario Cruces, IIS Biocruces Bizkaia, UPV/EHU, Barakaldo, Spain; [13]Pediatric Oncology Department, Hospital La Fe, Valencia, Spain and [14]Hematopathology Section, Laboratory of Pathology, National Cancer Institute, National Institutes of Health, Bethesda, MD, USA

BGF, JERZ, EC and IS contributed equally to this work.

ABSTRACT

Burkitt-like lymphoma with 11q aberration is characterized by pathological features and gene expression profile resembling those of Burkitt lymphoma but lacks the *MYC* rearrangement and carries an 11q-arm aberration with proximal gains and telomeric losses. Whether this lymphoma is a distinct category or a particular variant of other recognized entities is controversial. To improve the understanding of Burkitt-like lymphoma with 11q aberration we performed an analysis of copy number alterations and targeted sequencing of a large panel of B-cell lymphoma-related genes in 11 cases. Most patients had localized nodal disease and a favorable outcome after therapy. Histologically, they were high grade B-cell lymphoma, not otherwise specified (8 cases), diffuse large B-cell lymphoma (2 cases) and only one was considered as atypical Burkitt lymphoma. All cases had a germinal center B-cell signature and phenotype with frequent LMO2 expression. The patients with Burkitt-like lymphoma with 11q aberration had frequent gains of 12q12-q21.1 and losses of 6q12.1-q21, and lacked common Burkitt lymphoma or diffuse large B-cell lymphoma alterations. Potential driver mutations were found in 27 genes, particularly involving *BTG2, DDX3X, ETS1, EP300,* and *GNA13*. However, *ID3, TCF3,* or *CCND3* mutations were absent in all cases. These results suggest that Burkitt-like lymphoma with 11q aberration is a germinal center-derived lymphoma closer to high-grade B-cell lymphoma or diffuse large B-cell lymphoma than to Burkitt lymphoma.

Introduction

Our knowledge of lymphomas in children and young adults has increased dramatically in the last years with the identification of several subtypes that predominantly occur in this age subgroup.[1-4] One of these recently recognized categories is Burkitt-like lymphoma with 11q aberration (BLL-11q) which has morphological, phenotyp-

Correspondence:

ITZIAR SALAVERRIA
isalaver@clinic.cat

Received: October 5, 2018.

Accepted: February 7, 2019.

Pre-published: February 7, 2019.

doi:10.3324/haematol.2018.207928

Check the online version for the most updated information on this article, online supplements, and information on authorship & disclosures: www.haematologica.org/content/104/9/1822

ic, and gene expression profiles resembling those of Burkitt lymphoma (BL), but lacks *MYC* rearrangements according to standard methods of detection, such as fluorescence *in situ* hybridization (FISH). Alternatively, these tumors carry an 11q-arm aberration characterized by proximal gains and telomeric losses.[4] In comparison with BL, BLL-11q seems to have more complex karyotypes, a certain degree of cytological pleomorphism, sporadically a follicular pattern and a high incidence of nodal presentation.[4,5] Very similar cases have also been reported in the post-transplant setting,[6] although its incidence in other immunocompromised conditions, such as human immunodeficiency infection, is still unclear.[7,8]

BLL-11q has been incorporated in the revised World Health Organization (WHO) classification as a provisional category[1] because its precise taxonomy as a particular variant of BL, diffuse large B-cell lymphoma (DLBCL) or a distinct form of high-grade B-cell lymphoma (HGBCL) is still controversial.[1,4-6,9-11] The clarification of the biological nature of this uncommon subtype of lymphoma is clinically relevant because of increasing interest in defining the most appropriate management strategies for specific subtypes of lymphomas in pediatric and young adult patients.[12] Recent DNA copy number alteration and next-generation sequencing studies have provided a comprehensive catalog of genomic aberrations in BL and DLBCL which clearly distinguish these entities.[13-17] In this study we performed an integrated analysis of genomic and mutational alterations with a complete annotation of clinical and pathological features of BLL-11q with the goal of obtaining insights to refine the understanding of the pathogenesis of these tumors and improve their diagnosis.

Methods

Sample selection and DNA/RNA extraction

To identify BLL-11q cases we initially reevaluated the presence of *MYC* translocations in 95 cases diagnosed as BL, atypical BL or HGBCL, not otherwise specified (NOS), in our Hematopathology Unit between 2000-2016. Three consultation cases from centers belonging to the *Sociedad Española de Hematología y Oncología Pediátricas* (SEHOP) were also analyzed. Cases were reviewed by three pathologists (BG-F, EC, ESJ). DNA and RNA were extracted using standard protocols (Qiagen, Hilden, Germany). This study was approved by the Institutional Review Board of the Hospital Clinic of Barcelona. Informed consent was obtained from all patients in accordance with the Declaration of Helsinki.

Immunohistochemistry and fluorescence *in situ* hybridization

Immunohistochemical analysis using a panel of antibodies detecting common B- and T-cell markers as well as LMO2 and MYC was performed and interpreted as previously reported (*Online Supplementary Table S1*).[18,19]

MYC breaks and *MYC*/IGH fusions were analyzed by FISH using the XL MYC BA Probe (Metasystems, Altlussheim, Germany) and LSI IGH/MYC/CEP 8 Tri-Color Dual Fusion Probe Kit (Vysis-Abbott, Abbott Park, IL, USA) respectively. The 11q alteration was studied with a custom FISH probe using BAC clones (Invitrogen Inc.) for proximal gains (RP11-414G21-spectrum green) and terminal losses (RP11-629A20-spectrum red) combined with CEP11-spectrum aqua (Vysis-Abbott Inc.). The FISH constellation in a normal case is characterized by two signals per probe, while the pattern corresponding to the 11q gain/loss or gain/amplification/loss aberration would be two blue, three up to five green signals and one red signal. The probe was tested in an independent series of eight non-Hodgkin B-cell lymphomas and four *MYC*-negative HGBCL with lack of the 11q alteration by array analysis and all showed the normal pattern described above.

Copy number analysis

DNA was hybridized on Oncoscan FFPE or SNP array platform (ThermoFisher Scientific, Waltham, MA, USA) and analyzed as described previously (*Online Supplementary Methods*).[2] Published copy number data on *MYC*-positive BL[20] and DLBCL[13] were reanalyzed for comparison.

Sequencing approaches

The mutational status of 96 B-cell lymphoma-related genes (*Online Supplementary Table S2*) was examined by target next-generation sequencing in ten BLL-11q cases and four *MYC*-negative 11q-negative cases using a NGS SureSelect XT Target Enrichment System Capture strategy (Agilent Technologies, Santa Clara, CA, USA) before sequencing in a MiSeq instrument (Illumina, San Diego, CA, USA) (*Online Supplementary Methods*). Additionally, analysis of hotspots of mutation in *ID3*, *TCF3* and *CCND3* genes, *ETS1* exon 1 (transcript NM_005238) and verification of variants in specific cases was performed by Sanger sequencing using primers described in *Online Supplementary Table S3*.

Gene expression analysis

Cell of origin was determined by Lymph2Cx assay (Nanostring, Seattle, WA, USA) as previously published.[21] Gene expression levels of *MYC* and *ETS1* were investigated by real-time quantitative polymerase chain reaction (*Online Supplementary Methods*) using Taqman assays described in *Online Supplementary Table S4*.

Statistical methods

The χ^2 method was used for categorical variables and Student *t*-tests for continuous variables. Non-parametric tests were applied when necessary. The *P*-values for multiple comparisons were adjusted using the Benjamini–Hochberg correction. Survival curves were estimated with the Kaplan-Meier method. Statistical analyses were carried out with SPSS v22 and R software v3.1.3.

Results

Identification of cases with Burkitt-like lymphoma with 11q aberration

To identify BLL-11q cases we reevaluated the presence of *MYC* translocations in 95 cases diagnosed as having BL, atypical BL or HGBCL, NOS. We confirmed the presence of *MYC* rearrangements in 78 cases (82.1%), of which 67 (70.5%) were classified as BL. Since the 11q aberration has been found mainly in children and young adults (<40 years old),[4] we analyzed the 60 patients under 40 years and the 35 older patients separately (*Online Supplementary Figure S1*).

In the younger cohort (n=60), the 46 (76.7%) cases with *MYC* translocations were classified as having BL. To find BLL-11q cases, we initially used the Oncoscan platform in the remaining 14 *MYC*-negative patients and detected the presence of the 11q gain/loss alteration in eight of them. Additionally, we found a copy number pattern consistent with the presence of 11q alteration in three recent consultation cases from SEHOP (*Online Supplementary Figures S1* and *S2*). Then, among those BLL-11q cases we were able

to verify the presence of the 11q aberration by FISH in all ten evaluable cases (*Online Supplementary Figure S3* and *Supplementary Table S5*). The morphological, clinical, and genetic features and consensus diagnosis of the 11 BLL-11q identified in our files are summarized in Table 1. The six cases negative for the *MYC* rearrangement and 11q aberrations by Oncoscan were re-classified as DLBCL (3 cases) or HGBCL, NOS (3 cases). The DLBCL had predominant centroblastic morphology, germinal center phenotype, very high proliferative index and a focal "starry sky" pattern (see *Online Supplementary Results*). The absence of 11q alterations was also verified using the 11q FISH probe in four of these *MYC*/11q-negative cases with available material (*Online Supplementary Figure S1A*).

In the 35 older patients (≥40 years old), a *MYC* translocation was found in 32 cases; one was classified as DLBCL, 21 as BL, and ten were HGBCL with double- or triple-hit aberrations (*BCL2* and/or *BCL6* translocations). Only three cases were negative for *MYC* translocations and were classified as HGBCL, NOS (*Online Supplementary Figure S1B* and *Online Supplementary Results*). We screened these cases with the 11q FISH probe and all three were negative for the 11q aberration.

Clinical and morphological results of cases of Burkitt-like lymphoma with 11q aberration

The 11 patients with BLL-11q had a mean age of 15 years (range, 8-37 years); eight were male (Table 1). Eight tumors were reclassified morphologically as HGBCL, NOS, two as DLBCL and only one case was considered atypical BL. None of the cases was considered as typical BL (Figure 1). Six cases showed a "starry sky" pattern and two had a nodular growth pattern with the presence of a disrupted follicular dendritic cell meshwork (Figure 1C). Ki67 was very high in all the samples, as in BL. All cases had a germinal center (GC) phenotype and GC B-cell (GCB) signature by Nanostring Lymph2Cx assay. MUM1/IRF4 was negative in all 11 cases. One case expressed BCL2 (Figure 1D). LMO2, a germinal center marker that is usually seen in GCB-DLBCL but not in BL[18] was expressed in five cases (Figure 1A, B). Interestingly, using a 40% cutoff,[19] five cases were positive for *MYC* expression. However, only one case showed diffuse and intense positivity while the other four cases had either only positivity in around 50% of the cells or the intensity was not that expected in typical BL. Additionally, MYC RNA levels were significantly lower in BLL-11q than in *MYC*-positive BL (relative expression 0.07 *vs.* 0.36, *P*=0.019) (*Online Supplementary Figure S4A*). Epstein-Barr virus hybridization was negative in the nine cases tested.

Clinically, BLL-11q frequently had a nodal localized presentation (8/11) in the head and neck region. Two cases had an extranodal presentation, one in the context of an acute appendicitis and the other debuted as an omental mass. Eight patients (73%) had stage I-II, and one patient presented in an advanced stage (IV-E) with

Table 1. Pathological and clinical features of 11 cases of Burkitt-like lymphoma with 11q aberration.

Case	Age/ gender	Biopsy site	Original diagnosis	Final diagnosis	Immunophenotype					Stage*	COO Nanostring (Lymph2Cx)	Chemo-therapy	Rituximab	Outcome/ follow-up
					CD10& BCL6	IRF4/ MUM1	BCL2	LMO2	MYC					
#1	27, M	Laterocervical LN	Atypical BL	HGBCL, NOS	+	-	-	-	+	I	GCB	A	Yes	CR, 72m
#2**	37,M	Axillary LN	Atypical BL	DLBCL	+	-	-	+	-	IV-E	GCB	A	Yes	CR, 112m
#3	8,F	Tonsil	HGBCL	DLBCL & HGBCL blastoid	+	-	-	-	-	II	GCB	P	No	CR, 54m
#4	17,F	Submaxilar LN	HGBCL	HGBCL, NOS	+	-	-	+	+	I	GCB	A	Yes	CR, 22m
#5	14,F	Laterocervical LN	HGBCL	HGBCL with features intermediate between BL and DLBCL	+	-	+	+	-	I	GCB	P	No	CR, 29m
#6	14,M	Appendix	HGBCL	DLBCL	+	-	-	+	-	II	GCB	P	No	CR, 25m
#7	8, M	Laterocervical LN	BL	Atypical BL	+	-	-	-	-	I	GCB	P	No	CR, 113m
#14	8,M	Laterocervical LN	BL	HGBCL blastoid	+	-	-	-	Weak +	II	GCB	P	No	CR, 15m
#15	12,M	Laterocervical mass	DLBCL	HGBCL, NOS	+	-	-	-	+	I	GCB	P	No	CR, 35m
#16	14, M	Laterocervical LN	DLBCL	HGBCL, NOS	+	-	-	+	-	III	GCB	P	Yes	CR, 12m
#17	16, M	Omentum	HGBCL	HGBCL, NOS	+	-	-	-	+	III	GCB	A	Yes	CR, 4m

*Stage was established according to the St. Jude/International Pediatric NHL Staging System (IPNHLSS) or Ann Arbor staging system for pediatric and adult patients, respectively. COO: cell of origin; M: male; F: female; LN: lymph node; BL: Burkitt lymphoma; HGBCL: high-grade B-cell lymphoma; NOS: not otherwise specified; DLBCL: diffuse large B-cell lymphoma; Epstein-Barr virus *in situ* hybridization (EBER) was negative in all nine tested cases. E: extranodal; GCB: germinal center B-cell; A: adult schema protocol (R-CHOP or burkimab); P: pediatric schema protocol; CR: complete response; m: months. All patients received central nervous system prophylaxis. **Human immunodeficiency virus (HIV)-positive patient

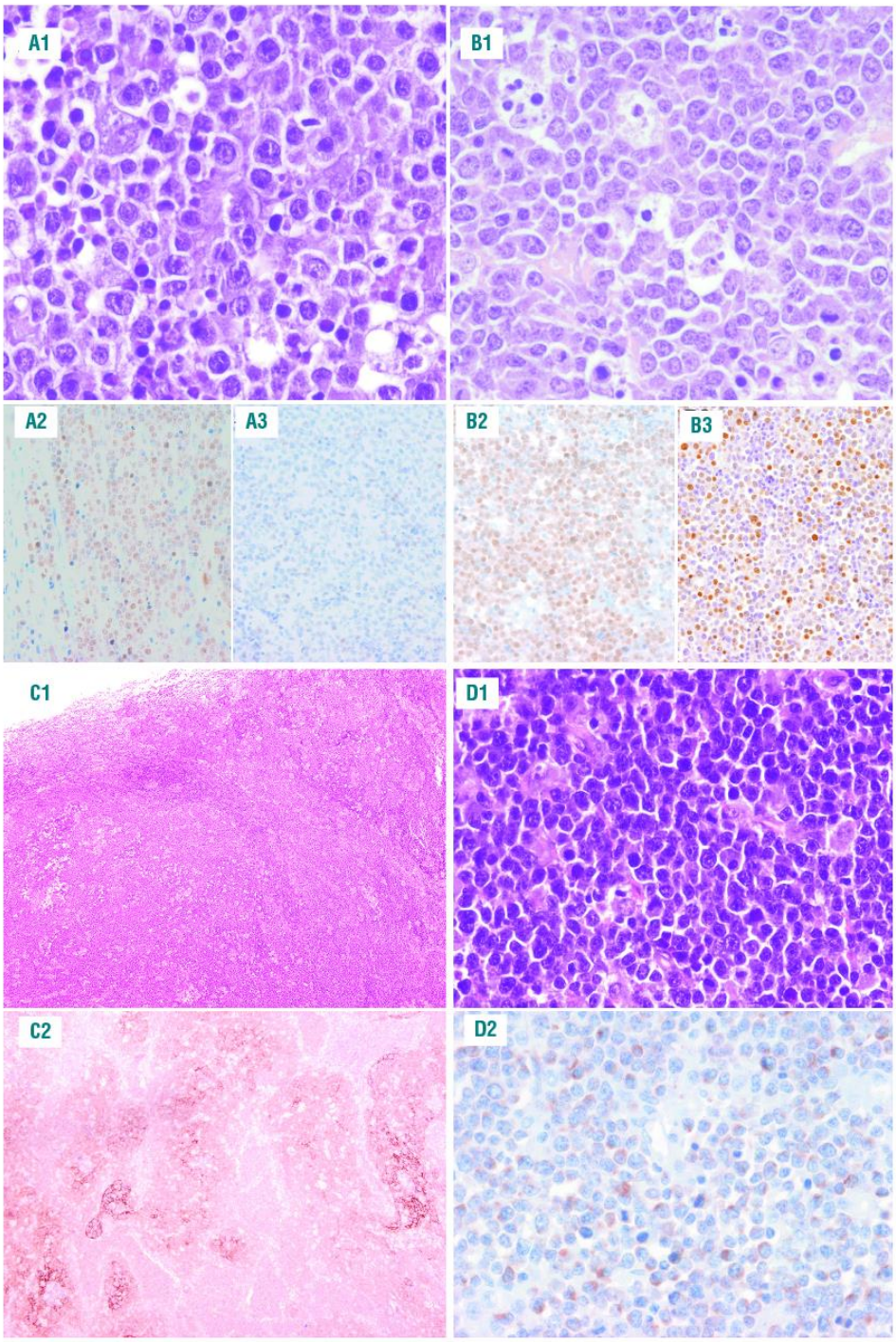

Figure 1. Morphological features of cases of Burkitt-like lymphoma with 11q aberration. (A1-A3) Case #2 shows the typical morphology of diffuse large B-cell lymphomas with large and irregular cells resembling centroblasts. This case was positive for (A2) LMO2 and negative for (A3) MYC. (B1-B3) Case #4 corresponds to a tumor with high-grade B-cell lymphoma (HGBCL) morphology. It is composed mostly of medium-sized cells with mild heterogeneity. Note the "starry sky" pattern. This case was positive for (B2) MYC and (B3) LMO2 expression. (C1-C2; case #7) Lymph node with nodular architecture and a "starry sky" pattern with large follicles and a disrupted follicular cell meshwork highlighted with (C2) CD21. (D1-D2; case #5) This is a case with HGBCL features with expression of (D2) BCL2 in the neoplastic cells.

widespread disease in the context of chronic human immunodeficiency virus infection. All cases were treated with chemotherapy, including rituximab in five. All patients were alive with no disease after a median follow-up of 29 months (Table 1).

Copy number analysis

The copy number analysis of all the 11 BLL-11q cases showed a total of 78 alterations (mean 7.1; range, 2-15) (*Online Supplementary Tables S5* and *S6*). Seven cases had the typical 11q gain/loss pattern (Figure 2A-B, *Online*

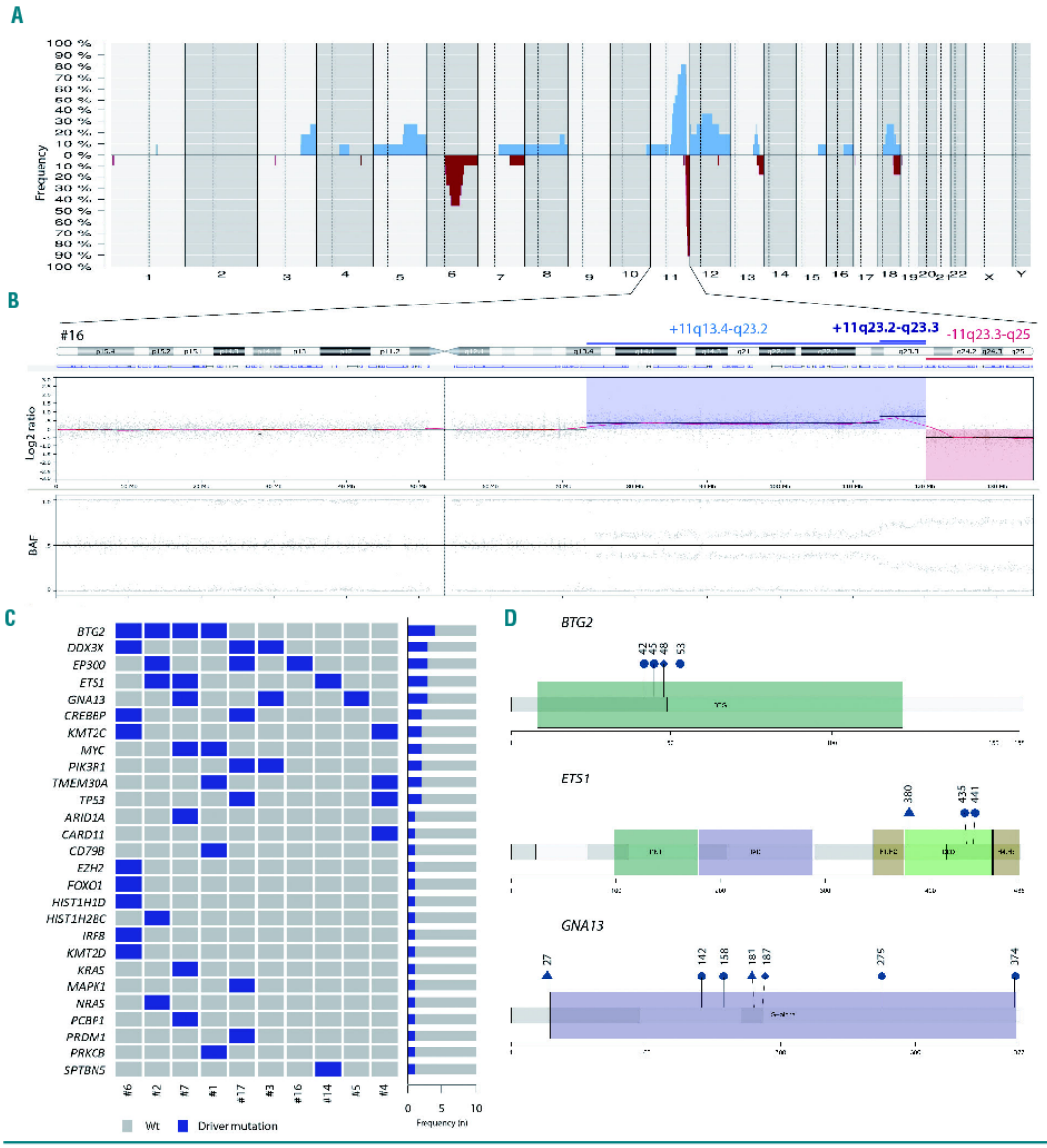

Figure 2. Genetic features of cases of Burkitt-like lymphoma with 11q aberration. (A) Global copy number profile of the 11 cases of Burkitt-like lymphoma (BLL) with 11q aberration. The horizontal axis indicates chromosomes from 1 to Y and p to q. The vertical axis indicates the frequency of the genomic aberration among the cases analyzed. Gains are depicted in blue, losses are depicted in red. (B) Individual copy number profile of case #16 showing a prototypical, gain, loss and amplification in the 11q region. Each probe is aligned from chromosome 1 to Y and p to q arm. (C) Mutational overview of ten cases of BLL with 11q aberration. The heat map shows the case-specific pattern of driver mutations found by next-generation sequencing. Each column represents a case and each row represents a gene. The right bar graph illustrates the mutation frequency of each gene. (D) A diagram of the relative positions of driver mutations is shown for *BTG2*, *ETS1* and *GNA13* genes. Domains BTG2: BTG family domain. Domains ETS1: PNT: pointed domain; TAD: transactivation domain; H-1/2: inhibitory α-helices 1/2; DBD: DNA binding domain; H4-5: α-helix 4/5. Domains GNA13: G-alpha: G protein α subunit. Circles indicate missense mutations, triangles indicate truncating mutations and rhombi indicate splicing mutations.

Supplementary Figure S2), two cases had only an 11q terminal deletion, one case showed a complex 11q alteration with two gains and two losses, and finally one case had an 11q23.3-q25 copy number neutral loss of heterozygosity in addition to gain (*Online Supplementary Figure S2*). Two minimal regions of gain were identified (chr11:103326831-111737912/11q22.3-q23.1 and chr11:114767237-116764582/11q23.3,hg19) whereas the minimal region of loss was in chr11:128214400-132020453/11q24.3-q25 (including the *ETS1* and *FLI1* genes). No cases with homozygous deletions of these two targets were observed in our series. The breakpoint region between gain and loss was not conserved and spanned from chr11:118352769 to chr11:121062860. Amplifications in the 11q arm were observed in four cases, with a minimal region chr11:118347020-120155799/11q23.3, including the *USP2* gene (*Online Supplementary Figure S5*). The most recurrent copy number aberrations other than 11q were 12q12-q21.1 gains and 6q12.1-q21 losses (Figure 2A).

BLL-11q cases displayed similar levels of complexity as *MYC*-positive BL (7.1 *vs.* 6 alterations/case),[20] but significantly lower than those of GCB-DLBCL (7.1 *vs.* 19, alterations/case $P<0.0001$).[13] The BLL-11q genomic profile differed from that of BL and DLBCL (*Online Supplementary Figure S6*). BLL-11q had frequent gains of 5q21.3-q32 and losses of 6q12.1-q21 and lacked the 1q gains seen in *MYC*-positive BL. BLL-11q also lacked alterations typically seen in GCB-DLBCL such as gains of 2p16.1 and 7p and losses of 1p36.32.

The six tumors negative for both *MYC* and 11q-aberrations in patients younger than 40 years had similar levels of genomic complexity as those observed in BLL-11q (11.8 *vs.* 7.1 alterations/case) (*Online Supplementary Figure S7A*). The unique significant aberration that distinguished the two groups was the presence/absence of the 11q aberration.

The review of the literature regarding other lymphoid neoplasms confirmed that the 11q alteration observed in BLL-11q is mainly absent in other lymphoma entities with the exception of transformed follicular lymphoma (16%) (*Online Supplementary Results*).[22]

Next-generation sequencing and gene expression analysis

Target next-generation sequencing showed a total of 49 potential driver mutations affecting 27 different genes (mean=4.9 mutations per case) (Figure 2C, D, *Online Supplementary Figures S8* and *S9*; *Online Supplementary Table S7*). Interestingly, all cases lacked the typical BL mutations in *ID3*, *TCF3*, or *CCND3* genes, and their mutational profile was more similar to that of other GC-derived lymphomas with recurrent mutations affecting *BTG2* (4 cases), *DDX3X*, *ETS1*, *EP300*, and *GNA13* (3 cases each) (*Online Supplementary Table S8*). Five cases had mutations in epigenetic modifier genes such as *EP300*, *CREBBP*, *KMT2C*, *EZH2*, *ARID1A*, *KMT2D*, *HIST1H1D* and *HIST1H2BC*. Two cases had concomitant *TMEM30A* deleterious mutations associated with a 6q14.1 deletion as seen in DLBCL but not in BL (Figure 2C).[14-16]

BTG2 mutations, found in four cases, comprised three missense mutations and one deletion in a splicing site. *BTG2* is a tumor suppressor gene with an important role in G1/S transition through inhibition of CCND1 in a pRb-dependent mechanism.[23] These *BTG2*-inactivating mutations could release CCND1 inhibition and accelerate G1/S transition. *GNA13* mutations were found in three cases including four missense and two nonsense mutations, and one missense mutation in a splicing site. Two *MYC* missense mutations occurred in the central domain of the protein, but did not affect threonine phosphorylation sites (*Online Supplementary Table S7*).[24] *ETS1* mutations have been previously described in BLL-11q and activated B-cell DLBCL[13,17] but not in conventional BL (*Online Supplementary Table S8*).[14,15] We detected three coding mutations located on the winged helix-turn-helix DNA-binding domain but the previously described exon 1 mutations (NM_005238) were absent in this series. *ETS1* RNA expression was lower in BLL-11q than in *MYC*-positive BL (relative expression 6.6 *vs.* 19.3, $P<0.001$) and was also lower in *ETS1*-mutated than wild-type BLL-11q (relative expression 1.9 *vs.* 8.6, $P=0.03$) (*Online Supplementary Figure S4B*).

The mutational profile of four *MYC*-negative/11q alteration-negative cases with material available was analyzed using the same approach. No mutations in *BTG2*, *EP300* or *ETS1* genes were observed. Moreover, three out of four did not harbor any BL-related mutation on *ID3*, *TCF3* and *CCND3* whereas the fourth case had a mutational profile commonly seen in BL with *MYC*, *DDX3X*, *SMARC4*, *CCND3* and *TP53* mutations (*Online Supplementary Figure S7B*).

Discussion

BLL-11q was initially recognized as a particular subset of HGBCL that had an expression profile and some pathological characteristics similar to those of BL but lacked *MYC*-translocations and alternatively shared a common pattern of gains at 11q23 associated with losses at 11q24-qter. The particular features of these cases raise some uncertainty on their precise categorization as a variant of BL or a tumor related to other HGBCL.[1,4-6,9-11] On the other hand, the limited number of cases reported and the different methodologies used for their recognition do not provide a clear view of their incidence and clinico-pathological characteristics.

In this study we searched our files for cases that could be reclassified as BLL-11q among 95 tumors previously classified as BL, atypical BL, or HGBCL, NOS and found eight (8%) cases with the chromosomal aberration. These cases, together with three additional cases received on consultation, were investigated for copy number alterations and mutational profiles and compared to the genomic aberrations recently identified in BL, DLBCL, and HGBCL.[13-17] The complexity of BLL-11q was similar to that of *MYC*-positive BL,[20] but significantly lower than that of GCB-DLBCL.[13] The BLL-11q genomic profile differed from that of BL and DLBCL (*Online Supplementary Figure S6*). BLL-11q had frequent gains of 5q21.3-q32 and losses of 6q12.1-q21 and lacked the 1q gains seen in *MYC*-positive BL. BLL-11q also lacked alterations typically seen in GCB-DLBCL such as gains of 2p16.1 and 7p and losses of 1p36.32. Additionally, we identified a mutational profile in BLL-11q which was different from that of *MYC*-positive BL since all cases lacked the typical BL mutations in *ID3*, *TCF3*, or *CCND3* genes and had mutations in *BTG2*, *DDX3X*, and *ETS1* not seen in BL. In addition, BLL-11q had mutations in epigenetic modifier genes such as *EP300*, *CREBBP*, *KMT2C*, *EZH2*, *ARID1A*, *KMT2D*, *HIST1H1D* and *HIST1H2BC*, which are common in DLBCL, particu-

larly of the GCB subtype. Other genes frequently mutated in GCB-DLBCL but not in BL were *GNA13* and *TMEM30A* associated with 6q14.1.[14-16]

We also compared our results with those of two recent studies on HGBCL (including double- and triple-hit lymphomas).[25,26] These cases also have recurrent mutations in histone modifier genes such as *KMT2D*, *CREBBP* and *EZH2* (*Online Supplementary Table S8*). Intriguingly, HGBCL, NOS, mainly with *MYC*-translocations, shared mutations in genes frequently mutated in both BL and GC-DLBCL.[25,26] All these observations suggest that BLL-11q is a neoplasm closer to other GC-derived lymphomas rather than BL in which the 11q aberration together with other mutations may play a relevant role in their pathogenesis. While this manuscript was under revision, Wagener *et al.* published a mutational study of 15 BLL-11q cases. Similar to our findings, no mutations in *ID3/TCF3* were identified and those cases carried frequent mutations in GC-DLBCL-associated genes such as *GNA13*, *FOXO1* and *EZH2*. Intriguingly, that study did not find mutations in *BTG2*, *KMT2D*, *KMT2C* or *CREBBP* observed in our study.[27] Collectively, these findings indicate that the genomic and mutational profiles of BLL-11q are different from those of BL and more similar to those of other GC-derived lymphomas.

In addition to the genetic differences, our BLL-11q cases differed clinically, morphologically and phenotypically from conventional BL and instead showed features more consistent with HGBCL or DLBCL. As in previous studies, all our patients were younger than 40 years, although occasional cases in older patients have been reported.[4,5,27] Contrary to BL, most of our cases of BLL-11q presented with localized lymphadenopathy.[4,5,27] These cases have a favorable outcome after therapy, although the optimal clinical management remains to be determined. Morphologically, our cases had a prominent "starry sky" pattern and high proliferation rate (>90%) but did not have the typical cytological features of BL since they were better classified as HGBCL with blastoid or intermediate features between HGBCL (8 cases) and DLBCL (2 cases) and only one had features of atypical BL. As previously reported,[4] two of our cases displayed a follicular growth pattern, with an underlying meshwork of follicular dendritic cells, raising the differential diagnosis with other pediatric lymphomas such as large B-cell lymphoma with *IRF4* rearrangement.[3] However, BLL-11q did not express IRF4/MUM1 and often exhibited a "starry sky" pattern with frequent mitotic figures, features that are not usual in large B-cell lymphoma with *IRF4* rearrangement. We also identified different immunohistochemical stains that could help in the differential diagnosis from other lymphomas entities. LMO2, a GC marker that is typically downregulated in BL and other lymphomas with *MYC* translocation,[18] was detected in 46% of our BLL-11q cases. In addition, and contrary to BL, MYC expression with a diffuse and intense pattern was only detected in one of our cases while the other four positive cases either exhibited partial positivity or the intensity was weak contrary to the pattern seen in BL.

Negativity for *MYC* rearrangement is a crucial element for the recognition of these cases. The recommended technique for detecting *MYC* translocations in clinical practice is FISH analysis using break-apart probes, with the limitation that a subset of 4% of *MYC*-positive cases are not detected with this method but picked up using *MYC*/IGH probes.[28] The genetic feature that distinguishes BLL-11q is an alteration of the 11q arm that prototypically is characterized by an 11q23.2-q23.3 gain/amplification and 11q24.1-qter loss. Additionally, isolated cases have been recognized with single 11q24.1-qter terminal loss or 11q23 gain with 11q24-qter copy number neutral loss of heterozygosity.[4,11] In our study we identified the presence of these 11q alterations using copy number arrays. We also confirmed the presence of 11q alterations by FISH analysis with a custom probe in all tested cases, suggesting that this approach may be useful in clinical practice to identify such cases (*Online Supplementary Table S8*). The specificity of this FISH approach was also confirmed by the fact that no false positive cases were observed in the 12 lymphoma cases in which the array showed a normal 11q pattern. Nevertheless, more studies on the clinical value of this probe are needed and, for the time being, confirmation of the finding by copy number array would be desirable. The specific 11q alteration observed in BLL-11q should be distinguished from other 11q aberrations such as 11q gains of the 11q24 region that include *ETS1* and *FLI1*, detected in DLBCL,[29] or the 11q25 losses missing *ETS1* and *FLI1* described in some post-transplant lymphoproliferative disorders.[30,31] On the other hand, although the 11q23 gain/11q24-qter loss of BLL-11q is mainly absent in other lymphoma entities, its detection should not be considered as a unique feature to diagnose BLL-11q cases since some transformed follicular lymphomas may carry a similar 11q aberration pattern.[22]

In summary, BLL-11q is a GC-derived lymphoma with genomic and mutational profiles closer to those of HGBCL or GCB-DLBCL rather than BL in which the 11q aberration, together with other mutations, may play a relevant role in pathogenesis. These observations support a reconsideration of the "Burkitt-like" term for these tumors. Although, the most appropriate name is not easy to propose and requires broader discussion and consensus, we think that the term "aggressive B-cell lymphoma with 11q aberration" captures their pathological features. To identify these cases we suggest performing copy number arrays or FISH with the 11q probe in cases with BL, DLBCL, and HGBCL morphology, a GC phenotype and very high proliferative index (>90%), without *MYC* rearrangements, in young patients. The recognition of these tumors is clinically relevant because they have a favorable outcome after therapy, although further studies are needed to determine the optimal clinical management.

Funding

This work was supported by Asociación Española Contra el Cáncer (AECC CICPFI6025SALA), Fondo de Investigaciones Sanitarias Instituto de Salud Carlos III (Miguel Servet program CP13/00159 and PI15/00580, to IS), Spanish Ministerio de Economía y Competitividad, Grant SAF2015-64885-R (EC), Generalitat de Catalunya Suport Grups de Recerca (2017-SGR-1107 I.S. and 2017-SGR-1142 to EC), and the European Regional Development Fund "Una manera de fer Europa". JER-Z was supported by a fellowship from the Generalitat de Catalunya AGAUR FI-DGR 2017 (2017 FI_B01004). EC is an Academia Researcher of the "Institució Catalana de Recerca i Estudis Avançats" (ICREA) of the Generalitat de Catalunya. This work was developed at the Centro Esther Koplowitz, Barcelona, Spain. The group is supported by Acció Instrumental d'Incorporació de Científics i Tecnòlegs PERIS 2016 (SLT002/16/00336) from the Generalitat de Catalunya.

The copy-number data reported in this article have been deposited at the GEO database under accession number GSE116527. Sequencing data have been deposited at the European Nucleotide Archive (ENA, accession number ERP110085).

Acknowledgments

We thank the centers of the Sociedad Española de Hematología y Oncología Pediátricas that submitted cases for consultation and Noelia Garcia, Silvia Martín, and Helena Suarez for their excellent technical assistance. We are indebted to the IDIBAPS Genomics Core Facility and to HCB-IDIBAPS Biobank-Tumor Bank and Biobanc de l'HospitaI Infantil Sant Joan de Déu, both integrated in the National Network Biobanks of ISCIII for the sample and data procurement. We thank Prof. Reiner Siebert from the University of Ulm for sharing the 11q

References

1. Swerdlow SH, Campo E, Harris NL, Jaffe ES, Pileri SA, Stein H, Thiele J (Eds) WHO Classification of Tumours of Haematopoietic and Lymphoid Tissues. (Revised 4th edition) IARC: Lyon 2017.
2. Schmidt J, Gong S, Marafioti T, et al. Genome-wide analysis of pediatric-type follicular lymphoma reveals low genetic complexity and recurrent alterations of TNFRSF14 gene. Blood. 2016;128(8):1101-1111.
3. Salaverria I, Philipp C, Oschlies I, et al. Translocations activating IRF4 identify a subtype of germinal center-derived B-cell lymphoma affecting predominantly children and young adults. Blood. 2011;118(1):139-147.
4. Salaverria I, Martin-Guerrero I, Wagener R, et al. A recurrent 11q aberration pattern characterizes a subset of MYC-negative high-grade B-cell lymphomas resembling Burkitt lymphoma. Blood. 2014;123(8):1187-1198.
5. Rymkiewicz G, Grygalewicz B, Chechlinska M, et al. A comprehensive flow-cytometry-based immunophenotypic characterization of Burkitt-like lymphoma with 11q aberration. Mod Pathol. 2018;31(5):732-743.
6. Ferreiro JF, Morscio J, Dierickx D, et al. Post-transplant molecularly defined Burkitt lymphomas are frequently MYC-negative and characterized by the 11q-gain/loss pattern. Haematologica. 2015;100(7):e275-e279.
7. Capello D, Scandurra M, Poretti G, et al. Genome wide DNA-profiling of HIV-related B-cell lymphomas. Br J Haematol. 2010;148(2):245-255.
8. Deffenbacher KE, Iqbal J, Liu Z, Fu K, Chan WC. Recurrent chromosomal alterations in molecularly classified AIDS-related lymphomas: an integrated analysis of DNA copy number and gene expression. J Acquir Immune Defic Syndr. 2010;54(1):18-26.
9. Poirel HA, Cairo MS, Heerema NA, et al. Specific cytogenetic abnormalities are associated with a significantly inferior outcome in children and adolescents with mature B-cell non-Hodgkin's lymphoma: results of the FAB/LMB 96 international study. Leukemia. 2009;23(2):323-331.
10. Havelange V, Ameye G, Theate I, et al. The peculiar 11q-gain/loss aberration reported in a subset of MYC-negative high-grade B-cell lymphomas can also occur in a MYC-rearranged lymphoma. Cancer Genet. 2016;209(3):117-118.
11. Grygalewicz B, Woroniecka R, Rymkiewicz G, et al. The 11q-gain/loss aberration occurs recurrently in MYC-negative Burkitt-like lymphoma with 11q aberration, as well as MYC-positive Burkitt lymphoma and MYC-positive high-grade B-cell lymphoma, NOS. Am J Clin Pathol. 2017;149(1):17-28.
12. Dunleavy K, Gross TG. Management of aggressive B-cell NHLs in the AYA population: an adult vs pediatric perspective. Blood. 2018;132(4):369-375.
13. Karube K, Enjuanes A, Dlouhy I, et al. Integrating genomic alterations in diffuse large B-cell lymphoma identifies new relevant pathways and potential therapeutic targets. Leukemia. 2018;32(3):675-684.
14. Richter J, Schlesner M, Hoffmann S, et al. Recurrent mutation of the ID3 gene in Burkitt lymphoma identified by integrated genome, exome and transcriptome sequencing. Nat Genet. 2012;44(12):1316-1320.
15. Schmitz R, Young RM, Ceribelli M, et al. Burkitt lymphoma pathogenesis and therapeutic targets from structural and functional genomics. Nature. 2012;490(7418):116-120.
16. Love C, Sun Z, Jima D, et al. The genetic landscape of mutations in Burkitt lymphoma. Nat Genet. 2012;44(12):1321-1325.
17. Morin RD, Mungall K, Pleasance E, et al. Mutational and structural analysis of diffuse large B-cell lymphoma using whole-genome sequencing. Blood. 2013;122(7):1256-1265.
18. Colomo L, Vazquez I, Papaleo N, et al. LMO2-negative expression predicts the presence of MYC translocations in aggressive B-cell lymphomas. Am J Surg Pathol. 2017;41(7):877-886.
19. Johnson NA, Slack GW, Savage KJ, et al. Concurrent expression of MYC and BCL2 in diffuse large B-cell lymphoma treated with rituximab plus cyclophosphamide, doxorubicin, vincristine, and prednisone. J Clin Oncol. 2012;30(28):3452-3459.
20. Scholtysik R, Kreuz M, Klapper W, et al. Detection of genomic aberrations in molecularly defined Burkitt's lymphoma by array-based, high resolution, single nucleotide polymorphism analysis. Haematologica. 2010;95(12):2047-2055.
21. Scott DW, Wright GW, Williams PM, et al. Determining cell-of-origin subtypes of diffuse large B-cell lymphoma using gene expression in formalin-fixed paraffin-embedded tissue. Blood. 2014;123(8):1214-1217.
22. Bouska A, McKeithan TW, Deffenbacher KE, et al. Genome-wide copy-number analyses reveal genomic abnormalities involved in transformation of follicular lymphoma. Blood. 2014;123(11):1681-1690.
23. Guardavaccaro D, Corrente G, Covone F, et al. Arrest of G(1)-S progression by the p53-inducible gene PC3 is Rb dependent and relies on the inhibition of cyclin D1 transcription. Mol Cell Biol. 2000;20(5):1797-1815.
24. Bahram F, von der LN, Cetinkaya C, Larsson LG. c-Myc hot spot mutations in lymphomas result in inefficient ubiquitination and decreased proteasome-mediated turnover. Blood. 2000;95(6):2104-2110.
25. Evrard SM, Pericart S, Grand D, et al. Targeted next generation sequencing reveals high mutation frequency of CREBBP, BCL2 and KMT2D in high-grade B-cell lymphoma with MYC and BCL2 and /or BCL6 rearrangements. Haematologica. 2019;104(4):e154-e157.
26. Momose S, Weissbach S, Pischimarov J, et al. The diagnostic gray zone between Burkitt lymphoma and diffuse large B-cell lymphoma is also a gray zone of the mutational spectrum. Leukemia. 2015;29(8):1789-1791.
27. Wagener R, Seufert J, Raimondi F, et al. The mutational landscape of Burkitt-like lymphoma with 11q aberration is distinct from that of Burkitt lymphoma. Blood. 2019;133(9):962-966.
28. King RL, McPhail ED, Meyer RG, et al. False-negative rates for MYC FISH probes in B-cell neoplasms. Haematologica. 2019;104(6):e248-e251.
29. Bonetti P, Testoni M, Scandurra M, et al. Deregulation of ETS1 and FLI1 contributes to the pathogenesis of diffuse large B-cell lymphoma. Blood. 2013;122(13):2233-2241.
30. Rinaldi A, Kwee I, Poretti G, et al. Comparative genome-wide profiling of post-transplant lymphoproliferative disorders and diffuse large B-cell lymphomas. Br J Haematol. 2006;134(1):27-36.
31. Rinaldi A, Capello D, Scandurra M, et al. Single nucleotide polymorphism-arrays provide new insights in the pathogenesis of post-transplant diffuse large B-cell lymphoma. Br J Haematol. 2010;149(4):569-577.

Selected Supplementary Material

Gonzalez-Farre & Ramis-Zaldivar et al

Supplementary Figure S1. Diagram of the strategy used for the identification of Burkitt-like with 11q aberration in a cohort of **A)** 60 patients <40 years old and **B)** 35 patients ≥ 40 years old with a morphological diagnosis of Burkitt lymphoma (BL)/atypical BL and high grade B-cell lymphoma, not otherwise specified (HGBCL, NOS) according to the updated WHO Classification 2016. Seven out of nine cases negative for both *MYC* and 11q alterations with material available were tested by MYC/IGH double color double fusion probe, and all resulted to be negative for the fusion. Abbreviations: DLBCL, diffuse large B-cell lymphoma; DHL, double hit lymphoma; THL, triple hit lymphoma.

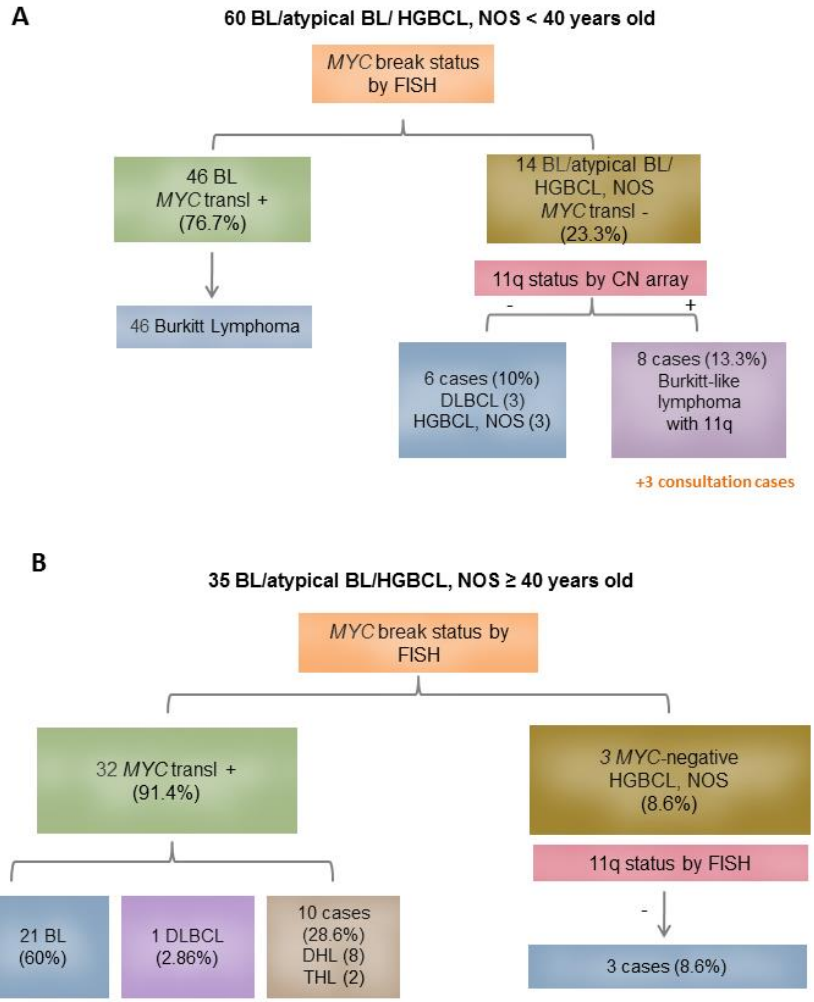

Supplementary Figure S2. Individual and integrative copy number plots of A) eleven Burkitt-like with 11q and **B)** six *MYC*-negative 11q-negative lymphoma cases. The vertical axis indicates frequency of the genomic aberration among the analyzed cases. Gains are depicted in blue, losses are depicted in red, and regions of CNN-LOH are represented in yellow.

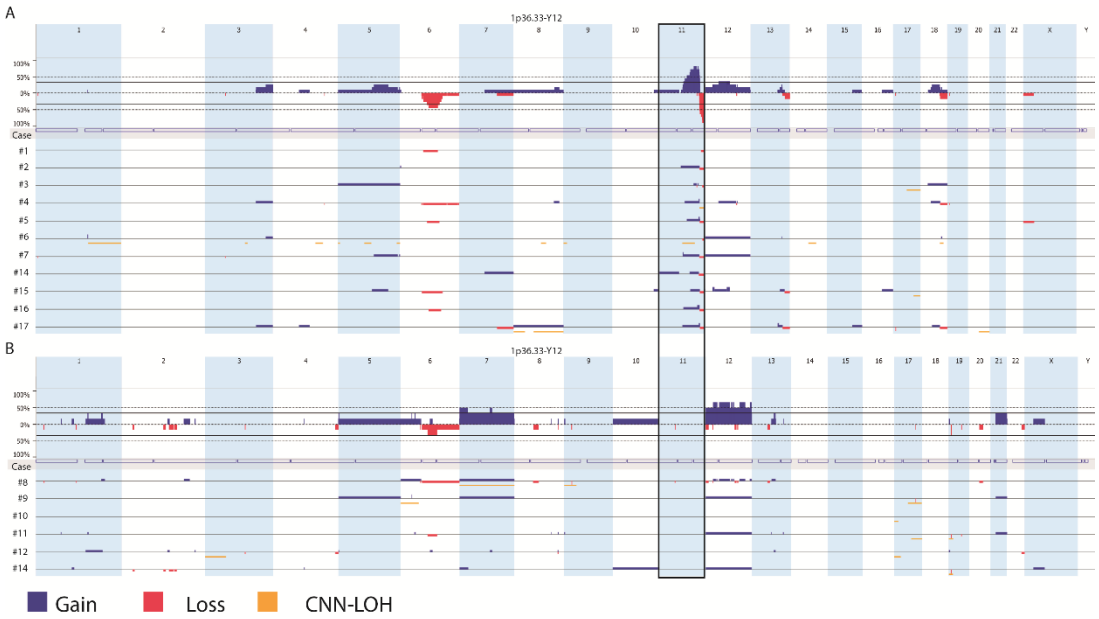

Supplementary Figure S3. Representative 11q aberration by FISH. A) FISH image of a representative case (#17) harboring 11q aberration using a custom probe combining CEP11 (Spectrum Aqua), RP11-414G21 (Spectrum Green) and R11-629A20 (Spectrum Red) bac clones. **B)** Two blue signals are observed per cell corresponding to the two chr11 centromeres, **C)** the presence of three green signals per cell indicates 11q gain and **(D)** the presence of only one red is indicative of the 11q terminal loss.

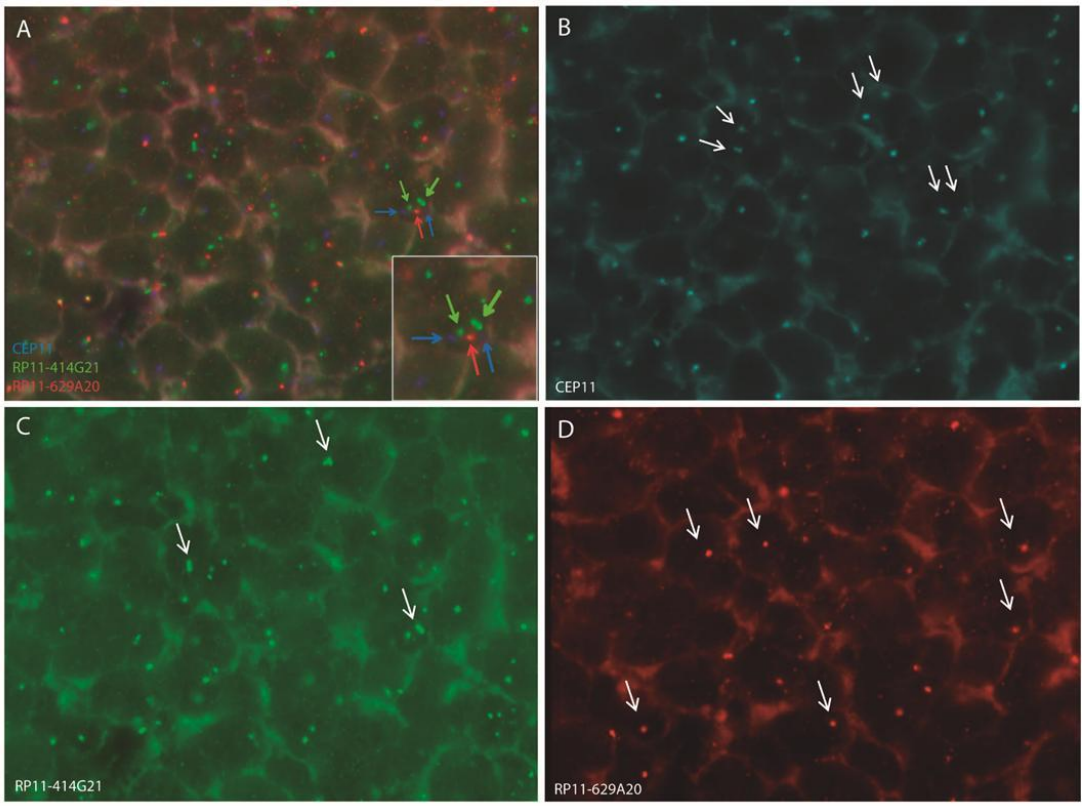

Supplementary Figure S4. *MYC* and *ETS1* RNA expression levels in BLL-11q. **A)** Box plot of the percentage of *MYC* expression analyzed by qPCR in BLL-11q (n=9) vs. *MYC*-positive BL (n=9). **B)** Box plot of the percentage of *ETS1* expression analyzed by qPCR in BLL-11q (n=10) vs. *MYC*-positive BL (n=12). The significance of difference was determined by t-test and Mann-Whitney test respectively.

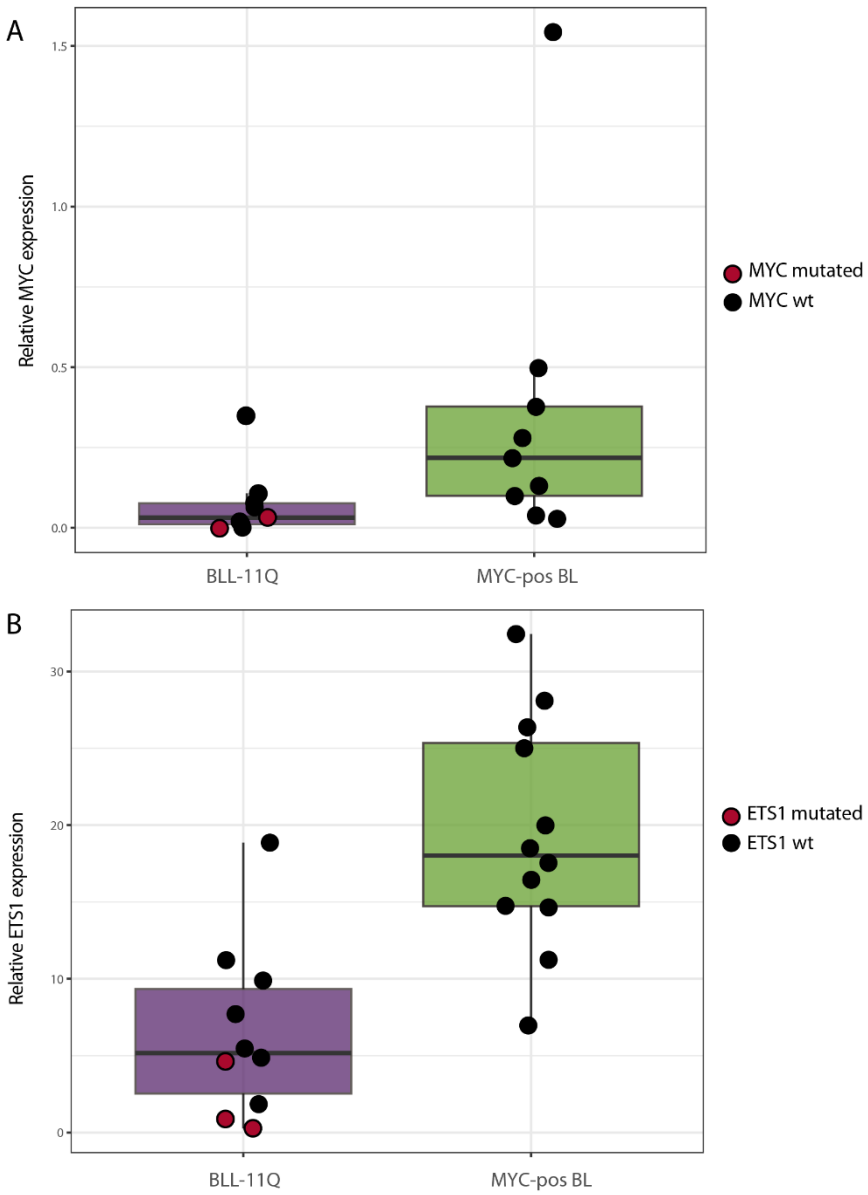

Supplementary Figure S5. Ideogram of chromosome 11q arm of 11 *MYC*-negative cases harboring 11q aberration by CN array. Gains are represented in blue, red corresponds to losses and CNN-LOH are represented in yellow. Two minimal regions of gain (MRGs) and one minimal region of loss (MRL) are pointed with blue and red boxes, respectively, and the minimal region of amplification (MRA) is indicated with the green box.

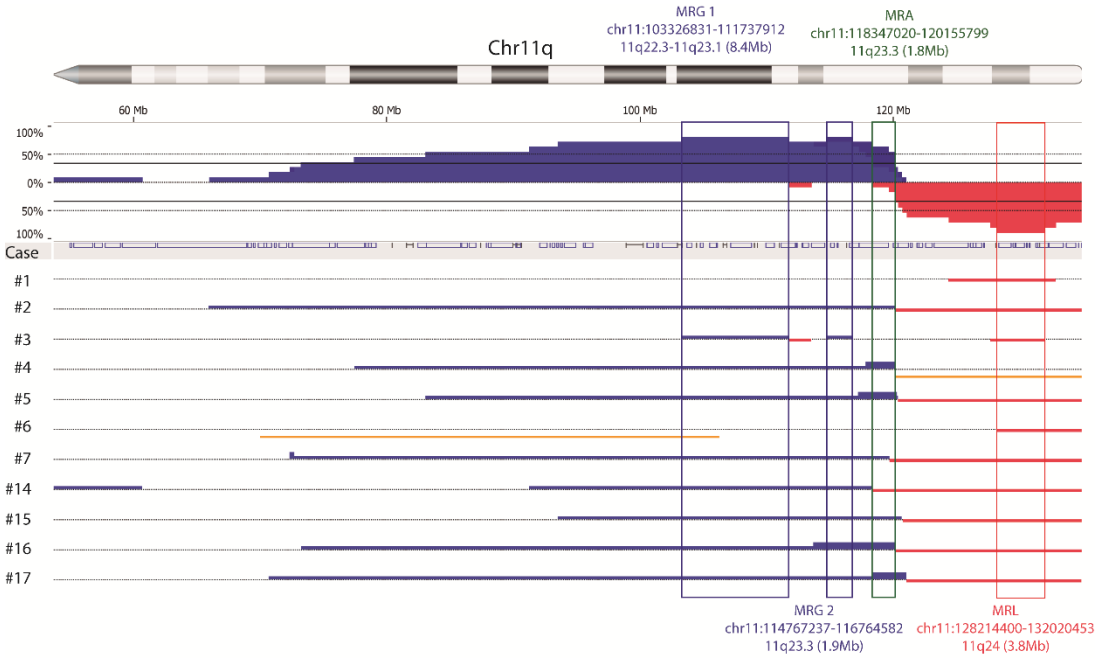

Supplementary Figure S6. Comparative plot of copy number aberrations between Burkitt-like lymphoma with 11q aberration (n=11) and **A)** conventional *MYC*-positive Burkitt Lymphoma (n=35) (Scholtysik *et al.*, 2010), **B)** GCB-Diffuse Large B-cell lymphoma (n=45) and (Karube *et al.*, 2018) **C)** ABC-Diffuse Large B-cell lymphoma (n=49) (Karube *et al.*, 2018). X-axis depicts chromosome positions with dotted lines pointing centromeres. Y-axis indicates frequency of the genomic aberration among the analyzed cases. Significantly different regions of alterations among groups (Fisher test non-adjusted $P \leq 0.01$) are labeled with corresponding color asterisks.

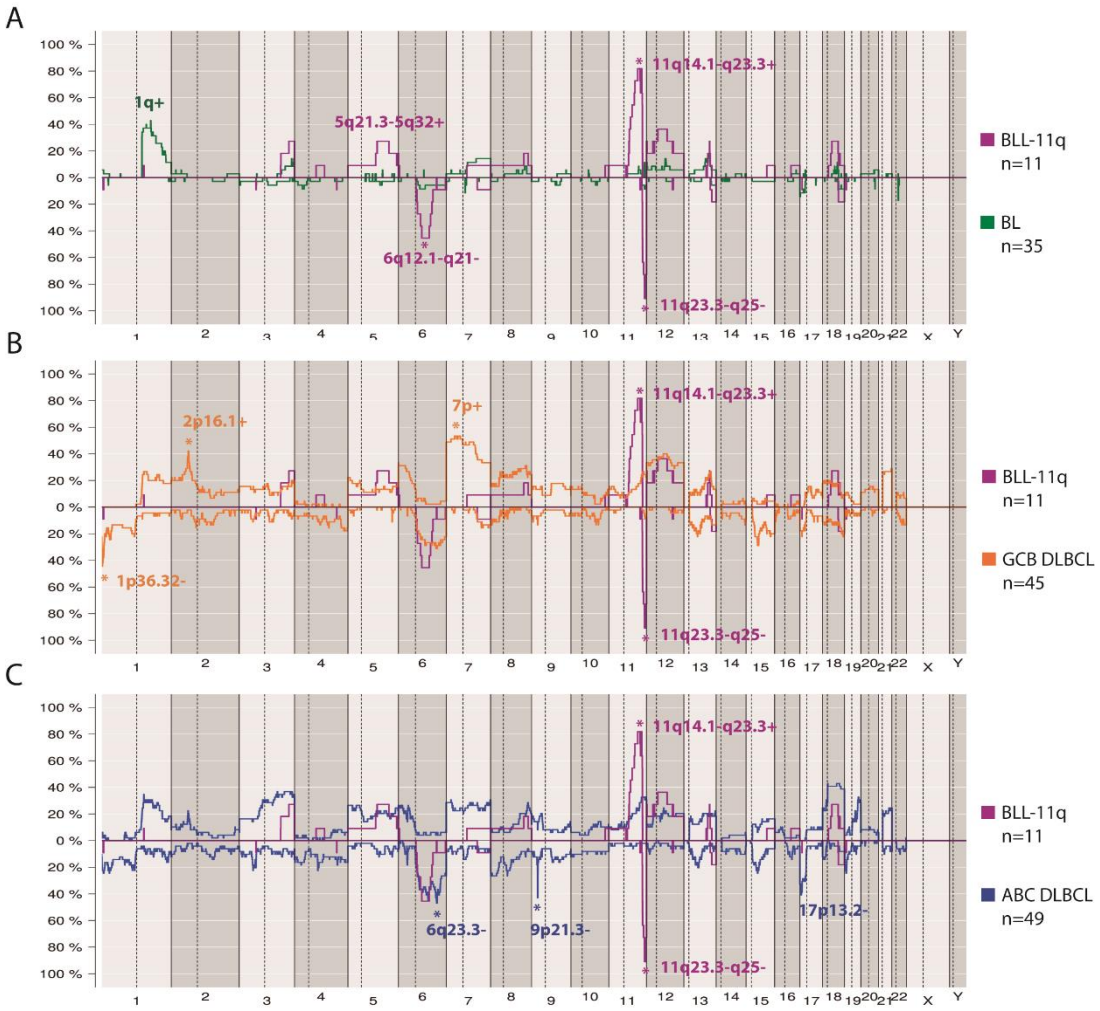

Supplementary Figure S7. A) Comparative plot of copy number aberrations between Burkitt-like lymphoma with 11q aberration (n=11) and 6 *MYC*-negative 11q-negative cases **B)** Mutational overview of 4 *MYC*-negative 11q negative cases in comparison with BLL with 11q aberration. The heat map shows the case specific pattern of driver mutations found by next generation sequencing. Each column represents a case and each row represents a gene. The right bar graph illustrates the mutation frequency of each gene.

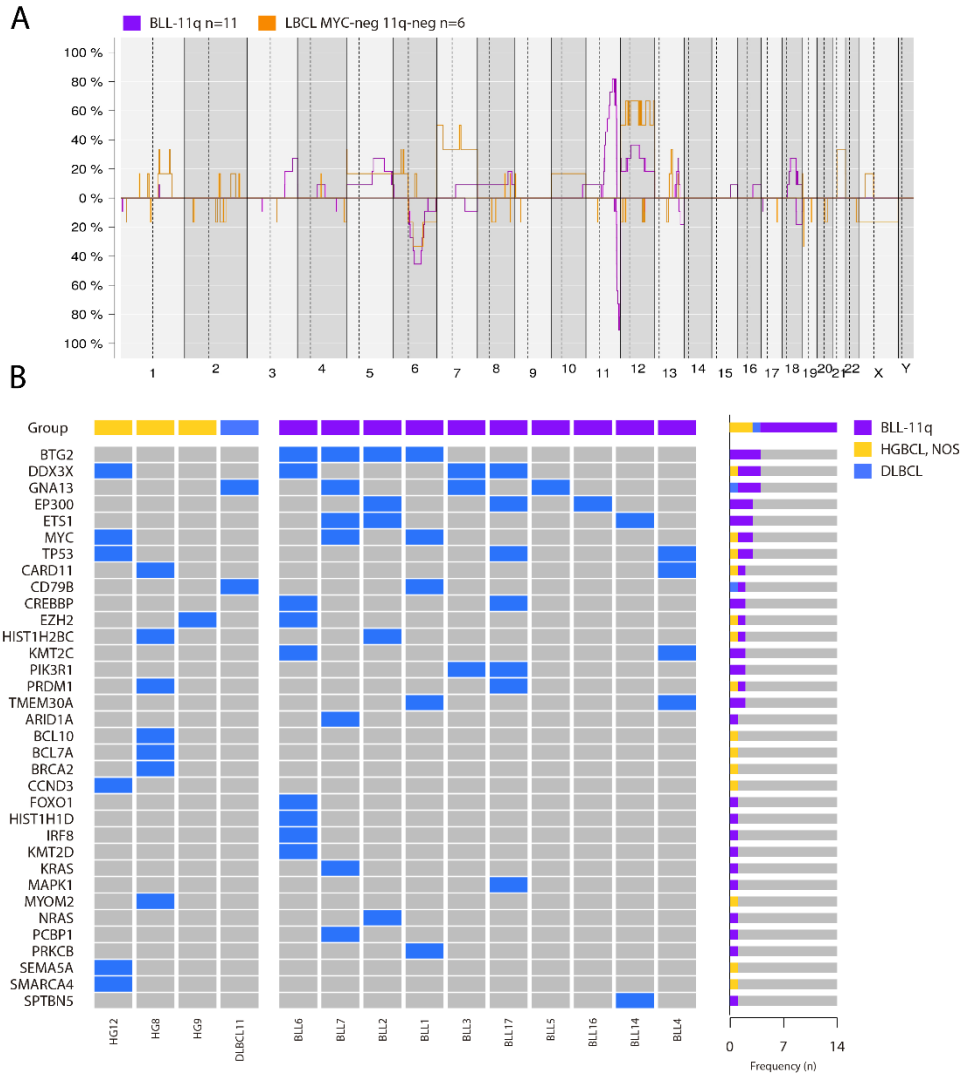

Supplementary Figure S8. Mean coverage distribution per gene of the 10 BLL-11q cases analyzed by target NGS. Y-axis indicates the mean number of reads. The red line depicts the mean coverage of all 10 cases. DNA from #2, #4 and #7 BLL-11q cases were extracted from frozen tissue.

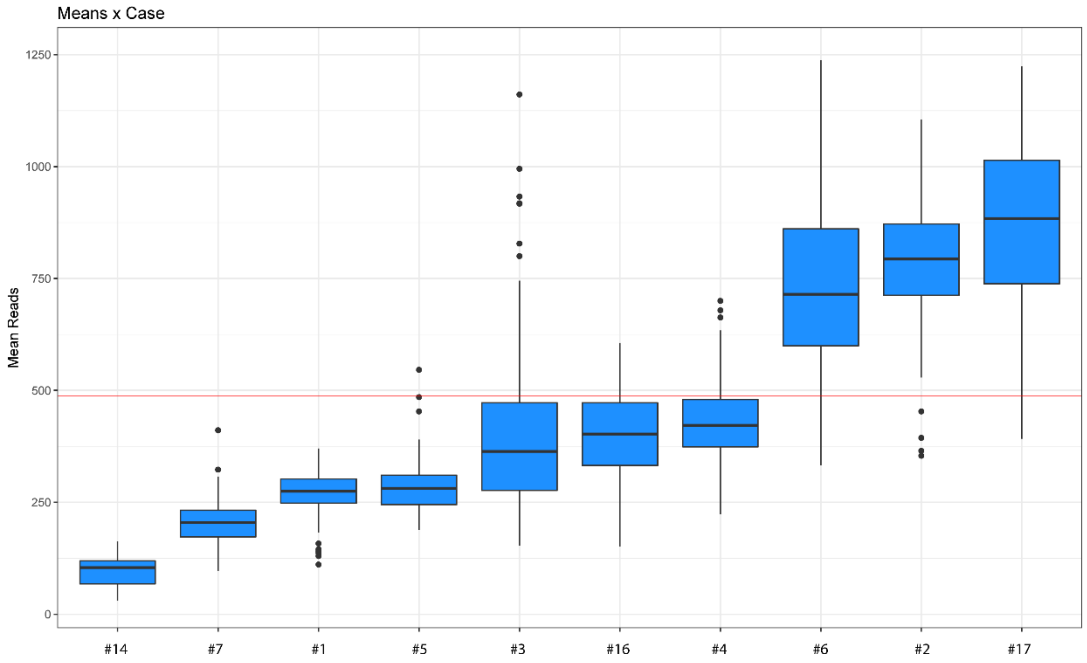

Supplementary Figure S9. NGS analysis pipeline followed to identify potential driver mutations in 10 BLL-11q samples. Two different variant callers were used: Somatic Variant Caller (Illumina) and Mutect2 (GATK version 4.0.3) and potential driver mutations were predicted according to previously published criteria (Karube *et al.*, 2018). SIFT predictor was only used for mutations in which a definitive score was not provided by Mutation Assessor.

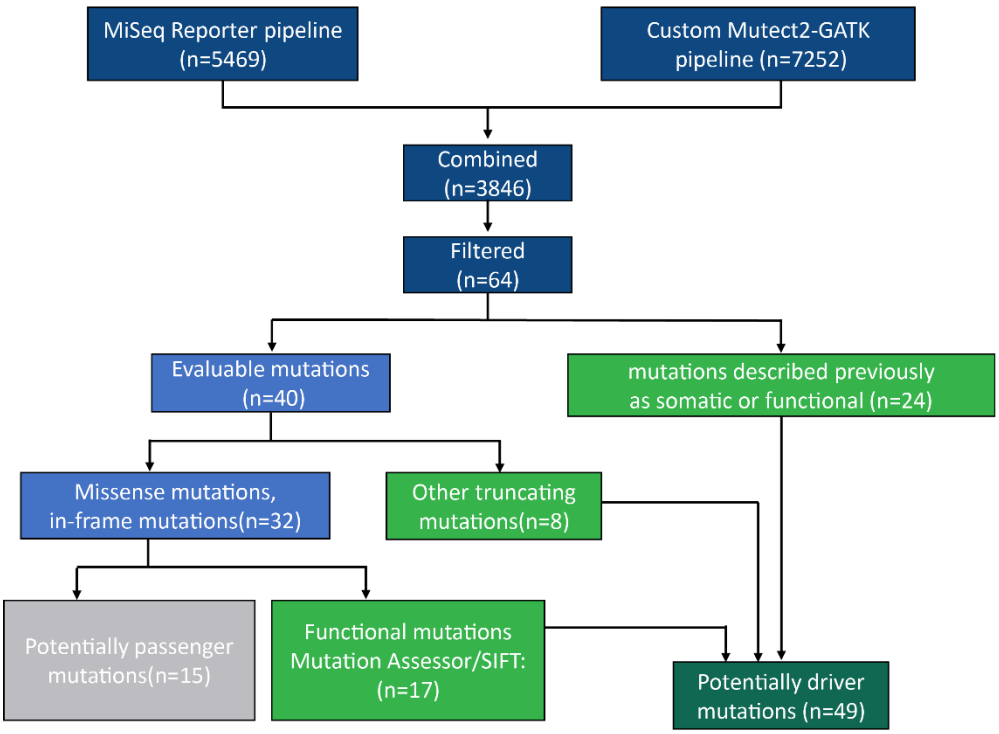

Supplementary Table S5. Summary of copy number findings and FISH pattern constellation of the 11q aberration in the current series of BLL-11q.

Case	CN array		11q FISH (CEP11 [D11Z1] + RP11-414G21+RP11-629A20)	
	Pattern of chr11	**Number of alterations**	**11q FISH constellation pattern[20]**	**11q FISH result**
#1	Only terminal loss	2 CNA	nuc ish (D11Z1x2,RP11-414G21x2,RP11-629A20x1)	Only terminal loss
#2	Gain/terminal loss	3 CNA	nuc ish (D11Z1x2,RP11-414G21x2,RP11-629A20x1)	Only terminal loss
#3	Gain/terminal loss	6 CNA, 1 CNN-LOH	nuc ish (D11Z1x2,RP11-414G21x2-3,RP11-629A20x1)	Gain*/terminal loss
#4	Gain/amplification/CNN-LOH	15 CNA+ 1CNN-LOH	nuc ish (D11Z1x2,RP11-414G21x2-5,RP11-629A20x2)	Amplification
#5	Gain/amplification/terminal loss	4 CNA	nuc ish (D11Z1x2,RP11-414G21x4-5,RP11-629A20x1)	Amplification/terminal loss
#6	Only terminal loss	6 CNA + 11 CNN-LOH	nuc ish (D11Z1x2,RP11-414G21x2,RP11-629A20x1)	Only terminal loss
#7	Gain/terminal loss	8 CNA	nuc ish (D11Z1x2,RP11-414G21x3,RP11-629A20x1)	Gain/terminal loss
#14	Gain/terminal loss	4 CNA	nuc ish (D11Z1x2,RP11-414G21x2,RP11-629A20x1)	Only terminal loss
#15	Gain/terminal loss	12 CNA + 1CNN-LOH	Not done	
#16	Gain/amplification/ terminal loss	4 CNA	nuc ish (D11Z1x2,RP11-414G21x3,RP11-629A20x1)	Gain/terminal loss
#17	Gain/amplification/ terminal loss	14 CNA +3 CNN-LOH	nuc ish (D11Z1x2,RP11-414G21x3-4,RP11-629A20x1)	Amplification* /terminal loss

CNA: copy number alteration. CNN-LOH: copy number neutral loss of heterozygosity. *Only observed in a few cells. CN and FISH results were not concordant in cases #2, and #14 most likely due to the fact that gained region covered by BAC RP11-414G21 was most likely inverted and then both copies were very narrow to be clearly distinguished as independent signals in the FISH constellation.

Supplementary Table S8. Mutational patterns across different germinal center derived lymphoma subgroups including BL (Richter *et al.*, 2012; Schmitz *et al.*, 2012), DLBCL (Morin *et al.*, 2013; Karube *et al.*, 2018), DH/TH (Momose *et al.*, 2015; Evrard *et al.*, 2019), and HGBCL, NOS with or without MYC rearrangement (Momose *et al.*, 2015). The BL pattern includes mutations in BL-associated genes and the GCB-DLBCL pattern includes mutations associated with GCB phenotype according to literature. BLL-11q mutational pattern includes genes mutated in more than 2 BLL-11q cases, not included in the other two signatures.

Mutational patterns	Gene	BLL-11q current series n=10 (%)	GCB-DLBCL n=83 (%)	HGBCL DH/TH n=44 (%)	HGBCL with or without *MYC*-R n=9 (%)	BL n=32 (%)
BLL-11q	***BTG2***	40	4.8*	-	-	0*
	ETS1	30	1.2*	-	-	0*
	EP300	30	6*	6.8	0	0*
Burkitt Lymphoma	***ID3***	0	0	25	88.9*	59.4*
	TCF3	0	0	4.5	0	31.3
	CCND3	0	3,6	29.2[b]	22.2	9.4
	MYC	20	2.4	43.2	44.4	71.9*
	DDX3X	30	0[a]*	-	-	31.3
GCB-DLBCL	***KMT2D***	20	32.5	60[c]	-	6.3
	CREBBP	20	25.3	50	44.4	6.3
	TNFRSF14	0	20.5	20[c]	-	0
	B2M	0	20.5	10[c]	-	0
	EZH2	10	21.7	27.3	0	0
	GNA13	30	21.7	15[c]	-	9.4
	FOXO1	10	13.3	30[c]	-	6.3
	ACTB	0	13.3	-	-	0
	SOCS1	0	15.7	30[c]	-	0

* Significant differences of mutated gene prevalence between BLL-11q series and the other germinal center entities ($P<0.05$).

[a] Only in Morin et al series n=23. [b] Only in Momose et al. n=24. [c] Only in Evrard et al. n=20.

Study 2:

Mutations of MAP2K1 are frequent in pediatric-type follicular lymphoma and result in ERK pathway activation.

Schmidt J*, **Ramis-Zaldivar JE***, Nadeu F, Gonzalez-Farre B, Navarro A, Egan C, Montes-Mojarro IA, Marafioti T, Cabeçadas J, van der Walt J, Dojcinov S, Rosenwald A, Ott G, Bonzheim I, Fend F, Campo E, Jaffe ES, Salaverria I, Quintanilla-Martinez L. ***Co-first author.**

Blood. 2017 Jul 20;130(3):323-327.

Summary

Pediatric-type follicular lymphoma (PTFL) is a distinct B-cell lymphoma entity which displays clinical, morphological, immunophenotypic and genetical differences with conventional FL from the adults. Recently, recurrent genetic alterations of potential importance for its pathogenesis that disrupt pathways associated with the germinal center reaction (*IRF8*), immune escape (*TNFRSF14*), and anti-apoptosis (*MAP2K1*) have been described. In an attempt to expand the knowledge onto the pathogenesis of PTFL, an integrative analysis of these mutations was undertaken in a large cohort of 43 cases previously characterized by targeted next-generation sequencing and copy number array. Mutations in *MAP2K1* were found in 49% of the cases, second in frequency to *TNFRSF14* alterations (54%). Immunohistochemical analysis of the *MAP2K1* downstream target extracellular signal-regulated kinase demonstrated its phosphorylation in the evaluable cases and revealed a good correlation with the allelic frequency of the *MAP2K1* mutation. On the other hand, the IRF8 p.K66R hot spot mutation was present only in 15% of the cases and was concomitant with *TNFRSF14* mutations in 4 cases. This hot spot seems to be highly characteristic for PTFL. Overall, *TNFRSF14* and *MAP2K1* mutations are the most frequent genetic alterations found in PTFL and occur independently in most cases, suggesting that both mutations might play an important role in PTFL lymphomagenesis.

Brief Report

blood

LYMPHOID NEOPLASIA

Mutations of *MAP2K1* are frequent in pediatric-type follicular lymphoma and result in ERK pathway activation

Janine Schmidt,[1,*] Joan Enric Ramis-Zaldivar,[2,*] Ferran Nadeu,[2] Blanca Gonzalez-Farre,[2] Alba Navarro,[2] Caoimhe Egan,[3] Ivonne Aidee Montes-Mojarro,[1] Teresa Marafioti,[4] Jose Cabeçadas,[5] Jon van der Walt,[6] Stefan Dojcinov,[7] Andreas Rosenwald,[8,9] German Ott,[10,11] Irina Bonzheim,[1] Falko Fend,[1] Elias Campo,[2] Elaine S. Jaffe,[3,†] Itziar Salaverria,[2,†] and Leticia Quintanilla-Martinez[1,†]

[1]Institute of Pathology and Neuropathology, Eberhard Karls University of Tübingen and Comprehensive Cancer Center, Tübingen University Hospital, Tübingen, Germany; [2]Hematopathology Unit, Hospital Clinic, Institut d'Investigacions Biomèdiques August Pi Sunyer, Centro de Investigación Biomédica en Red de Cáncer, Barcelona, Spain; [3]Hematopathology Section, Laboratory of Pathology, National Cancer Institute, Bethesda, MD; [4]Department of Cellular Pathology, Barts and The London National Health Service Trust, London, United Kingdom; [5]Pathology Department, Instituto Portugues de Oncologia, Lisbon, Portugal; [6]Department of Histopathology, Guy's and St Thomas' Hospitals, London, United Kingdom; [7]Department of Pathology, All Wales Lymphoma Panel, University Hospital of Wales, Cardiff, United Kingdom; [8]Institute of Pathology, University of Würzburg, Würzburg, Germany; [9]Comprehensive Cancer Center Mainfranken, Würzburg, Germany; [10]Department of Clinical Pathology, Robert Bosch Hospital, Stuttgart, Germany; and [11]Dr. Margarete Fischer-Bosch Institute of Clinical Pharmacology, Stuttgart, Germany

Key Points

- *TNFRSF14* and *MAP2K1* mutations are frequent in PTFL but do not occur together in the majority of cases.
- *MAP2K1* mutations lead to activation of the downstream target phosphorylated extracellular signal-regulated kinase.

Pediatric-type follicular lymphoma (PTFL) is a B-cell lymphoma with distinctive clinicopathological features. Recently, recurrent genetic alterations of potential importance for its pathogenesis that disrupt pathways associated with the germinal center reaction (*TNFRSF14*, *IRF8*), immune escape (*TNFRSF14*), and anti-apoptosis (*MAP2K1*) have been described. In an attempt to shed more light onto the pathogenesis of PTFL, an integrative analysis of these mutations was undertaken in a large cohort of 43 cases previously characterized by targeted next-generation sequencing and copy number array. Mutations in *MAP2K1* were found in 49% (20/41) of the cases, second in frequency to *TNFRSF14* alterations (22/41; 54%), and all together were present in 81% of the cases. Immunohistochemical analysis of the *MAP2K1* downstream target extracellular signal-regulated kinase demonstrated its phosphorylation in the evaluable cases and revealed a good correlation with the allelic frequency of the *MAP2K1* mutation. The *IRF8* p.K66R mutation was present in 15% (6/39) of the cases and was concomitant with *TNFRSF14* mutations in 4 cases. This hot spot seems to be highly characteristic for PTFL. In conclusion, *TNFRSF14* and *MAP2K1* mutations are the most frequent genetic alterations found in PTFL and occur independently in most cases, suggesting that both mutations might play an important role in PTFL lymphomagenesis. (*Blood*. 2017;130(3):323-327)

Introduction

Pediatric-type follicular lymphoma (PTFL) has been recognized as a definitive entity in the revised 2016 World Health Organization Lymphoma Classification.[1,2] Until recently, little was known about the genetic alterations involved in the pathogenesis of this disease. Nevertheless, several groups have described a specific mutational profile in PTFL distinct from other non-Hodgkin lymphomas, including conventional follicular lymphoma (FL), by using next-generation sequencing (NGS) technologies and copy number (CN) arrays.[3-5] Overall, PTFL lacks mutations of histone modifying genes frequently found in FL and shows low levels of genomic complexity in concordance with its indolent clinical behavior. The most frequently mutated genes reported in PTFL are *TNFRSF14*, *MAP2K1*, and *IRF8,* albeit at different frequencies in published series.[3-6] Furthermore, aberrations including CN neutral loss of heterozygosity (CNN-LOH) of the 1p36 region, containing *TNFRSF14,* have also been found in PTFL, suggesting a tumor suppressor function of this gene in this disease.[3,5-7]

Mutations observed in PTFL are not restricted to this disease and are well known to occur in other types of non-Hodgkin lymphoma. Mutations in *TNFRSF14* occur at high frequencies also in adult FL (18% to 44%)[8] and diffuse large B-cell lymphoma (DLBCL, 22%).[9] *MAP2K1* mutations have been described as driver mutations in hairy-cell leukemia variant (HCLv) and/or conventional HCL with immunoglobulin heavy-chain V4-34$^+$,[10,11] Langerhans cell histiocytosis,[12-14] and in isolated cases of chronic lymphocytic leukemia (CLL),[15,16] splenic marginal zone lymphoma,[17,18] and

Submitted 28 March 2017; accepted 13 May 2017. Prepublished online as *Blood* First Edition paper, 22 May 2017; DOI 10.1182/blood-2017-03-776278.

*J.S. and J.E.R.-Z. are joint first authors.

†E.S.J., I.S., and L.Q.-M. are joint senior authors.

The online version of this article contains a data supplement.

The publication costs of this article were defrayed in part by page charge payment. Therefore, and solely to indicate this fact, this article is hereby marked "advertisement" in accordance with 18 USC section 1734.

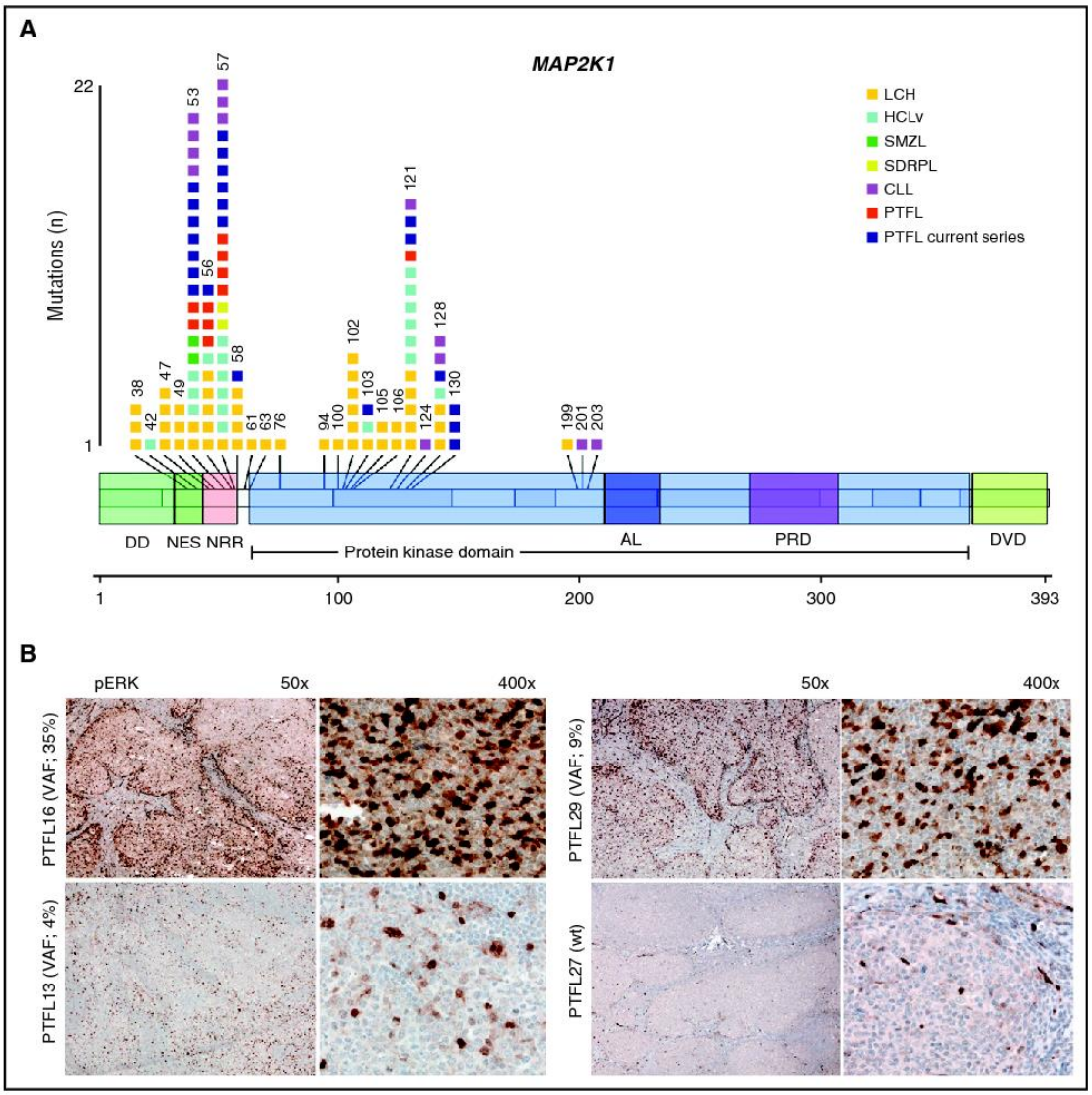

Figure 1. Distribution of *MAP2K1* mutations at protein and exon level in PTFL in comparison with other hematological neoplasias. (A) Schematic diagram of *MAP2K1* mutations in PTFL,[3,4] Langerhans cell histiocytosis (LCH),[12-14] hairy cell leukemia[10,11] (including HCLv and conventional HCL [HCLc] with IGHV4-34^{+}), splenic diffuse red pulp small B-cell lymphoma (SDRPL),[19] splenic marginal zone lymphoma (SMZL),[17,18] CLL,[15,16] according to NGS studies and/or Sanger analysis. Exons are represented by boxes on the body of MEK1 protein and the main protein domains are represented by larger colored boxes. AL, activation loop; DD, docking domain for ERK1 and ERK2; DVD, domain of versatile docking (MAP3K docking domain); NES, nuclear export sequence; NRR, negative regulatory region; PRD: proline-rich domain. (B) Immunohistochemical analysis of pERK in *MAP2K1* mutated and wild-type PTFL cases. Note that the variant allelic frequency (VAF, indicated in parentheses) of *MAP2K1* mutations by NGS analysis correlates with the amount of pERK-positive cells.

splenic diffuse red pulp lymphoma.[19] *IRF8* gene mutations have also been identified in DLBCL and FL, but without apparent functional consequences.[9,20-22]

A drawback in understanding the genetic landscape of PTFL is that the occurrence of these alterations has been described in different, mostly small cohorts of PTFL cases, and the cooccurrence of these mutations and their relevance for PTFL lymphomagenesis is not known. By expanding the genetic analysis of our published PTFL cohort[5] for *MAP2K1* and *IRF8* mutations, and performing an integrative analysis, we wanted to clarify their frequency and overlap with *TNFRSF14* mutations.

Study design

Cases

A total of 43 well-characterized PTFL cases were included. Clinical and morphological features were previously reported.[5]

Mutational analysis

All cases have been genetically characterized by targeted NGS and CN arrays using formalin-fixed paraffin-embedded tissue. Forty-one PTFL cases were

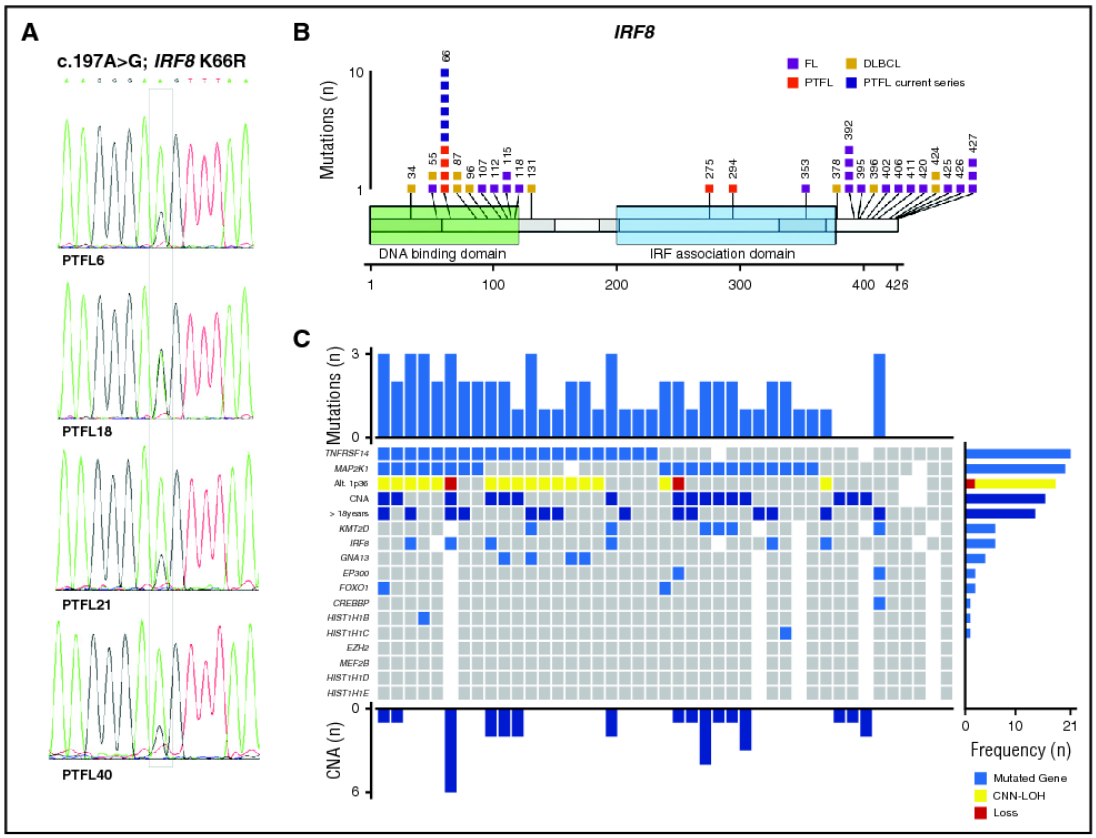

Figure 2. *IRF8* mutations and global mutational landscape in PTFL. (A) Sequence electropherograms from cases PTFL6, PTFL18, PTFL21, and PTFL40 showing *IRF8* p.K66R (c.197A>G) mutation by Sanger sequencing. PTFL18 carried a concomitant 16q11.2-q24.3 CNN-LOH, including an *IRF8* gene. (B) Schematic diagram of *IRF8* mutations in FL,[20-22] DLBCL,[9,25] and PTFL,[3,4] according to NGS studies. Exons are represented by boxes on the body of the protein and the main protein domains are represented by larger colored boxes. Domains of the protein are represented according to Uniprot database (www.uniprot.org).[4] (C) Overview of the global mutational landscape in 43 PTFL cases. Each column of the heat map represents 1 PTFL case and each line 1 specific analysis. On the right side of the figure, the frequency of the particular result of the analysis is shown.

additionally investigated for *MAP2K1* mutations using a single-amplicon NGS approach covering exons 2 and 3. The amplicons were analyzed on the Ion Torrent PGM (Thermo Fisher Scientific, Schwerte, Germany), as previously described.[5] The mean coverage of the amplicons was 18 132 reads (range, 104-79 524 reads). Sanger sequencing was performed to detect the *IRF8* p.K66R variant in 39 PTFL using primers previously described.[4] Allelic frequencies of these mutations are in the range of Sanger sequencing detection.[4] Sequence analysis was performed using Mutation Surveyor software (SoftGenetics LLC, State College, PA). The mutational analysis results were integrated to the previous genetic analysis.

Immunohistochemical analysis

Immunohistochemical analysis of phosphorylated extracellular signal-regulated kinase protein (pERK) (Cell Signaling Technologies) was performed in formalin-fixed paraffin-embedded sections in an automated immunostainer (Ventana Medical System, Tucson, AZ).

Results and discussion

Twenty of 41 PTFL (49%) cases carried *MAP2K1* mutations (Figure 1A). *MAP2K1* mutations were identified mainly in 2 hot spots within exon 2 (codons 53 and 57), which encode the negative regulatory region domain of MEK1 protein, corroborating previous results in PTFL,[3] HCLv,[10,11] and CLL.[15,16] In contrast, mutations in Langerhans cell histiocytosis spread across exons 2 and 3.[12-14] The allelic frequencies of *MAP2K1* mutations ranged between 4% and 35% (median, 10%). The frequency of *MAP2K1* mutations identified is similar to what we reported for *TNFRSF14* (21/41; 51%).[5] *MAP2K1* and/or *TNFRSF14* mutations were observed in 33/41 cases (81%); however, only 8 cases (8/41; 20%) showed mutations in both genes, whereas the majority of cases had either a *TNFRSF14* (13/41; 32%) or a *MAP2K1* (12/41; 29%) mutation. This finding indicates that both genes independently are of importance for the pathogenesis of PTFL, despite their different functional properties. *TNFRSF14* mutations abrogate the interaction between TNFRSF14 and BTLA (B and T lymphocyte attenuator) receptors disrupting an important tumor suppressor axis that leads to B-cell receptor activation.[7] The frequent *TNFRSF14* mutations together with CNN-LOH of 1p36 indicate a powerful selection against the *TNFRSF14* gene during PTFL development.

Because *MAP2K1* mutations are predicted to constitutively activate the downstream ERK1/2 proteins by phosphorylation, 12 PTFL cases (6 *MAP2K1* mutated cases and 6 wild-type cases), 3 reactive lymph nodes, and 3 tonsils were analyzed with a pERK antibody by

immunohistochemistry.[12-14] In normal lymph nodes, tonsils, and PTFL cases without *MAP2K1* mutation, the staining was negative in the germinal center (GC) cells with positive internal control in the endothelial cells (Figure 1B). The analysis in the PTFL cases revealed a good correlation of pERK staining and allelic frequency of *MAP2K1* mutation in the GC cells in the different cases, and confirmed the downstream activation of ERK in PTFL (Figure 1B; supplemental Table 1, available on the *Blood* Web site). Despite different functions, both genes/proteins have in common the control of signaling pathways important for B-cell proliferation.

Another interesting finding is the higher allelic frequency of *TNFRSF14* mutations in comparison with *MAP2K1* mutations, including 5 cases with both mutations (median ± standard deviation, 17.8 ± 6.3, vs 10 ± 8.6, $P = .046$), even after correcting for concomitant CNN-LOH of 1p36 found in 14/20 *TNFRSF14*-mutated cases. This suggests that *TNFRSF14* mutations occur earlier in tumorigenesis than *MAP2K1* mutations (supplemental Figure 1).

The *IRF8* mutations at the hotspot p.K66R (c.197A>G), affecting the DNA binding domain, were recently reported to be specific for PTFL.[4] Accordingly, 6 of 39 cases analyzed (15%) carried this mutation (Figure 2A), and only 1 case (PTFL18) showed a concomitant 16q CNN-LOH alteration. The frequency of *IRF8* mutations found in the present study was lower than that described by Ozawa et al (15 vs 50%).[4] The difference might be explained by the small cohort of 6 cases analyzed in that study. The *IRF8* gene has been described as potential tumor suppressor in myeloid neoplasms and has recently also been linked to the pathogenesis of B-cell lymphomas. Specifically, *IRF8* mutations have been observed in adult FL and DLBCL in 5% to 10% of cases.[9,20,21] However, in contrast to PTFL where the *IRF8* p.K66R mutation is predicted to affect DNA-protein interaction,[4] these mutations are frequently indel and missense mutations predominantly located in the IRF8 C-terminal domain (Figure 2B) with still unidentified functional consequences.[9,20-22] Of note, *IRF8* and *TNFRSF14* are critical regulators of the immune system development and function.[7,23] Both genes regulate GC B-cell activation,[7,23] and deficiency of *IRF8* has been reported to induce a hyperproliferative phenotype in pre-B cells.[24] Interestingly, 4 of 6 *IRF8* mutated cases also showed *TNFRSF14* mutations, suggesting possible cooperation between these 2 genes.

In conclusion, this integrative genetic analysis demonstrated that in 88% of PTFL cases (38/43), 1 or several alterations/genetic events were identified (Figure 2C). Only 5 cases (12%) did not show genetic alterations other than immunoglobulin heavy-chain rearrangement. *TNFRSF14* and *MAP2K1* mutations are found in about half of the cases each, but do not occur together in the majority of the cases, indicating important but distinct roles in lymphomagenesis for both genes. We confirmed that *IRF8* p.K66R mutations are highly specific for PTFL but occur less commonly than other events. Nevertheless, the similar functions and often cooccurrence of *IRF8* and *TNFRSF14* mutations suggest that these 2 mutations might cooperate in the pathogenesis of PTFL.

Acknowledgments

The authors are grateful to Noelia Garcia, Silvia Martín, Sieglinde Baisch, Claudia Hermann, and Sema Colak for excellent technical assistance.

This work was partially developed at the Centro Esther Koplowitz, Barcelona, Spain. This work was supported by Fondo de Investigaciones Sanitarias Instituto de Salud Carlos III (CP13/00159 and PI15/00580) (I.S.), Generalitat de Catalunya Suport Grups de Recerca (2013-SGR-378 I.S. and 2014-SGR-795) (E.C.), the European Regional Development Fund "Una manera de fer Europa" and the Wilhelm-Sander-Stiftung (2015.058.1) (L.Q.-M. and F.F.). J.S. was supported by the Wilhelm-Sander-Stiftung. J.E.R.-Z. was supported by a fellowship from Generalitat de Catalunya AGAUR FI-DGR 2017 (2017 FI_B01004). E.C. is an Academia Researcher of the "Institució Catalana de Recerca i Estudis Avançats" of the Generalitat de Catalunya.

Authorship

Contribution: L.Q.-M. and I.S. conceived and designed the study, supervised the experimental work, and wrote the manuscript; J.S., I.B., J.E.R.-Z., A.N., and I.S. performed genetic analysis and interpreted the data; F.N. performed bioinformatics analysis; B.G.-F., T.M., J.C., J.v.d.W., A.R., G.O., S.D., C.E., E.S.J., F.F., E.C., and L.Q.-M. contributed with cases; I.A.M.-M. and L.Q.-M. performed and interpreted the immunohistochemical analysis; and J.S., E.S.J., E.C., and F.F. analyzed the data and helped writing the manuscript.

Conflict-of-interest disclosure: The authors declare no competing financial interests.

ORCID profiles: J.E.R.-Z., 0000-0001-7108-7738; F.N., 0000-0003-2910-9440; B.G.-F., 0000-0002-1796-7248; A.N., 0000-0002-4041-0974; E.C., 0000-0001-9850-9793; I.S., 0000-0002-2427-9822; L.Q.-M., 0000-0001-7156-5365.

Correspondence: Leticia Quintanilla-Martinez, Institute of Pathology, Tübingen University Hospital, Liebermeisterstr 8, 72076 Tübingen, Germany; e-mail: leticia.quintanilla-fend@med.uni-tuebingen.de; and Itziar Salaverria, Institut d'Investigacions Biomèdiques August Pi i Sunyer, Rosselló 153, Barcelona, 08036, Spain; e-mail: isalaver@clinic.ub.es.

References

1. Quintanilla-Martinez L, Sander B, Chan JK, et al. Indolent lymphomas in the pediatric population: follicular lymphoma, IRF4/MUM1+ lymphoma, nodal marginal zone lymphoma and chronic lymphocytic leukemia. *Virchows Arch.* 2016;468(2):141-157.
2. Swerdlow SH, Campo E, Pileri SA, et al. The 2016 revision of the World Health Organization classification of lymphoid neoplasms. *Blood.* 2016;127(20):2375-2390.
3. Louissaint A Jr, Schafernak KT, Geyer JT, et al. Pediatric-type nodal follicular lymphoma: a biologically distinct lymphoma with frequent MAPK pathway mutations. *Blood.* 2016;128(8):1093-1100.
4. Ozawa MG, Bhaduri A, Chisholm KM, et al. A study of the mutational landscape of pediatric-type follicular lymphoma and pediatric nodal marginal zone lymphoma. *Mod Pathol.* 2016;29(10):1212-1220.
5. Schmidt J, Gong S, Marafioti T, et al. Genome-wide analysis of pediatric-type follicular lymphoma reveals low genetic complexity and recurrent alterations of TNFRSF14 gene. *Blood.* 2016;128(8):1101-1111.
6. Martin-Guerrero I, Salaverria I, Burkhardt B, et al. Recurrent loss of heterozygosity in 1p36 associated with TNFRSF14 mutations in IRF4 translocation negative pediatric follicular lymphomas. *Haematologica.* 2013;98(8):1237-1241.
7. Boice M, Salloum D, Mourcin F, et al. Loss of the HVEM tumor suppressor in lymphoma and restoration by modified CAR-T cells. *Cell.* 2016;167(2):405-418.
8. Launay E, Pangault C, Bertrand P, et al. High rate of TNFRSF14 gene alterations related to 1p36 region in de novo follicular lymphoma and impact on prognosis. *Leukemia.* 2012;26(3):559-562.
9. Lohr JG, Stojanov P, Lawrence MS, et al. Discovery and prioritization of somatic mutations in diffuse large B-cell lymphoma (DLBCL) by

whole-exome sequencing. *Proc Natl Acad Sci USA*. 2012;109(10):3879-3884.

10. Mason EF, Brown RD, Szeto DP, et al. Detection of activating MAP2K1 mutations in atypical hairy cell leukemia and hairy cell leukemia variant. *Leuk Lymphoma*. 2017;58(1):233-236.
11. Waterfall JJ, Arons E, Walker RL, et al. High prevalence of MAP2K1 mutations in variant and IGHV4-34-expressing hairy-cell leukemias. *Nat Genet*. 2014;46(1):8-10.
12. Brown NA, Furtado LV, Betz BL, et al. High prevalence of somatic MAP2K1 mutations in BRAF V600E-negative Langerhans cell histiocytosis. *Blood*. 2014;124(10):1655-1658.
13. Chakraborty R, Hampton OA, Shen X, et al. Mutually exclusive recurrent somatic mutations in MAP2K1 and BRAF support a central role for ERK activation in LCH pathogenesis. *Blood*. 2014; 124(19):3007-3015.
14. Zeng K, Ohshima K, Liu Y, et al. BRAFV600E and MAP2K1 mutations in Langerhans cell histiocytosis occur predominantly in children [published online ahead of print 6 Sept 2016]. *Hematol Oncol*. doi: 10.1002/hon.2344.
15. Landau DA, Tausch E, Taylor-Weiner AN, et al. Mutations driving CLL and their evolution in progression and relapse. *Nature*. 2015; 526(7574):525-530.
16. Puente XS, Beà S, Valdés-Mas R, et al. Non-coding recurrent mutations in chronic lymphocytic leukaemia. *Nature*. 2015; 526(7574):519-524.
17. Rossi D, Trifonov V, Fangazio M, et al. The coding genome of splenic marginal zone lymphoma: activation of NOTCH2 and other pathways regulating marginal zone development. *J Exp Med*. 2012;209(9):1537-1551.
18. Spina V, Khiabanian H, Messina M, et al. The genetics of nodal marginal zone lymphoma. *Blood*. 2016;128(10):1362-1373.
19. Martinez D, Navarro A, Martinez-Trillos A, et al. NOTCH1, TP53, and MAP2K1 mutations in splenic diffuse red pulp small B-cell lymphoma are associated with progressive disease. *Am J Surg Pathol*. 2016;40(2):192-201.
20. Okosun J, Bödör C, Wang J, et al. Integrated genomic analysis identifies recurrent mutations and evolution patterns driving the initiation and progression of follicular lymphoma. *Nat Genet*. 2014;46(2):176-181.
21. Li H, Kaminski MS, Li Y, et al. Mutations in linker histone genes HIST1H1 B, C, D, and E; OCT2 (POU2F2); IRF8; and ARID1A underlying the pathogenesis of follicular lymphoma. *Blood*. 2014; 123(10):1487-1498.
22. Green MR, Kihira S, Liu CL, et al. Mutations in early follicular lymphoma progenitors are associated with suppressed antigen presentation. *Proc Natl Acad Sci USA*. 2015;112(10): E1116-E1125.
23. Lu R. Interferon regulatory factor 4 and 8 in B-cell development. *Trends Immunol*. 2008;29(10): 487-492.
24. Ma S, Pathak S, Mandal M, Trinh L, Clark MR, Lu R. Ikaros and Aiolos inhibit pre-B-cell proliferation by directly suppressing c-Myc expression. *Mol Cell Biol*. 2010;30(17): 4149-4158.
25. Morin RD, Johnson NA, Severson TM, et al. Somatic mutations altering EZH2 (Tyr641) in follicular and diffuse large B-cell lymphomas of germinal-center origin. *Nat Genet*. 2010; 42(2):181-185.

Supplemental Data

Supplemental Figure Legend

Supplemental Figure 1. Hierarchy in somatic mutations in PTFL according to VAF. Representation of variant allelic frequencies (VAF) values of the *TNFRSF14*, *MAP2K1* and *KMT2D* by case. Values for mutations with concomitant CNN-LOH were corrected. *TNFRSF14* mutation in case PTFL18 is not represented because mutations of this gene were analyzed only by Sanger sequencing.

Supplemental Figure 1

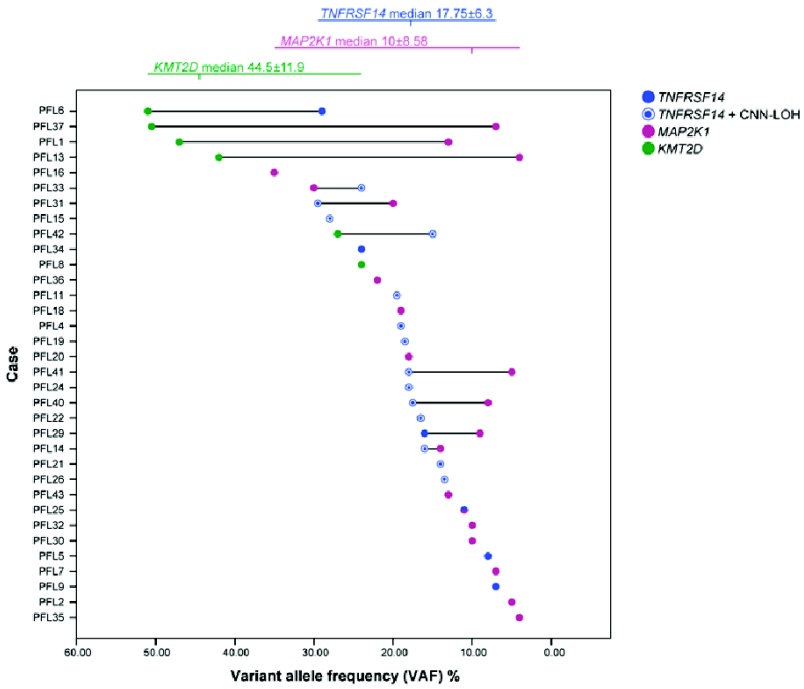

Supplementary Table

Supplemental Table 1 Correlation of allelic frequency of *MAP2K1* mutation and pERK staining in 12 analyzed PTFL cases.

Case number	*MAP2K1* mutation VAF	IHC pERK % of positive cells
PTFL 16	35%	30%
PTFL 31	20%	60%
PTFL 18	19%	25%
PTFL 29	9%	15%
PTFL 7	7%	15%
PTFL 13	4%	5%
PTFL 3	WT	neg
PTFL 10	WT	neg
PTFL 17	WT	neg
PTFL 27	WT	neg
PTFL 28	WT	neg
PFL 42	WT	neg

Abbreviations: VAF, variant allele frequency; WT, wild type; neg, negative; pERK, phospho-ERK

Study 3

Distinct molecular profile of IRF4-rearranged large B-cell lymphoma.

Ramis-Zaldivar JE*, Gonzalez-Farre B*, Balague O, Celis V, Nadeu F, Salmerón-Villalobos J, Andrés M, Martin-Guerrero I, Garrido G, Gaafar A, Suñol M, Bárcena C, Garcia-Bragado F, Andión M, Azorín D, Astigarraga I, Sagaseta de Ilurdoz M, Sábado C, Gallego S, Verdú-Amorós J, Fernandez-Delgado R, Perez V, Tapia G, Mozos A, Torrent M, Solano-Páez P, Rivas- Delgado A, Dlouhy I, Clot G, Enjuanes A, Lopez-Guillermo A, Galera P, Oberley M, Maguire A, Ramsower C, Rimsza LM, Quintanilla-Martinez L, Jaffe ES,Campo E, Salaverria I. ***Co-first autor.**

Blood, 2020:135(4):274–286.

Summary

Pediatric large B-cell lymphomas (LBCLs) share morphological and phenotypic features with adult types but have better prognosis. The higher frequency of some subtypes such as LBCL with *IRF4* rearrangement (LBCL-*IRF4*) in children suggests that some age-related biological differences may exist. To characterize the genetic and molecular heterogeneity of these tumors, we studied 31 diffuse large B-cell lymphomas (DLBCLs); 20 LBCL-IRF4 cases; and 12 cases of high-grade B-cell lymphoma, not otherwise specified (HGBCL, NOS) in patients ≤25 years using an integrated approach, including targeted gene sequencing, copy number arrays, and gene expression profiling. Each subgroup displayed different molecular profiles. LBCL-*IRF4* had frequent mutations in frequent mutations in *IRF4* and NF-kB related genes (*CARD11* and *CD79B*), losses of 17p13 without concomitant *TP53* mutations, gains of chromosome 7 and 11q12.3-q25 and overexpression of downstream target genes of the NF-kB pathway. On the other hand, DLBCL was predominantly of germinal center B-cell (GCB) subtype and carried gene mutations similar to the adult GCB-DLBCL counterpart (e.g., *SOCS1* and *KMT2D*), gains of 2p16, and losses of 19p13. Finally, a subset of HGBCL, NOS displayed recurrent alterations of Burkitt lymphoma-related genes such as *MYC*, *ID3*, and *DDX3X* and homozygous deletions of 9p21/*CDKN2A*, whereas other cases were genetically closer to GCB DLBCL. Regarding prognostic aspects, we could identified the prognostic value of several clinical and molecular features such as age higher than 18 years old, high LDH levels, ABC-subtype, high genetic complexity including chromothripsis and *TP53* mutations, as seen in adult population, in addition to 19p13/*TNFSF7*/*TNFSF9* homozygous deletions and 1q21-q44/*MDM4/MCL1* gains. In conclusion, these findings further unravel the molecular heterogeneity of pediatric and young adult LBCL and may help to improve the classification of this group of tumors and to provide new parameters for risk stratification.

blood®
Regular Article

LYMPHOID NEOPLASIA

Distinct molecular profile of *IRF4*-rearranged large B-cell lymphoma

Joan Enric Ramis-Zaldivar,[1,2,*] Blanca Gonzalez-Farré,[1-3,*] Olga Balagué,[3] Verónica Celis,[4] Ferran Nadeu,[1,2] Julia Salmerón-Villalobos,[1] Mara Andrés,[5] Idoia Martin-Guerrero,[6,7] Marta Garrido-Pontnou,[8] Ayman Gaafar,[9] Mariona Suñol,[10] Carmen Bárcena,[11] Federico Garcia-Bragado,[12] Maitane Andión,[13] Daniel Azorín,[14] Itziar Astigarraga,[7] Maria Sagaseta de Ilurdoz,[15] Constantino Sábado,[16] Soledad Gallego,[16] Jaime Verdú-Amorós,[17] Rafael Fernandez-Delgado,[17] Vanesa Perez,[18] Gustavo Tapia,[19] Anna Mozos,[20] Montserrat Torrent,[21] Palma Solano-Páez,[22] Alfredo Rivas-Delgado,[3] Ivan Dlouhy,[3] Guillem Clot,[1,2] Anna Enjuanes,[1,2] Armando López-Guillermo,[3] Pallavi Galera,[23] Matthew J. Oberley,[24] Alanna Maguire,[25] Colleen Ramsower,[25] Lisa M. Rimsza,[26] Leticia Quintanilla-Martinez,[27] Elaine S. Jaffe,[23] Elías Campo,[1-3] and Itziar Salaverria[1,2]

[1]Institut d'Investigacions Biomèdiques August Pi i Sunyer, Barcelona, Spain; [2]Centro de Investigación Biomédica en Red de Cáncer, Madrid, Spain; [3]Hematopathology Unit, Hospital Clínic de Barcelona, University of Barcelona, Barcelona, Spain; [4]Pediatric Oncology Department, Hospital Sant Joan de Déu, Esplugues de Llobregat, Spain; [5]Pediatric Oncology Department, Hospital Universitario y Politécnico La Fe de Valencia, Valencia, Spain; [6]Department of Genetics, Physical Anthropology, and Animal Physiology, Faculty of Science and Technology, University of the Basque Country, Universidad del Pais Vasco/Euskal Herriko Unibertsitatea, Leioa, Spain; [7]Pediatric Oncology Unit, Hospital Universitario Cruces Osakidetza, Biocruces Bizkaia Health Research Institute, Barakaldo, Spain; [8]Pathology Department, Hospital Universitari Vall d'Hebron, Barcelona, Spain; [9]Pathology Department, Hospital Universitario Cruces Osakidetza, Biocruces Bizkaia Health Research Institute, Barakaldo, Spain; [10]Pathology Department, Hospital Sant Joan de Déu, Esplugues de Llobregat, Spain; [11]Pathology Department, Hospital Universitario 12 de Octubre, Madrid, Spain; [12]Pathology Department, Complejo Hospitalario de Navarra, Pamplona, Spain; [13]Pediatric Oncology Department and [14]Pathology Department, Hospital Universitario Infantil Niño Jesus, Madrid, Spain; [15]Pediatric Oncology Department, Complejo Hospitalario de Navarra, Pamplona, Spain; [16]Pediatric Oncology Department, Hospital Universitari Vall d'Hebron, Barcelona, Spain; [17]Pediatric Oncology Department, Hospital Clínico Universitario de Valencia, Valencia, Spain; [18]Pediatric Oncology Department, Hospital Universitario 12 de Octubre, Madrid, Spain; [19]Pathology Department, Hospital Trias i Pujol, Badalona, Spain; [20]Pathology Department and [21]Pediatric Oncology Department, Hospital de Sant Pau i la Santa Creu, Barcelona, Spain; [22]Pediatric Oncology Department, Hospital Virgen del Rocio, Sevilla, Spain; [23]Laboratory of Pathology, National Institutes of Health, Bethesda, MD; [24]Department of Pathology and Laboratory Medicine, Children's Hospital Los Angeles, Los Angeles, CA; [25]Department of Research, Mayo Clinic, Scottsdale, AZ; [26]Department of Laboratory Medicine and Pathology, Mayo Clinic, Phoenix, AZ; and [27]Institute of Pathology, University Hospital Tübingen, Eberhard Karls University of Tübingen, Tübingen, Germany

KEY POINTS

- **LBCL with *IRF4* rearrangement displays a mutational profile distinct from other LBCLs affecting pediatric and young adult patients.**
- **Age, high genetic complexity, ABC profile, and *TP53* mutations are associated with poor prognosis in pediatric and young adult LBCL.**

Pediatric large B-cell lymphomas (LBCLs) share morphological and phenotypic features with adult types but have better prognosis. The higher frequency of some subtypes such as LBCL with *IRF4* rearrangement (LBCL-*IRF4*) in children suggests that some age-related biological differences may exist. To characterize the genetic and molecular heterogeneity of these tumors, we studied 31 diffuse LBCLs (DLBCLs), not otherwise specified (NOS); 20 LBCL-*IRF4* cases; and 12 cases of high-grade B-cell lymphoma (HGBCL), NOS in patients ≤25 years using an integrated approach, including targeted gene sequencing, copy-number arrays, and gene expression profiling. Each subgroup displayed different molecular profiles. LBCL-*IRF4* had frequent mutations in *IRF4* and NF-κB pathway genes (*CARD11*, *CD79B*, and *MYD88*), losses of 17p13 and gains of chromosome 7, 11q12.3-q25, whereas DLBCL, NOS was predominantly of germinal center B-cell (GCB) subtype and carried gene mutations similar to the adult counterpart (eg, *SOCS1* and *KMT2D*), gains of 2p16/*REL*, and losses of 19p13/*CD70*. A subset of HGBCL, NOS displayed recurrent alterations of Burkitt lymphoma–related genes such as *MYC*, *ID3*, and *DDX3X* and homozygous deletions of 9p21/*CDKN2A*, whereas other cases were genetically closer to GCB DLBCL. Factors related to unfavorable outcome were age >18 years; activated B-cell (ABC) DLBCL profile, HGBCL, NOS, high genetic complexity, 1q21-q44 gains, 2p16/*REL* gains/amplifications, 19p13/*CD70* homozygous deletions, and *TP53* and *MYC* mutations. In conclusion, these findings further unravel the molecular heterogeneity of pediatric and young adult LBCL, improve the classification of this group of tumors, and provide new parameters for risk stratification. (*Blood*. 2020;135(4):274-286)

Introduction

Large B-cell lymphomas (LBCLs) in children and young adults have morphological and phenotypic features similar to those observed in their adult counterparts. However, the more favorable outcome of most pediatric patients after high-dose chemotherapy may be due, among other factors, to a different underlying biology.[1] Recent molecular studies of diffuse LBCLs (DLBCLs) not otherwise specified (NOS) in adults revealed that

the heterogeneity of these tumors is mainly related to cell-of-origin (COO) subtyping into germinal center B cells (GCBs) or activated B cells (ABCs), and a plethora of genomic alterations defining specific clusters with different clinical manifestations and outcome.[2-7]

Aggressive mature B-cell lymphomas in children and young adults include Burkitt lymphoma (BL), primary mediastinal large B-cell lymphoma (PMBL), and DLBCL, NOS. The first 2 subtypes have been extensively studied with now well-established profiles of genomic alterations.[8-12] However, the molecular characterization of DLBCL, NOS in this age group is less defined. In fact, the constellation of LBCL in these patients seems more diverse than initially recognized. Clinicopathologic studies of LBCL in children have identified 2 additional tumors subtypes, included in the recent update of the World Health Organization (WHO) classification as provisional entities, that have overlapping features with BL and DLBCL.[13] Burkitt-like lymphoma with 11q aberration (BLL-11q) is a high-grade B-cell lymphoma (HGBCL) that was initially considered BL related but without *MYC* translocations.[14] However, 2 recent molecular studies have identified that these tumors lack the common BL mutations in the TCF3-ID3 axis and carry alterations closer to those found in GCB-DLBCL, although with differences suggesting they are a specific DLBCL subtype.[15,16] LBCL with *IRF4* rearrangement (LBCL-*IRF4*) predominates in pediatric population, has a favorable outcome after therapy, and consistently expresses IRF4 due to translocation.[17-20] These cases display a complex pattern of chromosomal changes, but their mutational profile and possible relationship to other LBCLs is not known.[21] The last WHO classification has also recognized the category of HGBCL that encompasses a spectrum of morphological appearances from blastoid to cases with intermediate features between BL and DLBCL.[13] The mutational profile of these tumors is not well known, but some studies in adults have identified the simultaneous presence of characteristic mutations of both BL and DLBCL.[22,23] The genomic features of these tumors in pediatric populations and their relationship to other LBCLs in this group of patients are not known.

Pediatric LBCLs and BL are treated using the same therapeutic protocols.[1,24] Although generally curable with this intensive chemotherapy, ~10% of cases relapse.[1] Biological prognostic parameters predicting an adverse outcome have been extensively studied in adult DLBCL[5,6,25,26] but are less well defined in pediatric and young adult tumors, with only few studies reported.[24,27] A better understanding of the molecular pathogenesis of these tumors may assist in defining management protocols better suited to the biology of the disease. In the present study, we aimed to extensively characterize the molecular landscape of LBCL in the pediatric and young adult population and identify clinically relevant molecular features specific to different subtypes that are distinct from adult cases.

Methods

Patients and samples

Sixty-three patients <26 years with LBCL were included in the study and centrally reviewed by 3 hematopathologists (B.G.-F., O.B., and E.C.). Cases were classified according to WHO criteria[13] into DLBCL, NOS (n = 31); LBCL-*IRF4* (n = 20); and HGBCL, NOS (n = 12). No HGBCLs with *MYC* and *BCL2*/*BCL6* rearrangements were identified. Fifty-three cases (51 primary and 2 relapses obtained 10 and 23 months after first diagnosis) were gathered in a centralized review supported by Sociedad Española de Hematología y Oncología Pediátrica or from the hematopathology files of Hospital Clínic of Barcelona, Spain. Additionally, 9 LBCL-*IRF4* and 1 DLBCL, NOS were consultation cases from the University of Tübingen (Tübingen, Germany), National Institutes of Health (Bethesda, MD), and Children's Hospital Los Angeles (Los Angeles, CA). Moreover, samples at relapse from 3 patients with primary tumor available were investigated. BL, BLL-11q, and PMBL cases were excluded. This study was approved by our institutional review board and in accordance with the Declaration of Helsinki.

Immunohistochemistry and FISH

Immunohistochemistry and fluorescence in situ hybridization (FISH) analyses were performed using standard protocols. The morphology, growth pattern, cytology, and immunohistochemical stains together with Epstein-Barr virus (EBV) in situ hybridization were evaluated as part of the diagnostic workup (supplemental Table 1, available on the *Blood* Web site). Cases were classified as germinal center (GC) and non-GC subtypes according to the Hans algorithm.[28] Genetic alterations of *BCL2*, *BCL6*, *MYC*, *IRF4*, *CIITA*, and IGH were analyzed by commercial (Metasystems, Altlußheim, Germany) or homemade FISH probes.[17,29]

Targeted NGS and mutational analysis

Fifty-five LBCLs from 52 patients were examined for the mutational status of 96 B-cell lymphoma–related genes (supplemental Table 2) using the SureSelectXT Target Enrichment System Capture next-generation sequencing (NGS) strategy library (Agilent Technologies, Santa Clara, CA) before sequencing on MiSeq equipment (Illumina, San Diego, CA) (supplemental Methods; supplemental Figures 1 and 2). The contribution of previously defined mutational signatures was calculated for each gene (supplemental Methods). Variant verification was performed using the Ampliseq NGS method (Illumina) (supplemental Table 3) and/or by Sanger sequencing analysis using the primers detailed in supplemental Table 4. The previously published mutational profile of 144 adult DLBCLs was used for comparisons.[26]

DNA CN alteration analysis

Copy-number (CN) alterations were examined in 59 LBCLs from 55 patients using Oncoscan or single-nucleotide polymorphism array platforms (Thermo Fisher Scientific, Waltham, MA) according to standard protocols (supplemental Methods). Gains and losses and CN neutral loss of heterozygosity (CNN-LOH) regions were evaluated using Nexus Biodiscovery v9.0 software (Biodiscovery, Hawthorne, CA). Additional previously published CN data were used for comparison.[26,30]

Gene expression profile by NanoString

COO classification was performed using Lymph2Cx assay (NanoString, Seattle, WA).[31] The Lymph3Cx assay was used for detection of molecular PMBL (mPMBL).[32] The NanoString Pan-Cancer Immune Profiling Panel was also used to investigate additional gene expression differences between different subsets of LBCL (supplemental Methods).

Statistical methods

Survival probabilities were estimated with the Kaplan-Meier method and differences assessed by the log-rank test. Event-free survival (EFS) was calculated as previously described.[33] Differences in the distribution of individual parameters among patient subsets were analyzed by Fisher's exact test for categorized variables, and the Student *t* test for continuous variables. Nonparametric tests were applied when necessary. Only mutations and genomic aberrations present in 5% of the cases and affecting a minimum of 4 cases were accounted for comparisons. The *P* values for multiple comparisons were adjusted using the Benjamini-Hochberg correction (false discovery rate). A cutoff of $P = .05$ was considered significant unless otherwise indicated. Statistical analyses were carried out using R software v3.5.0.

Results

Clinicopathological characteristics

Twenty cases were classified as LBCL-*IRF4* (11 females, 9 males; median age, 14 years; range, 5-22 years). Eight patients had nodal involvement, mainly in the head and neck region, and 8 had tonsillar disease (Table 1). The other 4 patients (20%) had primary extranodal presentation in the gastrointestinal tract (2 cases), liver, and larynx. Histologically, 9 cases were purely diffuse, 5 cases showed a nodular growth pattern, and 6 displayed both follicular and diffuse areas. All cases showed positivity for MUM1/IRF4 and BCL6, whereas CD10 and BCL2 were positive in 11 and 10 cases, respectively (Figure 1). Five out of 12 cases coexpressed CD5, and all cases analyzed were negative for EBV. FISH studies identified the *IRF4* translocation in 17 out of the 19 investigated cases, and the remaining 2 negative cases had breaks of the IGH locus (Figure 2). None of the 11 LBCL-*IRF4* cases interrogated carried *BCL6* or *BCL2* rearrangements. The Lymph2Cx assay predicted 10 cases (72%) as GCB, 3 (21%) as unclassified, and only 1 (7%) as ABC. The IRF4/MUM1 messenger RNA levels detected by this assay were significantly higher than in DLBCL, NOS and HGBCL, NOS ($P < .01$) (supplemental Figure 3).

Thirty-one cases (22 males and 9 females; median age, 14 years; range, 1-25 years) were classified as DLBCL, NOS, all with a diffuse pattern of large, mainly centroblastic cells. Most cases showed a GC-phenotype (20/31, 65%) in line with the Lymph2Cx results that showed a GCB profile in 67%, followed by 22% ABC and 11% UNC. *MYC* breaks were detected in 3 cases, *BCL6* rearrangement in 2 cases (supplemental Table 5), and, contrary to adult DLBCL, NOS, only 1 case presented *BCL2* translocation. EBV was positive in 5 out of 25 (20%) cases, 4 of which had an ABC phenotype. Seven patients had primary extranodal presentation.

Finally, 12 cases were classified as HGBCL, NOS (8 males and 4 females; median age, 9.5 years; range, 3-23 years), 8 with intermediate features between DLBCL and BL and 4 with blastoid morphology (Figure 3). These cases mainly had a GC phenotype (91%) and were classified as GCB (7/9 cases) by the Lymph2Cx assay. Inmunohistochemically, BCL2 was positive in 5 out of 11 cases (45%) and MYC in 3, but without typical BL morphology (supplemental Figure 4). *MYC* and *BCL6* translocations were detected in 4 cases and 1 case, respectively. No double/triple hits were identified. EBV was detected in 2 cases. Most patients had a primary extranodal presentation (75%) (Figure 2; supplemental Table 6).

A recent gene expression study has recognized PMBL at non-mediastinal sites and/or with atypical clinical presentations.[34] To identify any potential PMBL not recognized based on conventional clinicopathological criteria, we investigated the mPMBL signature using the Lymph3Cx assay[32] in 39 cases (21 DLBCL, NOS; 14 LBCL-IRF4; and 4 HGBCL, NOS) with available RNA. This analysis predicted 4 DLBCL, NOS as mPMBL. Three of these cases had mediastinal involvement but were not considered initially as PMBL due to concomitant disseminated disease involving bone marrow, lymph nodes, and multiple extranodal sites (supplemental Table 7). However, 1 DLBCL, NOS case predicted as mPMBL had a solitary axillary lymph node without apparent mediastinal involvement. These 4 cases were analyzed as a separate category in subsequent molecular analyses. Finally, the assay predicted 5 DLBCL, NOS, as "uncertain," ie, with a gene expression signature probability score between DLBCL and PMBL. None of these 5 cases had clinicopathological features of PMBL (supplemental Table 7). Additionally, Lymph2Cx/Lymph3Cx had 100% concordance for COO prediction (Figure 2).

Identification of mutational profiles by targeted NGS

Fifty-five tumors (50 primary, including 22 DLBCL, NOS; 17 LBCL-*IRF4*; 8 HGBCL, NOS; 3 mPMBL; and 5 relapsed samples) were analyzed by NGS (mean coverage, 447×; range, 28-1439×). After filtering, 496 mutations were identified in 50 out of 55 samples analyzed with a verification rate of 97% (147/151) of the selected variants (supplemental Table 8). A total of 331 variants (67%) were predicted as potential driver mutations (supplemental Methods). After exclusion of mPMBL and relapsed samples, the remaining 47 cases displayed a total of 245 driver mutations with a mean of 5.2 driver mutations per case. The most recurrently mutated genes were *IRF4* (14/47, 30%), *CARD11* and *CCND3* (8/47, 17%), *KMT2D*, *MYC*, *PIM1*, or *SOCS1* (6/47, 13%), and *FOXO1* (5/47, 11%) (Figure 4A).

The number of mutations per case was similar among the 3 subtypes (mean: LBCL-*IRF4*, 5.2 mutations/case; DLBCL, NOS, 5.8; and HGBCL, NOS, 6.6), but they exhibited different mutational profiles (Figure 4). The most frequently mutated genes in LBCL-*IRF4* were *IRF4* (76%), *CARD11* (35%), and *CCND3* (24%). Interestingly, mutations in 3 genes activating the NF-κB pathway (*CARD11*, *CD79B*, and *MYD88*) were observed in 6 out of the 17 analyzed cases. Of note, these 6 cases showed a purely diffuse morphology. The majority of *CARD11* mutations (4/6) occurred in the coiled-coil domain, which is known to produce a constitutive NF-κB activation and enhanced NF-κB activity in adult DLBCL.[35] All *CD79B* mutated cases carried a Y197 hot spot mutation affecting the immunoreceptor tyrosine-based activation motif domain (Figure 4B). Mutations on this residue reduce its negative regulation by the kinase LYN.[36] *MAP2K1* mutations, typically seen in pediatric-type follicular lymphoma, were detected in 2 cases with predominant follicular growth pattern and confirmed *IRF4*-rearrangement (supplemental Figure 5).[37,38] Multiple *IRF4* mutations (>4 mutations/case including synonymous variants) were observed in 9 cases, all of which carried the *IRF4* rearrangement. These mutations had the pattern of aberrant somatic hypermutation (aSHM) and predominant AID

Table 1. Pathological and clinical features of 20 LBCL cases with *IRF4* rearrangement

Case	Age (y), gender	Biopsy site	Growth pattern	Immunohistochemistry				FISH		COO NanoString (Lymph2Cx)	Stage*	Treatment	Outcome, follow-up
				CD10	BCL6	BCL2	IRF4/MUM1	*IRF4*	IGH				
D1	5, F	LN	Follicular and diffuse	+	+	+	+						
D2	14, M	LN	Follicular	+	+	−	+	R		GCB		Surgical excision	
D15	5, F	Tonsil	Diffuse	−	+	+	+	R	R	GCB	II	CT-P	CR, 49 mo
D16	14, F	Tonsil	Diffuse	−	+	−	+	R			II	CT-P	CR, 99 mo
D17	21, M	Liver	Diffuse	−	+	+	+	R		ABC	I-E	CT-A	CR, 10 mo †
D20	17, M	Ileum	Diffuse	+	+	+	+	N	R	UNC	II	CT-P	CR, 72 mo
D21	8, M	Tonsil	Follicular	+	+	+	+	R			I	CT-P	CR, 36 mo
D23	21, F	Inguinal LN	Diffuse	−	+		+	R	R	GCB	IV-A	CT-A	CR, 40 mo
D31	12, F	Cervical LN	Diffuse	−	+	+	+	N	R	UNC			
D32	7, M	Tonsil	Follicular	+	+	+	+	R		GCB	I	CT-P	CR, 22 mo
D35	6, F	Cervical LN	Diffuse	+	+	−	+	R		GCB	I	CT-P	CR, 63 mo
D46	11, M	Tonsil	Follicular and diffuse	+	+	−	+	R	R	GCB		Surgical excision	
D47	22, M	Tonsil	Follicular and diffuse	+	+	−	+	R	R		I	CT-A	CR, 24 mo
D48	18, F	Tonsil	Follicular and diffuse	−	+	−	+	R		UNC	I	CT-A	CR, 29 mo
D50	17, F	Cervical LN	Follicular	−	+	−	+	R	R			Surgical excision	
D51	10, F	Tonsil	Follicular and diffuse	+	+	−	+	R		GCB	III	CT-P	CR, 14 mo
D54	18, F	Cervical LN	Diffuse	+	+	+	+	R		GCB	III	CT-P	CR, 14 mo
D62	17, M	Cervical LN	Follicular	−	+	−	+	R		GCB	II	CT-P	CR, 45 mo
D63	14, F	Larynx	Diffuse	+	+	+	+	R		GCB	I	CT-P	CR, 18 mo
D69	15, M	Intestine	Follicular and diffuse	−	+	+	+	R				CT-P	CR, 10 mo

CR, complete response; CT-A, chemotherapy with adult schema protocol (R-CHOP/ESHAP); CT-P, chemotherapy with pediatric schema protocol; F, female; LN, lymph node; M, male; N, normal; R, rearrangement; UNC, intermediate/unclassified.

*Stage was established according St. Jude/International Pediatric NHL Staging System or Ann Arbor staging system for pediatric and adult patients, respectively.

†Patients who had a relapse/progression and needed rescue treatment.

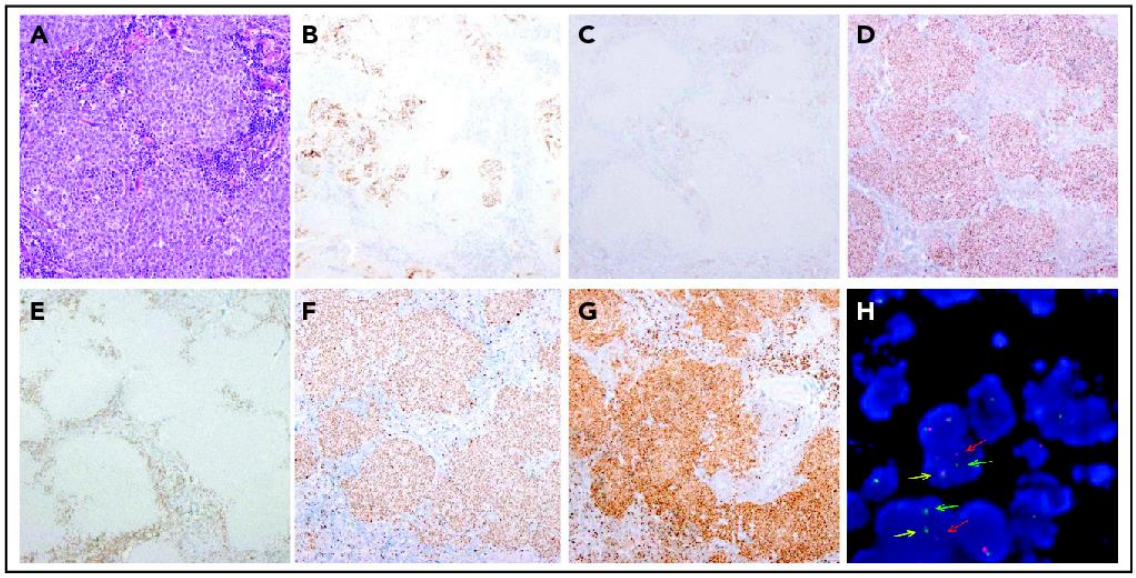

Figure 1. Morphological, immunophenotypic, and genetic features of a LBCL with *IRF4* rearrangement (case D62). Architecture effacement by an atypical lymphoid proliferation with nodular growth pattern (A; hematoxylin and eosin) that corresponds to expanded follicles with highly disrupted follicular dendritic cell meshwork (B; CD21). The atypical cells were negative for CD10 (C) and positive for BCL6 (D). BCL2 was positive in the accompanying reactive T cells but negative in the tumor (E), which exhibits a high proliferation rate (F; Ki67). The immunohistochemical study for IRF4/MUM1 (G; MUM1) shows strong and diffuse positivity in the neoplastic proliferation, and FISH with *IRF4* break-apart probe shows a signal constellation of 1 colocalization (yellow arrow) and 1 split signal (red and green arrows) consistent with the gene rearrangement (H). Original magnification ×100 (A), ×40 (B-G).

mutational signature (supplemental Results; supplemental Figure 6; supplemental Table 9). In agreement with previous observations,[17] 8 out of 16 primary *LBCL-IRF4* cases investigated carried somatic intronic *BCL6* mutations. Of note, these mutations affected the predicted *IRF4*-binding site in 5 cases (supplemental Table 10).[39]

Among the 22 DLBCL, NOS cases, the most frequently mutated genes were *SOCS1* (27%), *KMT2D* (23%), and *BTG1*, *EZH2*, *GNA13*, *MYD88*, and *PIM1* (14%), consistent with a predominantly GCB-DLBCL profile but with absence of *TNFRSF14* and *SGK1* mutations (supplemental Figure 7). Compared with adult DLBCL, NOS, no significant differences were detected in the number of mutations affecting commonly interrogated genes (pediatric/young adult LBCL mean 4.3 vs adult DLBCL 4.8 mutations/case, $P < .15$). However, we observed a higher frequency of *SOCS1* mutations in pediatric and young adult DLBCL, NOS (27% vs 8% respectively, $P = .01$), and the practical absence of some mutations affecting genes was strongly associated with the definition of established mutational clusters in adult DLBCL, NOS, such as *MYD88*-L265P, *NOTCH1*, *NOTCH2*, *BCL2*, and *SGK1* (supplemental Figure 8A).[5,6]

Of the 8 HGBCL, NOS cases examined, 4 had mutations in ≥3 genes predominately associated with BL (supplemental Figure 5). The remaining 4 cases had mutations in *CARD11* (2 cases) or *EZH2* and *TNFRSF14* (1 case each) akin to DLBCL, NOS.[22,23] Interestingly, *MYC* mutations clustered around known phosphorylation sites required for the ubiquitination and degradation of MYC protein as previously described (Figure 4B).[40] Of note, all *MYC* mutated cases (5 HGBCL, NOS and 1 DLBCL, NOS) had multiple mutations (>4 mutations/case including intronic and synonymous variants) with an aSHM pattern (supplemental Table 9).[40,41] Four out of these 6 cases also carried *MYC* rearrangement, and in the 2 remaining ones, the presence of cryptic translocations could not be completely ruled out.[13,42]

We evaluated the presence of recurrent mutated pathways in the different morphological subtypes.[26] This analysis showed frequent mutations in chromatin modifiers in HGBCL, NOS, whereas mutations in B-cell differentiation and JAK-STAT pathway genes were more frequently seen in LBCL-*IRF4* and DLBCL, respectively (supplemental Figure 9).

The mutational profile of the 3 cases predicted as mPMBL was closer to PMBL than DLBCL, NOS, with mutations in *SOCS1*, *NFKBIE*, *STAT6*, *B2M*, and *CIITA*, which appeared to confirm the mPMBL gene expression prediction (supplemental Figure 7).

Finally, the mutational profile of the 3 paired diagnostic-relapse samples analyzed showed marked differences between both biopsy specimens with a total of 13 (mean 4.3, range 0-9) shared and 23 acquired variants (mean 7.7, range 2-16) in the relapsed samples. Additionally, in the 5 relapsed samples available, we identified recurrent *KLHL6* and *BTG2* mutations (2 cases each) (supplemental Figure 10A).

CN alteration profile

CN analysis detected 302 genetic alterations in 43 out of 49 LBCL primary tumors (mean, 6.2 alterations per case; range, 0-34 alterations) and 45 CNN-LOH in 25 out of 49 cases (supplemental Table 11). Recurrent CN alterations (>15%) included gains of 1q21.2-q42.13, 11q22.3-q25, trisomies 7 and 12, and recurrent losses of 1p36.33-p36.13/*TNFRSF14* and 6q21/*PRDM1*.

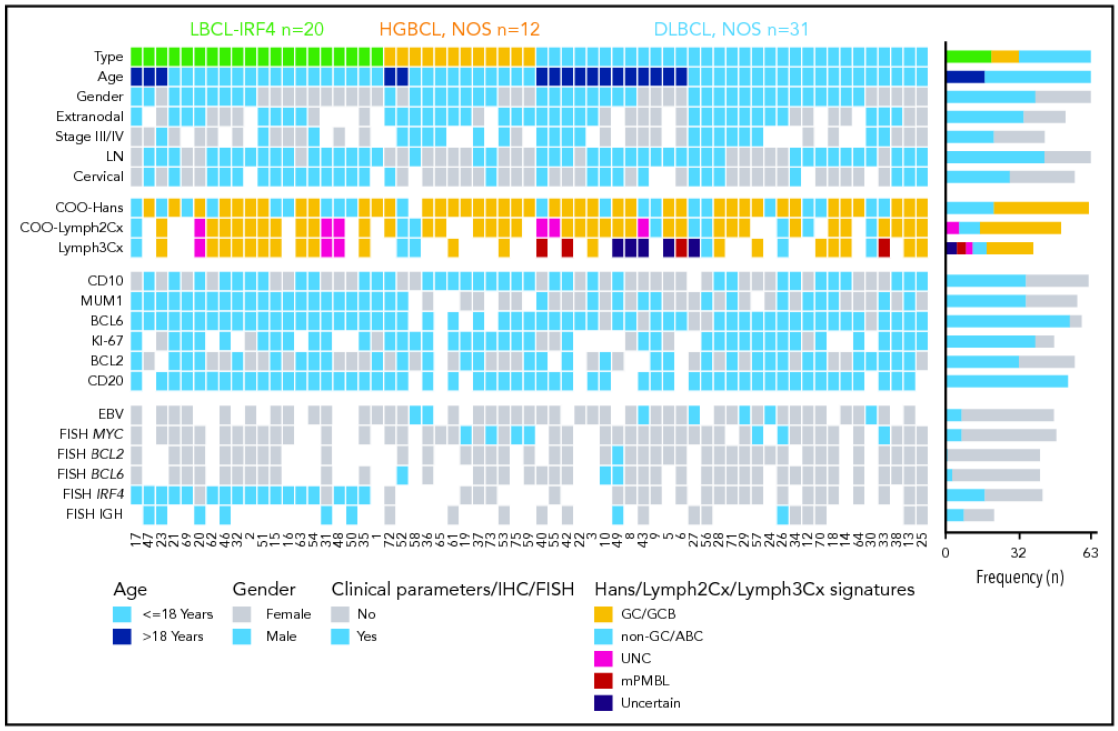

Figure 2. Overview of clinical and histological findings in 63 pediatric and young adult LBCL cases. Each column of the heatmap represents 1 LBCL case and each line a specific analysis. On the right side of the figure, the frequency of the particular result of the analysis is shown. LN, lymph node; UNC, unclassified.

Frequent CNN-LOH (>10%) affected 17q21.3-q25.3 and 19p13.3-p13.2 regions (supplemental Figure 11). Recurrent homozygous deletions were observed at 19p13.3/*CD70* (5 cases) and 9p21.3/*CDKN2A* (3 cases) in addition to single events in 13q14.2/*RB1* and 17q24.1/*GNA13* loci. Alteration patterns suggestive of chromothripsis[43] were found in 4 out of 49 cases (8%) affecting chromosomes 1, 9, 12, and 13, respectively. Of note, all 4 cases carried *MYC*, *IRF4*, or *BCL6* translocations.

The 3 LBCL subtypes displayed different CN profiles despite having similar number of aberrations (mean, LBCL-*IRF4*, 6.2; DLBCL, NOS, 5.8; and HGBCL, NOS, 7.1 alterations per case). LBCL-*IRF4* had frequent 17p/*TP53* deletions (25%), without gene mutations, and gains of chromosome 7 (45%) and 11q12.3-q25 (35%). DLBCL, NOS had recurrent 2p16 gains targeting *REL* and 19p13 homozygous deletions targeting *CD70* (23% each). HGBCL, NOS had 1q gains (3 cases), similar to BL,[30] but also carried trisomies/gains of 7 (4 cases) and 12 (3 cases), and 9p21.3/*CDKN2A* homozygous deletions (2 cases) (Figure 5).

Compared with adult DLBCL, NOS, pediatric and young adult DLBCL, NOS had a similar CN profile without any specific alteration but significantly lower levels of genetic complexity (mean, 5.8 vs 20 CN alterations; $P < .01$) (supplemental Figure 8B). Our current pediatric and young adult series lacked alterations present in adults such as 6q13-q14.1/*TMEM30A* and 6q22.1-q25.3/*TNFAIP3* deletions as well as those typically associated with ABC-DLBCL as 9p21.3/*CDKN2A* and 17p13.3-p11.2/*TP53* losses, which probably reflects the predominance of GCB cases in our cohort. In fact, these differences were not observed when compared only to adult *BCL2*-negative GCB-DLBCL. Nevertheless, results should be taken with caution, since different CN platforms were used.

Finally, analysis of 3 paired diagnostic-relapsed biopsy specimens showed the acquisition of a mean of 15 additional events (range, 12-16) in the relapsed samples. Recurrent alterations in these cases included gains of 1q21.2-q41 (*MDM4*), 12p13.3-q21.1, and 18q22.2-q23 and biallelic inactivation of 19p13/*CD70*, which was also present in both samples (diagnosis/relapse) in the 3 cases (supplemental Figure 10B) and even in a second relapse in 1 case.

Gene expression patterns

Differential gene expression analysis between LBCL-*IRF4* (n = 11) and DLBCL, NOS (n = 10) identified 48 differentially expressed genes (log2 fold change greater than ±1 and false discovery rate <.05), including 14 NF-κB target genes (29%; eg, *IRF4*, *LTF*, and *CSF1*), which suggests a deregulation of this pathway in LBCL-*IRF4* (http://www.bu.edu/nf-kb/gene-resources/target-genes/) (supplemental Figure 12; supplemental Table 12). No gene expression differences were observed between LBCL-*IRF4* cases with and without *CD79B* or *CARD11* mutations.

Prognostic value of clinical and molecular features

The 5-year EFS of the 46 LBCL patients with available follow-up was 68.4%. All received chemotherapy as first-line treatment, including rituximab in 35% of the patients with no differences in

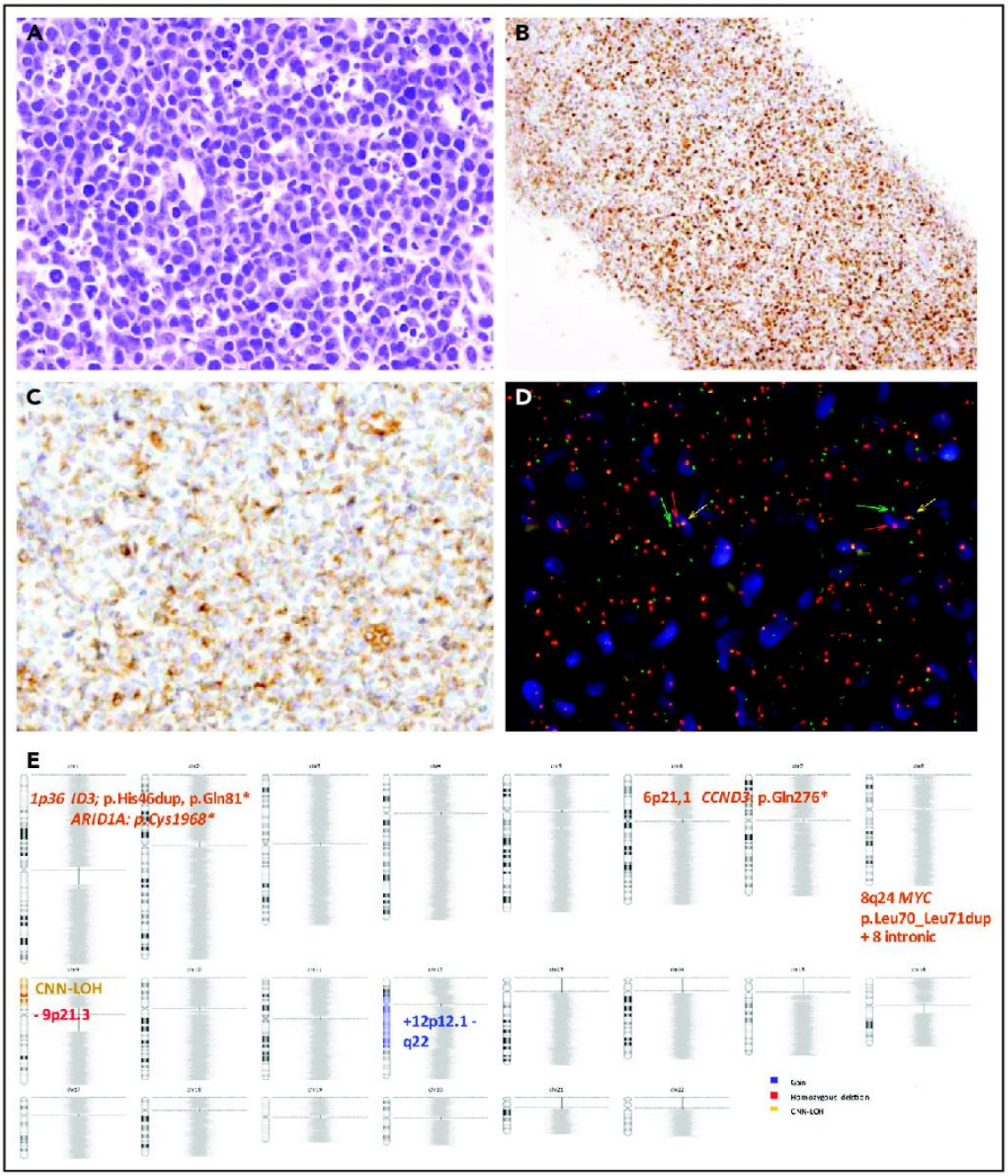

Figure 3. Morphological, immunophenotypic and genetic features of an HGBCL, NOS with *MYC* rearrangement (Case D59). Hematoxylin and eosin stain (A) depicting mild heterogeneity with certain cellular irregularity of the neoplastic cells that are BCL6 positive (B) with partial expression of BCL2 (C). (D) FISH with *MYC* break-apart shows a signal constellation of 1 colocalization (yellow arrow) and 1 split signal (green and red arrows). (E) Ideogram of the CN, CNN-LOH, and mutational features of this case. Original magnification ×400 (A,C), ×100 (B).

EFS (log-rank test $P = .75$). Complete response was achieved in 83% of patients, whereas 8 died of disease. Cases predicted as ABC-DLBCL had significantly worse 5-year EFS compared with GCB-DLBCL patients (26% vs 74% $P = .002$) (Figure 6; supplemental Figure 13), even when the LBCL-*IRF4* cases were excluded from the comparison (30% vs 68%, $P = .033$). Interestingly, the clinical outcome of GCB-DLBCL was similar to LBCL-*IRF4*, whereas ABC-DLBCL and HGBCL, NOS had significantly worse 5-year EFS (78% vs 48%; $P = .005$). Similarly, high lactate dehydrogenase (LDH) levels; a high number of CN

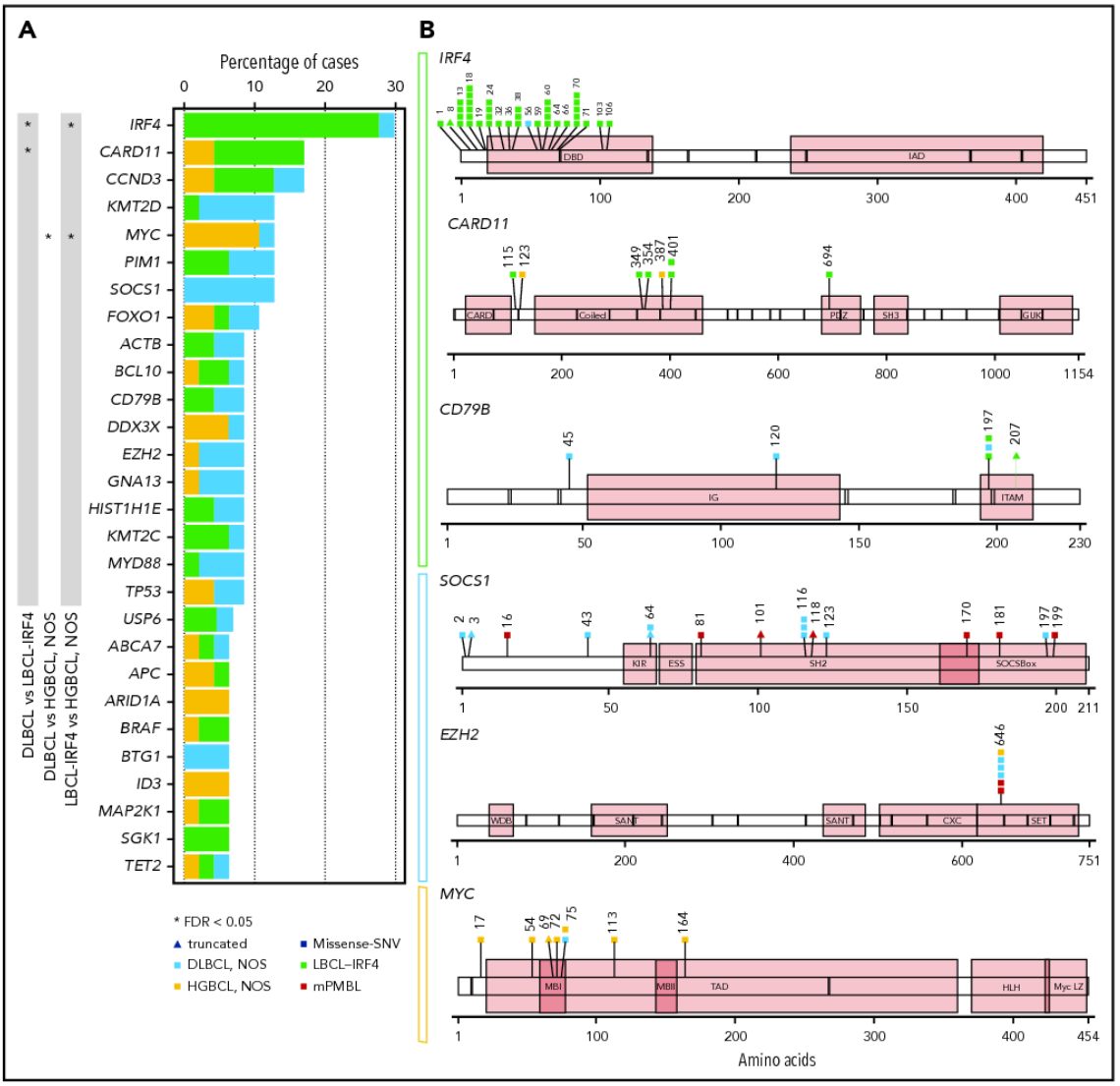

Figure 4. Mutational landscape of 47 pediatric and young adult LBCL cases. (A) Bar graphs show mutated genes in >5% of 47 pediatric and young adult primary LBCL cases excluding mPMBL. Each color bar indicates histological subtypes. An asterisk represents mutated genes significantly enriched in 1 of the subtypes. SNV, single-nucleotide variant. (B) A diagram of the relative positions of driver mutations is shown for *IRF4*, *CARD11*, *CD79B*, *SOCS1*, *EZH2*, and *MYC* genes. x-axes indicate amino acid position: IRF4 domains (DBD, DNA-binding domain; IAD, IRF association domain), CARD11 domains (CARD, caspase activation and recruitment domain; SH, Src homology 3 domain), CD79B domains (IG, immunoglobulin-like; ITAM, immunoreceptor tyrosine-based activation motif), SOCS1 domains (ESS, extended SH2 subdomain; KIR, kinase inhibitory region), EZH2 domains (CXC, cysteine-rich domain; SANT, SWI3-ADA2-*N*-CoR-TFIIIB domains; WDB, WD-40 binding domain), and MYC domains (HLH, helix-loop-helix; LZ, leucine zipper; MBI/II, Myc box I and II; TAD, transactivation domain).

alterations (>10), including cases with chromothripsis-like patterns; *TP53* and *MYC* mutations; gains of 2p16/*REL* and 1q21-q44/*MDM4*; and biallelic inactivation of 19p13/*CD70* correlated with a significant lower EFS rate (Figure 6; supplemental Figure 13).

When patients were examined according to age, pediatric patients (≤18 years) had better 5-year EFS than young adults (19-25 years) (76% vs 46%, log-rank test $P = .044$) (Figure 6; supplemental Figure 13). Young adults had more frequent *BCL6* rearrangements, high genetic complexity, and chromothripsis-like patterns (supplemental Table 13). Finally, when the clinical parameters were compared among the 3 different lymphoma entities, HGBCL, NOS presented more frequently in primary extranodal sites and had a higher incidence of *MYC* rearrangements (supplemental Table 14).

Discussion

Genomic studies of adult LBCL have revealed a large number of somatic mutations and structural alterations related to the

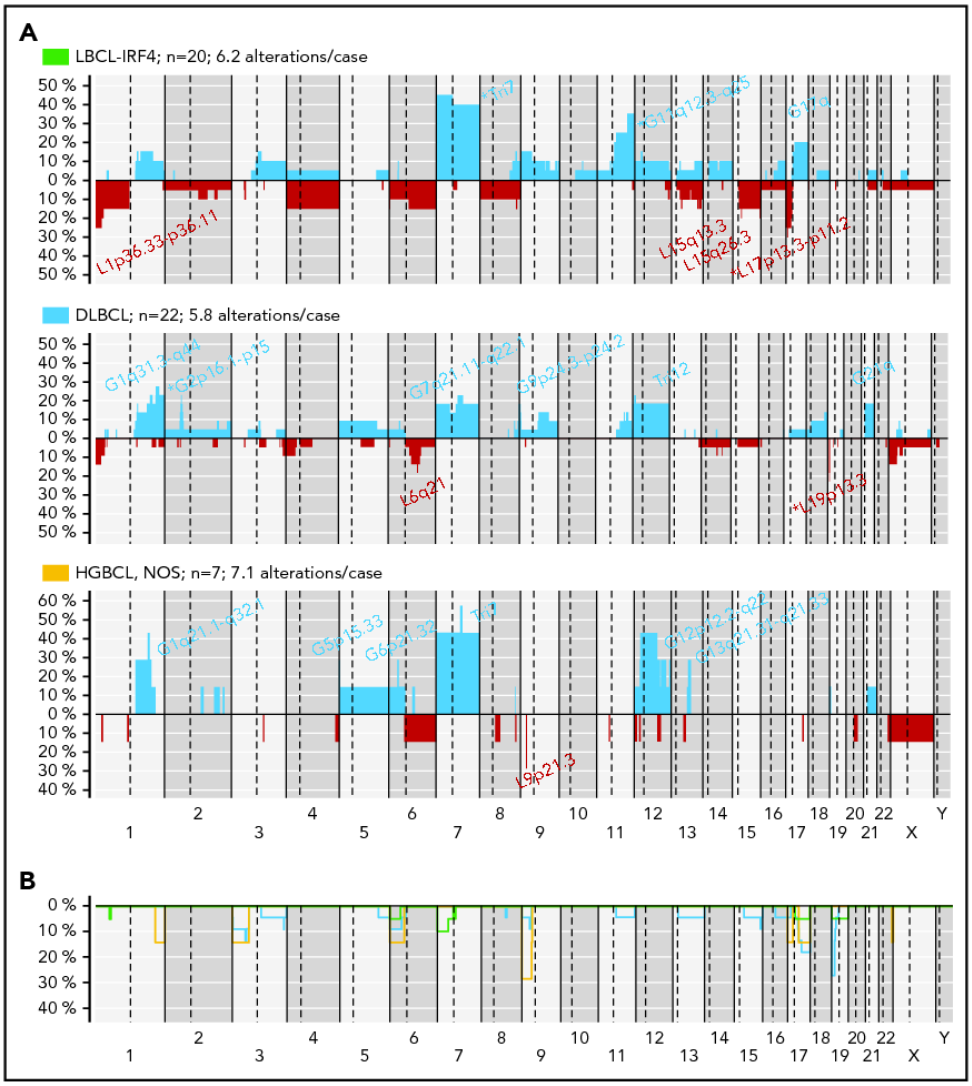

Figure 5. CN profile of pediatric and young adult LBCL cases. (A) Global CN profiles of 20 LBCL-*IRF4* cases; 22 DLBCL, NOS cases; and 7 HGBCL, NOS cases. x-axis indicates chromosomes from 1 to Y and p to q. The vertical axis indicates frequency of each genomic aberration among the analyzed cases. Gains are depicted in blue and losses in red. Most frequently recurrent regions are indicated for LBCL-*IRF4*; DLBCL, NOS (>20%); and HGBCL, NOS (≥2 cases). Asterisks indicate significant differences between LBCL-*IRF4* and DLBCL (Fisher's test, $P < .05$). (B) Comparative plot of CNN-LOH among the 3 morphological groups described above. Green identifies LBCL-*IRF4*; blue DLBCL, NOS; and yellow HGBCL, NOS.

pathogenesis of these diseases.[3,4,7] However, the genetic landscape of these tumors in pediatric populations is poorly known. In this study, through an integrative targeted NGS, CN, and transcriptome data analyses, we show that pediatric and young adult LBCLs are a heterogeneous group of tumors including different entities with specific molecular profiles and clinical behavior. A better understanding of these differences is relevant to design management strategies more adapted to the particular biological behavior of these tumors.

LBCL-*IRF4* was recently recognized as a specific entity genetically characterized b *IRF4* translocation, clinical presentation localized in the head and neck or abdominal regions, and a favorable outcome after chemotherapy.[17,19] We have now expanded these observations to show that these tumors have a distinct molecular profile characterized by frequent mutations in *IRF4* and NF-κB-related genes (*CARD11*, *CD79B*, and *MYD88*) and overexpression of downstream target genes of the NF-κB pathway. These findings are intriguing, because most of these tumors have a GC phenotype and gene expression profile, whereas mutations in these genes and NF-κB activation have mainly been found in ABC-DLBCL in adults.[5] The activation of the NF-κB pathway in these tumors may be also related to the IRF4 overexpression.[44] The presence of multiple mutations

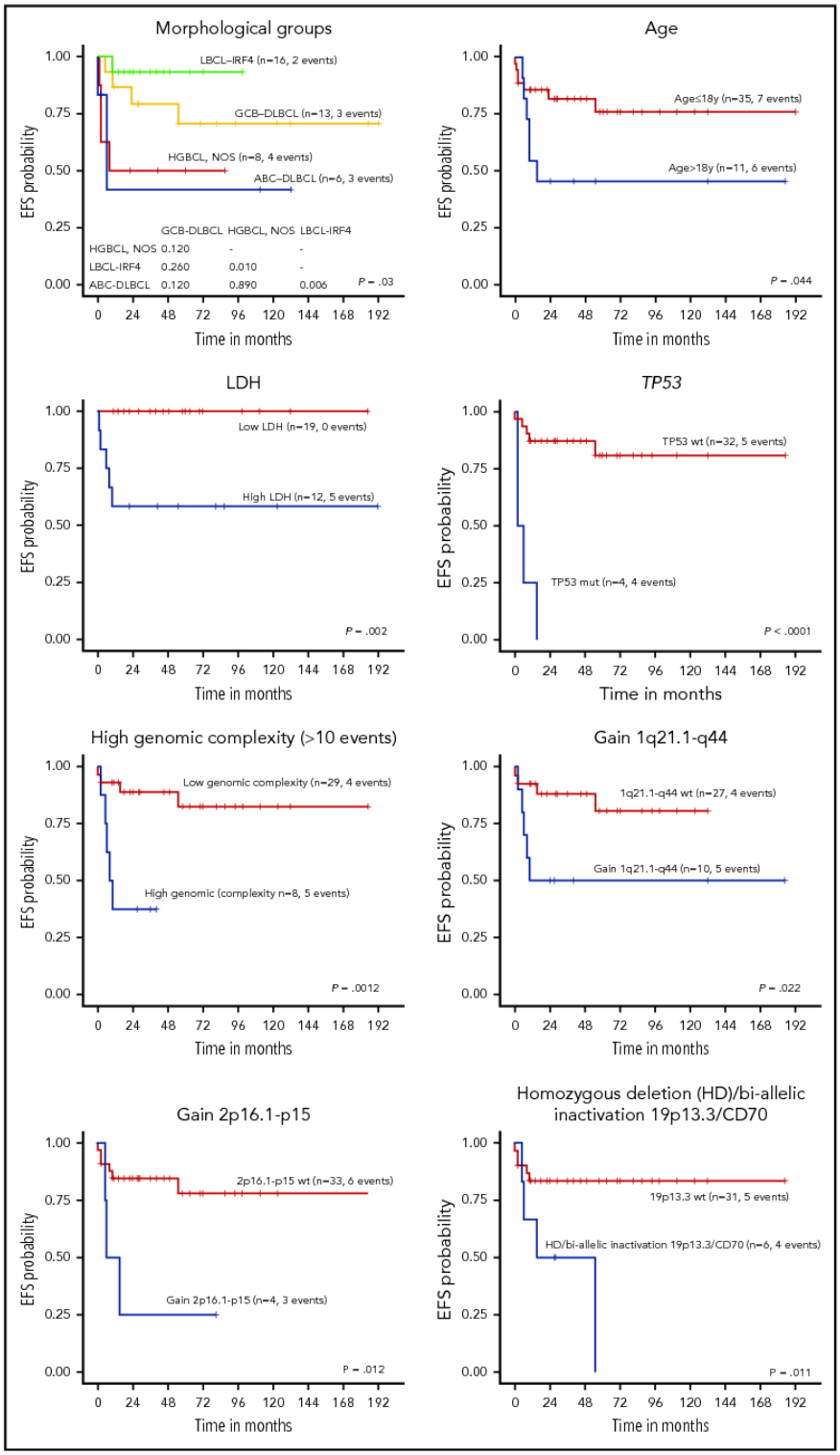

Figure 6. EFS of 45 pediatric and young adult LBCL cases according to morphological and molecular subtypes, age, LDH levels, and specific molecular features. wt, wild type.

affecting the *IRF4* gene with an aSHM pattern appears to be a hallmark of the *IRF4* translocation. Further studies are needed to define the potential functional effect of these mutations. Morphologically, LBCL-*IRF4* may have predominantly diffuse or follicular pattern. Interestingly, *CARD11* mutations were seen exclusively in cases with diffuse growth pattern, whereas *MAP2K1* mutations, characteristic of pediatric-type follicular lymphoma,[37,38] were detected in 2 cases with a predominantly follicular pattern (supplemental Figure 8), suggesting that the underlying mutational profile may influence the morphological features of the tumors. No differences in terms of CN mutational profile, including *IRF4* mutations and IRF4 expression at the RNA and protein level (supplemental Figure 3), were seen in the 2 LBCL-*IRF4* cases with an IGH split without concomitant *IRF4* breaks, confirming the idea that these tumors belong to the same entity. The presence of cryptic *IRF4* translocations cannot be excluded.[45] The outcome of LBCL-*IRF4* was very favorable, but most of the patients were treated with aggressive pediatric or adult-type chemotherapy protocols. The identification of the translocation and the related mutational profile may be relevant to identify these patients and design management strategies better suited to the biology of the tumors.[17,19]

The genetic and expression profile of our DLBCL, NOS was relatively similar to that previously observed in pediatric cohorts with a predominance of GCB-DLBCL, low CN complexity, few *MYC* and *BCL6* rearrangements, and, in contrast to adults, the virtual absence of *BCL2* translocations (supplemental Table 15).[46-48] Our study expands these observations, showing that these cases have a mutational profile similar to adult DLBCL with predominance of mutations in GCB-DLBCL–related genes (supplemental Figures 5 and 8). Nevertheless, pediatric and young adult DLBCL had higher frequency of *SOCS1* mutations and virtually lacked *MYD88*-L265P, *NOTCH1*, *NOTCH2*, *BCL2*, and *SGK1* mutations that have been associated with the definition of established mutational clusters in adult DLBCL.[5,6] Further studies using whole-exome/genome approaches may expand the genomic profile of alterations of these tumors.

The application of the Lymph3Cx in our DLBCL, NOS cohort recognized 4 cases predicted as mPMBL with an atypical clinical presentation for this entity.[32] Although 3 of these patients had mediastinal lymph node involvement, they also had disseminated disease including bone marrow and extranodal involvement. Intriguingly, 1 case predicted as mPMBL only had axillary nodal involvement. The mutational profile of these cases was consistent with PMBL, including *NFKBIE* mutations recently associated with poor outcome in these tumors.[49] These observations, together with similar cases recently described in adults, suggest that a subset of DLBCL, NOS in pediatric and young adult populations may correspond to PMBL.[34,50]

The genetic features of HGBCL, NOS were heterogeneous. Four out of the 8 molecularly investigated cases had mutational profile closer to BL (supplemental Figure 5), with concomitant *MYC* rearrangements and 1q21-q31 gains identified in 2 cases each (Figure 3E; supplemental Figure 4). Nevertheless, those cases did not have the typical BL morphology and expressed strong BCL2 or MUM1. Similar to HGBCL, NOS in adults,[22,23] no *TCF3* mutations were seen in our cases. Other HGBCL, NOS cases had mutational profiles closer to GCB-DLBCL with *TNFRSF14*, *CARD11*, and *EZH2* mutations and lacked *MYC* translocations. Of note, genes frequently mutated in BLL-11q, such as *BTG2*, *ETS1*, and *EP300*,[15,16] were significantly absent in both DLBCL and HGBCL, NOS ($P < .05$), suggesting that they correspond to different entities (supplemental Figure 5).

Regarding prognostic aspects, advanced stage, high LDH, and combined bone marrow and central nervous system disease have been significantly associated with unfavorable outcome in pediatric mature B-cell lymphomas, whereas the adverse prognosis of 8q24-*MYC* rearrangements and ABC-COO is still controversial.[24,27] In our series, we found the prognostic value of several clinical and molecular features such as age >18 years, high LDH levels, and ABC-subtype, as seen in adult populations. We also found that *TP53* mutations, high genetic complexity, including chromothripsis, and gains in 1q21-q44/*MDM4* conferred poor EFS.

In conclusion, LBCLs in the pediatric and young adult population are a heterogeneous group of tumors with distinct genomic and mutational alterations. LBCL-*IRF4* reveals a GC phenotype with frequent mutations in *IRF4*, NF-κB-related genes (*CARD11*, *CD79B*, and *MYD88*), and overexpression of genes of the NF-κB pathway, whereas DLBCL, NOS cases in this population are predominantly of GCB subtype. Our study also suggests that PMBL may present with disseminated disease, and ancillary tools may recognize these cases, with implications for treatment. The integration of molecular and genetic studies may improve the classification of LBCL in pediatric and young adult populations and provide parameters for risk stratification.

Acknowledgments

The authors thank the centers of the Sociedad Española de Hematología y Oncología Pediátricas that submitted cases for consultation, as well as Noelia Garcia, Silvia Martín, and Helena Suarez for their excellent technical assistance. They also thank Miguel Angel Piris from Fundación Jimenez Díaz for performing immunohistochemical analyses and Pedro Jares and Magda Pinyol from Hospital Clínic, Institut d'Investigacions Biomèdiques August Pi i Sunyer (IDIBAPS) for their support with gene expression analyses. The authors are indebted to the IDIBAPS Genomics Core Facility and the HCB-IDIBAPS Biobank-Tumor Bank and Biobanc de l'Hospital Infantil Sant Joan de Déu, Hospital Universitario Virgen del Rocío-Instituto de Biomedicina de Sevilla Biobank (ISCIII-Red de Biobancos PT13/0010/0056), all 3 integrated in the National Network Biobanks of ISCIII, for the sample and data procurement.

This work was supported by Asociación Española Contra el Cáncer (AECC CICPFI6025SALA), Fondo de Investigaciones Sanitarias Instituto de Salud Carlos III (Miguel Servet Program CP13/00159 and PI15/00580 to I.S.), Spanish Ministerio de Economía y Competitividad (SAF2015-64885-R to E.C.), Generalitat de Catalunya Suport Grups de Recerca (2017-SGR-1107 to I.S. and 2017-SGR-1142 to E.C.), SPECS II grant (National Cancer Institute 1U01CA157581), and the European Regional Development Fund (Una manera de fer Europa). J.E.R.-Z. was supported by a fellowship from Generalitat de Catalunya AGAUR FI-DGR 2017 (2017 FI_B01004). E.C. is an Academia Researcher of the Institució Catalana de Recerca i Estudis Avançats of the Generalitat de Catalunya. This work was developed at the Centro Esther Koplowitz, Barcelona, Spain. The group is supported by Acció instrumental d'incorporació de científics i tecnòlegs PERIS 2016 (SLT002/16/00336 to Noelia Garcia) from Generalitat de Catalunya.

Authorship

Contribution: J.E.R.-Z. performed research, analyzed data, and wrote the manuscript; B.G.-F. performed morphological diagnosis, analyzed data, and wrote the paper; F.N., J.S.-V., I.M.-G., G.C., A.E., A. Maguire, and

C.R. performed research and analyzed data; O.B., M.G.-P., A.G., M.S., D.A., C.B., F.G.-B., G.T., A. Mozos, L.M.R., L.Q.-M., and E.S.J. reviewed and interpreted pathological data; V.C., M. Andrés, M. Andión, I.A., M.S.d.l., C.S., S.G., J.V.-A., R.F.-D., A.R.-D., V.P., M.T., P.S.-P., I.D., A.L.-G., P.G., and M.J.O. reviewed and interpreted clinical data; E.C. performed morphological analysis, designed research, and wrote the manuscript; and I.S. performed research, analyzed data, designed research, and wrote the manuscript; and all authors approved the final manuscript.

Conflict-of-interest disclosure: E.C. and L.M.R. are co-inventors of the Lymph2Cx and Lymph3Cx gene expression profiling assay used in this study. The remaining authors declare no competing financial interests.

ORCID profiles: J.E.R.-Z., 0000-0001-7108-7738; B.G.-F., 0000-0002-1796-7248; O.B., 0000-0002-5099-3675; F.N., 0000-0003-2910-9440; I.M.-G., 0000-0002-0098-1908; M.G.-P., 0000-0002-7762-7085; A.G., 0000-0003-0324-2251; M.S.d.l., 0000-0002-8054-9698; C.S., 0000-0003-3956-5466; S.G., 0000-0002-4712-9624; V.P., 0000-0002-2668-3263; A. Mozos, 0000-0002-3350-1827; M.J.O., 0000-0001-6419-2513; A. Maguire, 0000-0002-1193-5528; L.Q.-M., 0000-0001-7156-5365; E.S.J., 0000-0003-4632-0301; E.C., 0000-0001-9850-9793; I.S., 0000-0002-2427-9822.

Correspondence: Itziar Salaverria, Institut d'Investigacions Biomèdiques August Pi i Sunyer (IDIBAPS), Rosselló 149-153, 08036 Barcelona, Spain; e-mail: isalaver@clinic.cat.

Footnotes

Submitted 8 August 2019; accepted 31 October 2019; prepublished online on *Blood* First Edition 18 November 2019. DOI 10.1182/blood.2019002699.

*J.E.R.-Z. and B.G.-F. contributed equally to this study.

The CN and gene expression data reported in this article have been deposited to the GEO database under accession number GSE128294. Sequencing data have been deposited to the European Nucleotide Archive under accession number ERP114095.

The online version of this article contains a data supplement.

The publication costs of this article were defrayed in part by page charge payment. Therefore, and solely to indicate this fact, this article is hereby marked "advertisement" in accordance with 18 USC section 1734.

REFERENCES

1. Dunleavy K, Gross TG. Management of aggressive B-cell NHLs in the AYA population: an adult vs pediatric perspective. *Blood*. 2018; 132(4):369-375.
2. Pasqualucci L, Trifonov V, Fabbri G, et al. Analysis of the coding genome of diffuse large B-cell lymphoma. *Nat Genet*. 2011;43(9): 830-837.
3. Morin RD, Mungall K, Pleasance E, et al. Mutational and structural analysis of diffuse large B-cell lymphoma using whole-genome sequencing. *Blood*. 2013;122(7):1256-1265.
4. Lohr JG, Stojanov P, Lawrence MS, et al. Discovery and prioritization of somatic mutations in diffuse large B-cell lymphoma (DLBCL) by whole-exome sequencing. *Proc Natl Acad Sci USA*. 2012;109(10):3879-3884.
5. Chapuy B, Stewart C, Dunford AJ, et al. Molecular subtypes of diffuse large B cell lymphoma are associated with distinct pathogenic mechanisms and outcomes [published correction appears in *Nat Med*. 2018;24(8): 1290-1291]. *Nat Med*. 2018;24(5):679-690.
6. Schmitz R, Wright GW, Huang DW, et al. Genetics and pathogenesis of diffuse large B-cell lymphoma. *N Engl J Med*. 2018;378(15): 1396-1407.
7. Reddy A, Zhang J, Davis NS, et al. Genetic and functional drivers of diffuse large B cell lymphoma. *Cell*. 2017;171(2):481-494.e15.
8. Savage KJ, Monti S, Kutok JL, et al. The molecular signature of mediastinal large B-cell lymphoma differs from that of other diffuse large B-cell lymphomas and shares features with classical Hodgkin lymphoma. *Blood*. 2003;102(12):3871-3879.
9. Richter J, Schlesner M, Hoffmann S, et al; ICGC MMML-Seq Project. Recurrent mutation of the ID3 gene in Burkitt lymphoma identified by integrated genome, exome and transcriptome sequencing. *Nat Genet*. 2012; 44(12):1316-1320.
10. Love C, Sun Z, Jima D, et al. The genetic landscape of mutations in Burkitt lymphoma. *Nat Genet*. 2012;44(12):1321-1325.
11. Schmitz R, Young RM, Ceribelli M, et al. Burkitt lymphoma pathogenesis and therapeutic targets from structural and functional genomics. *Nature*. 2012;490(7418):116-120.
12. Dunleavy K. Primary mediastinal B-cell lymphoma: biology and evolving therapeutic strategies. *Hematology Am Soc Hematol Educ Program*. 2017;2017:298-303.
13. In: Swerdlow SH, Campo E, Harris NL, eds., et al. WHO Classification of Tumours of Haematopoietic and Lymphoid Tissues, Revised 4th ed, Lyon: IARC; 2017:
14. Salaverria I, Martin-Guerrero I, Wagener R, et al; Berlin-Frankfurt-Münster Non-Hodgkin Lymphoma Group. A recurrent 11q aberration pattern characterizes a subset of MYC-negative high-grade B-cell lymphomas resembling Burkitt lymphoma. *Blood*. 2014; 123(8):1187-1198.
15. Gonzalez-Farre B, Ramis-Zaldivar JE, Salmeron-Villalobos J, et al. Burkitt-like lymphoma with 11q aberration: a germinal center-derived lymphoma genetically unrelated to Burkitt lymphoma. *Haematologica*. 2019; 104(9):1822-1829.
16. Wagener R, Seufert J, Raimondi F, et al. The mutational landscape of Burkitt-like lymphoma with 11q aberration is distinct from that of Burkitt lymphoma. *Blood*. 2019;133(9): 962-966.
17. Salaverria I, Philipp C, Oschlies I, et al; Berlin-Frankfurt-Münster-NHL trial group. Translocations activating IRF4 identify a subtype of germinal center-derived B-cell lymphoma affecting predominantly children and young adults. *Blood*. 2011;118(1):139-147.
18. Quintanilla-Martinez L, Sander B, Chan JK, et al. Indolent lymphomas in the pediatric population: follicular lymphoma, IRF4/MUM1+ lymphoma, nodal marginal zone lymphoma and chronic lymphocytic leukemia. *Virchows Arch*. 2016;468(2):141-157.
19. Chisholm KM, Mohlman J, Liew M, et al. IRF4 translocation status in pediatric follicular and diffuse large B-cell lymphoma patients enrolled in Children's Oncology Group trials. *Pediatr Blood Cancer*. 2019;66(8):e27770.
20. Woessmann W, Quintanilla-Martinez L. Rare mature B-cell lymphomas in children and adolescents. *Hematol Oncol*. 2019;37(suppl 1):53-61.
21. Salaverria I, Martin-Guerrero I, Burkhardt B, et al. High resolution copy number analysis of IRF4 translocation-positive diffuse large B-cell and follicular lymphomas. *Genes Chromosomes Cancer*. 2013;52(2):150-155.
22. Momose S, Weißbach S, Pischimarov J, et al. The diagnostic gray zone between Burkitt lymphoma and diffuse large B-cell lymphoma is also a gray zone of the mutational spectrum. *Leukemia*. 2015;29(8):1789-1791.
23. Sha C, Barrans S, Cucco F, et al. Molecular high-grade B-cell lymphoma: defining a poor-risk group that requires different approaches to therapy. *J Clin Oncol*. 2019;37(3):202-212.
24. Poirel HA, Cairo MS, Heerema NA, et al; FAB/LMB 96 International Study Committee. Specific cytogenetic abnormalities are associated with a significantly inferior outcome in children and adolescents with mature B-cell non-Hodgkin's lymphoma: results of the FAB/LMB 96 international study. *Leukemia*. 2009; 23(2):323-331.
25. Rosenwald A, Wright G, Chan WC, et al; Lymphoma/Leukemia Molecular Profiling Project. The use of molecular profiling to predict survival after chemotherapy for diffuse large-B-cell lymphoma. *N Engl J Med*. 2002; 346(25):1937-1947.
26. Karube K, Enjuanes A, Dlouhy I, et al. Integrating genomic alterations in diffuse large B-cell lymphoma identifies new relevant pathways and potential therapeutic targets. *Leukemia*. 2018;32(3):675-684.
27. Szczepanowski M, Lange J, Kohler CW, et al. Cell-of-origin classification by gene expression and MYC-rearrangements in diffuse large B-cell lymphoma of children and adolescents. *Br J Haematol*. 2017;179(1):116-119.
28. Hans CP, Weisenburger DD, Greiner TC, et al. Confirmation of the molecular classification of diffuse large B-cell lymphoma by immunohistochemistry using a tissue microarray. *Blood*. 2004;103(1):275-282.

29. Steidl C, Shah SP, Woolcock BW, et al. MHC class II transactivator CIITA is a recurrent gene fusion partner in lymphoid cancers. *Nature*. 2011;471(7338):377-381.

30. Scholtysik R, Kreuz M, Klapper W, et al; Molecular Mechanisms in Malignant Lymphomas Network Project of Deutsche Krebshilfe. Detection of genomic aberrations in molecularly defined Burkitt's lymphoma by array-based, high resolution, single nucleotide polymorphism analysis. *Haematologica*. 2010; 95(12):2047-2055.

31. Scott DW, Wright GW, Williams PM, et al. Determining cell-of-origin subtypes of diffuse large B-cell lymphoma using gene expression in formalin-fixed paraffin-embedded tissue. *Blood*. 2014;123(8):1214-1217.

32. Mottok A, Wright G, Rosenwald A, et al. Molecular classification of primary mediastinal large B-cell lymphoma using routinely available tissue specimens. *Blood*. 2018;132(22): 2401-2405.

33. Cheson BD, Pfistner B, Juweid ME, et al; International Harmonization Project on Lymphoma. Revised response criteria for malignant lymphoma. *J Clin Oncol*. 2007; 25(5):579-586.

34. Yuan J, Wright G, Rosenwald A, et al; Lymphoma Leukemia Molecular Profiling Project (LLMPP). Identification of primary mediastinal large B-cell lymphoma at nonmediastinal sites by gene expression profiling. *Am J Surg Pathol*. 2015;39(10):1322-1330.

35. Lenz G, Davis RE, Ngo VN, et al. Oncogenic CARD11 mutations in human diffuse large B cell lymphoma. *Science*. 2008;319(5870): 1676-1679.

36. Davis RE, Ngo VN, Lenz G, et al. Chronic active B-cell-receptor signalling in diffuse large B-cell lymphoma. *Nature*. 2010; 463(7277):88-92.

37. Louissaint A Jr., Schafernak KT, Geyer JT, et al. Pediatric-type nodal follicular lymphoma: a biologically distinct lymphoma with frequent MAPK pathway mutations. *Blood*. 2016; 128(8):1093-1100.

38. Schmidt J, Ramis-Zaldivar JE, Nadeu F, et al. Mutations of *MAP2K1* are frequent in pediatric-type follicular lymphoma and result in ERK pathway activation. *Blood*. 2017; 130(3):323-327.

39. Saito M, Gao J, Basso K, et al. A signaling pathway mediating downregulation of BCL6 in germinal center B cells is blocked by BCL6 gene alterations in B cell lymphoma. *Cancer Cell*. 2007;12(3):280-292.

40. López C, Kleinheinz K, Aukema SM, et al; ICGC MMML-Seq Consortium. Genomic and transcriptomic changes complement each other in the pathogenesis of sporadic Burkitt lymphoma. *Nat Commun*. 2019;10(1):1459.

41. Khodabakhshi AH, Morin RD, Fejes AP, et al. Recurrent targets of aberrant somatic hypermutation in lymphoma. *Oncotarget*. 2012; 3(11):1308-1319.

42. Wagener R, Bens S, Toprak UH, et al. Cryptic insertion of *MYC* exons 2 and 3 into the IGH locus detected by whole genome sequencing in a case of MYC-negative Burkitt lymphoma [published online ahead of print 9 May 2019]. *Haematologica*. doi:10.3324/haematol.2018.208140.

43. Edelmann J, Holzmann K, Miller F, et al. High-resolution genomic profiling of chronic lymphocytic leukemia reveals new recurrent genomic alterations. *Blood*. 2012;120(24): 4783-4794.

44. Yang Y, Shaffer AL III, Emre NC, et al. Exploiting synthetic lethality for the therapy of ABC diffuse large B cell lymphoma. *Cancer Cell*. 2012;21(6):723-737.

45. Liu Q, Salaverria I, Pittaluga S, et al. Follicular lymphomas in children and young adults: a comparison of the pediatric variant with usual follicular lymphoma. *Am J Surg Pathol*. 2013; 37(3):333-343.

46. Oschlies I, Klapper W, Zimmermann M, et al. Diffuse large B-cell lymphoma in pediatric patients belongs predominantly to the germinal-center type B-cell lymphomas: a clinicopathologic analysis of cases included in the German BFM (Berlin-Frankfurt-Munster) Multicenter Trial. *Blood*. 2006;107(10): 4047-4052.

47. Klapper W, Kreuz M, Kohler CW, et al; Molecular Mechanisms in Malignant Lymphomas Network Project of the Deutsche Krebshilfe. Patient age at diagnosis is associated with the molecular characteristics of diffuse large B-cell lymphoma. *Blood*. 2012;119(8):1882-1887.

48. Deffenbacher KE, Iqbal J, Sanger W, et al. Molecular distinctions between pediatric and adult mature B-cell non-Hodgkin lymphomas identified through genomic profiling. *Blood*. 2012;119(16):3757-3766.

49. Mansouri L, Noerenberg D, Young E, et al. Frequent NFKBIE deletions are associated with poor outcome in primary mediastinal B-cell lymphoma. *Blood*. 2016;128(23): 2666-2670.

50. Chen BJ, Ruminy P, Roth CG, et al. Cyclin D1-positive mediastinal large B-cell lymphoma with copy number gains of CCND1 gene: a study of 3 cases with nonmediastinal disease. *Am J Surg Pathol*. 2019;43(1):110-120.

Selected Supplementary Material

Ramis-Zaldivar & Gonzalez-Farre et al

Supplemental Results

DNA and RNA quality analysis according to sample age

Time frame sample collection was from 1993 to 2019. In our series, we observed that the FFPE antiquity affected DNA quality according to qPCR values. The FFPE antiquity and the DNA quality according to qPCR values did not affect the number of variants or the C>T changes rate (**Supplemental Figure 2**). The antiquity affected the coverage, nevertheless 83% of the FFPE samples had ≥90% of the regions covered at ≥50x. Regarding RNA when we correlated binding density quality score from nSolver software (NanoString inc.) with sample antiquity, more ancient samples tend to have less binding density.

Mutational signatures analysis

The relative contribution of mutational signatures previously described in DLBCL (Arthur *et al.*, 2018; Chapuy *et al.*, 2018) was investigated for the global cohort of 47 primary LBCL (415 variants including driver, synonymous and MYC intron1). Three mutational signatures were identified, including the canonical activation-induced cytidine deaminase (cAID) (SBS.C1 in 43% of the variants) and two age related signatures (SBS1 and SBS5 in 10 and 47% respectively) with a cosine similarity of 0.92. When the relative contribution of these three mutational signatures was investigated for genes with at least 10 mutations, AID signature was detected in genes previously known to be targets of aSHM such as *SOCS1*, *IRF4*, *PIM1*, *SGK1* and *MYC* (Khodabakhshi *et al.*, 2012) (**Supplemental Figure 5, Supplemental Table 9**).

RHOA mutational analysis by Sanger sequencing

Due to the presence of *GNA13* mutations in 14% and 13% of DLBCL and HGBCL, NOS of our series respectively, we hypothesized that another gene of the same pathway as *RHOA* could be also mutated in our series. Mutations of *RHOA* have been rarely observed in DLBCL (1-

3%) (Arthur *et al.*, 2018; Chapuy *et al.*, 2018; Schmitz *et al.*, 2018) but is highly recurrent in BL (Lopez *et al.*, 2019). We then performed Sanger sequencing of RHOA exon 2 and 3 in 16 cases (9 DLBCL, 5 HGBCL, NOS and 2 DLBCL relapsed samples with DNA available). Only one DLBCL case presented a SNV in 5R>W position.

Supplemental Figure 1. Next generation sequencing (NGS) analysis pipeline followed to identify potential driver mutations in the 55 large B-cell lymphomas analyzed. Two different variant callers were used, Somatic Variant Caller (Illumina inc.) and Mutect2 (GATK version 4.0.3). Potential driver mutations were predicted according to previously published criteria (Karube *et al.*, 2018).

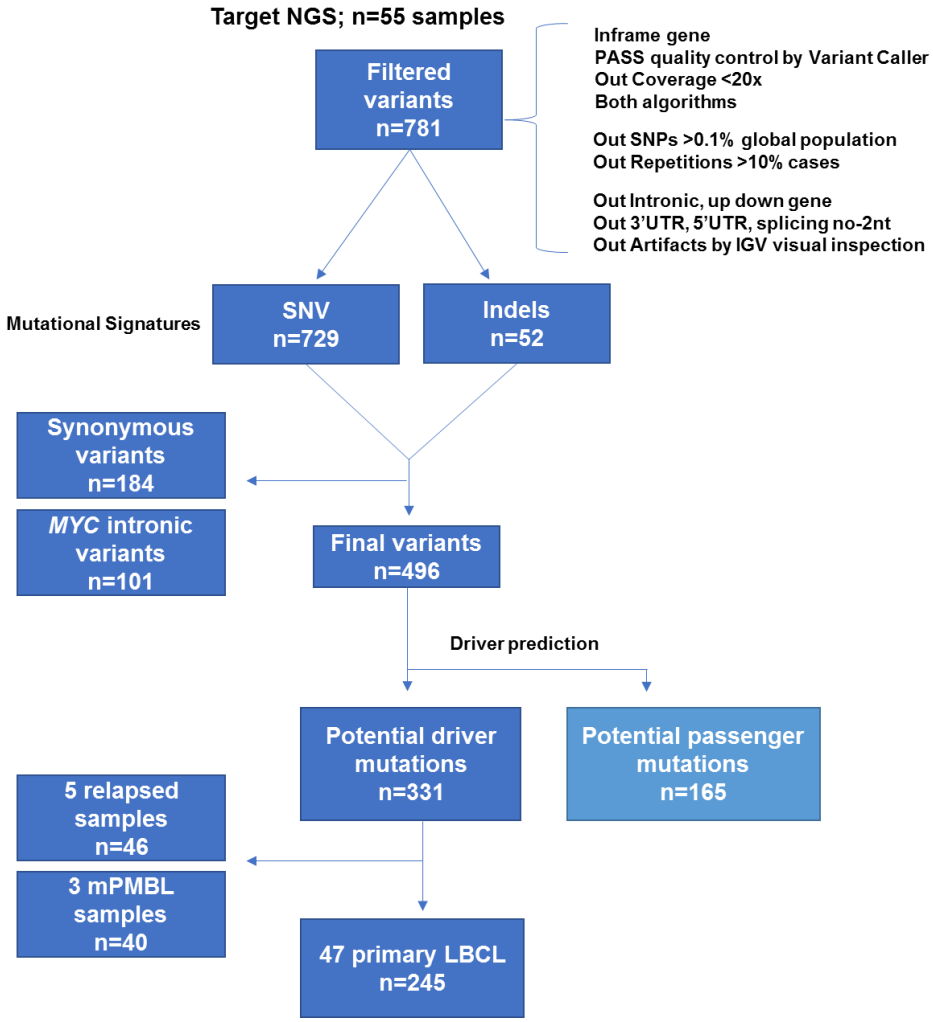

Supplemental Figure 2. Quality control of NGS data after filtering according to pipeline. **A)** Coverage, **B)** number of variants and **C)** C<T proportion were assessed in terms of tissue type (FFPE and FT DNA samples) and FFPE DNA antiquity and quality. **D)** Relative contribution of SNV changes of 47 FFPE and 8 frozen DNA samples. FFPE: formalin-fixed paraffin-embedded; FT: frozen tissue.

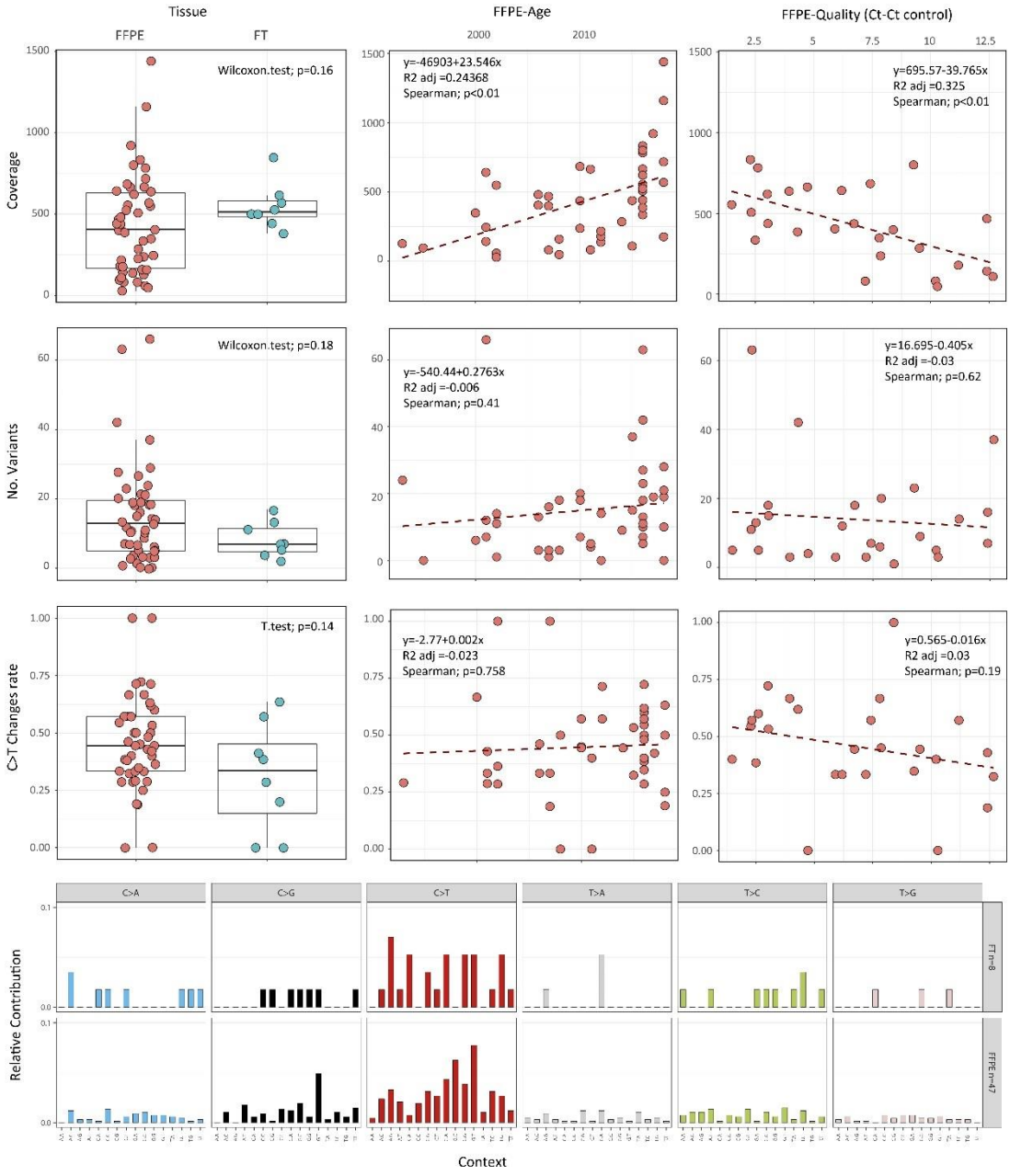

Supplemental Figure 3. *IRF4* expression at RNA and protein level between morphological groups. **A)** Boxplot representing *IRF4* gene expression (number of counts of IRF4_NM_002460.1 on Lymph2Cx assay) between LBCL-*IRF4* (n=14), DLBCL, NOS (n=25) and HGBCL, NOS (n=9). *IRF4*-R: *IRF4* rearrangement; IGH-R: IGH rearrangement; neg: negative; pos: positive; TCC: tumor cell content. Immunostaining of MUM1/IRF4 from **B-C)** D20 and D31 which are *IRF4*-negative IGH-positive LBCL-*IRF4* cases, **D-E)** cases D17 and D15 which are *IRF4*-positive LBCL-*IRF4*.

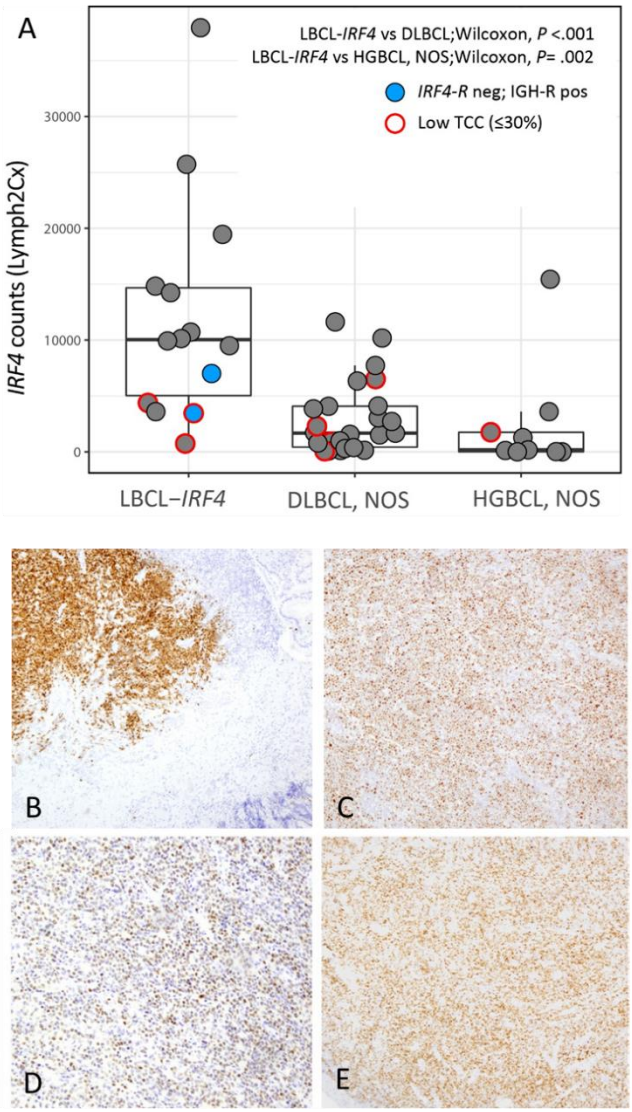

Supplemental Figure 4. Morphological, immunophenotypical and genetic features of a high grade B-cell lymphoma, NOS with *MYC* rearrangement. (Case D73) **A, H&E)** showing cytological features intermediate between DLBCL and BL and **B)** FISH with *MYC* break-apart depicting a signal constellation of one colocalization (yellow arrow) and one split signal (red and green arrows), and **C)** ideogram of the copy number, copy number neutral-loss of heterozygosity (CNN-LOH) and mutational features of this case.

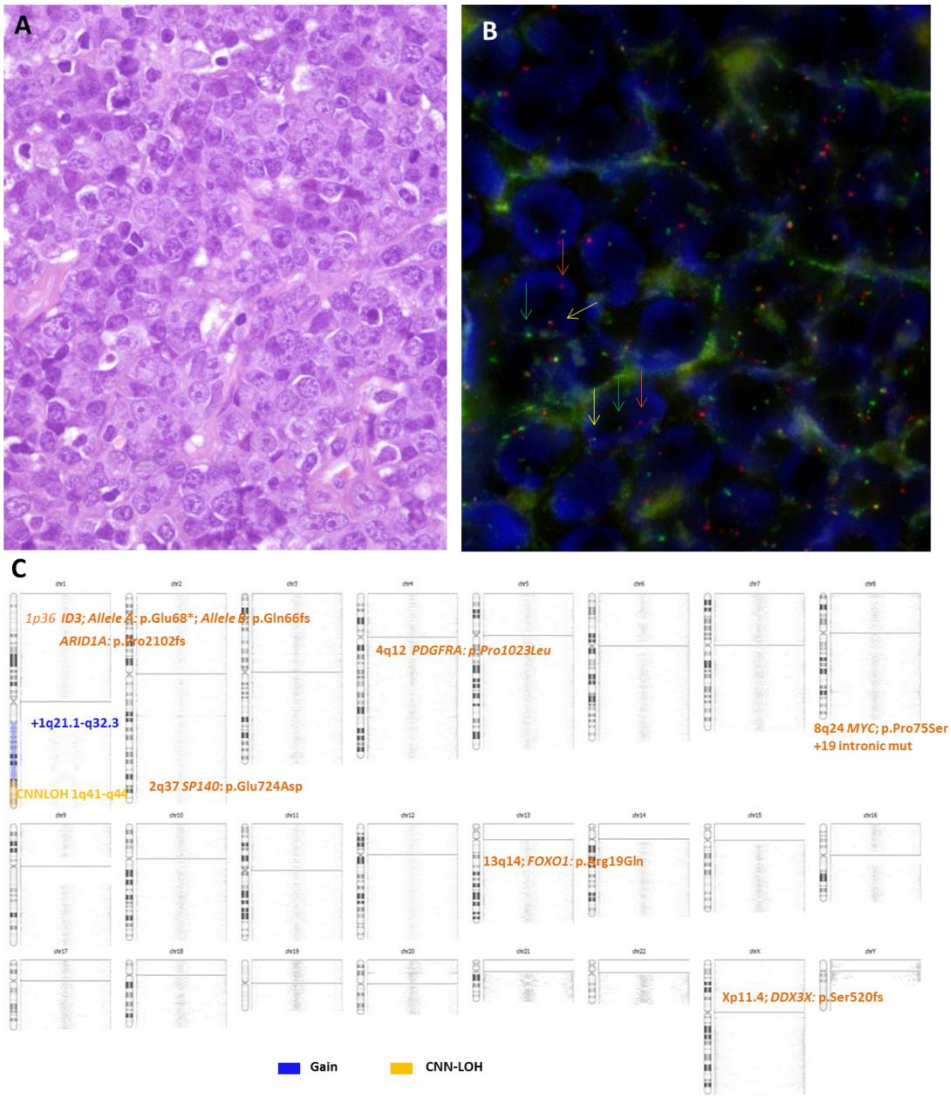

Supplemental Figure 5. Molecular features of current LBCL series according to recurrent mutational profiles on Primary mediastinal large B-cell lymphoma (PMBL), Burkitt Lymphoma (BL), pediatric type follicular lymphoma (PTFL) and Burkitt like lymphoma with 11q aberration (BLL-11q).

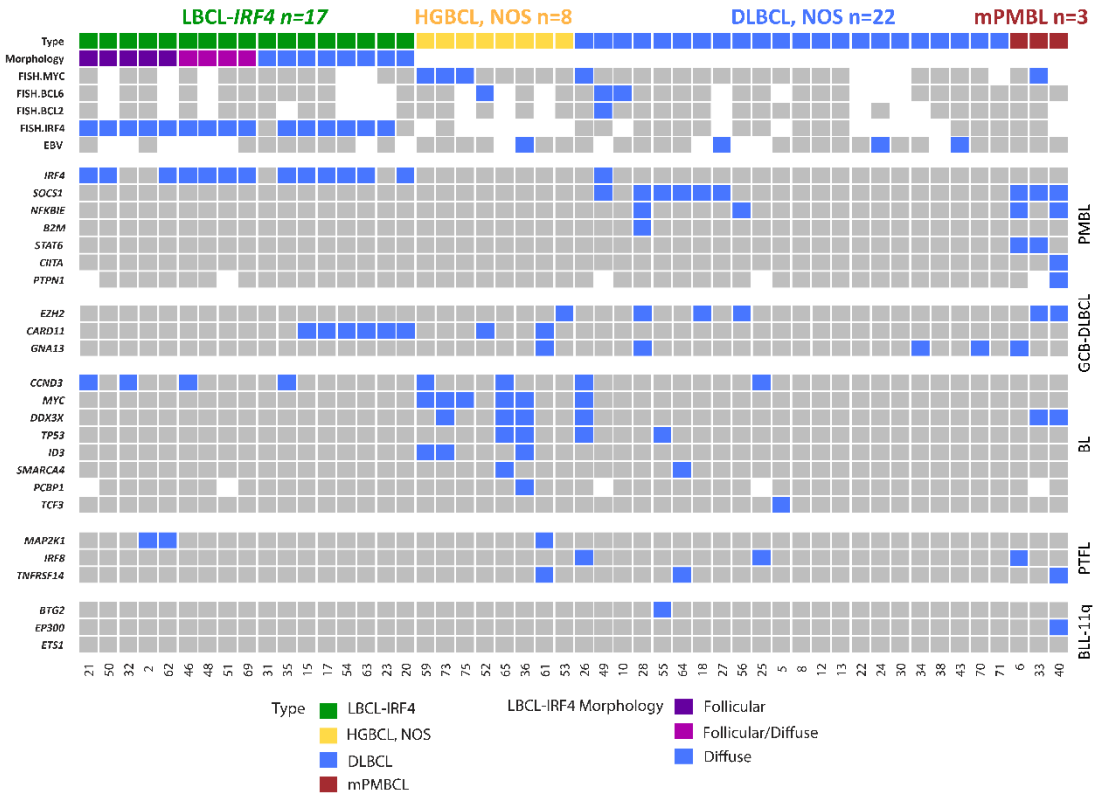

Supplemental Figure 6. Relative contribution of previously described signatures in DLBCL, NOS (Arthur *et al.*, 2018; Chapuy *et al.*, 2018) for both all the variants found in 47 primary LBCL and per frequently mutated genes (at least 10 mutations). Single nucleotide variants including both driver and non-driver predicted mutations, synonymous and *MYC*-intronic mutations were considered for the analysis.

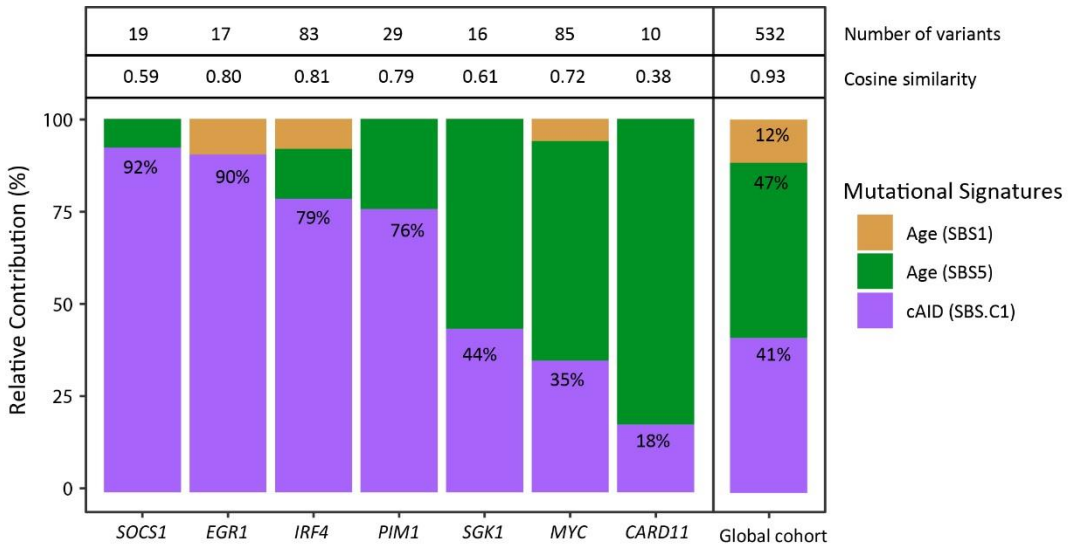

Supplemental Figure 7. Mutational profile of 25 pediatric/young-adult DLBCL, NOS according to cell of origin (Lymph2Cx and Lymph3Cx) determination. No significant differences in terms of mutation frequencies were observed between ABC and GCB (Fisher-test; NS).

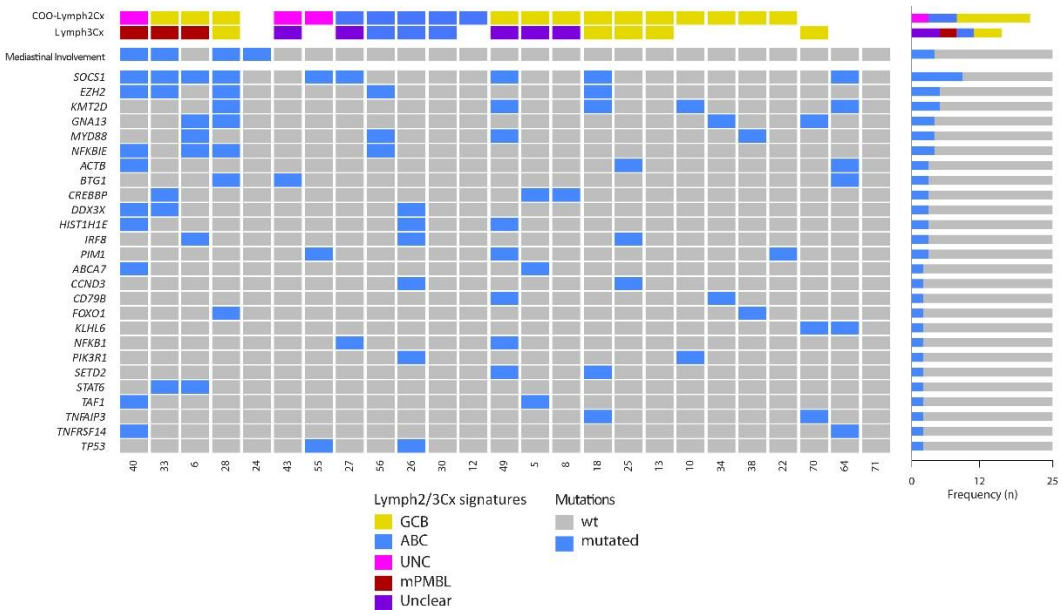

Supplemental Figure 8. Comparison of pediatric/young-adult versus adult DLBCL, NOS (Karube *et al.*, 2018)**. A)** Percentage of mutated cases in pediatric/young-adult (upper panel) and adult DLBCL, NOS (lower panel) of the most frequently mutated genes interrogated in both series (at least 5 cases). Asterisk indicates differentially mutated genes between age groups (*P* <.05). **B)** Comparative plot of copy number and copy number neutral-loss of heterozygosity (CNN-LOH) between 22 pediatric/young-adult DLBCL, NOS and 116 adult DLBCL, NOS. Significant different regions are indicated in the plot and the color denotes the enriched group (FDR<.1). GCB: germinal center B-cell; ABC: activated B-cell; UC: unclassified/intermediate; ND/NE: not done/not evaluable.

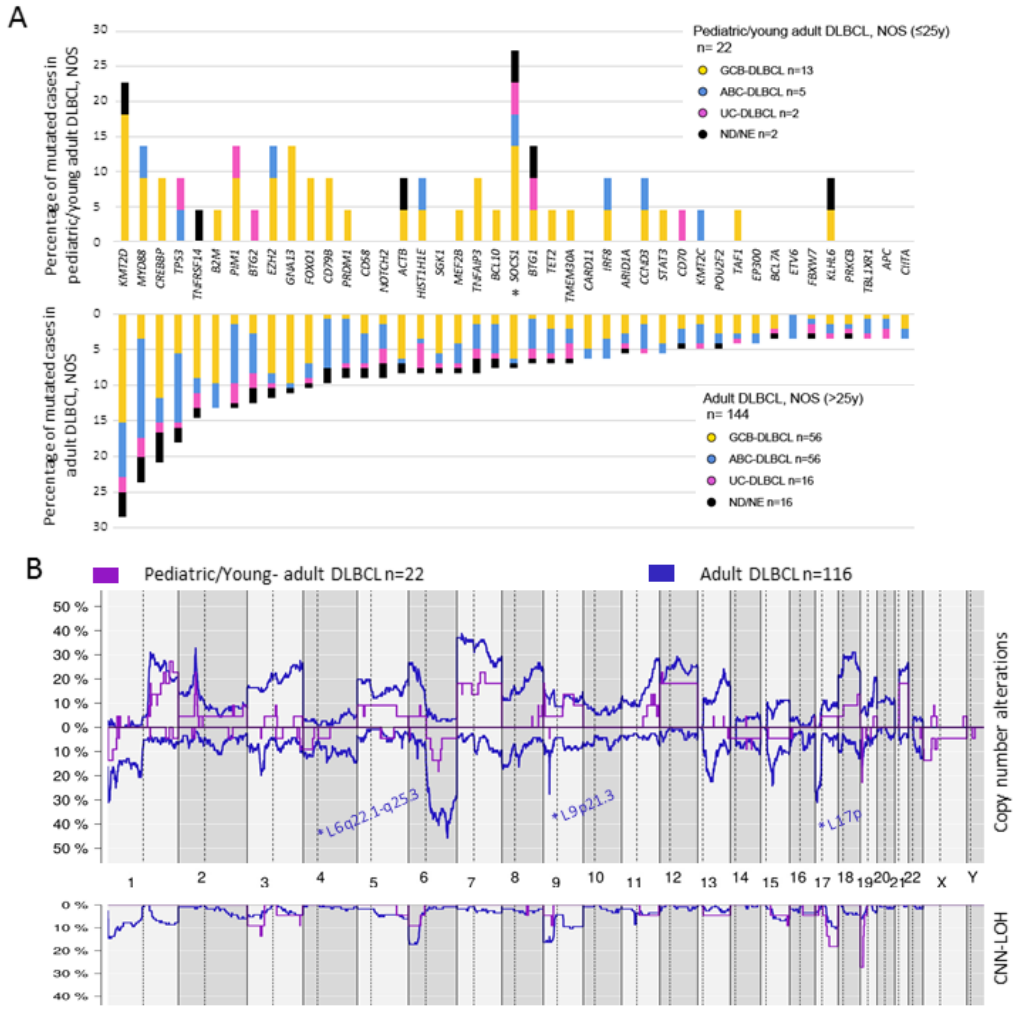

Supplemental Figure 9. Recurrent mutated pathways (Karube *et al.*, 2018) in 47 LBCL primary tumors. Bar-graph shows the total number of mutated cases for each pathway. Each color bar indicates morphological subtypes. Asterisks represents significant mutated pathway in a morphological subtype.

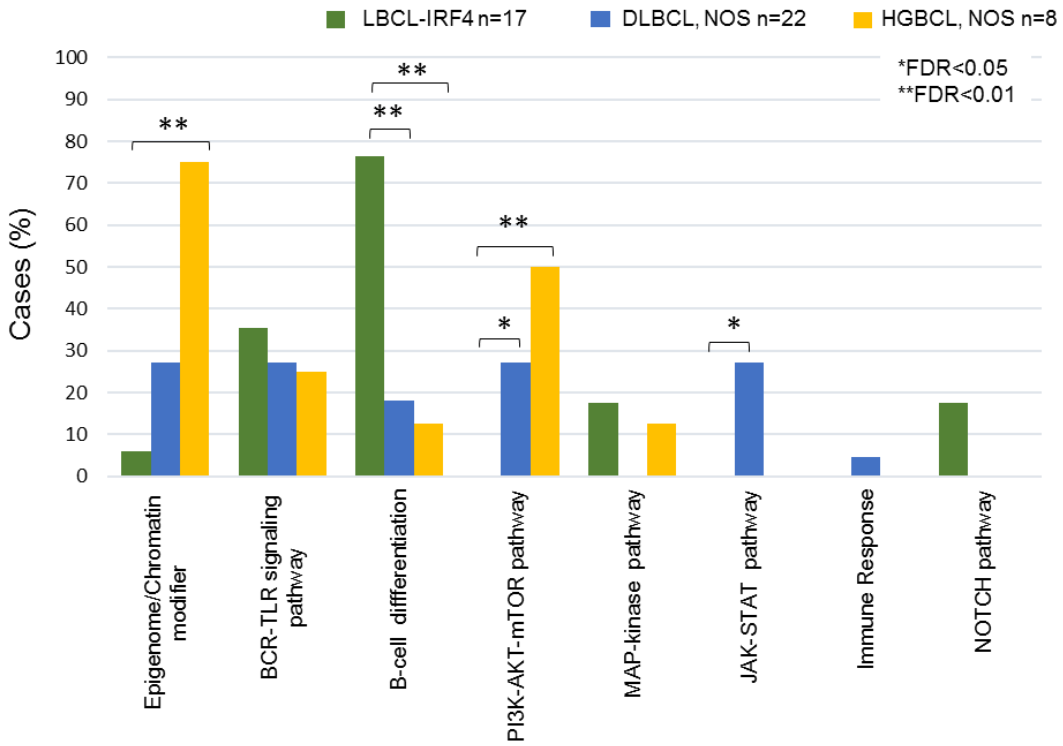

Supplemental Figure 10. A) Detailed representation of mutational landscape by variant allele frequency (VAF) **B)** and CN profiles of three paired cases (primary tumor-relapsed samples). In **A**, multiple mutations on a single gene are represented as the mean of mutation VAFs. CN information for each locus is indicated behind each gene. Asterisk denotes that some variants of specific gene are not shared between primary tumor and relapse sample. Acquired mutations are depicted in green, mutations only observed at diagnosis in red and shared mutations in orange. Note that VAF has not been corrected by tumor cell content since it was not available for all samples.

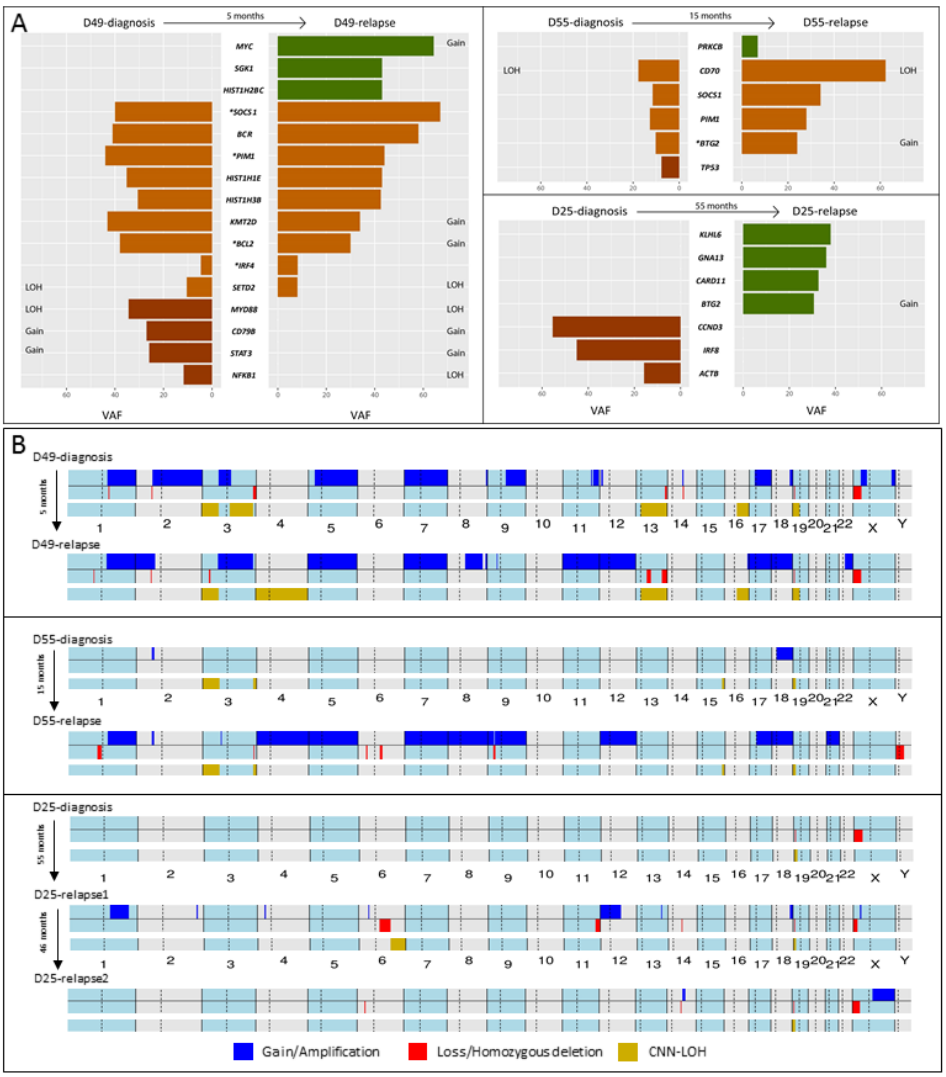

Supplemental Figure 11. Copy number (CN) analysis. **A)** Global copy number and **B)** copy number neutral loss of heterozygosity (CNN-LOH) profile of 49 pediatric/young-adult LBCL primary tumors excluding the four cases predicted as molecular PMBL. X-axis indicates chromosomes from 1 to Y and p to q. The vertical axis indicates frequency of the genomic aberration among the analyzed cases. Gains are depicted in blue, losses are depicted in red and CNN-LOH are depicted in yellow. Recurrent CN and CNN-LOH regions (>10% of cases) are indicated.

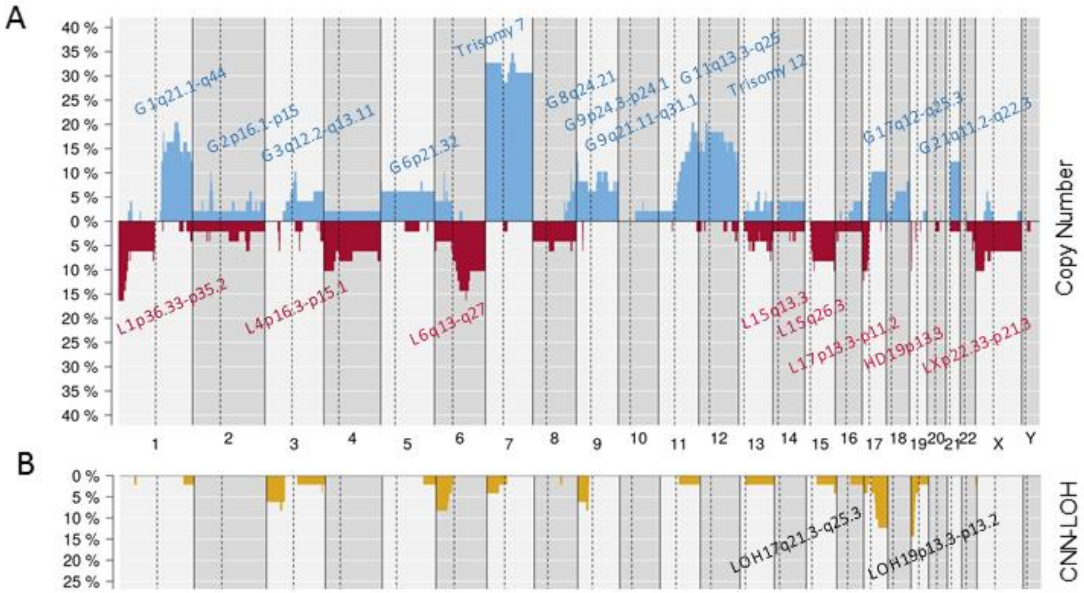

Supplemental Figure 12. Heatmap of differentially expressed genes in LBCL-*IRF4* (n=11) versus DLBCL (n=10) based on the nCounter PanCancer Immune Profiling Panel (NanoString inc.). Asterisk indicates NF-κB target gene according to http://www.bu.edu/nf-kb/gene-resources/target-genes/.

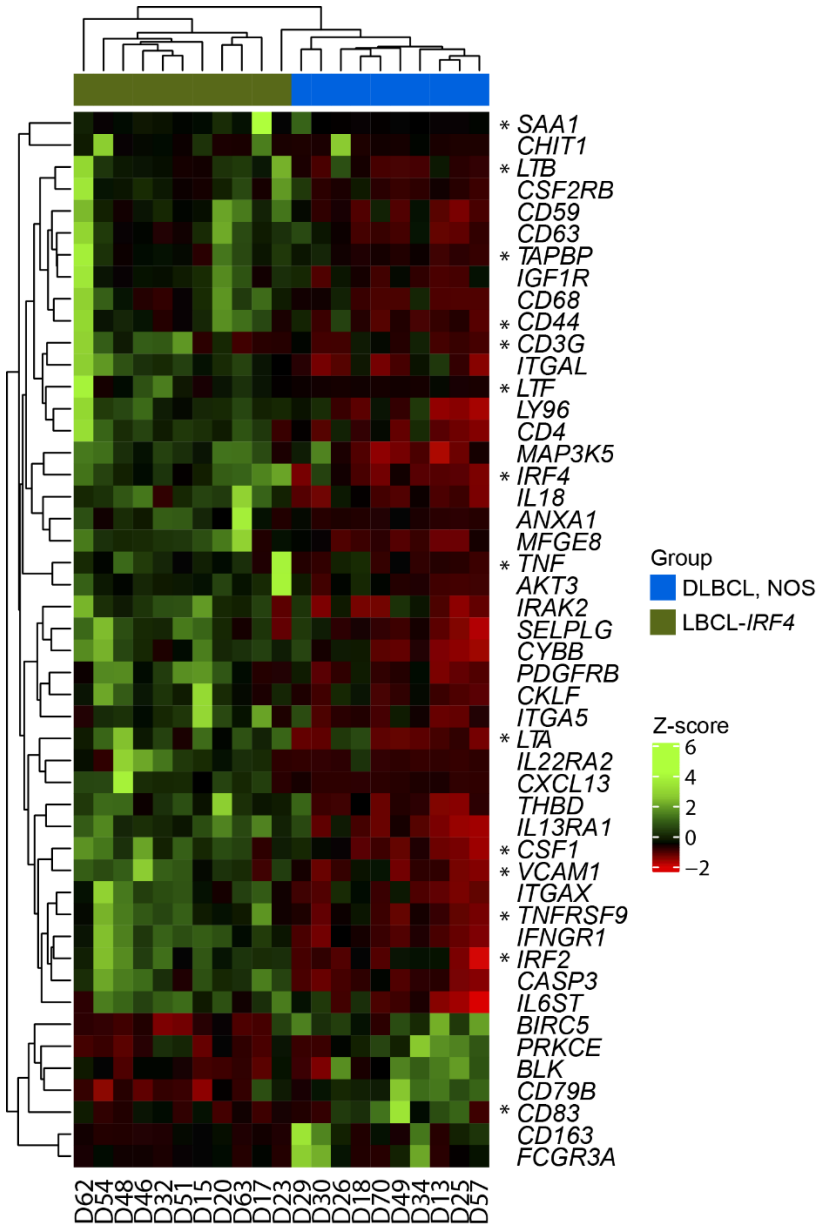

Supplemental Figure 13. Clinical and molecular parameters associated to worse EFS in the 46 current series with available follow up. COO: Cell of origin; UNC: unclassified/intermediate.

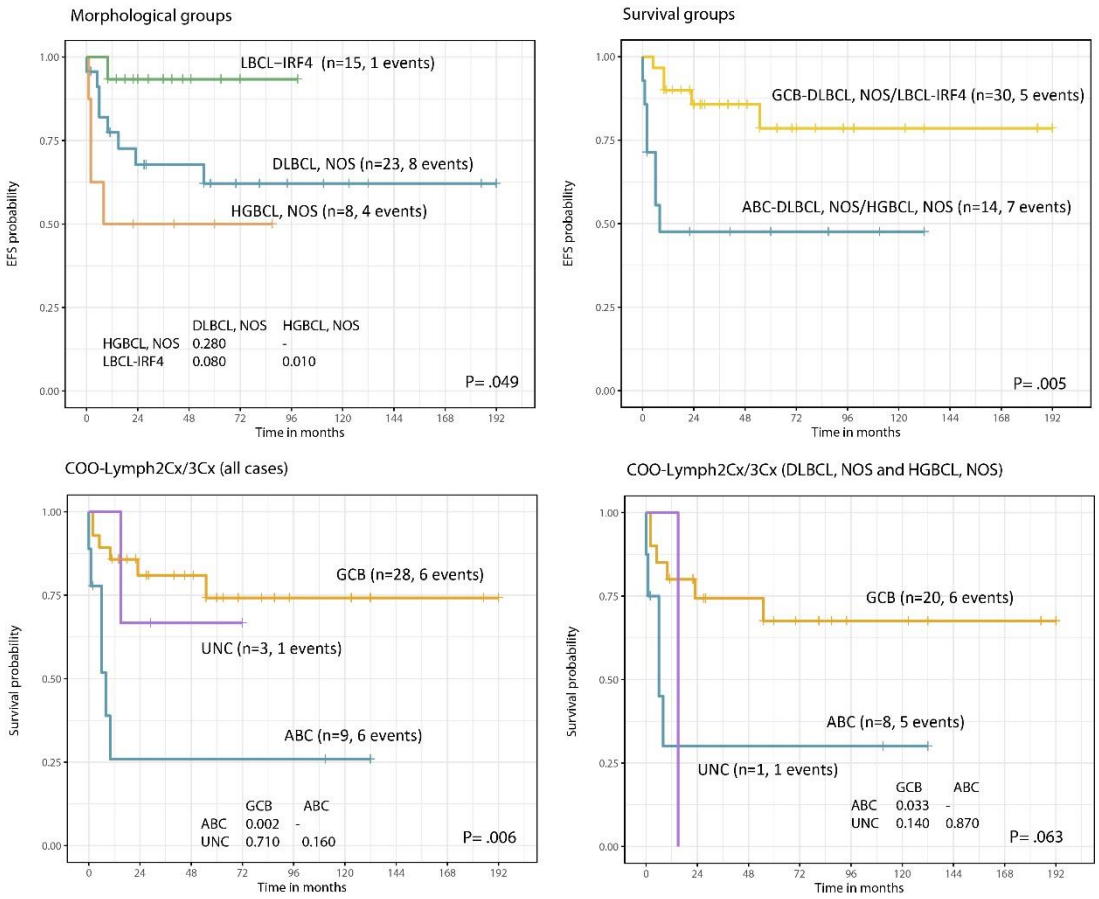

Supplemental Table 5. Clinicopathological features of 31 Diffuse large B-cell lymphoma, NOS.

Case	Age, gender	Biopsy site	Immunophenotype					*In situ* hybridization			Stage*	COO Nanostring (Lymph2Cx)	Treatment	Outcome, Follow-up
			CD10	BCL6	MUM1	BCL2	EBER	*MYC*	*BCL2*	*BCL6*				
D3R	20, M	Supraclavicular LN	+	+	+	-	-					GCB	CT-A	CR, 197m**
D5	20, F	LN	-	+	-	+	-	N	N			GCB		
D6	25, F	Axillary LN	-	+	-		-	N	N	N	II	GCB#	CT-A	CR, 164m
D8	25, M	Inguinal LN	-	+	-		-	N	N	N	II	GCB	CT-A	CR, 185m
D9	22, F	LN	-	+	+	+	-	N	N	N	II	ABC	CT-A	DwD, 20m**
D10	21, M	Cervical LN	-	-	-	+	-	N	N	R	II	GCB	CT-A	CR, 132m
D12	17, M	LN	-	+	+	+	-	N	N	N	I	ABC	CT-A	CR, 111m
D13	4, F	Supraclavicular LN	+	+	+	+	-	N	N	N	I	GCB	CT-P	CR, 70m
D14R	11, M	Abdominal LN	+	+	-	-	-					GCB	CT-P	DwD, 80m**
D18	16, M	Inguinal LN	+	+	+	-		N	N	N	I-A	GCB	CT-A	CR, 94m
D22	24, M	Liver	-	+	-		-				IV	GCB	CT-A	CR, 55m
D24	2, M	Lung	-	+	-	+	+		N				CT-P	CR, 58m
D25	5, F	Cervical LN	+	+	-	-		N	N	N	I	GCB	CT-P	CR, 145m**
D26	12, M	Spleen	+	+	+	+	-	R	N	N		ABC	CT-P	DwD, 6m**
D27	11, M	Cervical LN		-	-	-	+	N			IV-B	ABC	CT-P	CR, 132m

D28	14, M	Cervical LN	+	+	-	-	-	N	N	N	IV-A	GCB	CT-P	CR, 81m
D29	1, M	Small bowel	-	+	-	-	+	N	N	N	III	GCB	CT-P	CR, 192m
D30	1, F	LN	-	-	-	+	+				IV	ABC		DwD, 0m**
D33	9, F	Mediastinal mass	-	+	+	+	-	R	N	N	IV	GCB#	CT-P	CR, 23m**
D34	11, M	Cervical LN	+	+	-	-	-	N		N		GCB	CT-P	CR, 27m
D38	12, F	Tonsil and submandibular LN	+	+	-	+		N	N	N	II	GCB	CT-P	CR, 28m
D40	24, M	Supraclavicular LN	-	+	+	+	-			N	III	UNC#	CT-A	DwD, 11m**
D42	22, M	Mediastinal LN	+	+	-	+		N	N	N	IV	GCB#	CT-A	CR, 184m**
D43	22, F	Cervical LN	-	-	+		+	N	N	N	II	UNC		
D49	21, M	Tonsil	+	+	+	-		N	R	R		GCB	CT-A	CR, 34m**
D55	25, M	Axillary LN	+	+	-		-	N	N	N	IV	UNC	CT-A	DwD, 31m**
D56	1, M	Cervical LN	-	-	+	+		N	N	N	IV	ABC	CT-P	CR, 2m
D57	5, M	Abdominal mass	-	+		+	-	R	N	N	III		CT-P	CR, 123m
D64	16, M	Inguinal LN	-	+	-	+	-	N	N	N				
D70	9, M	Axillary LN	+	+	+	+	-	N	N	N				
D71	10, M	Appendix	+	+	+	+	-		N	N	III	GCB	CT-P	CR, 8m

Abbreviations: R: relapse; M: male; F: Female; LN: Lymph node; R: rearrangement; N: Normal; COO: Cell of origin; GCB: Germinal center B-cell; ABC: Activated B-cell; UNC: Intermediate/unclassified; CT-P: Chemotherapy with pediatric schema protocol; CT-A: Chemotherapy with adult schema protocol (R-CHOP/ESHAP); CR: Complete response; DwD: Dead with disease; m: months.

*Stage was established according St. Jude/International pediatric NHL staging system (IPNHLSS) or Ann Arbor staging system for pediatric and adult patients respectively.

**Patients who had a relapse/progression

#Predicted as mPMBL by Lymph3Cx and are also described in Supplementary Table 7.

Supplemental Table 6. Pathological and clinical features of 12 High grade B-cell lymphoma, NOS.

Case	Age, gender	Biopsy site	Morphology	Immunophenotype						*In situ* hybridization				Stage*	COO Nanostring (Lymph2Cx)	Treatment	Outcome, Follow-up
				CD10	BCL6	MUM1	BCL2	TdT	MYC	EBER	*MYC*	*BCL2*	*BCL6*				
D19	7, M	Retroperitoneum	Blastoid	+		-	+	-	+		R	N				CT-P	CR, 41m
D36	14, M	Abdominal tumor	DLBCL/BL	+	+	-	+			+	N	N	N	III	GCB	CT-P	DwD, 2m
D37	3, M	Abdominal LN	DLBCL/BL	+	+	-	+	-		-	N	N	N	III	GCB	CT-P	CR, 22m
D52	23, F	Breast	DLBCL/BL	-	+	+	+	-		-	N	N	R	IV-A	ABC	CT-P	CR, 191m**
D53	13, F	Stomach	DLBCL/BL	+	+	-	-	-		-	N	N	N	IV	GCB	CT-P	CR, 87m
D58	4, M	LN	DLBCL/BL	-			-			+				IV	ABC	CT-P	DwD, 1m
D59	5, F	Kidney	DLBCL/BL	+	+		+	-	+	-	R	N	N				D, 1m#
D61	12, M	Intestine	Blastoid	+	+		-	-	-	-	N						
D65	4, M	Retroperitoneum	Blastoid	+				-			N			III	GCB	CT-P	DwD, 7m**
D72	19, M	Palate	DLBCL/BL	+	+	+	-		+	-	N	N	N		GCB		
D73	12, M	Tonsil	DLBCL/BL	+			-		-	-	R	N	N		GCB		
D75	6, F	Intestine	Blastoid	+	+	-	-	-		-	R			II	GCB	CP-P	CR, 60m

Abbreviations: M: male; F: Female; LN: Lymph node; R: rearrangement; N: Normal; COO: Cell of origin; GCB: Germinal center B-cell; ABC: Activated B-cell; CT-P: Chemotherapy with pediatric schema protocol; CR: Complete response; D: died: DwD: Dead with disease; m: months.
*Stage was established according St. Jude/International pediatric NHL staging system (IPNHLSS) or Ann Arbor staging system for pediatric and adult patients respectively.
** Patients who had a relapse/progression and need rescue treatment.
# This patient died before treatment due to cardiac arrest during port-a cath insertion, so this event is excluded of survival analysis.

Supplemental Table 7. Clinical, morphological and genetic data of four cases predicted as PMBL and 5 cases predicted as uncertain between mPMBL and DLBCL by Lymph3Cx assay.

Case	Age, Gender	Diagnosis	Biopsy Site	Other sites	PMBL morphological features	Hans	EBV	FISH *MYC*	FISH *CIITA*	9p24 *JAK2*	2p16 *REL*	Lymph3Cx	Lymph2Cx
D6	25, F	DLBCL	Axillary LN		Not typical	GC	-	-		Tri 9	WT	PMBL	GCB
D33	9, F	DLBCL	Mediastinal mass	BM, pelvis and ovary	Not typical	Non-GC	-	+		WT	Ampli	PMBL	GCB
D40	24, M	DLBCL	Supraclavicular LN	Multiple LN in thoracic region and mediastinum, bone and spleen	Typical	Non-GC	-		-	Tri 9	WT	PMBL	UNC
D42	22, M	DLBCL	Mediastinal LN	BM, lung, liver, suprarenal and renal	Not typical	GC		-	-	WT	WT	PMBL	GCB
D5	20, F	DLBCL	LN		Not typical	GC	-	-		WT	WT	Uncertain PMBL/GCB	GCB
D8	25, M	DLBCL	Inguinal LN		Not typical	GC	-	-				Uncertain PMBL/GCB	GCB
D27	11, M	DLBCL	Cervical LN	BM and spleen	Not typical	Non-GC	+	-		Ampli	WT	Uncertain PMBL/UNC	ABC
D43	22, F	DLBCL	Cervical LN		Not typical	Non-GC	+	-		Gain	WT	Uncertain PMBL/GCB	UNC
D49	21, M	DLBCL	Tonsil		Not typical	GC		-		WT	Ampli	Uncertain PMBL/GCB	GCB

Abbreviations: F: Female; M: Male; LN: Lymph node; BM: bone marrow; GC: germinal center; Tri: trisomy; Ampli: amplification; GCB: Germinal Center B-cell derived; ABC: Activated B-cell derived; PMBL: Primary mediastinal large B-cell lymphoma; UNC: Unclassified; WT: wild type.
Copy number alterations obtained from Oncoscan/SNP-array analysis.

Supplemental Table 9. Aberrant somatic hypermutation (aSHM) hallmarks in frequently mutated genes[#]

Gene name	Total SNV	Mutated cases	Mutations/ case	Variants within AID target region	AID-target region bias (*P*-value)	Transition over transversions bias (*P*-value)	AID-motif bias (*P*-value)
MYC	85	11	7.73	75	0.88 (<0.001)	0.74 (0.111)	0.59 (0.002)
IRF4	83	16	5.19	80	0.96 (<0.001)	1.10 (<0.001)	0.55 (0.172)
PIM1	29	12	2.42	29	1.00 (0.001)	1.64 (0.002)	0.66 (0.758)
SOCS1	19	7	2.71	19	1.00 (1.000)	0.58 (0.935)	0.42 (0.470)
EGR1	17	6	2.83	16	0.94 (0.091)	2.20 (0.006)	0.69 (1.000)
SGK1	16	6	2.67	16	1.00 (<0.001)	2.20 (0.006)	0.81 (0.044)
CARD11	10	10	1.00	0	-	-	-

[#] Ten single nucleotide variants including driver and passengers predicted, synonymous and *MYC*-intronic.
AID-target region is defined as 2Kb region after 150bp from a transcript start site)
AID-motifs correspond to sequences WA/TW/WRCY/RGYW/WGCW)[16]
Significance value was calculated using Test of Equal or Given Proportions.

Supplemental Table 13. Clinicopathological features of the different age groups.

Characteristics	0-18 y	19-25 y	All LBCL	>25 y ¶	Significance (*P*-value) Age (0-18y) vs (19-25y)	Pediatric/young-adult vs adult (>25 y)
Num. Patients	45	14	59	144		
Type						
DLBCL, NOS	18/45 (40%)	9/14 (64%)	27/59 (46%)		0.134	
HGBCL, NOS	10/45 (22%)	2/14 (14%)	12/59 (20%)		0.712	
LBCL-*IRF4*	17/45 (38%)	3/14 (21%)	20/59 (34%)		0.342	
Ratio M:F	28:17	9:5	37:22	74:70	1.000	0.163
Primary extranodal involvement	15/45 (33%)	4/14 (29%)	19/59 (32%)		1.000	
Head and neck	21/40 (53%)	6/12 (50%)	27/52 (52%)		1.000	
Stage III/IV	14/29 (48%)	4/10 (40%)	18/39 (46%)	78/143 (55%)	0.726	0.371
LDH high	8/25 (32%)	4/7 (57%)	12/32 (38%)	65/142 (46%)	0.379	0.436
In situ Hybridization						
EBV (EBER)	6/32 (19%)	1/12 (8%)	7/44 (16%)		0.653	
FISH MYC	6/34 (18%)	0/11 (0%)	6/45 (13%)	11/119 (9%)	0.311	0.566
FISH BCL2	0/29 (0%)	1/9 (11%)	1/38 (3%)	25/125 (20%)	0.237	**0.010**
FISH BCL6	0/29 (0%)	3/8 (38%)	3/37 (8%)	24/117 (21%)	**0.007**	0.134
FISH IRF4	14/31 (45%)	3/9 (33%)	17/40 (43%)		0.707	
COO-Hans						
GC	31/44 (70%)	8/14 (57%)	39/58 (67%)		0.514	
Non-GC	13/44 (30%)	6/14 (43%)	19/58 (33%)		0.514	
COO-Nanostring #						
GCB	27/36 (75%)	8/13 (62%)	35/49 (71%)	43/105 (41%)	0.476	**<0.001**
ABC	6/36 (17%)	3/13 (23%)	9/49 (18%)	49/105 (47%)	0.683	**0.009**
UC	3/36 (8%)	2/13 (15%)	5/49 (10%)	13/105 (12%)	0.598	1.000
Genetics						
No. Mutations	5.1 (0-16)	5.8 (1-20)	5.2 (0-20)		0.969	
No. CNA	4.5 (0-24)	12.8 (1-34)	6.2 (0-34)	20 (1-108)	**0.046**	**<0.001**
Chromothripsis	1/39 (3%)	3/10 (30%)	4/49 (8%)	28/116 (24%)	**0.023**	0.077
CR rate of first line treatment	29/35 (83%)	9/11 (82%)	38/46 (83%)	96/142 (68%)	1.000	0.061
Rituximab	7/35 (20%)	9/11 (82%)	16/46 (35%)	116/143 (81%)	**<0.001**	**<0.001**
No. of deads	6/35 (17%)	2/11 (18%)	8/46 (17%)	82/144 (57%)	1.000	**<0.001**
Relapse/Progress	7/35 (20%)	6/11 (55%)	13/46 (28%)	70/144 (49%)	0.051	**0.017**
Median Follow-up	38.5 months	40 months	40 months	84 months	0.234	0.581
5-year OS	86%	79%	83%	63%	0.910	**0.007**
5-year EFS	76%	46%	68%	65%	**0.044**	0.490

#Cell of origin by Lymph2Cx or Lymph3Cx.
Abbreviations; y: years; M: male; F: female; GC: germinal center; CR: Complete response; OS: Overall survival; EFS: Event free survival.
¶ Clinical data from patients older than 25 years old was recruited and updated from Karube et al.[5]

Supplemental Table 14. Clinical and morphological features of the different lymphoma entitites.

Characteristics	LBCL-*IRF4*	DLBCL, NOS	HGBCL, NOS	Significance (*P*-value) LBCL-IRF4 vs DLBCL	LBCL-IRF4 vs HGBCL, NOS	DLBCL vs HGBCL, NOS
Num. Patients	20	27	12			
Median Age	14 (5-22)	12 (1-25)	9.5 (3-23)	0.889	0.093	0.330
0-18y	17/20 (85%)	18/27 (67%)	10/12 (83%)	0.191	1.000	0.446
19-25y	3/20 (15%)	9/27 (33%)	2/12 (17%)	0.191	1.000	0.446
Ratio M:F	9:11	20:7	8:4	0.069	0.291	0.709
Primary extranodal involvement	4/20 (20%)	6/27 (22%)	9/12 (75%)	1.000	**0.004**	**0.004**
Head and neck	14/18 (78%)	11/23 (48%)	2/11 (18%)	0.063	**0.003**	0.140
Stage III/IV	3/14 (21%)	9/18 (50%)	6/7 (86%)	0.147	**0.016**	0.179
LDH high	2/12 (17%)	5/12 (42%)	5/8 (63%)	0.371	0.062	0.650
Immunohistochemistry						
CD10	11/20 (55%)	13/26 (50%)	10/12 (83%)	0.774	0.139	0.077
MUM1	20/20 (100%)	11/26 (42%)	2/7 (29%)	**<0.001**	**<0.001**	0.676
BCL6	20/20 (100%)	22/27 (81%)	8/8 (100%)	0.063	1.000	0.315
KI-67>75%	11/14 (79%)	15/19 (79%)	11/11 (100%)	1.000	0.230	0.268
BCL2	10/19 (53%)	14/23 (61%)	5/11 (45%)	0.756	1.000	0.475
CD20	19/19 (100%)	22/22 (100%)	9/9 (100%)	1.000	1.000	1.000
In situ Hybridization						
EBV (EBER)	0/12 (0%)	5/22 (23%)	2/10 (20%)	0.137	0.195	1.000
FISH MYC	0/13 (0%)	2/21 (10%)	4/11 (36%)	0.513	**0.031**	0.148
FISH BCL2	0/10 (0%)	1/21 (5%)	0/7 (0%)	1.000	1.000	1.000
FISH BCL6	0/11 (0%)	2/20 (10%)	1/6 (17%)	0.527	0.353	1.000
FISH IRF4	17/19 (89%)	0/17 (0%)	0/4 (0%)	**<0.001**	**0.002**	1.000
COO-Hans						
GC	11/20 (55%)	18/27 (67%)	10/11 (91%)	0.546	0.055	0.225
Non-GC	9/20 (45%)	9/27 (33%)	1/11 (9%)	0.546	0.055	0.225
COO-Nanostring[#]						
GCB	10/14 (71%)	17/25 (68%)	8/10 (80%)	1.000	1.000	0.686
ABC	1/14 (7%)	6/25 (24%)	2/10 (20%)	0.386	0.550	1.000
UC	3/14 (21%)	2/25 (8%)	0/10 (0%)	0.329	0.239	1.000
Genetics						
No. Mutations	5.2 (0-11)	4.7 (0-20)	6.6 (1-11)	0.247	0.278	0.143
No. CNA	6.2 (0-27)	5.8 (0-34)	7.1 (0-27)	0.518	0.697	0.939
Chromothripsis	2/20 (10%)	1/22 (5%)	1/7 (14%)	0.598	1.000	0.431
CR rate of first line treatment	14/15 (93%)	19/23 (83%)	5/8 (63%)	0.630	0.103	0.335
Rituximab	6/15 (40%)	10/23 (43%)	0/8 (0%)	1.000	0.058	**0.032**
No. of deads	0/15 (0%)	5/23 (22%)	3/8 (38%)	0.136	**0.032**	0.393
Relapse/Progress	1/15 (7%)	8/23 (35%)	4/8 (50%)	0.061	**0.033**	0.676
Median Follow-up	29 months	70 months	22 months	0.060	0.531	0.126
5-year EFS	93%	62%	50%	0.075	**0.010**	0.280

[#]Cell of origin by Lymph2Cx or Lymph3Cx.
Abbreviations; y: years; M: male; F: female; GC: germinal center; CR: Complete response; OS: Overall survival; EFS: Event free survival.

Supplemental Table 15. Clinical and morphological features of the different age groups of DLBCL					Significance (*P*-value)		
Characteristics	**0-18 y**	**19-25 y**	**All pDLBCL, NOS**	**>25 y¶**	**Age (0-18y) vs (19-25y)**	**Pediatric/young-adult vs adult (>25 y)**	**Young-adult (19-25y) vs adult (>25 y)**
Num. Patients	18	9	27	144			
Ratio M:F	14:4	6:3	20:07	74:70	0.653	**0.035**	0.721
Primary extranodal involvement	5/18 (28%)	1/9 (11%)	6/27 (22%)		0.628		
Head and neck	7/16 (44%)	4/7 (57%)	11/23 (48%)		0.667		
Stage III/IV	7/12 (58%)	2/6 (33%)	9/18 (50%)	78/143 (55%)	0.620	0.804	0.416
LDH high	3/8 (38%)	2/4 (50%)	5/12 (42%)	65/142 (46%)	1.000	1.000	1.000
In situ Hybridization							
EBV (EBER)	4/14 (29%)	1/8 (13%)	5/22 (23%)		0.613		
FISH MYC	2/14 (14%)	0/7 (0%)	2/21 (10%)	11/119 (9%)	0.533	1.000	1.000
FISH BCL2	0/14 (0%)	1/7 (14%)	1/21 (5%)	25/125 (20%)	0.333	0.125	0.595
FISH BCL6	0/14 (0%)	2/6 (33%)	2/20 (10%)	24/117 (21%)	0.079	0.364	1.000
FISH IRF4	0/12 (0%)	0/5 (0%)	0/17 (0%)		1.000		
COO-Hans							
GC	12/18 (67%)	6/9 (67%)	18/27 (67%)		1.000		
Non-GC	6/18 (33%)	3/9 (33%)	9/27 (33%)		1.000		
COO-Nanostring							
GCB	11/16 (69%)	6/9 (67%)	17/25 (68%)	43/105 (41%)	1.000	**0.009**	0.268
ABC	5/16 (31%)	1/9 (11%)	6/25 (24%)	49/105 (47%)	0.364	0.182	0.259
UC	0/16 (0%)	2/9 (22%)	2/25 (8%)	13/105 (12%)	0.120	1.000	0.241
Genetics							
No. Mutations	4.4 (0-16)	5.4 (1-20)	4.7 (0-20)		0.803		
No. CNA	4.9 (0-24)	8.2 (1-34)	5.8 (0-34)	20 (1-108)	0.682	**<0.001**	**0.001**
Chromothripsis	1/16 (6%)	0/6 (0%)	1/22 (5%)	28/116 (24%)	1.000	0.129	0.584
CR rate of first line treatment	13/16 (81%)	6/7 (86%)	19/23 (83%)	96/142 (68%)	1.000	0.221	0.665
Rituximab	4/16 (25%)	6/7 (86%)	10/23 (43%)	116/143 (81%)	**0.019**	**<0.001**	1.000
No. of deads	3/16 (19%)	2/7 (29%)	5/23 (22%)	82/144 (57%)	0.621	**0.003**	0.405
Relapse/Progress	4/16 (25%)	4/7 (57%)	8/23 (35%)	70/144 (49%)	0.182	0.264	1.000
Median Follow-up	75 months	55 months	70 months	84 months	0.504	0.287	0.138
5-year OS	87%	71%	81%	63%	0.740	**0.035**	0.190
5-year EFS	71%	43%	62%	65%	0.150	0.900	0.320

[#]Cell of origin by Lymph2Cx or Lymph3Cx.
Abbreviations; y: years; M: male; F: female; GC: germinal center; CR: Complete response; OS: Overall survival; EFS: Event free survival.
[¶]Clinical data from patients older than 25 years old was recruited and updated from Karube et al.[5]

DISCUSSION

B-NHL in pediatric population is a heterogeneous group of lymphomas that comprises different entities, mainly represented by GC-derived aggressive high-grade tumors including BL, PMBCL and DLBCL (Sandlund and Martin, 2016). The two first subtypes have been extensively studied and are now characterized by well-established genomic profiles (Savage *et al.*, 2003; Love *et al.*, 2012; Richter *et al.*, 2012; Schmitz *et al.*, 2012). On the other hand, DLBCL of pediatric population is still not well genetically characterized since the majority of the molecular studies did not take into account the age of the patients, diluting in that way the biology of the pediatric variants (Reddy *et al.*, 2017; Karube *et al.*, 2018). Other less frequent but well characterized subgroup of lymphomas is PTFL, which has become a separate entity from their adult counterpart due to their clear morphological, immunophenotypic, and molecular differences (Louissaint *et al.*, 2016; Schmidt *et al.*, 2016).

Nevertheless, the knowledge of this group of lymphomas has been recently increased thanks to clinicopathologic and genetic studies of mature B-NHL in pediatric and young adult population, which have led to the identification of additional tumor subtypes previously classified as BL or DLBCL. Those new subtypes have been recognized as provisional entities in the recent update of the WHO classification (Swerdlow *et al.*, 2017). One of these entities is BLL-11q that is a HGBCL that was initially considered to have overlapping features with BL but without *MYC* translocations (Salaverria *et al.*, 2014). Secondly, LBCL-*IRF4* is also a newly defined subgroup of LBCL that constitutively expresses *IRF4* due to a translocation of the gene (Salaverria *et al.*, 2011; Quintanilla-Martinez *et al.*, 2016; Chisholm *et al.*, 2019; Woessmann and Quintanilla-Martinez, 2019). Finally, HGBCL, NOS encompasses a spectrum of morphological appearances from blastoid variants to cases with intermediate features between BL and DLBCL (Swerdlow *et al.*, 2017). Genomic features of these new subtypes in pediatric populations and their relationship to other mature B-NHL in this group of patients have not been extensively investigated. This is in part due to the rareness and novelty of some of these lymphomas that makes difficult the collection of large series.

Unfortunately, overlapping immunophenotypic, morphological and clinical features between some of these pediatric entities make the differential diagnosis challenging. For that reason, the elucidation of their genetic landscape must be relevant to improve their diagnosis and design management strategies more adapted to the particular biological behavior of these tumors.

Therefore, this doctoral thesis has aimed to address this gap of knowledge by performing a genetic and molecular characterization of large series of pediatric and young adult variants of GC-derived B-NHL including the BLL-11q, PTFL and LBCL such as DLBCL, HGBCL, NOS and LBCL-*IRF4* entities. To achieve this goal, an integrative targeted NGS, CN and transcriptome data analysis of these different pediatric and young adult entities has been performed. This has been possible thanks to the recent adaptation of molecular analysis to FFPE biopsies, along with the consortium efforts to gather these rare samples with the support of Sociedad Española de Hematología y Oncología Pediátricas (SEHOP), that accounts all pediatric hospital centers throughout Spain, and by stablishing collaborations with reference centers in the field of pediatric lymphoma diagnosis.

As it was mentioned, BLL-11q is a provisional entity that represents cases which have morphological, phenotypic, and gene expression profiles resembling those of BL, but lack *MYC* rearrangements according to standard detection methods such as FISH, and are characterized by an 11q-arm aberration (Salaverria *et al.*, 2014; Swerdlow *et al.*, 2017). In order to improve our understanding of BLL-11q, in the **Study 1** we aimed to elucidate its genomic landscape. Therefore, we searched our files for cases that could be reclassified as BLL-11q among 95 tumors previously classified as BL, atypical BL, or HGBCL, NOS. We screened for the 11q-arm alterations using CN arrays and/or FISH probes identifying 8 cases (8%) with the 11q-arm aberration and negative for *MYC* rearrangement. As in previous studies, all identified cases were younger than 41 years, although occasional cases in adult patients have been reported (Klapper *et al.*, 2012; Salaverria *et al.*, 2014; Rymkiewicz *et al.*, 2018; Wagener *et al.*, 2018; Au-Yeung *et al.*, 2020). When we restricted the analysis to cases

under the age of 41-year-old, the incidence increased to a 13% of the cases. The same frequency has been reported by the German NHL-BFM group when screening 11q alterations in a series of 82 BL and HGBCL, unclassifiable between BL and DLBCL under the age of 18 years old (11/82 cases; 13%) (Au-Yeung *et al.*, 2020). In this way, the 8 identified BLL-11q cases together with three additional cases received on consultation with a previous suspicious of BLL-11q were investigated for the CN and mutational profiles and compared to those genomic aberrations of BL, DLBCL, and HGBCL (Love *et al.*, 2012; Richter *et al.*, 2012; Schmitz *et al.*, 2012; Morin *et al.*, 2013; Karube *et al.*, 2018).

Our data from 11 BLL-11q cases showed that, BLL-11q CN profile differed from that of BL and DLBCL. BLL-11q lacked the 1q gains seen in *MYC*-positive BL or gains of 2p16.1 and 7p and 1p36.32 losses typical of GCB-DLBCL. Additionally, we identified a mutational profile in BLL-11q different from that of *MYC*-positive BL since all cases lacked the typical BL mutations in *ID3*, *TCF3*, *CCND3* or *SMARCA4* genes and had recurrent mutations in *BTG2* and *ETS1* not present in BL (Love *et al.*, 2012; Richter *et al.*, 2012; Schmitz *et al.*, 2012). Even that, few genes were found to be commonly mutated in both BL and BLL-11q entities such as *GNA13* or *DDX3X.* Interestingly, coding mutations in the *MYC* gene, which is the most frequently mutated gene in conventional BL (79%) (Richter *et al.*, 2012; Schmitz *et al.*, 2012), were only found in 2 out of 10 cases. Despite of that, these two cases did not show an aSHM pattern as typically observed in BL (Lopez *et al.*, 2019). BLL-11q mutational landscape was also characterized by the presence of mutations in epigenetic modifier genes such as *EP300*, *CREBBP*, *KMT2C*, *EZH2*, *ARID1A*, *KMT2D*, *HIST1H1D* and *HIST1H2BC,* which are common in DLBCL, particularly of the GCB subtype (Lunning and Green, 2015; Karube *et al.*, 2018). We also compared our results with two recent genetic studies on HGBCL (including DH/TH lymphomas) (Momose *et al.*, 2015; Evrard *et al.*, 2019). As in BLL-11q, HGBCL cases also presented mutations on histone modifier genes such as *KMT2D*, *CREBBP* or *EZH2*. All these observations suggest that BLL-11q is a neoplasm closer to other GC-derived lymphomas rather than BL.

Whereas our manuscript was under revision, Wagener et al published a mutational study of 15 BLL-11q analyzed by WES (Wagener *et al.*, 2018). In line with our findings, BLL-11q of the Wagener study presented no mutations in *ID3* nor *TCF3* and carried frequent mutations in GCB-DLBCL associated genes such as *GNA13*, *FOXO1* and *EZH2*. Besides, they also identified *NFRKB* gene as a candidate gene in the deleted region in 11q24.3, which was also target of recurrent stop-gain mutations. Intriguingly, this study did not find mutations in *BTG2*, *KMT2D*, *KMT2C* or *CREBBP* genes observed in our study. These differences might be explained by the small sizes of the cohorts analyzed in both studies and the fact that only recurrent mutations (>15% of the cases) were reported by Wagener et al. Again, these findings indicate that the genomic and mutational profile of BLL-11q is different from those of BL and more similar to other GC derived lymphomas.

Interestingly, the *ETS1* gene, which is located in the minimal region of loss of the 11q alteration, has been reported to be affected by loss of function mutations and homozygous deletion in previous BLL-11q series (Salaverria *et al.*, 2014), suggesting that it could be the candidate gene in the 11q deleted region. In fact, our results on *ETS1* RNA expression showed lower expression in BLL-11q than in MYC-positive BL, identifying lower values in ETS1-mutated than wild-type BLL-11q cases. This gene is a member of the ETS family of transcription factors involved in fundamental processes in normal and neoplastic cells (Testoni *et al.*, 2015). Mutations in *ETS1* gene has been previously observed in B-NHL (Morin *et al.*, 2011), precisely in ABC-DLBCL (Morin *et al.*, 2013; Karube *et al.*, 2018). Despite of that, *ETS1* mutations in DLBCL have been described to affect the first exon of the gene, contrary to BLL-11q, in which mutations are located in the last exons targeting the DNA binding domain. In fact, in DLBCL, *ETS1* is considered an oncogene since it is frequently gained and cooperates in sustaining proliferation, viability and regulates genes involved in GC differentiation (Pasqualucci, Trifonov, *et al.*, 2011; Bonetti *et al.*, 2013) whereas our findings in BLL-11q rather suggest a tumor-suppressive function.

In addition to the genetic differences, BLL-11q differed clinically, morphologically, and phenotypically from conventional BL and instead showed features more consistent with HGCBL or DLBCL. As previously observed (Salaverria *et al.*, 2014) and contrary to BL, BLL-11q presented with localized lymphadenopathy in most of our cases. Morphologically, cases identified in our study had a prominent "starry sky" pattern and high proliferation (>90% ki67) but did not have the typical cytological features of BL since they were better classified as HGBCL with blastoid or intermediate features between HGBCL (8 cases) and DLBCL (2 cases) and only one had features of atypical BL. Interestingly, LMO2, a GC marker that is typically downregulated in BL and other lymphomas with *MYC* translocation (Colomo *et al.*, 2017), was found to be expressed in BLL-11q (45%) as previously observed in an independent series (46%) (Rymkiewicz *et al.*, 2018), suggesting its use as a biomarker to differentiate from BL.

The negativity for *MYC* rearrangement is a crucial element for the recognition of these cases. The gold-standard technique for interrogating *MYC* translocations in the clinical practice is the FISH analysis using break-apart probes, with the limitation that approximately ~4% of *MYC* positive cases are not detected with this method but picked up using *MYC*/IGH fusion probes (King *et al.*, 2019). Interestingly, when the MYC expression was evaluated by immunohistochemistry, using a 40% cut-off (Johnson *et al.*, 2012), five out of 11 cases were positive. However, *MYC* expression with a diffuse and intense pattern was only detected in one of our cases while the other four positive cases either exhibited partial positivity or the intensity was weak contrary to the pattern seen in BL. Additionally, *MYC* RNA levels evaluated by qPCR were significantly lower in BLL-11q than in *MYC*-positive BL, suggesting the absence of *MYC* rearrangements. Only one BLL-11q case showed high *MYC* expression with no gains in the MYC region that could explained the high expression or any mutation affecting MYC functionality. Only using the break apart FISH probe is difficult to assure that it has not a cryptic translocation, but it is important to note that this case did not have a typical BL mutational profile, which led us to think that this case do not correspond to a *MYC*-positive BL with cryptic translocation (Wagener *et al.*, 2019).

In addition to the absence of *MYC* rearrangement, the genetic feature that distinguishes BLL-11q is the alteration of the 11q arm that is prototypically characterized by an 11q23.2-q23.3 gain/amplification and 11q24.1-qter loss. Additionally, isolated cases have been recognized with single 11q24.1-qter terminal loss or 11q23 gain with 11q24 CNN-LOH (Poirel *et al.*, 2009; Grygalewicz *et al.*, 2017). What all these 11q alteration patterns shared between them is the minimal region of loss at 11q24.3-q25, which targets the *ETS1* and *FLI1* genes. In this study we identified the presence of these 11q alterations using CN array and confirmed the presence of 11q alterations by FISH analysis with a custom probe in all tested cases, suggesting that this approach may be useful in the clinical practice to identify these cases. Same results were obtained by Wagener et al, who could verify the presence of 11q alteration in all the cases tested using the same FISH probes (Wagener *et al.*, 2018). Additionally, the specificity of this FISH approach was also confirmed by the fact that no false positive cases were observed in the 12 NHL control cases tested with this probe in which a normal 11q pattern was observed by CN array. As probe that the identification of patients with the 11q-gain/loss aberration is clinically important, a commercial FISH probe has been recently commercialized for its detection (ZytoLight SPEC 11q gain/loss Triple Color Probe). Nevertheless, FISH approaches (custom and commercial probes) have limitations to detect some of the 11q alterations such as gain/CNN-LOH and 11q patterns with gain but no amplification. This comes from the fact that a CNN-LOH cannot be distinguished from a wild type since both display two copies. Besides, since the gained region is most likely inverted (Pienkowska-Grela *et al.*, 2011) the two copies in the der(11) are too close to each other to be clearly distinguished as independent signals in the FISH constellation, making difficult the differentiation between wild type and gain. Thus, for the time being, confirmation of the finding by CN array would be desirable.

Moreover, although the 11q23 gain/11q24-qter loss of BLL-11q is mainly absent in other lymphoma entities, its detection should not be considered as a unique tool to diagnose BLL-11q cases since some transformed FL and few typical *MYC*-positive BL and *MYC*-positive HGBCL may carry a similar 11q aberration pattern (Bouska *et al.*, 2014; Grygalewicz *et al.*,

2017). Even that, this specific 11q alteration observed in BLL-11q should be distinguished from other 11q aberrations such as gains of the 11q24 region that include *ETS1* and *FLI1* detected in DLBCL (Bonetti *et al.*, 2013) or 11q25 losses missing the *ETS1* and *FLI1* described in some adult post-transplant lymphoproliferative disorders (Rinaldi *et al.*, 2006, 2010). Only the cases reported by Ferreiro et al, described the same 11q alteration pattern in an immunodeficiency setting of *MYC*-negative adult post-transplant molecular BL, suggesting that this entity exists in the context of post-transplant lymphoproliferative disease (Ferreiro *et al.*, 2015; Swerdlow *et al.*, 2017). Nevertheless, results from our 34 pediatric B cell monomorphic post-transplant lymphoproliferative disease (<18 years old) showed no evidence of 11q aberration in any of the cases (Salmeron et al, data not published).

Altogether, the genetic analyses performed in the **Study 1** indicate that BLL-11q is a GC-derived lymphoma with a genomic and mutational profile closer to HGBCL or GCB-DLBCL rather than BL in which the 11q aberration, together with other mutations, may play a relevant role in their pathogenesis. These observations support a reconsideration of the "Burkitt-like" term for these tumors. Although, the most appropriate name is not easy to propose and requires broader discussion and consensus, we think that the term "aggressive B-cell lymphoma with 11q aberration" better captures their pathological features.

Another lymphoma entity of the pediatric population that has been recently recognized by the WHO as a separate entity due to its clinical, morphological, immunophenotypic and genetical differences with conventional FL from the adults is the PTFL (Oschlies *et al.*, 2010; Swerdlow *et al.*, 2017). This entity is characterized by lack of t(14;18)/*BCL2* rearrangement and weak or negative BCL2 expression. In 2016 our group performed a collaborative study with the University of Tübingen and the National Institute of Health-Bethesda in the global genetic profiling of PTFL which included a CN analysis by Oncoscan and a mutational analysis using a targeted panel interrogating FL frequently mutated genes. The study concluded that PTFL were characterized by frequent *TNFRSF14* alterations including losses, CNN-LOH and mutations, as previously observed (Martin-Guerrero *et al.*, 2013). In addition, PTFL virtually

lacked mutations in histone and chromatin-modifying genes (*CREBBP*, *KMT2D*, *EZH2*, *MEF2B* and *EP300*) typically seen in FL (Schmidt *et al.*, 2016). In parallel, two different molecular studies also interrogated the mutational landscape of the PTFL. Louissant et al identified frequent activating mutations in the negative regulatory region (exon2) and the catalytic core domain (exon3) of *MAP2K1*, in addition to *TNFRSF14* mutations and the lack of mutations in epigenetic modifier genes (Louissaint *et al.*, 2016). On the other hand, Ozawa et al identified recurrent *IRF8* mutations at the hotspot p.K66R (Ozawa *et al.*, 2016). In order to validate the information reported in these last publications, in the **Study 2** included in this doctoral thesis, we expanded our knowledge on the genetic alterations associated to PTFL by analyzing the frequency of *MAP2K1* and *IRF8* mutations in our previously well characterized series of 43 PTFL (Schmidt *et al.*, 2016).

Results of **Study 2** confirmed previous observations, since *MAP2K1* mutations were identified in 49% of the PTFL investigated. Those mutations were mainly located in two hot spots within exon 2 (codons 53 and 57), which encode the negative regulatory region domain of MEK1 protein, corroborating previous results in PTFL (Louissaint *et al.*, 2016). These positions were also reported to be mutated in hairy cell leukemia (Waterfall *et al.*, 2014; Mason *et al.*, 2017) and chronic lymphocytic leukemia (Landau *et al.*, 2015; Puente *et al.*, 2015) but not in conventional FL (Li *et al.*, 2014; Okosun *et al.*, 2014; Green *et al.*, 2015). The same mutations have been previously demonstrated to result in constitutive activation of the MAPK pathway by activating the downstream target extracellular signal-regulated kinase (ERK1/2) proteins through phosphorylation (Marks *et al.*, 2008; Brown *et al.*, 2014; Chakraborty *et al.*, 2014; Zeng *et al.*, 2017). By Immunohistochemical analysis we confirmed the downstream activation of ERK proteins in *MAP2K1* mutated PTFL cases and revealed a good correlation with the allelic frequency of the *MAP2K1* mutations.

The incidence of *MAP2K1* mutations identified was similar to what we previously reported for *TNFRSF14* (51%) (Schmidt *et al.*, 2016). Even that, only 8 cases showed mutations in both genes, indicating that mutations in these two genes are mutually exclusive and that both

genes independently are of importance for the pathogenesis of PTFL, despite their different functional properties. The higher allelic frequency of *TNFRSF14* mutations in comparison with *MAP2K1* mutations (median variant allelic frequency, 17.8 vs 10%), even after correcting for concomitant CNN-LOH of 1p36, indicates that *TNFRSF14* mutations occur earlier than *MAP2K1* mutations in tumorigenesis. Although *TNFRSF14* mutations have been described to be late events in FL tumor evolution (Green *et al.*, 2013), they have been also demonstrated to occur in an *in situ* follicular neoplasia (ISFN), a preliminary stage before the appearance of FL, corroborating in that way the early occurrence in FL tumor evolution (Schmidt *et al.*, 2018).

On the other hand, we could also identify *IRF8* mutations at the hotspot p.K66R (c.197A>G) in 15% of cases analyzed. The frequency of *IRF8* mutations found in the present study was lower than that described by Ozawa et al (15 vs 50%) (Ozawa *et al.*, 2016). The difference might be explained by the small cohort of 6 cases analyzed by Ozawa *et al*. The *IRF8* gene has been described as potential tumor suppressor in myeloid neoplasms and has recently also been linked to the pathogenesis of B-cell lymphomas (Shukla and Lu, 2014). Specifically, *IRF8* mutations have been observed in adult FL and DLBCL in 5% to 10% of cases (Lohr *et al.*, 2012; Li *et al.*, 2014; Okosun *et al.*, 2014). However, in contrast to PTFL where the *IRF8* p.K66R mutation is predicted to affect DNA-protein interaction (Ozawa *et al.*, 2016), these mutations in adults are frequently indel and missense mutations predominantly located in the *IRF8* C-terminal domain with still unidentified functional consequences (Lohr *et al.*, 2012; Li *et al.*, 2014; Okosun *et al.*, 2014; Green *et al.*, 2015). Of note, *IRF8* and *TNFRSF14* are critical regulators of the immune system development and function (Shukla and Lu, 2014; Boice *et al.*, 2016). Both genes regulate GC B-cell activation, and deficiency of *IRF8* has been reported to induce a hyperproliferative phenotype in pre-B cells (Ma *et al.*, 2010). Interestingly, 4 of 6 *IRF8* mutated PTFL cases also showed *TNFRSF14* mutations, suggesting possible cooperation between these two genes.

Since some PTFL may occur in adults (Louissaint *et al.*, 2012), the differential diagnosis with other FL without t(14;18) translocation of the adult might be crucial for therapy selection, especially when PTFL can be diagnosed in the adult setting. Our group has recently participated in the genetic characterization of t(14;18) negative FL, a FL entity that mainly affects adult and also lacks the typical *BCL2* rearrangement or expression as PTFL (Nann *et al.*, 2020). Results showed that t(14;18) negative FL display a distinct mutational landscape characterized by *STAT3* mutations and lack of *MAP2K1*. Thus, the interrogation of these mutations might improve differential diagnosis of PTFL.

Overall, in the **Study 2** we have verified the presence of *MAP2K1* and *IRF8* mutations in a large series of PTFL expanding in that way the knowledge on the genetic landscape associated to this disease. Additionally, the high specificity of these mutations makes them valuable for improving diagnosis in those adult critical cases.

Finally, in the **Study 3** we reveal the genetic landscape of 63 pediatric and young adult LBCL (up to 25 years-old) including DLBCL and HGBCL, NOS and the new provisional entity LBCL-*IRF4.*

As already mentioned in the introduction, LBCL-*IRF4* has been recently recognized as a specific provisional entity characterized by the *IRF4* translocation, clinical presentation localized in the head and neck or abdominal regions and a favorable outcome after intensive chemotherapy (Salaverria *et al.*, 2011; Chisholm *et al.*, 2019; Au-Yeung *et al.*, 2020). The number of cases previously identified was limited and the genetic landscape was unknown. Therefore, in the **study 3**, we expanded these observations by analyzing 20 LBCL-*IRF4*. Results showed that these tumors have a specific molecular profile characterized by frequent mutations in *IRF4* and NF-kB related genes (*CARD11* and *CD79B*), losses of 17p13 without concomitant *TP53* mutations, gains of chromosome 7 and 11q12.3-q25 and overexpression of downstream target genes of the NF-kB pathway.

Despite all LBCL-*IRF4* cases showed a high *IRF4*/MUM1 positivity by IHC, the *IRF4* rearrangement could not be demonstrated in two of the investigated LBCL-*IRF4* cases. However, the constellation of pathological and clinical features together with the demonstration of an IGH break in the absence of rearrangements in the most common partners, *BCL2*, *BCL6* and *MYC*, supported the idea that these two cases may correspond to the same diagnostic category. CN and mutational profiles of the two LBCL-*IRF4* cases without *IRF4* rearrangement were similar to the ones of *IRF4* rearranged cases, confirming the idea that these tumors belong to the same entity. Additionally, relatively similar *IRF4* expression levels (according to NanoString Lymph2Cx counts) could also be observed between LBCL-*IRF4* cases with and without the *IRF4* rearrangement, which were significantly higher than other *IRF4*-negative LBCL such as DLBCL or HGBCL, NOS. These high levels of *IRF4* expression suggest the presence of a cryptic rearrangement in these cases with no demonstrable *IRF4* rearrangement (Liu *et al.*, 2013). Even that, we could not rule out the possibility that other mechanisms such as the activation of NF-kB pathway could also be leading these high levels of *IRF4* expression (Klein and Dalla-Favera, 2008).

LBCL-*IRF4* mutational landscape was characterized by recurrent *IRF4* mutations located in the second exon targeting the DNA binding domain. These *IRF4* mutations were predicted to have a predominant AID mutational signature, characterized by C>T/G mutations at AID hotspots associated with the SHM patterns (Alexandrov *et al.*, 2013; Chapuy *et al.*, 2018). In fact, *IRF4* gene was previously described as a potential SHM target in adult DLBCL (Khodabakhshi *et al.*, 2012). Interestingly, all cases with multiple *IRF4* mutations had an aSHM pattern (characterized by at least one *IRF4* transition change was within the 2000bp from the TSS and affecting AID motif) and concomitant *IRF4* rearrangement, suggesting that the presence of multiple mutations affecting the *IRF4* gene with aSHM pattern could be a hallmark of the *IRF4* translocation. In fact, this coexistence between rearrangements and aSHM has been reported previously for *BCL2* and *BCL6* genes in adult DLBCL (Küppers and Dalla-Favera, 2001; Khodabakhshi *et al.*, 2012). This is explained by the fact that the process of SHM by AID machinery not only generates nucleotide exchanges but also double-strand

DNA breaks that are potentially recombinogenic which may lead to a chromosomal translocation (Küppers and Dalla-Favera, 2001). Interestingly, *IRF4* mutations with aSHM pattern of *IRF4* rearranged cases seem to be more clonal than those in cases affected by non-aSHM mutations (mean, 70% vs 36% of cancer cell fraction; P = 0.04), suggesting that *IRF4* aSHM and rearrangement may occur early in the tumor evolution whereas non-aSHM single mutations might occur in a later stage subsequently to the translocation. On the other hand, not all *IRF4* translocated cases displayed an aSHM pattern with multiple mutations targeting the *IRF4* gene. Even that, we cannot discard the presence of multiple mutations outside the exon2 since the AID machinery target region (2Kb after the TSS) was not entirely included in our panel design focused on the detection of mutations in the coding region. Further studies are needed to define the potential functional effect of these *IRF4* mutations located in the DNA binding domain.

If we checked the literature, the *IRF4* transcription factor has been previously described to play role in lymphoid pathogenesis of different B-cell malignancies. For instance, *IRF4* has been demonstrated to be overexpressed in plasma cell myeloma, where it is required for their survival (Shaffer *et al.*, 2008). Additionally, in a little subset of plasma cell myeloma cases, this *IRF4*/MUM1 overexpression is also explained by t(6;14) rearrangements (Iida *et al.*, 1997; Yoshida *et al.*, 1999) or mutations mainly affecting the hotspot K123R located in the DNA-binding domain (Chapman *et al.*, 2011; Lohr *et al.*, 2014). *IRF4* overexpression has also been identified in ABC-DLBCL and Hodgkin lymphoma, where it acts as a pro-survival factor (Aldinucci *et al.*, 2010; Yang *et al.*, 2012). In the spectrum of pediatric aggressive B-cell lymphoma entities, *IRF4* mutations, specifically affected by aSHM pattern, seem to be specific of LBCL-*IRF4* since no mutations could be observed in DLBCL, HGBCL, NOS or BLL-11q. Previous results of our group and the literature, also demonstrated the absence of *IRF4* mutations in BLL-11q and PTFL (Louissaint *et al.*, 2016; Ozawa *et al.*, 2016; Wagener *et al.*, 2018).

Moreover, unpublished data from a collaborative study performed by our group have also demonstrated the presence of *IRF4* translocations in a subset of triple positive (CD10/BCL6/MUM1) adult DLBCL. Interestingly, genetic studies of these cases with *IRF4* rearrangement confirmed the presence of *IRF4* and NF-kB mutations, although they were were more often ABC-type and showed higher genetic complexity when compared with pediatric LBCL-*IRF4* (Frauenfeld L, Castrejon-de-Anta N, in preparation).

The presence of mutations affecting NF-kB related genes in LBCL-*IRF4* cases is intriguing since most of these tumors (72%) have a GCB phenotype and NF-kB activation have been associated to ABC-DLBCL in adults (Chapuy *et al.*, 2018). The *IRF4* gene is a downstream gene upregulated by NF-kB pathway activation (Klein and Dalla-Favera, 2008) but at the same time it has been demonstrated to sustain survival by transactivating *CARD11* and potentiating NF-kB signaling in ABC-DLBCL (Yang *et al.*, 2012). In a similar way, *IRF4* was observed to be regulated by a NF-kB positive feedback loop in peripheral T-cell lymphoma (Boddicker *et al.*, 2015). Therefore, the activation of NF-kB pathway in LBCL-*IRF4* tumors may also be related with the *IRF4* overexpression.

Interestingly, *CARD11* mutations were seen exclusively in cases with diffuse growth pattern whereas *MAP2K1* mutations, characteristic of PTFL (Louissaint *et al.*, 2016) could be detected in two cases with predominantly follicular pattern suggesting that the underlying mutational profile may influence the morphological features of the tumors.

In the same **Study 3**, 31 DLBCL of pediatric and young adult cases were also analyzed. As observed in previous pediatric DLBCL series, DLBCL were mainly GCB phenotype, displayed low CN complexity, few *MYC* and *BCL6* rearrangements and, in contrast to adults, lacked *BCL2* translocations (Oschlies *et al.*, 2006; Deffenbacher *et al.*, 2012; Klapper *et al.*, 2012).

Since some cases presented mediastinal affection, the Lymph3Cx gene expression assay was applied to the entire LBCL cohort identifying four DLBCL cases predicted as mPMBCL with an

atypical clinical presentation for PMBCL diagnosis (Mottok *et al.*, 2018). Although three of these patients had mediastinal lymph node involvement, they also had disseminated disease including BM and extranodal involvement, not frequent of PMBCL. The mutational profile of three of these mPMBCL was closer to PMBCL than DLBCL, with mutations in *SOCS1*, *NFKBIE*, *STAT6*, *B2M*, and *CIITA* genes, which appeared to confirm the mPMBCL gene expression prediction. These observations, together with similar cases recently described in adults suggest that a subset of DLBCL in pediatric and young adult population without mediastinal involvement may correspond to PMBCL and are only detected by the analysis of gene expression profiles (Yuan *et al.*, 2015; Chen *et al.*, 2019).

Mutational results from the remaining DLBCL without mPMBCL signature showed a homogeneous molecular landscape with predominance of mutations in GCB- related genes including *SOCS1*, *EZH2*, *GNA13*, but with absence of other recurrent GCB-associated alterations such as *TNFRSF14* and *SGK1* mutations. Additionally, CN analysis showed lack of alterations present in adult DLBCL such as 6q13-q14.1/*TMEM30A* and 6q22.1-q25.3/*TNFAIP3* deletions as well as those typically associated with ABC-DLBCL as 9p21.3/*CDKN2A* and 17p13.3-p11.2/*TP53* losses, which probably reflects the predominance of GCB cases in our cohort.

On the other hand, genetic analysis of 8 HGBCL, NOS demonstrate a heterogeneous mutational landscape identifying two different genetic patterns associated to BL and DLBCL molecular landscapes respectively, as previously observed (Momose *et al.*, 2015). Five out of the eight molecularly investigated cases had mutational profile closer to BL (including *MYC, ID3, CCND3* and *SMARCA4* mutations), four of them with concomitant *MYC* rearrangements. These cases were not diagnosed as BL since they did not have the typical BL morphology or immunophenotype (high pleomorphism and/or BCL2 expression). Nevertheless, two of these five cases with BL mutational landscape had typical BL immunophenotype in concert with a single *MYC* translocation, which has been recently demonstrated to be uncommon in HGBCL, NOS, a fact that could favor the BL diagnosis

(Hüttl *et al.*, 2021). On the other hand, the other three HGBCL, NOS had mutational profiles closer to GCB-DLBCL with *TNFRSF14*, *CARD11* and *EZH2* mutations, and lack of *MYC* translocations. These results open again the discussion about if some HGBCL, NOS could be reclassified as BL or DLBCL based mainly on the genetic profile even without fitting the morphological and/or immunophenotypic diagnosis and reinforces the importance of a multidisciplinary approach to improve the disease classification.

Regarding prognostic aspects, advanced stage, high LDH and combined BM and CNS disease have been significantly associated with unfavorable outcome in pediatric mature B-NHL, whereas the adverse prognosis of *MYC* rearrangements and ABC-COO is still controversial (Poirel *et al.*, 2009; Szczepanowski *et al.*, 2017). The comprehensive genomic analyses performed in **Study 3** has not only allowed a better molecular characterization of pediatric and young adult LBCL but also has identified the prognostic value of several clinical and molecular features such as the higher age than 18 years old, high LDH levels (International Non-Hodgkin's Lymphoma Prognostic Factors Project, 1993), ABC-subtype (Rosenwald *et al.*, 2002), high genetic complexity including the presence of chromothripsis-like patterns (Monti *et al.*, 2012) and *TP53* mutations (Young *et al.*, 2008; Xu-Monette *et al.*, 2012), as previously seen in adult population. In addition, we could also identify novel genetic features associated with poor EFS such as 1q21-q44/*MDM4/MCL1* gains and 19p13.3/*TNFSF7*/*TNFSF9* homozygous deletions, which have been associated with higher genetic complexity (Monti *et al.*, 2012). These results offer novel opportunities in patient risk stratification and management. However, these findings should be verified in other large cohorts and the independent prognostic value should be demonstrated in a multivariate analysis in addition to other well-known prognostic markers.

Molecular subgroups based on their genetic alterations integrating mutations, CN and structural variants have been recently stablished in adult DLBCL cohorts but not in pediatric (Chapuy *et al.*, 2018; Schmitz *et al.*, 2018; Lacy *et al.*, 2020). Subsequently to the publication of our study, Wright et al stablished an available tool to predict DLBCL into the different

genetic subgroups achieving 54% of the cases classified (Wright *et al.*, 2020). When this tool was applied to our series of LBCL pediatric and young adult cohort (**Study 3**) only 24% of the cases could be classified into the different 6 molecular subgroups, suggesting that cases diagnosed in this age range might not fit in any of the molecular subgroups previously stablished in adults (**Figure 25**). This make sense since pediatric cases virtually lacked *MYD88*-L265P, *NOTCH1*, *NOTCH2*, *BCL2* and *SGK1* mutations and *BCL2* and *BCL6* rearrangements that have been associated with the definition of the established subgroups in adult DLBCL (Chapuy *et al.*, 2018; Schmitz *et al.*, 2018; Wright *et al.*, 2020).

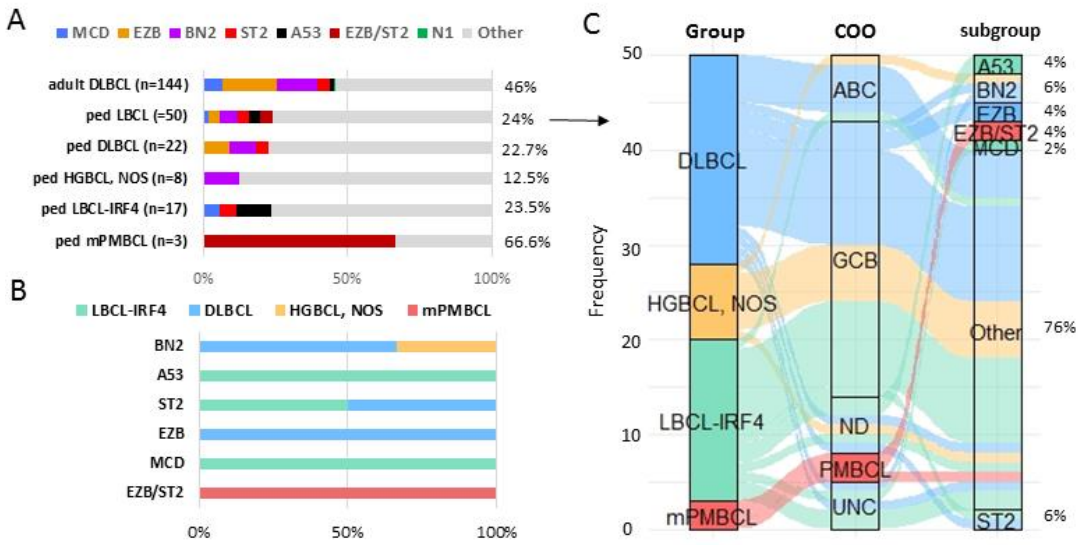

Figure 25. Pediatric and adult LBCL molecular subgroup prediction by *Lymphgen* tool (Wright *et al.*, 2020) using mutational information of 43 out of 114 genes required for the prediction. A) Prevalence of molecular subtypes in adult DLBCL (Karube *et al.*, 2018) and pediatric and young adult LBCL subtypes. B) prevalence of pediatric LBCL subtypes within each genetic subtype. C) Alluvial plot shows the frequency and relationship between pediatric LBCL groups, COO classification according to Lymph2Cx/3Cx and molecular subgroup prediction.

From the clinical point of view, the proper diagnosis of these pediatric GC-derived B-NHL entities may be of major importance for the outcome of the patients since some of these entities might require different therapeutic strategies (Sandlund and Martin, 2016). When all the cases analyzed in this thesis (**Study 1, 2 and 3**) including pediatric and young BLL-11q, PTFL, DLBCL, HGBCL, NOS and LBCL-*IRF4* variants were compared in terms of survival, a

different clinical behavior could be observed between entities (**Figure 26**). All LBCL including LBCL-*IRF4*, DLBCL, HGBCL, NOS and BLL-11q received chemotherapy following pediatric (LMB/BFM/Inter-B-NHL protocols) or adult (R-CHOP/CODOX) schema protocols as first-line treatment, including rituximab in 35% of the patients. Despite of different therapeutic strategies no differences in EFS could be observed comparing adult vs pediatric protocols (log-rank test p=0.27) or with or without Rituximab (log-rank test p=0.9). Whereas LBCL-*IRF4* and BLL-11q had excellent prognosis (93% and 100% 5-year EFS, respectively), DLBCL and HGBCL, NOS had worse prognosis (62% and 50% 5-year EFS). The recently published clinicopathological study of LBCL-*IRF4* and BLL-11q in pediatric patients of the NHL-BFM group corroborate also the excellent outcome (both 100% overall survival) after treated according to pediatric BFM strategies (Au-Yeung *et al.*, 2020). These results are not surprising since these lymphomas frequently present as localized disease (stage 1 or 2). Therefore, both diseases could be targets for therapy de-escalation in future clinical trials.

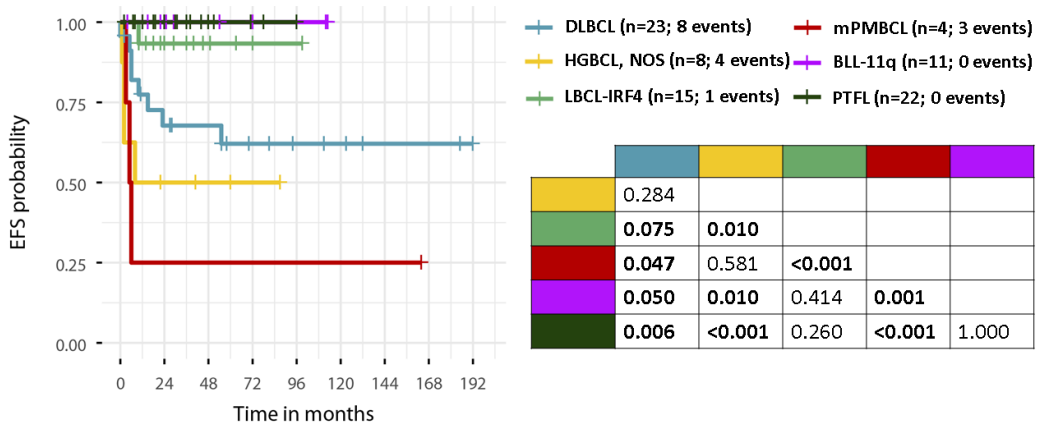

Figure 26. EFS of different pediatric and young adult GC-derived B-NHL. Cases included correspond to cases from Study 1-3. P-values of pairwise comparisons are indicated in the right side of the figure corresponding to its color legend.

On the other hand, only 10 out of the 22 PTFL received chemotherapy whereas the rest followed a watch and wait strategy after complete resection achieving the same excellent results as the ones treated with chemotherapy (both 100% 5-years EFS). Similar response to treatment were observed in other PTFL series (Louissaint *et al.*, 2012; Attarbaschi *et al.*, 2013; Martin-Guerrero *et al.*, 2013). These results suggest that a complete resection followed by a watch and wait strategy could be a reasonable therapeutic option for localized disease (stage 1) PTFL patients.

Interestingly, those DLBCL cases predicted as mPMBCL by Lymph3Cx gene expression assay displayed worse prognosis compared to DLBCL. As it was previously mentioned, these cases were closer to PMBCL than DLBCL, suggesting that may correspond to PMBCL with atypical clinical presentation. Detection of these cases may have clinical implications since PMBCL have worse prognosis than other LBCL with standard pediatric protocols (LMB) but respond well with more aggressive chemotherapies including rituximab (DA-EPOCH-R) with or without radiotherapy (>90% 3-year OS) (Seidemann *et al.*, 2003; Dunleavy, Pittaluga, Maeda, *et al.*, 2013; Gerrard *et al.*, 2013).

The morphological, immunophenotypic and genetic characterization of large series of pediatric lymphoma entities we have performed in the context of this thesis has allowed to better understand the pathogenesis of these entities identifying biomarkers that might be helpful to improve their diagnosis and to design management strategies more adapted to the particular biological behavior of these tumors (**Figure 27**).

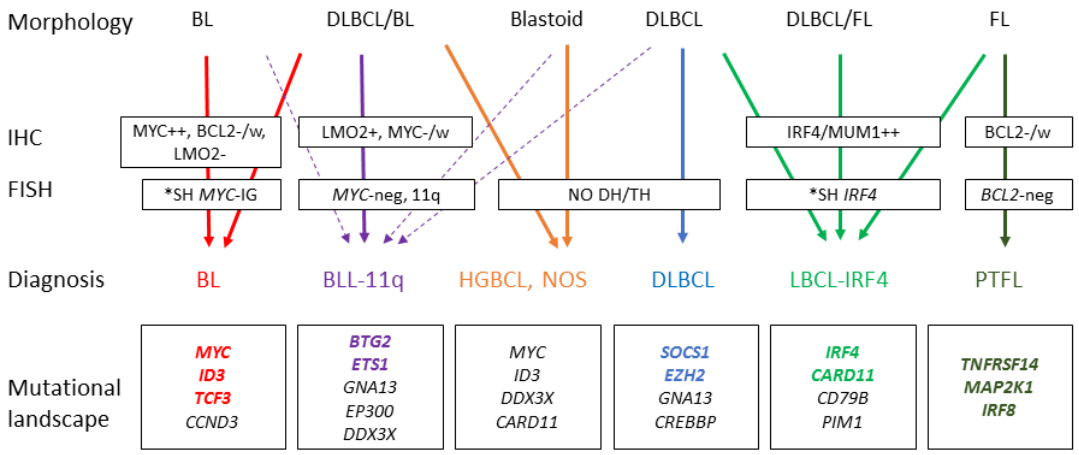

Figure 27. Diagnostic algorithm useful in the differential diagnosis of germinal center-derived B-NHL in pediatric and young adult population. It includes morphology, immunohistochemistry, FISH analysis and mutational landscape. Colored genes indicate specific mutations of each pediatric entity. Asterisk indicates that negative cases might be included suggesting a cryptic insertion/alteration. DH/TH: double hit/triple hit; SH: single hit; w: weak.

Mutational characterization has also allowed the identification of different mutational profiles among pediatric GC-derived B-NHL. The specificity of some of these mutations to a particular lymphoma entity may help to clarify the diagnosis of those challenging cases with overlapping morphologies and immunophenotypes. For instance, we could observe that mutations in *ETS1* and *BTG2* genes are specific of BLL-11q. Mutations in *IRF4* and *CARD11* genes are specific of LBCL-*IRF4* whereas *SOCS1* mutations of pediatric DLBCL. Finally, *MAP2K1* mutations seem to be specific of PTFL and its presence in some LBCL-*IRF4* might indicate a follicular morphology of the disease. Regarding BL-associated mutations including *MYC*, *ID3* and *CCND3*, they have only been observed in a subset of HGBCL, NOS with *MYC* translocations but with atypical BL morphology and/or immunophenotype.

With all the results generated in this thesis we can conclude that, to identify BLL-11q, CN arrays or FISH with the 11q probe in cases with BL, DLBCL, and HGBCL morphology, GC phenotype and very high proliferative index (>90%), without *MYC* rearrangements, in young patients should be performed. Additionally, lack of BL-associated mutated genes (*ID3,*

CCND3, TCF3) or presence of *BTG2* or *ETS1* might help to differentially diagnose from BL. On the other hand, to identify LBCL-*IRF4*, we suggest performing FISH analysis for *IRF4* in the context of a child/young adult patient with head and neck or intestinal lymphoma with FL, DLBCL and FL/DLBCL morphology, in addition to IG, *BCL2*, *BCL6* and *MYC* FISH analyses to demonstrate the presence of IG rearrangement in absence of other B-cell associated lymphoma genes. Additionally, mutational status of *IRF4* may help to predict *IRF4* rearrangements.

Despite of all this findings, targeted NGS approach is a limitation since we have only been able to interrogate the mutational status of those genes previously observed to be mutated in adult series. This approach does not allow the identification of novel mutated genes of the pediatric and young adult variants. This may explain why there are still 12% of the PTFL with no genetic alterations other than immunoglobulin heavy-chain rearrangements (clonal expansion). However, we consider that capture-based targeted NGS was the most appropriate technology for those FFPE samples without paired normal DNA available in order to avoid bad quality results related with the low number of amplifiable templates available for PCR amplification. Despite of that, further studies of pediatric and young variants of B-NHL should be performed using WES/WGS approaches, which may expand the genomic profile of alterations of these tumors.

In summary, in this thesis we have observed that GC-derived B-NHL in pediatric and young adult population are a heterogeneous group of tumors including different entities with specific molecular profiles and clinical behavior. A better understanding of these differences and the integration of some molecular and genetic markers in clinics might be relevant to improve their classification and to design management strategies more adapted to the particular biological behavior of these tumors.

CONCLUSIONS

- BLL-11q is a GC-derived lymphoma with a genomic and mutational profile closer to HGBCL or GCB-DLBCL rather than BL in which the 11q aberration, together with other mutations, may play a relevant role in their pathogenesis.
- PTFL is a separated entity from its adult counterpart characterized by frequent *TNFRSF14* aberrations and *MAP2K1* activating mutations, in addition to specific *IRF8*-K66R hot spot mutations.
- LBCL-*IRF4* is an aggressive lymphoma characterized by frequent mutations in *IRF4* and NF-kB related genes (*CARD11* and *CD79B*), losses of 17p13 without concomitant *TP53* mutations, gains of chromosome 7 and 11q12.3-q25 and overexpression of downstream target genes of the NF-kB pathway.
- Pediatric and young adult DLBCL are mainly GCB-phenotype characterized by mutations in GCB-DLBCL associated genes, and, in comparison with their adult counterpart, display low genetic complexity and virtually lack primary alterations as *BCL2* or *BCL6* translocations.
- Pediatric and young adult HGBCL, NOS are a heterogeneous disease with a subset of cases presenting recurrent mutations in BL-related genes whereas others in GCB-DLBCL-related genes.
- Pediatric and young adult LBCL do not fit into the different molecular subgroups previously stablished in adults since virtually lack significant alterations that have been associated with the definition of the established subgroups in adult DLBCL.
- Clinical and molecular features related to unfavorable outcome in pediatric and young adult LBCL includes age >18 years, high LDH levels, ABC-phenotype, high genetic complexity and *TP53* mutations, as in adults, in addition to 1q21-q44/*MDM4*/*MCL1* gains and 19p13.3/*TNFSF7*/*TNFSF9* homozygous deletions.
- Overall, GC-derived B-NHL in pediatric and young adult population are a heterogeneous group of tumors including different entities with specific molecular profiles and clinical behavior. Thus, a multidisciplinary approach including interrogation of different molecular alterations may help in its diagnosis and disease classification.

REFERENCES

Aldinucci, D. *et al.* (2010) 'IRF4 is modulated by CD40L and by apoptotic and anti-proliferative signals in Hodgkin lymphoma.', *British journal of haematology*. England, 148(1), pp. 115–118. doi: 10.1111/j.1365-2141.2009.07945.x.

Alexandrov, L. B. *et al.* (2013) 'Signatures of mutational processes in human cancer.', *Nature*, 500(7463), pp. 415–421. doi: 10.1038/nature12477.

Alexandrov, L. B. *et al.* (2020) 'The repertoire of mutational signatures in human cancer.', *Nature*, 578(7793), pp. 94–101. doi: 10.1038/s41586-020-1943-3.

Alizadeh, A. A. *et al.* (2000) 'Distinct types of diffuse large B-cell lymphoma identified by gene expression profiling.', *Nature*. England, 403(6769), pp. 503–511. doi: 10.1038/35000501.

Angi, M. *et al.* (2017) 'The t(8;14)(q24.1;q32) and its variant translocations: A study of 34 cases.', *Hematology/oncology and stem cell therapy*. England, 10(3), pp. 126–134. doi: 10.1016/j.hemonc.2017.03.002.

Araf, S. and Fitzgibbon, J. (2016) 'Pediatric-type FL: simply different.', *Blood*. United States, 128(8), pp. 1030–1031. doi: 10.1182/blood-2016-07-725002.

Arthur, S. E. *et al.* (2018) 'Genome-wide discovery of somatic regulatory variants in diffuse large B-cell lymphoma.', *Nature communications*. England, 9(1), p. 4001. doi: 10.1038/s41467-018-06354-3.

Astolfi, A. *et al.* (2015) 'Whole exome sequencing (WES) on formalin-fixed, paraffin-embedded (FFPE) tumor tissue in gastrointestinal stromal tumors (GIST).', *BMC genomics*, 16, p. 892. doi: 10.1186/s12864-015-1982-6.

Attarbaschi, A. *et al.* (2013) 'Children and adolescents with follicular lymphoma have an excellent prognosis with either limited chemotherapy or with a "Watch and wait" strategy after complete resection.', *Annals of hematology*. Germany, 92(11), pp. 1537–1541. doi: 10.1007/s00277-013-1785-2.

Au-Yeung, R. K. H. *et al.* (2020) 'Experience with provisional WHO-entities large B-cell lymphoma with IRF4-rearrangement and Burkitt-like lymphoma with 11q aberration in paediatric patients of the NHL-BFM group.', *British journal of haematology*. England, 190(5), pp. 753–763. doi: 10.1111/bjh.16578.

Aukema, S. M. *et al.* (2011) 'Double-hit B-cell lymphomas.', *Blood*. United States, 117(8), pp. 2319–2331. doi: 10.1182/blood-2010-09-297879.

Bahram, F. *et al.* (2000) 'c-Myc hot spot mutations in lymphomas result in inefficient ubiquitination and decreased proteasome-mediated turnover.', *Blood*. United States, 95(6), pp. 2104–2110.

Barrans, S. *et al.* (2010) 'Rearrangement of MYC is associated with poor prognosis in patients with diffuse large B-cell lymphoma treated in the era of rituximab.', *Journal of clinical oncology : official journal of the American Society of Clinical Oncology*. United States, 28(20), pp. 3360–3365. doi: 10.1200/JCO.2009.26.3947.

Barth, T. F. E. *et al.* (2002) 'Mediastinal (thymic) large B-cell lymphoma: where do we stand?', *The Lancet. Oncology*. England, 3(4), pp. 229–234. doi: 10.1016/s1470-2045(02)00714-3.

Basso, K. and Dalla-Favera, R. (2015) 'Germinal centres and B cell lymphomagenesis.', *Nature reviews. Immunology*. England, 15(3), pp. 172–184. doi: 10.1038/nri3814.

Batlevi, C. L. *et al.* (2020) 'Follicular lymphoma in the modern era: survival, treatment outcomes, and identification of high-risk subgroups.', *Blood cancer journal*, 10(7), p. 74. doi: 10.1038/s41408-020-00340-z.

Bea, S. *et al.* (2005) 'Diffuse large B-cell lymphoma subgroups have distinct genetic profiles that influence tumor biology and improve gene-expression-based survival prediction.', *Blood*. United States, 106(9), pp. 3183–3190. doi: 10.1182/blood-2005-04-1399.

Béguelin, W. *et al.* (2013) 'EZH2 is required for germinal center formation and somatic EZH2 mutations promote lymphoid transformation.', *Cancer cell*, 23(5), pp. 677–692. doi: 10.1016/j.ccr.2013.04.011.

Bentz, M. *et al.* (2001) 'Gain of chromosome arm 9p is characteristic of primary mediastinal B-cell lymphoma (MBL): comprehensive molecular cytogenetic analysis and presentation of a novel MBL cell line.', *Genes, chromosomes & cancer*. United States, 30(4), pp. 393–401. doi: 10.1002/1098-2264(2001)9999:9999<::aid-gcc1105>3.0.co;2-i.

Boddicker, R. L. *et al.* (2015) 'The oncogenic transcription factor IRF4 is regulated by a novel CD30/NF-κB positive feedback loop in peripheral T-cell lymphoma.', *Blood*, 125(20), pp. 3118–3127. doi: 10.1182/blood-2014-05-578575.

Boice, M. *et al.* (2016) 'Loss of the HVEM Tumor Suppressor in Lymphoma and Restoration by Modified CAR-T Cells.', *Cell*, 167(2), pp. 405-418.e13. doi: 10.1016/j.cell.2016.08.032.

Bonetti, P. *et al.* (2013) 'Deregulation of ETS1 and FLI1 contributes to the pathogenesis of diffuse large B-cell lymphoma.', *Blood*. United States, 122(13), pp. 2233–2241. doi: 10.1182/blood-2013-01-475772.

Bouska, A. *et al.* (2014) 'Genome-wide copy-number analyses reveal genomic abnormalities involved in transformation of follicular lymphoma.', *Blood*. United States, 123(11), pp. 1681–1690. doi: 10.1182/blood-2013-05-500595.

Brown, N. A. *et al.* (2014) 'High prevalence of somatic MAP2K1 mutations in BRAF V600E-negative Langerhans cell histiocytosis.', *Blood*. United States, 124(10), pp. 1655–1658. doi: 10.1182/blood-2014-05-577361.

BURKITT, D. (1958) 'A sarcoma involving the jaws in African children.', *The British journal of surgery*. England, 46(197), pp. 218–223. doi: 10.1002/bjs.18004619704.

Büyüktaş, D. *et al.* (2020) 'IRF4-Rearranged Large B-Cell Lymphoma on Waldeyer's Ring: A Case Report.', *Turkish journal of haematology : official journal of Turkish Society of Haematology*, 37(4), pp. 292–294. doi: 10.4274/tjh.galenos.2020.2020.0086.

Carrick, D. M. *et al.* (2015) 'Robustness of next generation sequencing on older formalin-fixed paraffin-embedded tissue', *PLoS ONE*, 10(7), pp. 3–10. doi: 10.1371/journal.pone.0127353.

Casulo, C. and Friedberg, J. W. (2018) 'Burkitt lymphoma- a rare but challenging lymphoma.', *Best practice & research. Clinical haematology*. Netherlands, 31(3), pp. 279–284. doi: 10.1016/j.beha.2018.07.013.

Cattoretti, G. *et al.* (2005) 'Deregulated BCL6 expression recapitulates the pathogenesis of human diffuse large B cell lymphomas in mice.', *Cancer cell*. United States, 7(5), pp. 445–455. doi: 10.1016/j.ccr.2005.03.037.

Cazals-Hatem, D. *et al.* (1996) 'Primary mediastinal large B-cell lymphoma. A clinicopathologic study of 141 cases compared with 916 nonmediastinal large B-cell lymphomas, a GELA ("Groupe d'Etude des Lymphomes de l'Adulte") study.', *The American journal of surgical pathology*.

United States, 20(7), pp. 877–888. doi: 10.1097/00000478-199607000-00012.

Cerutti, A., Cols, M. and Puga, I. (2013) 'Marginal zone B cells: virtues of innate-like antibody-producing lymphocytes.', *Nature reviews. Immunology*, 13(2), pp. 118–132. doi: 10.1038/nri3383.

Chakraborty, R. *et al.* (2014) 'Mutually exclusive recurrent somatic mutations in MAP2K1 and BRAF support a central role for ERK activation in LCH pathogenesis.', *Blood*, 124(19), pp. 3007–3015. doi: 10.1182/blood-2014-05-577825.

Challa-Malladi, M. *et al.* (2011) 'Combined genetic inactivation of β2-Microglobulin and CD58 reveals frequent escape from immune recognition in diffuse large B cell lymphoma.', *Cancer cell*, 20(6), pp. 728–740. doi: 10.1016/j.ccr.2011.11.006.

Chalmers, Z. R. *et al.* (2017) 'Analysis of 100,000 human cancer genomes reveals the landscape of tumor mutational burden.', *Genome medicine*, 9(1), p. 34. doi: 10.1186/s13073-017-0424-2.

Chapman, M. A. *et al.* (2011) 'Initial genome sequencing and analysis of multiple myeloma.', *Nature*, 471(7339), pp. 467–472. doi: 10.1038/nature09837.

Chapuy, B. *et al.* (2018) 'Molecular subtypes of Diffuse Large B-cell Lymphoma are associated with distinct pathogenic mechanisms and outcomes', *Nature Medicine*, p. In press. doi: 10.1038/s41591-018-0016-8.

Chen, B.-J. *et al.* (2019) 'Cyclin D1-positive Mediastinal Large B-Cell Lymphoma With Copy Number Gains of CCND1 Gene: A Study of 3 Cases With Nonmediastinal Disease.', *The American journal of surgical pathology*. United States, 43(1), pp. 110–120. doi: 10.1097/PAS.0000000000001154.

Chisholm, K. M. *et al.* (2019) 'IRF4 translocation status in pediatric follicular and diffuse large B-cell lymphoma patients enrolled in Children's Oncology Group trials.', *Pediatric blood & cancer*. United States, p. e27770. doi: 10.1002/pbc.27770.

Chonabayashi, K. *et al.* (2014) 'Refractory IGκ/IRF4-positive DLBCL with CDKN2A/2B deletion.', *Annals of hematology*. Germany, pp. 893–894. doi: 10.1007/s00277-013-1889-8.

Choudhary, M. *et al.* (2017) 'AID Biology: A pathological and clinical perspective', *International Reviews of Immunology*. Taylor & Francis, 0(0), pp. 1–20. doi: 10.1080/08830185.2017.1369980.

Colomo, L. *et al.* (2017) 'LMO2-negative Expression Predicts the Presence of MYC Translocations in Aggressive B-Cell Lymphomas.', *The American journal of surgical pathology*. United States, 41(7), pp. 877–886. doi: 10.1097/PAS.0000000000000839.

Compagno, M. *et al.* (2009) 'Mutations of multiple genes cause deregulation of NF-kappaB in diffuse large B-cell lymphoma.', *Nature*, 459(7247), pp. 717–721. doi: 10.1038/nature07968.

Copie-Bergman, C. *et al.* (2015) 'MYC-IG rearrangements are negative predictors of survival in DLBCL patients treated with immunochemotherapy: a GELA/LYSA study.', *Blood*. United States, 126(22), pp. 2466–2474. doi: 10.1182/blood-2015-05-647602.

Dang, C. V (2013) 'MYC, metabolism, cell growth, and tumorigenesis.', *Cold Spring Harbor perspectives in medicine*. United States, 3(8). doi: 10.1101/cshperspect.a014217.

Dang, C. V, O'donnell, K. A. and Juopperi, T. (2005) 'The great MYC escape in tumorigenesis.', *Cancer cell*. United States, 8(3), pp. 177–178. doi: 10.1016/j.ccr.2005.08.005.

Dave, S. S. *et al.* (2006) 'Molecular diagnosis of Burkitt's lymphoma.', *The New England journal of medicine*. United States, 354(23), pp. 2431–2442. doi: 10.1056/NEJMoa055759.

Davis, R. E. *et al.* (2001) 'Constitutive nuclear factor kappaB activity is required for survival of activated B cell-like diffuse large B cell lymphoma cells.', *The Journal of experimental medicine*, 194(12), pp. 1861–1874. doi: 10.1084/jem.194.12.1861.

Davis, R. E. *et al.* (2010) 'Chronic active B-cell-receptor signalling in diffuse large B-cell lymphoma.', *Nature*. England, 463(7277), pp. 88–92. doi: 10.1038/nature08638.

Deffenbacher, K. E. *et al.* (2012) 'Molecular distinctions between pediatric and adult mature B-cell non-Hodgkin lymphomas identified through genomic profiling.', *Blood*. United States, 119(16), pp. 3757–3766. doi: 10.1182/blood-2011-05-349662.

Divine, M. *et al.* (2005) 'Burkitt lymphoma in adults: a prospective study of 72 patients treated with an adapted pediatric LMB protocol.', *Annals of oncology : official journal of the European Society for Medical Oncology*. England, 16(12), pp. 1928–1935. doi: 10.1093/annonc/mdi403.

Do, H. and Dobrovic, A. (2015) 'Sequence artifacts in DNA from formalin-fixed tissues: causes and strategies for minimization.', *Clinical chemistry*. England, 61(1), pp. 64–71. doi: 10.1373/clinchem.2014.223040.

Downing, J. R. *et al.* (2012) 'The Pediatric Cancer Genome Project.', *Nature genetics*, 44(6), pp. 619–622. doi: 10.1038/ng.2287.

Duan, S. *et al.* (2012) 'FBXO11 targets BCL6 for degradation and is inactivated in diffuse large B-cell lymphomas.', *Nature*, 481(7379), pp. 90–93. doi: 10.1038/nature10688.

Dunleavy, K., Pittaluga, S., Maeda, L. S., *et al.* (2013) 'Dose-adjusted EPOCH-rituximab therapy in primary mediastinal B-cell lymphoma.', *The New England journal of medicine*, 368(15), pp. 1408–1416. doi: 10.1056/NEJMoa1214561.

Dunleavy, K., Pittaluga, S., Shovlin, M., *et al.* (2013) 'Low-intensity therapy in adults with Burkitt's lymphoma.', *The New England journal of medicine*. United States, 369(20), pp. 1915–1925. doi: 10.1056/NEJMoa1308392.

Dunleavy, K. (2017) 'Primary mediastinal B-cell lymphoma: biology and evolving therapeutic strategies.', *Hematology. American Society of Hematology. Education Program*. United States, 2017(1), pp. 298–303. doi: 10.1182/asheducation-2017.1.298.

Dunleavy, K. and Gross, T. G. (2018) 'Management of aggressive B-cell NHLs in the AYA population: an adult vs pediatric perspective.', *Blood*. United States, 132(4), pp. 369–375. doi: 10.1182/blood-2018-02-778480.

Dunleavy, K., Little, R. F. and Wilson, W. H. (2016) 'Update on Burkitt Lymphoma.', *Hematology/oncology clinics of North America*. United States, 30(6), pp. 1333–1343. doi: 10.1016/j.hoc.2016.07.009.

Edelmann, J. *et al.* (2012) 'High-resolution genomic profiling of chronic lymphocytic leukemia reveals new recurrent genomic alterations.', *Blood*. United States, 120(24), pp. 4783–4794. doi: 10.1182/blood-2012-04-423517.

Ennishi, D. *et al.* (2019) 'Double-Hit Gene Expression Signature Defines a Distinct Subgroup of Germinal Center B-Cell-Like Diffuse Large B-Cell Lymphoma.', *Journal of clinical oncology : official journal of the American Society of Clinical Oncology*. United States, 37(3), pp. 190–201. doi: 10.1200/JCO.18.01583.

Evrard, S. M. *et al.* (2019) 'Targeted next generation sequencing reveals high mutation frequency of CREBBP, BCL2 and KMT2D in

high-grade B-cell lymphoma with MYC and BCL2 and/or BCL6 rearrangements.', *Haematologica*. Italy, pp. e154–e157. doi: 10.3324/haematol.2018.198572.

Ferreiro, J. F. *et al.* (2015) 'Post-transplant molecularly defined Burkitt lymphomas are frequently MYC-negative and characterized by the 11q-gain/loss pattern.', *Haematologica*. Italy, pp. e275-9. doi: 10.3324/haematol.2015.124305.

Ferry, J. A. (2020) 'Scientific Advances and the Evolution of Diagnosis, Subclassification and Treatment of Lymphoma.', *Archives of medical research*. United States. doi: 10.1016/j.arcmed.2020.05.022.

Frauenfeld L, Castrejon-de-Anta N, Ramis-Zaldivar JE, Otto F, Streich S, Salmerón-Villalobos J, Mayer A, Steinhilber J, Pinyol M, Mankel B, Bonzheim I, Fend F, Rimza L, Salaverria I, Campo E, Balagué O, Q.-M. L. (2021) *Triple positive (CD10+BCL6+MUM1+) diffuse large B-cell lymphomas in adults are a heterogeneous group enriched in large B-cell lymphomas with IRF4 rearrangement*.

Fugmann, S. D. *et al.* (2000) 'The RAG proteins and V(D)J recombination: complexes, ends, and transposition.', *Annual review of immunology*. United States, 18, pp. 495–527. doi: 10.1146/annurev.immunol.18.1.495.

Gallegos Ruiz, M. I. *et al.* (2007) 'EGFR and K-ras mutation analysis in non-small cell lung cancer: comparison of paraffin embedded versus frozen specimens.', *Cellular oncology : the official journal of the International Society for Cellular Oncology*, 29(3), pp. 257–264. doi: 10.1155/2007/568205.

Gerrard, M. *et al.* (2013) 'Outcome and pathologic classification of children and adolescents with mediastinal large B-cell lymphoma treated with FAB/LMB96 mature B-NHL therapy.', *Blood*, 121(2), pp. 278–285. doi: 10.1182/blood-2012-04-422709.

Goldman, S. *et al.* (2013) 'Rituximab and FAB/LMB 96 chemotherapy in children with Stage III/IV B-cell non-Hodgkin lymphoma: a Children's Oncology Group report.', *Leukemia*, pp. 1174–1177. doi: 10.1038/leu.2012.255.

Le Gouill, S. *et al.* (2007) 'The clinical presentation and prognosis of diffuse large B-cell lymphoma with t(14;18) and 8q24/c-MYC rearrangement.', *Haematologica*. Italy, 92(10), pp. 1335–1342. doi: 10.3324/haematol.11305.

Grande, B. M. *et al.* (2019) 'Genome-wide discovery of somatic coding and non-coding mutations in pediatric endemic and sporadic Burkitt lymphoma.', *Blood*. United States. doi: 10.1182/blood-2018-09-871418.

Green, M. R. *et al.* (2013) 'Hierarchy in somatic mutations arising during genomic evolution and progression of follicular lymphoma.', *Blood*, 121(9), pp. 1604–1611. doi: 10.1182/blood-2012-09-457283.

Green, M. R. *et al.* (2015) 'Mutations in early follicular lymphoma progenitors are associated with suppressed antigen presentation.', *Proceedings of the National Academy of Sciences of the United States of America*. United States, 112(10), pp. E1116-25. doi: 10.1073/pnas.1501199112.

Green, T. M. *et al.* (2012) 'Immunohistochemical double-hit score is a strong predictor of outcome in patients with diffuse large B-cell lymphoma treated with rituximab plus cyclophosphamide, doxorubicin, vincristine, and prednisone.', *Journal of clinical oncology : official journal of the American Society of Clinical Oncology*. United States, 30(28), pp. 3460–3467. doi: 10.1200/JCO.2011.41.4342.

Grimm, K. E. and O'Malley, D. P. (2019) 'Aggressive B cell lymphomas in the 2017 revised WHO classification of tumors of hematopoietic and lymphoid tissues.', *Annals of diagnostic pathology*. United States, 38, pp.

610.doi:10.1016/j.anndiagpath.2018.09.014.

Grygalewicz, B. *et al.* (2017) 'The 11q-Gain/Loss Aberration Occurs Recurrently in MYC-Negative Burkitt-like Lymphoma With 11q Aberration, as Well as MYC-Positive Burkitt Lymphoma and MYC-Positive High-Grade B-Cell Lymphoma, NOS.', *American journal of clinical pathology*. England, 149(1), pp. 17–28. doi: 10.1093/ajcp/aqx139.

Gunawardana, J. *et al.* (2014) 'Recurrent somatic mutations of PTPN1 in primary mediastinal B cell lymphoma and Hodgkin lymphoma.', *Nature genetics*. United States, 46(4), pp. 329–335. doi: 10.1038/ng.2900.

Hans, C. P. *et al.* (2004) 'Confirmation of the molecular classification of diffuse large B-cell lymphoma by immunohistochemistry using a tissue microarray.', *Blood*. United States, 103(1), pp. 275–282. doi: 10.1182/blood-2003-05-1545.

Harker-Murray, P. D., Pommert, L. and Barth, M. J. (2020) 'Novel Therapies Potentially Available for Pediatric B-Cell Non-Hodgkin Lymphoma.', *Journal of the National Comprehensive Cancer Network : JNCCN*. United States, 18(8), pp. 1125–1134. doi: 10.6004/jnccn.2020.7608.

Havelange, V. *et al.* (2016) 'Genetic differences between paediatric and adult Burkitt lymphomas.', *British journal of haematology*. England, 173(1), pp. 137–144. doi: 10.1111/bjh.13925.

Hemann, M. T. *et al.* (2005) 'Evasion of the p53 tumour surveillance network by tumour-derived MYC mutants.', *Nature*. England, 436(7052), pp. 807–811. doi: 10.1038/nature03845.

Hübschmann, D. *et al.* (2021) 'Mutational mechanisms shaping the coding and noncoding genome of germinal center derived B-cell lymphomas.', *Leukemia*. England. doi: 10.1038/s41375-021-01251-z.

Hullein, J. *et al.* (2019) 'MDM4 is targeted by 1q gain and drives disease in Burkitt lymphoma.', *Cancer research*. United States. doi: 10.1158/0008-5472.CAN-18-3438.

Hummel, M. *et al.* (2006) 'A biologic definition of Burkitt's lymphoma from transcriptional and genomic profiling.', *The New England journal of medicine*. United States, 354(23), pp. 2419–2430. doi: 10.1056/NEJMoa055351.

Hunt, K. E., Hall, B. and Reichard, K. K. (2010) 'Translocations involving MUM1 are rare in diffuse large B-cell lymphoma.', *Applied immunohistochemistry & molecular morphology : AIMM*. United States, 18(2), pp. 109–112. doi: 10.1097/PAI.0b013e31817fa43c.

Hüttl, K. S. *et al.* (2021) 'The "Burkitt-like" immunophenotype and genotype is rarely encountered in diffuse large B cell lymphoma and high-grade B cell lymphoma, NOS.', *Virchows Archiv : an international journal of pathology*. Germany. doi: 10.1007/s00428-021-03050-4.

Iida, S. *et al.* (1997) 'Deregulation of MUM1/IRF4 by chromosomal translocation in multiple myeloma.', *Nature genetics*. United States, 17(2), pp. 226–230. doi: 10.1038/ng1097-226.

International Non-Hodgkin's Lymphoma Prognostic Factors Project (1993) 'A predictive model for aggressive non-Hodgkin's lymphoma.', *The New England journal of medicine*. United States, 329(14), pp. 987–994. doi: 10.1056/NEJM199309303291402.

Jardin, F. *et al.* (2010) 'Diffuse large B-cell lymphomas with CDKN2A deletion have a distinct gene expression signature and a poor prognosis under R-CHOP treatment: a GELA study.', *Blood*. United States, 116(7), pp. 1092–1104. doi: 10.1182/blood-2009-10-247122.

Johnson, N. A. *et al.* (2012) 'Concurrent expression of MYC and BCL2 in diffuse large B-

cell lymphoma treated with rituximab plus cyclophosphamide, doxorubicin, vincristine, and prednisone.', *Journal of clinical oncology : official journal of the American Society of Clinical Oncology*. United States, 30(28), pp. 3452–3459. doi: 10.1200/JCO.2011.41.0985.

Joos, S. *et al.* (1996) 'Primary mediastinal (thymic) B-cell lymphoma is characterized by gains of chromosomal material including 9p and amplification of the REL gene.', *Blood*. United States, 87(4), pp. 1571–1578.

Kamranvar, S. A. *et al.* (2007) 'Epstein-Barr virus promotes genomic instability in Burkitt's lymphoma.', *Oncogene*. England, 26(35), pp. 5115–5123. doi: 10.1038/sj.onc.1210324.

Karube, K. *et al.* (2018) 'Integrating genomic alterations in diffuse large B-cell lymphoma identifies new relevant pathways and potential therapeutic targets.', *Leukemia*. England, 32(3), pp. 675–684. doi: 10.1038/leu.2017.251.

Khodabakhshi, A. H. *et al.* (2012) 'Recurrent targets of aberrant somatic hypermutation in lymphoma.', *Oncotarget*. United States, 3(11), pp. 1308–1319. doi: 10.18632/oncotarget.653.

King, R. L. *et al.* (2019) 'False-negative rates for MYC fluorescence in situ hybridization probes in B-cell neoplasms.', *Haematologica*, pp. e248–e251. doi: 10.3324/haematol.2018.207290.

Klapper, W. *et al.* (2008) 'Molecular profiling of pediatric mature B-cell lymphoma treated in population-based prospective clinical trials.', *Blood*. United States, 112(4), pp. 1374–1381. doi: 10.1182/blood-2008-01-136465.

Klapper, W. *et al.* (2012) 'Patient age at diagnosis is associated with the molecular characteristics of diffuse large B-cell lymphoma.', *Blood*. United States, 119(8), pp. 1882–1887. doi: 10.1182/blood-2011-10-388470.

Klein, U. and Dalla-Favera, R. (2008) 'Germinal centres: role in B-cell physiology and malignancy.', *Nature reviews. Immunology*. England, 8(1), pp. 22–33. doi: 10.1038/nri2217.

Komano, J. *et al.* (1999) 'Oncogenic role of Epstein-Barr virus-encoded RNAs in Burkitt's lymphoma cell line Akata.', *Journal of virology*. United States, 73(12), pp. 9827–9831.

Kramer, M. H. *et al.* (1998) 'Clinical relevance of BCL2, BCL6, and MYC rearrangements in diffuse large B-cell lymphoma.', *Blood*. United States, 92(9), pp. 3152–3162.

Küppers, R. and Dalla-Favera, R. (2001) 'Mechanisms of chromosomal translocations in B cell lymphomas.', *Oncogene*. England, 20(40), pp. 5580–5594. doi: 10.1038/sj.onc.1204640.

Kurosaki, T., Kometani, K. and Ise, W. (2015) 'Memory B cells.', *Nature reviews. Immunology*. England, 15(3), pp. 149–159. doi: 10.1038/nri3802.

Lacasce, A. *et al.* (2004) 'Modified magrath regimens for adults with Burkitt and Burkitt-like lymphomas: preserved efficacy with decreased toxicity.', *Leukemia & lymphoma*. United States, 45(4), pp. 761–767. doi: 10.1080/1042819031000141301.

Lacy, S. E. *et al.* (2020) 'Targeted sequencing in DLBCL, molecular subtypes, and outcomes: a Haematological Malignancy Research Network report.', *Blood*, 135(20), pp. 1759–1771. doi: 10.1182/blood.2019003535.

Landau, D. A. *et al.* (2015) 'Mutations driving CLL and their evolution in progression and relapse.', *Nature*, 526(7574), pp. 525–530. doi: 10.1038/nature15395.

LeBien, T. W. and Tedder, T. F. (2008) 'B lymphocytes: how they develop and function.', *Blood*, 112(5), pp. 1570–1580. doi: 10.1182/blood-2008-02-078071.

Lecluse, Y. *et al.* (2009) 't(11;14)-positive clones can persist over a long period of time in the peripheral blood of healthy individuals.', *Leukemia*. England, pp. 1190–1193. doi: 10.1038/leu.2009.31.

Lenz, G., Wright, G. W., *et al.* (2008) 'Molecular subtypes of diffuse large B-cell lymphoma arise by distinct genetic pathways.', *Proceedings of the National Academy of Sciences of the United States of America*, 105(36), pp. 13520–13525. doi: 10.1073/pnas.0804295105.

Lenz, G., Davis, R. E., *et al.* (2008) 'Oncogenic CARD11 mutations in human diffuse large B cell lymphoma.', *Science (New York, N.Y.)*. United States, 319(5870), pp. 1676–1679. doi: 10.1126/science.1153629.

Leucci, E. *et al.* (2008) 'MYC translocation-negative classical Burkitt lymphoma cases: an alternative pathogenetic mechanism involving miRNA deregulation.', *The Journal of pathology*. England, 216(4), pp. 440–450. doi: 10.1002/path.2410.

Leventaki, V. *et al.* (2012) 'TP53 pathway analysis in paediatric Burkitt lymphoma reveals increased MDM4 expression as the only TP53 pathway abnormality detected in a subset of cases.', *British journal of haematology*. England, 158(6), pp. 763–771. doi: 10.1111/j.1365-2141.2012.09243.x.

Li, H. *et al.* (2014) 'Mutations in linker histone genes HIST1H1 B, C, D, and E; OCT2 (POU2F2); IRF8; and ARID1A underlying the pathogenesis of follicular lymphoma.', *Blood*, 123(10), pp. 1487–1498. doi: 10.1182/blood-2013-05-500264.

Li, S. *et al.* (2012) 'B-cell lymphomas with MYC/8q24 rearrangements and IGH@BCL2/t(14;18)(q32;q21): an aggressive disease with heterogeneous histology, germinal center B-cell immunophenotype and poor outcome.', *Modern pathology : an official journal of the United States and Canadian Academy of Pathology, Inc*. United States, 25(1), pp. 145–156. doi: 10.1038/modpathol.2011.147.

Li, S. *et al.* (2015) 'B-cell lymphomas with concurrent MYC and BCL2 abnormalities other than translocations behave similarly to MYC/BCL2 double-hit lymphomas.', *Modern pathology : an official journal of the United States and Canadian Academy of Pathology, Inc*. United States, 28(2), pp. 208–217. doi: 10.1038/modpathol.2014.95.

Li, S., Young, K. H. and Medeiros, L. J. (2018) 'Diffuse large B-cell lymphoma.', *Pathology*. England, 50(1), pp. 74–87. doi: 10.1016/j.pathol.2017.09.006.

Li, Z. *et al.* (2004) 'The generation of antibody diversity through somatic hypermutation and class switch recombination.', *Genes & development*. United States, 18(1), pp. 1–11. doi: 10.1101/gad.1161904.

Lindstrom, M. S. and Wiman, K. G. (2002) 'Role of genetic and epigenetic changes in Burkitt lymphoma.', *Seminars in cancer biology*. England, 12(5), pp. 381–387. doi: 10.1016/s1044-579x(02)00058-5.

Liu, Q. *et al.* (2013) 'Follicular lymphomas in children and young adults: a comparison of the pediatric variant with usual follicular lymphoma.', *The American journal of surgical pathology*. United States, 37(3), pp. 333–343. doi: 10.1097/PAS.0b013e31826b9b57.

Lohr, J. G. *et al.* (2012) 'Discovery and prioritization of somatic mutations in diffuse large B-cell lymphoma (DLBCL) by whole-exome sequencing.', *Proceedings of the National Academy of Sciences of the United States of America*. United States, 109(10), pp. 3879–3884. doi: 10.1073/pnas.1121343109.

Lohr, J. G. *et al.* (2014) 'Widespread genetic heterogeneity in multiple myeloma: implications for targeted therapy.', *Cancer cell*. United States, 25(1), pp. 91–101. doi: 10.1016/j.ccr.2013.12.015.

Lopez, C. *et al.* (2019) 'Genomic and transcriptomic changes complement each other in the pathogenesis of sporadic Burkitt lymphoma.', *Nature communications*. England, 10(1), p. 1459. doi: 10.1038/s41467-019-08578-3.

Lorsbach, R. B. *et al.* (2002) 'Clinicopathologic analysis of follicular lymphoma occurring in children.', *Blood*. United States, 99(6), pp. 1959–1964. doi: 10.1182/blood.v99.6.1959.

Louissaint, A. J. *et al.* (2012) 'Pediatric-type nodal follicular lymphoma: an indolent clonal proliferation in children and adults with high proliferation index and no BCL2 rearrangement.', *Blood*. United States, 120(12), pp. 2395–2404. doi: 10.1182/blood-2012-05-429514.

Louissaint, A. J. *et al.* (2016) 'Pediatric-type nodal follicular lymphoma: a biologically distinct lymphoma with frequent MAPK pathway mutations.', *Blood*. United States, 128(8), pp. 1093–1100. doi: 10.1182/blood-2015-12-682591.

Love, C. *et al.* (2012) 'The genetic landscape of mutations in Burkitt lymphoma.', *Nature genetics*. United States, 44(12), pp. 1321–1325. doi: 10.1038/ng.2468.

Lunning, M. A. and Green, M. R. (2015) 'Mutation of chromatin modifiers; an emerging hallmark of germinal center B-cell lymphomas.', *Blood cancer journal*, 5(10), p. e361. doi: 10.1038/bcj.2015.89.

Lyons-Weiler, M. *et al.* (2008) 'Optimization of the Affymetrix GeneChip Mapping 10K 2.0 Assay for routine clinical use on formalin-fixed paraffin-embedded tissues.', *Diagnostic molecular pathology : the American journal of surgical pathology, part B*. United States, 17(1), pp. 3–13. doi: 10.1097/PDM.0b013e31815aca30.

Ma, S. *et al.* (2010) 'Ikaros and Aiolos inhibit pre-B-cell proliferation by directly suppressing c-Myc expression.', *Molecular and cellular biology*, 30(17), pp. 4149–4158. doi: 10.1128/MCB.00224-10.

Marks, J. L. *et al.* (2008) 'Novel MEK1 mutation identified by mutational analysis of epidermal growth factor receptor signaling pathway genes in lung adenocarcinoma.', *Cancer research*, 68(14), pp. 5524–5528. doi: 10.1158/0008-5472.CAN-08-0099.

Martin-Guerrero, I. *et al.* (2013) 'Recurrent loss of heterozygosity in 1p36 associated with TNFRSF14 mutations in IRF4 translocation negative pediatric follicular lymphomas.', *Haematologica*. Italy, 98(8), pp. 1237–1241. doi: 10.3324/haematol.2012.073916.

Martincorena, I. and Campbell, P. J. (2015) 'Somatic mutation in cancer and normal cells.', *Science (New York, N.Y.)*. United States, 349(6255), pp. 1483–1489. doi: 10.1126/science.aab4082.

Mason, E. F. *et al.* (2017) 'Detection of activating MAP2K1 mutations in atypical hairy cell leukemia and hairy cell leukemia variant.', *Leukemia & lymphoma*. United States, pp. 233–236. doi: 10.1080/10428194.2016.1185786.

Mc Sherry, E. A. *et al.* (2007) 'Formalin-fixed paraffin-embedded clinical tissues show spurious copy number changes in array-CGH profiles.', *Clinical genetics*. Denmark, 72(5), pp. 441–447. doi: 10.1111/j.1399-0004.2007.00882.x.

Mead, G. M. *et al.* (2002) 'An international evaluation of CODOX-M and CODOX-M alternating with IVAC in adult Burkitt's lymphoma: results of United Kingdom Lymphoma Group LY06 study.', *Annals of oncology : official journal of the European Society for Medical Oncology*. England, 13(8), pp. 1264–1274. doi: 10.1093/annonc/mdf253.

Mead, G. M. *et al.* (2008) 'A prospective clinicopathologic study of dose-modified CODOX-M/IVAC in patients with sporadic

Burkitt lymphoma defined using cytogenetic and immunophenotypic criteria (MRC/NCRI LY10 trial).', *Blood*. United States, 112(6), pp. 2248–2260. doi: 10.1182/blood-2008-03-145128.

Melzner, I. *et al.* (2005) 'Biallelic mutation of SOCS-1 impairs JAK2 degradation and sustains phospho-JAK2 action in the MedB-1 mediastinal lymphoma line.', *Blood*. United States, 105(6), pp. 2535–2542. doi: 10.1182/blood-2004-09-3701.

Mesin, L., Ersching, J. and Victora, G. D. (2016) 'Germinal Center B Cell Dynamics.', *Immunity*, 45(3), pp. 471–482. doi: 10.1016/j.immuni.2016.09.001.

Meyer, N. and Penn, L. Z. (2008) 'Reflecting on 25 years with MYC.', *Nature reviews. Cancer*. England, 8(12), pp. 976–990. doi: 10.1038/nrc2231.

Meyer, P. N. *et al.* (2011) 'Immunohistochemical methods for predicting cell of origin and survival in patients with diffuse large B-cell lymphoma treated with rituximab.', *Journal of clinical oncology : official journal of the American Society of Clinical Oncology*, 29(2), pp. 200–207. doi: 10.1200/JCO.2010.30.0368.

Miao, Y. *et al.* (2019) 'Genetic alterations and their clinical implications in DLBCL.', *Nature reviews. Clinical oncology*. England, 16(10), pp. 634–652. doi: 10.1038/s41571-019-0225-1.

Miles, R. R. *et al.* (2008) 'Pediatric diffuse large B-cell lymphoma demonstrates a high proliferation index, frequent c-Myc protein expression, and a high incidence of germinal center subtype: Report of the French-American-British (FAB) international study group.', *Pediatric blood & cancer*, 51(3), pp. 369–374. doi: 10.1002/pbc.21619.

Minard-Colin, V. *et al.* (2015) 'Non-Hodgkin Lymphoma in Children and Adolescents: Progress Through Effective Collaboration, Current Knowledge, and Challenges Ahead.', *Journal of clinical oncology : official journal of the American Society of Clinical Oncology*, 33(27), pp. 2963–2974. doi: 10.1200/JCO.2014.59.5827.

Minard-Colin, V. *et al.* (2020) 'Rituximab for High-Risk, Mature B-Cell Non-Hodgkin's Lymphoma in Children.', *The New England journal of medicine*, 382(23), pp. 2207–2219. doi: 10.1056/NEJMoa1915315.

Moleti, M. L., Testi, A. M. and Foa, R. (2020) 'Treatment of relapsed/refractory paediatric aggressive B-cell non-Hodgkin lymphoma.', *British journal of haematology*. England. doi: 10.1111/bjh.16461.

Momose, S. *et al.* (2015) 'The diagnostic gray zone between Burkitt lymphoma and diffuse large B-cell lymphoma is also a gray zone of the mutational spectrum', *Leukemia*, 29(8), pp. 1789–1791. doi: 10.1038/leu.2015.34.

Monroe, J. G. and Dorshkind, K. (2007) 'Fate decisions regulating bone marrow and peripheral B lymphocyte development.', *Advances in immunology*. United States, 95, pp. 1–50. doi: 10.1016/S0065-2776(07)95001-4.

Monti, S. *et al.* (2012) 'Integrative analysis reveals an outcome-associated and targetable pattern of p53 and cell cycle deregulation in diffuse large B cell lymphoma.', *Cancer cell*, 22(3), pp. 359–372. doi: 10.1016/j.ccr.2012.07.014.

Morin, R. D. *et al.* (2010) 'Somatic mutations altering EZH2 (Tyr641) in follicular and diffuse large B-cell lymphomas of germinal-center origin.', *Nature genetics*, 42(2), pp. 181–185. doi: 10.1038/ng.518.

Morin, R. D. *et al.* (2011) 'Frequent mutation of histone-modifying genes in non-Hodgkin lymphoma.', *Nature*, 476(7360), pp. 298–303. doi: 10.1038/nature10351.

Morin, R. D. *et al.* (2013) 'Mutational and structural analysis of diffuse large B-cell lymphoma using whole-genome sequencing.', *Blood*. United States, 122(7), pp. 1256–1265. doi: 10.1182/blood-2013-02-483727.

Morton, L. M. *et al.* (2007) 'Proposed classification of lymphoid neoplasms for epidemiologic research from the Pathology Working Group of the International Lymphoma Epidemiology Consortium (InterLymph).', *Blood*. United States, 110(2), pp. 695–708. doi: 10.1182/blood-2006-11-051672.

Mottok, A. *et al.* (2015) 'Genomic Alterations in CIITA Are Frequent in Primary Mediastinal Large B Cell Lymphoma and Are Associated with Diminished MHC Class II Expression.', *Cell reports*. United States, 13(7), pp. 1418–1431. doi: 10.1016/j.celrep.2015.10.008.

Mottok, A. *et al.* (2018) 'Molecular classification of primary mediastinal large B-cell lymphoma using routinely available tissue specimens', *Blood*, p. blood-2018-05-851154. doi: 10.1182/blood-2018-05-851154.

Mrozek-Gorska, P. *et al.* (2019) 'Epstein-Barr virus reprograms human B lymphocytes immediately in the prelatent phase of infection.', *Proceedings of the National Academy of Sciences of the United States of America*, 116(32), pp. 16046–16055. doi: 10.1073/pnas.1901314116.

Muppidi, J. R. *et al.* (2014) 'Loss of signalling via Gα13 in germinal centre B-cell-derived lymphoma.', *Nature*, 516(7530), pp. 254–258. doi: 10.1038/nature13765.

Muramatsu, M. *et al.* (2000) 'Class switch recombination and hypermutation require activation-induced cytidine deaminase (AID), a potential RNA editing enzyme.', *Cell*. United States, 102(5), pp. 553–563. doi: 10.1016/s0092-8674(00)00078-7.

Murphy, S. B. (1980) 'Classification, staging and end results of treatment of childhood non-Hodgkin's lymphomas: dissimilarities from lymphomas in adults.', *Seminars in oncology*. United States, 7(3), pp. 332–339.

Müschen, M. *et al.* (2000) 'Somatic mutation of the CD95 gene in human B cells as a side-effect of the germinal center reaction.', *The Journal of experimental medicine*, 192(12), pp. 1833–1840. doi: 10.1084/jem.192.12.1833.

Nakagawa, H. *et al.* (2015) 'Cancer whole-genome sequencing: present and future.', *Oncogene*. England, 34(49), pp. 5943–5950. doi: 10.1038/onc.2015.90.

Nann, D. *et al.* (2020) 'Follicular lymphoma t(14;18)-negative is genetically a heterogeneous disease.', *Blood advances*, 4(22), pp. 5652–5665. doi: 10.1182/bloodadvances.2020002944.

Nasri, S. *et al.* (2010) 'Oligonucleotide array outperforms SNP array on formalin-fixed paraffin-embedded clinical samples.', *Cancer genetics and cytogenetics*. United States, 198(1), pp. 1–6. doi: 10.1016/j.cancergencyto.2009.12.002.

Nguyen, L., Papenhausen, P. and Shao, H. (2017) 'The Role of c-MYC in B-Cell Lymphomas: Diagnostic and Molecular Aspects.', *Genes*. Switzerland, 8(4). doi: 10.3390/genes8040116.

Offit, K. *et al.* (1994) 'Rearrangement of the bcl-6 gene as a prognostic marker in diffuse large-cell lymphoma.', *The New England journal of medicine*. United States, 331(2), pp. 74–80. doi: 10.1056/NEJM199407143310202.

Ok, C. Y. and Medeiros, L. J. (2020) 'High-grade B-cell lymphoma: a term re-purposed in the revised WHO classification.', *Pathology*. England, 52(1), pp. 68–77. doi: 10.1016/j.pathol.2019.09.008.

Okosun, J. *et al.* (2014) 'Integrated genomic analysis identifies recurrent mutations and evolution patterns driving the initiation and progression of follicular lymphoma.', *Nature*

genetics. United States, 46(2), pp. 176–181. doi: 10.1038/ng.2856.

Onciu, M. *et al.* (2006) 'Secondary chromosomal abnormalities predict outcome in pediatric and adult high-stage Burkitt lymphoma.', *Cancer*. United States, 107(5), pp. 1084–1092. doi: 10.1002/cncr.22089.

Oschlies, I. *et al.* (2006) 'Diffuse large B-cell lymphoma in pediatric patients belongs predominantly to the germinal-center type B-cell lymphomas: a clinicopathologic analysis of cases included in the German BFM (Berlin-Frankfurt-Munster) Multicenter Trial.', *Blood*. United States, 107(10), pp. 4047–4052. doi: 10.1182/blood-2005-10-4213.

Oschlies, I. *et al.* (2010) 'Pediatric follicular lymphoma--a clinico-pathological study of a population-based series of patients treated within the Non-Hodgkin's Lymphoma--Berlin-Frankfurt-Munster (NHL-BFM) multicenter trials.', *Haematologica*. Italy, 95(2), pp. 253–259. doi: 10.3324/haematol.2009.013177.

Ozawa, M. G. *et al.* (2016) 'A study of the mutational landscape of pediatric-type follicular lymphoma and pediatric nodal marginal zone lymphoma.', *Modern pathology : an official journal of the United States and Canadian Academy of Pathology, Inc*. United States, 29(10), pp. 1212–1220. doi: 10.1038/modpathol.2016.102.

Pasqualucci, L. *et al.* (1998) 'BCL-6 mutations in normal germinal center B cells: evidence of somatic hypermutation acting outside Ig loci.', *Proceedings of the National Academy of Sciences of the United States of America*, 95(20), pp. 11816–11821. doi: 10.1073/pnas.95.20.11816.

Pasqualucci, L. *et al.* (2001) 'Hypermutation of multiple proto-oncogenes in B-cell diffuse large-cell lymphomas.', *Nature*. England, 412(6844), pp. 341–346. doi: 10.1038/35085588.

Pasqualucci, L. *et al.* (2003) 'Mutations of the BCL6 proto-oncogene disrupt its negative autoregulation in diffuse large B-cell lymphoma.', *Blood*. United States, 101(8), pp. 2914–2923. doi: 10.1182/blood-2002-11-3387.

Pasqualucci, L. *et al.* (2006) 'Inactivation of the PRDM1/BLIMP1 gene in diffuse large B cell lymphoma.', *The Journal of experimental medicine*, 203(2), pp. 311–317. doi: 10.1084/jem.20052204.

Pasqualucci, L. *et al.* (2008) 'AID is required for germinal center-derived lymphomagenesis.', *Nature genetics*. United States, 40(1), pp. 108–112. doi: 10.1038/ng.2007.35.

Pasqualucci, L., Trifonov, V., *et al.* (2011) 'Analysis of the coding genome of diffuse large B-cell lymphoma.', *Nature genetics*. United States, 43(9), pp. 830–837. doi: 10.1038/ng.892.

Pasqualucci, L., Dominguez-Sola, D., *et al.* (2011) 'Inactivating mutations of acetyltransferase genes in B-cell lymphoma.', *Nature*. England, 471(7337), pp. 189–195. doi: 10.1038/nature09730.

Pasqualucci, L. (2019) 'Molecular pathogenesis of germinal center-derived B cell lymphomas.', *Immunological reviews*. England, 288(1), pp. 240–261. doi: 10.1111/imr.12745.

Pasqualucci, L. and Dalla-Favera, R. (2015) 'The genetic landscape of diffuse large B-cell lymphoma.', *Seminars in hematology*, 52(2), pp. 67–76. doi: 10.1053/j.seminhematol.2015.01.005.

Pasqualucci, L. and Dalla-Favera, R. (2018) 'Genetics of diffuse large B-cell lymphoma.', *Blood*, 131(21), pp. 2307–2319. doi: 10.1182/blood-2017-11-764332.

Patte, C. *et al.* (2001) 'The Societe Francaise d'Oncologie Pediatrique LMB89 protocol: highly effective multiagent chemotherapy

tailored to the tumor burden and initial response in 561 unselected children with B-cell lymphomas and L3 leukemia.', *Blood*. United States, 97(11), pp. 3370–3379. doi: 10.1182/blood.v97.11.3370.

Perry, A. M. *et al.* (2013) 'B-cell lymphoma, unclassifiable, with features intermediate between diffuse large B-cell lymphoma and burkitt lymphoma: study of 39 cases.', *British journal of haematology*. England, 162(1), pp. 40–49. doi: 10.1111/bjh.12343.

Pienkowska-Grela, B. *et al.* (2011) 'Partial trisomy 11, dup(11)(q23q13), as a defect characterizing lymphomas with Burkitt pathomorphology without MYC gene rearrangement.', *Medical oncology (Northwood, London, England)*. United States, 28(4), pp. 1589–1595. doi: 10.1007/s12032-010-9614-0.

Pieper, K., Grimbacher, B. and Eibel, H. (2013) 'B-cell biology and development.', *The Journal of allergy and clinical immunology*. United States, 131(4), pp. 959–971. doi: 10.1016/j.jaci.2013.01.046.

Poirel, H. A. *et al.* (2009) 'Specific cytogenetic abnormalities are associated with a significantly inferior outcome in children and adolescents with mature B-cell non-Hodgkin's lymphoma: results of the FAB/LMB 96 international study.', *Leukemia*. England, 23(2), pp. 323–331. doi: 10.1038/leu.2008.312.

Puente, X. S. *et al.* (2015) 'Non-coding recurrent mutations in chronic lymphocytic leukaemia.', *Nature*. England, 526(7574), pp. 519–524. doi: 10.1038/nature14666.

Quintanilla-Martinez, L. *et al.* (2016) 'Indolent lymphomas in the pediatric population: follicular lymphoma, IRF4/MUM1+ lymphoma, nodal marginal zone lymphoma and chronic lymphocytic leukemia.', *Virchows Archiv : an international journal of pathology*. Germany, 468(2), pp. 141–157. doi: 10.1007/s00428-015-1855-z.

Reddy, A. *et al.* (2017) 'Genetic and Functional Drivers of Diffuse Large B Cell Lymphoma.', *Cell*. Elsevier Inc., 171(2), pp. 481-494.e15. doi: 10.1016/j.cell.2017.09.027.

Reiter, A. *et al.* (1999) 'Improved treatment results in childhood B-cell neoplasms with tailored intensification of therapy: A report of the Berlin-Frankfurt-Munster Group Trial NHL-BFM 90.', *Blood*. United States, 94(10), pp. 3294–3306.

Reiter, A. and Klapper, W. (2008) 'Recent advances in the understanding and management of diffuse large B-cell lymphoma in children.', *British journal of haematology*. England, 142(3), pp. 329–347. doi: 10.1111/j.1365-2141.2008.06988.x.

Richter, J. *et al.* (2012) 'Recurrent mutation of the ID3 gene in Burkitt lymphoma identified by integrated genome, exome and transcriptome sequencing.', *Nature genetics*. United States, 44(12), pp. 1316–1320. doi: 10.1038/ng.2469.

Rieger, M. A. and Schroeder, T. (2012) 'Hematopoiesis.', *Cold Spring Harbor perspectives in biology*, 4(12). doi: 10.1101/cshperspect.a008250.

Rinaldi, A. *et al.* (2006) 'Comparative genome-wide profiling of post-transplant lymphoproliferative disorders and diffuse large B-cell lymphomas.', *British journal of haematology*. England, 134(1), pp. 27–36. doi: 10.1111/j.1365-2141.2006.06114.x.

Rinaldi, A. *et al.* (2010) 'Single nucleotide polymorphism-arrays provide new insights in the pathogenesis of post-transplant diffuse large B-cell lymphoma.', *British journal of haematology*. England, 149(4), pp. 569–577. doi: 10.1111/j.1365-2141.2010.08125.x.

Ritz, O. *et al.* (2009) 'Recurrent mutations of the STAT6 DNA binding domain in primary mediastinal B-cell lymphoma.', *Blood*. United

States, 114(6), pp. 1236–1242. doi: 10.1182/blood-2009-03-209759.

Rohde, M. *et al.* (2017) 'Relevance of ID3-TCF3-CCND3 pathway mutations in pediatric aggressive B-cell lymphoma treated according to the non-Hodgkin Lymphoma Berlin-Frankfurt-Munster protocols.', *Haematologica*. Italy, 102(6), pp. 1091–1098. doi: 10.3324/haematol.2016.156885.

Ronceray, L. *et al.* (2018) 'Children and adolescents with marginal zone lymphoma have an excellent prognosis with limited chemotherapy or a watch-and-wait strategy after complete resection.', *Pediatric blood & cancer*. United States, 65(4). doi: 10.1002/pbc.26932.

Rosenwald, A. *et al.* (2002) 'The use of molecular profiling to predict survival after chemotherapy for diffuse large-B-cell lymphoma.', *The New England journal of medicine*. United States, 346(25), pp. 1937–1947. doi: 10.1056/NEJMoa012914.

Rosenwald, A. *et al.* (2003) 'Molecular diagnosis of primary mediastinal B cell lymphoma identifies a clinically favorable subgroup of diffuse large B cell lymphoma related to Hodgkin lymphoma.', *The Journal of experimental medicine*. United States, 198(6), pp. 851–862. doi: 10.1084/jem.20031074.

Rosolen, A. *et al.* (2015) 'Revised International Pediatric Non-Hodgkin Lymphoma Staging System.', *Journal of clinical oncology : official journal of the American Society of Clinical Oncology*, 33(18), pp. 2112–2118. doi: 10.1200/JCO.2014.59.7203.

Ruppert, A. S. *et al.* (2020) 'International prognostic indices in diffuse large B-cell lymphoma: a comparison of IPI, R-IPI, and NCCN-IPI.', *Blood*. United States, 135(23), pp. 2041–2048. doi: 10.1182/blood.2019002729.

Rymkiewicz, G. *et al.* (2018) 'A comprehensive flow-cytometry-based immunophenotypic characterization of Burkitt-like lymphoma with 11q aberration.', *Modern pathology : an official journal of the United States and Canadian Academy of Pathology, Inc*. United States. doi: 10.1038/modpathol.2017.186.

Saito, M. *et al.* (2007) 'A Signaling Pathway Mediating Downregulation of BCL6 in Germinal Center B Cells Is Blocked by BCL6 Gene Alterations in B Cell Lymphoma', *Cancer Cell*, 12(3), pp. 280–292. doi: 10.1016/j.ccr.2007.08.011.

Salaverria, I. *et al.* (2008) 'Chromosomal alterations detected by comparative genomic hybridization in subgroups of gene expression-defined Burkitt's lymphoma.', *Haematologica*. Italy, 93(9), pp. 1327–1334. doi: 10.3324/haematol.13071.

Salaverria, I. *et al.* (2011) 'Translocations activating IRF4 identify a subtype of germinal center-derived B-cell lymphoma affecting predominantly children and young adults', *Blood*. doi: 10.1182/blood-2011-01-330795.

Salaverria, I. *et al.* (2013) 'High resolution copy number analysis of IRF4 translocation-positive diffuse large B-cell and follicular lymphomas.', *Genes, chromosomes & cancer*. United States, 52(2), pp. 150–155. doi: 10.1002/gcc.22014.

Salaverria, I. *et al.* (2014) 'A recurrent 11q aberration pattern characterizes a subset of MYC-negative high-grade B-cell lymphomas resembling Burkitt lymphoma.', *Blood*. United States, 123(8), pp. 1187–1198. doi: 10.1182/blood-2013-06-507996.

Saleh, K. *et al.* (2020) 'Burkitt and Burkitt-Like Lymphomas: a Systematic Review.', *Current oncology reports*. United States, 22(4), p. 33. doi: 10.1007/s11912-020-0898-8.

Sandlund, J. T. (2007) 'Should adolescents with NHL be treated as old children or young adults?', *Hematology. American Society of Hematology. Education Program*. United States, pp. 297–303. doi: 10.1182/asheducation-2007.1.297.

Sandlund, J. T. and Martin, M. G. (2016) 'Non-Hodgkin lymphoma across the pediatric and adolescent and young adult age spectrum.', *Hematology. American Society of Hematology. Education Program*. United States, 2016(1), pp. 589–597. doi: 10.1182/asheducation-2016.1.589.

Savage, K. J. *et al.* (2003) 'The molecular signature of mediastinal large B-cell lymphoma differs from that of other diffuse large B-cell lymphomas and shares features with classical Hodgkin lymphoma.', *Blood*. United States, 102(12), pp. 3871–3879. doi: 10.1182/blood-2003-06-1841.

Savage, K. J. *et al.* (2009) 'MYC gene rearrangements are associated with a poor prognosis in diffuse large B-cell lymphoma patients treated with R-CHOP chemotherapy.', *Blood*. United States, 114(17), pp. 3533–3537. doi: 10.1182/blood-2009-05-220095.

Scarpa, A. *et al.* (1999) 'Molecular features of primary mediastinal B-cell lymphoma: involvement of p16INK4A, p53 and c-myc.', *British journal of haematology*. England, 107(1), pp. 106–113. doi: 10.1046/j.1365-2141.1999.01678.x.

Schiffman, J. D. *et al.* (2011) 'Genome wide copy number analysis of paediatric Burkitt lymphoma using formalin-fixed tissues reveals a subset with gain of chromosome 13q and corresponding miRNA over expression.', *British journal of haematology*. England, 155(4), pp. 477–486. doi: 10.1111/j.1365-2141.2011.08883.x.

Schmidt, J. *et al.* (2016) 'Genome-wide analysis of pediatric-type follicular lymphoma reveals low genetic complexity and recurrent alterations of TNFRSF14 gene.', *Blood*. United States, 128(8), pp. 1101–1111. doi: 10.1182/blood-2016-03-703819.

Schmidt, J. *et al.* (2018) 'CREBBP gene mutations are frequently detected in in situ follicular neoplasia.', *Blood*, pp. 2687–2690. doi: 10.1182/blood-2018-03-837039.

Schmitz, R. *et al.* (2009) 'TNFAIP3 (A20) is a tumor suppressor gene in Hodgkin lymphoma and primary mediastinal B cell lymphoma.', *The Journal of experimental medicine*. United States, 206(5), pp. 981–989. doi: 10.1084/jem.20090528.

Schmitz, R. *et al.* (2012) 'Burkitt lymphoma pathogenesis and therapeutic targets from structural and functional genomics.', *Nature*. England, 490(7418), pp. 116–120. doi: 10.1038/nature11378.

Schmitz, R. *et al.* (2014) 'Oncogenic mechanisms in Burkitt lymphoma.', *Cold Spring Harbor perspectives in medicine*. United States, 4(2). doi: 10.1101/cshperspect.a014282.

Schmitz, R. *et al.* (2018) 'Genetics and Pathogenesis of Diffuse Large B-Cell Lymphoma', *New England Journal of Medicine*, 378(15), pp. 1396–1407. doi: 10.1056/NEJMoa1801445.

Scholtysik, R. *et al.* (2010) 'Detection of genomic aberrations in molecularly defined Burkitt's lymphoma by array-based, high resolution, single nucleotide polymorphism analysis.', *Haematologica*. Italy, 95(12), pp. 2047–2055. doi: 10.3324/haematol.2010.026831.

Scholtysik, R. *et al.* (2015) 'Characterization of genomic imbalances in diffuse large B-cell lymphoma by detailed SNP-chip analysis.', *International journal of cancer*. United States, 136(5), pp. 1033–1042. doi: 10.1002/ijc.29072.

Schroeder, H. W., Radbruch, A. and Berek, C. (2019) '7 - B-Cell Development and Differentiation', in Rich, R. R. et al. (eds) *Clinical Immunology (Fifth Edition)*. Fifth Edit. London: Elsevier, pp. 107-118.e1. doi: https://doi.org/10.1016/B978-0-7020-6896-6.00007-7.

Scott, D. W. *et al.* (2012) 'TBL1XR1/TP63: a novel recurrent gene fusion in B-cell non-Hodgkin lymphoma.', *Blood*. United States, 119(21), pp. 4949–4952. doi: 10.1182/blood-2012-02-414441.

Scott, D. W. *et al.* (2014) 'Determining cell-of-origin subtypes of diffuse large B-cell lymphoma using gene expression in formalin-fixed paraffin-embedded tissue.', *Blood*. United States, 123(8), pp. 1214–1217. doi: 10.1182/blood-2013-11-536433.

Scott, D. W. *et al.* (2015) 'Prognostic Significance of Diffuse Large B-Cell Lymphoma Cell of Origin Determined by Digital Gene Expression in Formalin-Fixed Paraffin-Embedded Tissue Biopsies.', *Journal of clinical oncology : official journal of the American Society of Clinical Oncology*, 33(26), pp. 2848–2856. doi: 10.1200/JCO.2014.60.2383.

Sebastián, E. *et al.* (2016) 'High-resolution copy number analysis of paired normal-tumor samples from diffuse large B cell lymphoma.', *Annals of hematology*. Germany, 95(2), pp. 253–262. doi: 10.1007/s00277-015-2552-3.

Seidemann, K. *et al.* (2003) 'Primary mediastinal large B-cell lymphoma with sclerosis in pediatric and adolescent patients: treatment and results from three therapeutic studies of the Berlin-Frankfurt-Münster Group.', *Journal of clinical oncology : official journal of the American Society of Clinical Oncology*. United States, 21(9), pp. 1782–1789. doi: 10.1200/JCO.2003.08.151.

Seto, E. *et al.* (2010) 'Micro RNAs of Epstein-Barr virus promote cell cycle progression and prevent apoptosis of primary human B cells.', *PLoS pathogens*, 6(8), p. e1001063. doi: 10.1371/journal.ppat.1001063.

Sha, C. *et al.* (2019) 'Molecular High-Grade B-Cell Lymphoma: Defining a Poor-Risk Group That Requires Different Approaches to Therapy.', *Journal of clinical oncology : official journal of the American Society of Clinical Oncology*. United States, 37(3), pp. 202–212. doi: 10.1200/JCO.18.01314.

Shaffer, A. L. *et al.* (2008) 'IRF4 addiction in multiple myeloma.', *Nature*, 454(7201), pp. 226–231. doi: 10.1038/nature07064.

Shannon-Lowe, C. and Rickinson, A. (2019) 'The Global Landscape of EBV-Associated Tumors.', *Frontiers in oncology*. Switzerland, 9, p. 713. doi: 10.3389/fonc.2019.00713.

Shukla, V. and Lu, R. (2014) 'IRF4 and IRF8: Governing the virtues of B Lymphocytes.', *Frontiers in biology*, 9(4), pp. 269–282. doi: 10.1007/s11515-014-1318-y.

De Silva, N. S. and Klein, U. (2015) 'Dynamics of B cells in germinal centres', *Nature Reviews Immunology*. doi: 10.1038/nri3804.

Snuderl, M. *et al.* (2010) 'B-cell lymphomas with concurrent IGH-BCL2 and MYC rearrangements are aggressive neoplasms with clinical and pathologic features distinct from Burkitt lymphoma and diffuse large B-cell lymphoma.', *The American journal of surgical pathology*. United States, 34(3), pp. 327–340. doi: 10.1097/PAS.0b013e3181cd3aeb.

Srinivasan, M., Sedmak, D. and Jewell, S. (2002) 'Effect of fixatives and tissue processing on the content and integrity of nucleic acids.', *The American journal of pathology*, 161(6), pp. 1961–1971. doi: 10.1016/S0002-9440(10)64472-0.

Steidl, C. and Gascoyne, R. D. (2011) 'The molecular pathogenesis of primary mediastinal large B-cell lymphoma.', *Blood*. United States, 118(10), pp. 2659–2669. doi: 10.1182/blood-2011-05-326538.

Steinberg, M. W., Cheung, T. C. and Ware, C. F. (2011) 'The signaling networks of the herpesvirus entry mediator (TNFRSF14) in immune regulation.', *Immunological reviews*, 244(1), pp. 169–187. doi: 10.1111/j.1600-065X.2011.01064.x.

Stephens, P. J. *et al.* (2011) 'Massive genomic rearrangement acquired in a single catastrophic event during cancer development.', *Cell*, 144(1), pp. 27–40. doi: 10.1016/j.cell.2010.11.055.

Stratton, M. R., Campbell, P. J. and Futreal, P. A. (2009) 'The cancer genome.', *Nature*, 458(7239), pp. 719–724. doi: 10.1038/nature07943.

Swerdlow, S. H. *et al.* (2016) 'The 2016 revision of the World Health Organization classification of lymphoid neoplasms.', *Blood*. United States, 127(20), pp. 2375–2390. doi: 10.1182/blood-2016-01-643569.

Swerdlow, S. H. *et al.* (2017) *WHO Classification of Tumours of Haematopoietic and Lymphoid Tissues*. International Agency for Research on Cancer (IARC WHO Classification of Tumours Series). Available at: https://books.google.es/books?id=Qdt9swEACAAJ.

Swerdlow SH, Campo E, Harris NL, Jaffe ES, Pileri SA, Stein H, T. J. (2017) *WHO Classification of Tumours of Haematopoietic and Lymphoid Tissues*.

Szczepanowski, M. *et al.* (2017) 'Cell-of-origin classification by gene expression and MYC-rearrangements in diffuse large B-cell lymphoma of children and adolescents.', *British journal of haematology*. England, 179(1), pp. 116–119. doi: 10.1111/bjh.14812.

Testoni, M. *et al.* (2015) 'The transcription factor ETS1 in lymphomas: friend or foe?', *Leukemia & lymphoma*. England, 56(7), pp. 1975–1980. doi: 10.3109/10428194.2014.981670.

Thomas, D. A. *et al.* (2006) 'Chemoimmunotherapy with hyper-CVAD plus rituximab for the treatment of adult Burkitt and Burkitt-type lymphoma or acute lymphoblastic leukemia.', *Cancer*. United States, 106(7), pp. 1569–1580. doi: 10.1002/cncr.21776.

Traverse-Glehen, A. *et al.* (2005) 'Mediastinal gray zone lymphoma: the missing link between classic Hodgkin's lymphoma and mediastinal large B-cell lymphoma.', *The American journal of surgical pathology*. United States, 29(11), pp. 1411–1421. doi: 10.1097/01.pas.0000180856.74572.73.

Trinh, D. L. *et al.* (2013) 'Analysis of FOXO1 mutations in diffuse large B-cell lymphoma.', *Blood*, 121(18), pp. 3666–3674. doi: 10.1182/blood-2013-01-479865.

Tsang, P. *et al.* (1996) 'Molecular characterization of primary mediastinal B cell lymphoma.', *The American journal of pathology*, 148(6), pp. 2017–2025.

Tuefferd, M. *et al.* (2008) 'Genome-wide copy number alterations detection in fresh frozen and matched FFPE samples using SNP 6.0 arrays.', *Genes, chromosomes & cancer*. United States, 47(11), pp. 957–964. doi: 10.1002/gcc.20599.

Twa, D. D. W. *et al.* (2014) 'Genomic rearrangements involving programmed death ligands are recurrent in primary mediastinal large B-cell lymphoma.', *Blood*. United States, 123(13), pp. 2062–2065. doi: 10.1182/blood-2013-10-535443.

Twa, D. D. W. *et al.* (2015) 'Recurrent genomic rearrangements in primary testicular lymphoma.', *The Journal of pathology*. England, 236(2), pp. 136–141. doi: 10.1002/path.4522.

Valera, A. *et al.* (2013) 'MYC protein expression and genetic alterations have prognostic impact in patients with diffuse large B-cell lymphoma treated with immunochemotherapy.', *Haematologica*, 98(10), pp. 1554–1562. doi: 10.3324/haematol.2013.086173.

Vereide, D. T. *et al.* (2014) 'Epstein-Barr virus maintains lymphomas via its miRNAs.', *Oncogene*. England, 33(10), pp. 1258–1264. doi: 10.1038/onc.2013.71.

Victora, G. D. *et al.* (2012) 'Identification of human germinal center light and dark zone cells and their relationship to human B-cell lymphomas.', *Blood*. United States, 120(11), pp. 2240–2248. doi: 10.1182/blood-2012-03-415380.

Vigano, E. *et al.* (2018) 'Somatic IL4R mutations in primary mediastinal large B-cell lymphoma lead to constitutive JAK-STAT signaling activation.', *Blood*. United States, 131(18), pp. 2036–2046. doi: 10.1182/blood-2017-09-808907.

Wagener, R. *et al.* (2018) 'The mutational landscape of Burkitt-like lymphoma with 11q aberration is distinct from that of Burkitt lymphoma.', *Blood*. United States. doi: 10.1182/blood-2018-07-864025.

Wagener, R. *et al.* (2019) 'Cryptic insertion of MYC exons 2 and 3 into the IGH locus detected by whole genome sequencing in a case of MYC-negative Burkitt lymphoma.', *Haematologica*. Italy. doi: 10.3324/haematol.2018.208140.

Wang, Y. *et al.* (2009) 'High quality copy number and genotype data from FFPE samples using Molecular Inversion Probe (MIP) microarrays.', *BMC medical genomics*, 2, p. 8. doi: 10.1186/1755-8794-2-8.

Waterfall, J. J. *et al.* (2014) 'High prevalence of MAP2K1 mutations in variant and IGHV4-34-expressing hairy-cell leukemias.', *Nature genetics*, 46(1), pp. 8–10. doi: 10.1038/ng.2828.

von der Weid, N. X. (2008) 'Adult life after surviving lymphoma in childhood.', *Supportive care in cancer : official journal of the Multinational Association of Supportive Care in Cancer*. Germany, 16(4), pp. 339–345. doi: 10.1007/s00520-007-0369-x.

Weniger, M. A. *et al.* (2007) 'Gains of REL in primary mediastinal B-cell lymphoma coincide with nuclear accumulation of REL protein.', *Genes, chromosomes & cancer*. United States, 46(4), pp. 406–415. doi: 10.1002/gcc.20420.

Wessendorf, S. *et al.* (2007) 'Further delineation of chromosomal consensus regions in primary mediastinal B-cell lymphomas: an analysis of 37 tumor samples using high-resolution genomic profiling (array-CGH).', *Leukemia*. England, 21(12), pp. 2463–2469. doi: 10.1038/sj.leu.2404919.

Woessmann, W. *et al.* (2005) 'The impact of the methotrexate administration schedule and dose in the treatment of children and adolescents with B-cell neoplasms: a report of the BFM Group Study NHL-BFM95.', *Blood*. United States, 105(3), pp. 948–958. doi: 10.1182/blood-2004-03-0973.

Woessmann, W. and Quintanilla-Martinez, L. (2019) 'Rare mature B-cell lymphomas in children and adolescents.', *Hematological oncology*. England, 37 Suppl 1, pp. 53–61. doi: 10.1002/hon.2585.

Wong, S. Q. *et al.* (2013) 'Targeted-capture massively-parallel sequencing enables robust detection of clinically informative mutations from formalin-fixed tumours.', *Scientific reports*, 3, p. 3494. doi: 10.1038/srep03494.

Wright, G. W. *et al.* (2020) 'A Probabilistic Classification Tool for Genetic Subtypes of Diffuse Large B Cell Lymphoma with Therapeutic Implications.', *Cancer cell*. United States, 37(4), pp. 551-568.e14. doi: 10.1016/j.ccell.2020.03.015.

Xu-Monette, Z. Y. *et al.* (2012) 'Mutational profile and prognostic significance of TP53 in diffuse large B-cell lymphoma patients treated with R-CHOP: report from an International DLBCL Rituximab-CHOP Consortium Program Study.', *Blood*, 120(19), pp. 3986–3996. doi: 10.1182/blood-2012-05-433334.

Yang, Yibin *et al.* (2012) 'Exploiting synthetic lethality for the therapy of ABC diffuse large B cell lymphoma.', *Cancer cell*. United States, 21(6), pp. 723–737. doi:

10.1016/j.ccr.2012.05.024.

Ye, B. H. *et al.* (1995) 'Chromosomal translocations cause deregulated BCL6 expression by promoter substitution in B cell lymphoma.', *The EMBO journal*, 14(24), pp. 6209–6217.

Ying, C. Y. *et al.* (2013) 'MEF2B mutations lead to deregulated expression of the oncogene BCL6 in diffuse large B cell lymphoma.', *Nature immunology*, 14(10), pp. 1084–1092. doi: 10.1038/ni.2688.

Yoshida, S. *et al.* (1999) 'Detection of MUM1/IRF4-IgH fusion in multiple myeloma.', *Leukemia*. England, 13(11), pp. 1812–1816. doi: 10.1038/sj.leu.2401563.

Young, K. H. *et al.* (2008) 'Structural profiles of TP53 gene mutations predict clinical outcome in diffuse large B-cell lymphoma: an international collaborative study.', *Blood*, 112(8), pp. 3088–3098. doi: 10.1182/blood-2008-01-129783.

Yuan, J. *et al.* (2015) 'Identification of Primary Mediastinal Large B-cell Lymphoma at *diagnostics*, 5(6), pp. 539–550.

Nonmediastinal Sites by Gene Expression Profiling.', *The American journal of surgical pathology*. United States, 39(10), pp. 1322–1330. doi: 10.1097/PAS.0000000000000473.

Zayac, A. S. and Olszewski, A. J. (2020) 'Burkitt lymphoma: bridging the gap between advances in molecular biology and therapy.', *Leukemia & lymphoma*. United States, pp. 1–13. doi: 10.1080/10428194.2020.1747068.

Zech, L. *et al.* (1976) 'Characteristic chromosomal abnormalities in biopsies and lymphoid-cell lines from patients with Burkitt and non-Burkitt lymphomas.', *International journal of cancer*. United States, 17(1), pp. 47–56. doi: 10.1002/ijc.2910170108.

Zeng, K. *et al.* (2017) 'BRAFV600E and MAP2K1 mutations in Langerhans cell histiocytosis occur predominantly in children.', *Hematological oncology*. England, 35(4), pp. 845–851. doi: 10.1002/hon.2344.

Zhang, Y. *et al.* (2011) 'Risk Factors of Non-Hodgkin Lymphoma.', *Expert opinion on medical*

ABBREVIATIONS

ABC: activated B-cell type

AID: activation-induced cytidine deaminase

ALCL: anaplastic large cell lymphoma

aSHM: aberrant somatic hypermutation

BCR: B-cell receptor

BFM: Berlin-Frankfurt-Munster protocol

BL: Burkitt lymphoma

BLL-11q: Burkitt-like lymphoma with 11q aberration

BM: bone marrow

B-NHL: B-cell non-Hodgkin lymphoma

CGH: comparative genomic hybridization

CN: copy number

CNN-LOH: copy number neutral-loss of heterozygosity

CNS: central nervous system

COO: cell of origin

CSR: class switch recombination

DH/TH: double hit / triple hit

DLBCL: diffuse large B-cell lymphoma

DZ/LZ: dark zone / light zone

EBV: Epstein barr virus

FFPE: formalin-fixed paraffin embedded

FISH: Fluorescence *in situ* hybridization

FL: follicular lymphoma

GC: germinal center

GCB: germinal center B-cell

HGBCL: high grade B-cell lymphoma

IG: Immunoglobulin

IGH: heavy-chain immunoglobulin

IGK: Kappa-chain immunoglobulin

IGL: lambda-chain immunoglobulin

IPI: International prognostic index

LBCL: large B-cell lymphoma

LBCL-*IRF4*: large B-cell lymphoma with IRF4 rearrangement

LBL: lymphoblastic lymphoma

LDH: lactate dehydrogenase

LMB: French-American-British lymphomes Malins B protocol

LOH: loss of heterozygosity

mBL: molecular Burkitt lymphoma

MIP: molecular inversion probe

NGS: next generation sequencing

NHL: non-Hodgkin lymphoma

NMZL: nodal marginal zone lymphoma

NOS: not otherwise specified

OS: overall survival

PMBCL: primary mediastinal B-cell lymphoma

PNMZL: pediatric nodal marginal zone lymphoma

PTFL: pediatric type follicular lymphoma

SHM: somatic hypermutation

SNP: single nucleotide polymorphism

WES: whole exon sequencing

WGS: whole genome sequencing

WHO: World Health Organization

AKNOWLEDGMENTS

Aquesta tesi ha sigut per jo un llarg viatge d'aprenentatge, ple d'experiències i emocions. Un recorregut que no he fet sol sinó amb la companyia de mentors i companys de feina que han acabat formant part de les meves amistats més properes. A tota aquesta gent els hi vull donar les gràcies per haver compartit viatge amb jo, per ensenyar-me, per recolzar-me, per compartir la seva experiència en mi, per la seva paciència i per regalar-me moments únics que sempre m'acompanyaran allà on em porti la vida.

Començaré per donar les gràcies a la meva directora de tesi, la **Itziar**, per la qual estic plenament agraït per haver-me donat la oportunitat de formar part del seu propi viatge. Des del primer moment em vaig sentir molt afortunat de poder formar part d'un grup d'investigació novell el qual també he vist créixer durant els anys en que jo també ho feia. Un grup que ha crescut amb gran força gràcies a la feina de totes les seves treballadores, a la seva professionalitat i al bon vincle que hem creat entre nosaltres. Vull agrair una a una a totes les persones que formen part d'aquest grup, ja que la tesi aquí presentada és el fruit de la feina de totes i cada una de vosaltres. A la Iti, per la seva dedicació, tracte, professionalitat, per la seva confiança. Has sigut la millor *jefa* que un es pugui imaginar i una gran model a seguir. A la **Noe**, per ensenyar-me des de cero com funcionava el laboratori, per ser tant propera des del primer dia. A la **Blanca**, per compartir amb jo els seus coneixements, pel tracte proper i paciència, que tantes vegades he atabalat amb preguntes sobre patologia. También a **Julia**, por su sonrisa, su dedicación, su felicidad tan contagiosa y por haber podido compartir experiencias y anécdotas juntos. Ha sigut un gran plaer haver pogut treballar amb totes vosaltres aquets cinc anys.

També vull agrair a tots els *jefes* del grup, a grans professionals, pel seu suport, consells i coneixement que m'han pogut donar durant aquets anys. A **l'Elias**, gràcies per l'oportunitat de formar part d'aquesta gran família. Gràcies pels teus consells i per la teva amabilitat. A la **Silvia**, per ser tan extrovertida i divertida, a **l'Iñaki**, per la seva serenitat i per les classes de meditació. A la **Virginia**, **Lluis**, **Pedro**, **Guillem** i a **l'Olga** per tot el suport i consells. A la **Cristina**, per ser tan propera i aconsellar-me pel meu viatge a Alemanya. A totes les

treballadores de la plataforma genòmica, per la paciència amb les concentracions de DNA que tants mals de caps ens van donar; en especial a **l'Anna**, que tant ens ha ajudat.

En aquest gran grup del qual he format part també he tingut la sort de coincidir amb molts de companys i companyes de feina, grans amistats, amb les quals hem compartit no sols el dia a dia al laboratori treballant en les nostres respectives tesis sinó també gaudit de moments inoblidables en terrasses, cases rurals, congressos, concursos de cuina, al sharma, room scapes, festes de barri, platges e inclús en les pròpies cases d'algun d'ells. A tots vosaltres us vull agrair el fet d'acollir-me a la vostra família des del primer dia en que vaig trepitjar el laboratori quan tant sols era un estudiant de màster. Al **Robert**, per la seva amistat, per ser tan proper des del primer dia. Gràcies pel teu suport en els moments més difícils i per creure en jo. A la **Nuria** i el **David**, per la seva amabilitat, generositat i afecte, per totes les experiències que hem viscut plegats i per les que ens queden. A la **Roser**, per la seva energia i pel suport en aquesta darrera etapa de la tesi; a qui li desitjo molta sort per Anglaterra. A la **Rodri**, per tots els moments divertits, per les seves creacions artístiques amb el paint, pel seu humor i per les seves llistes de reproducció casposes. A **Patri**, por su compañía i aguante en los días de terraceo. A la **Sureda**, pel seu suport i consells, per ser tan propera i amable, amb qui puc parlar de tot. Al **Ferran**, per totes les hores que m'ha dedicat a ensenyar anàlisis bioinformàtic, per tenir tanta paciència però també pel seu suport, generositat i amabilitat. Al qual li dec tones de xocolata per tota l'ajuda rebuda. Al **Martí**, per tants moments plegats dins i fora del laboratori, pel suport i consells. A **Kulis**, por sus consejos, apoyo, por transmitir esa felicidad y por ser tan amable. A **Alfredo**, por sus consejos sobre clínica y por enseñarnos a todos la buena cocina mejicana. Al **Pepe** i a **l'Antonia**, per tants riures entre birres i per tot el xafardeig.

Com es pot apreciar, és un gran grup que creix i decreix amb els anys i així com unes persones han anat abandonant el grup durant els anys, n'hi ha de noves que s'han anat incorporant. A totes elles, pels que ja no hi són, pels que seguiu i pels nous vinguts, gràcies per fer-me els dies més fàcils.

I would like also to thank all the people whom I have had the pleasure to collaborate with. A **Leticia**, gracias por el trato i hospitalidad recibidos en Tübingen. Fue un placer visitarles y conocer a todos los componentes del grupo con los que he tenido el honor de trabajar. To **Reiner**, for giving me the opportunity to work in his group and being so kind and generous.

No menys important, gràcies a les meves amistats, a les genuïnes amistats mallorquines amb les que durant molt anys he pogut comptar. Gràcies pel vostre suport i per ser el meu refugi durant els moments més difícils, vos estim molt. Als Islanders, per la paciència i suport, per la vostra comprensió per no poder ser sempre allà fent música amb voltros. I a tota la gent de BCN, a les meves companyes "payasas" de pis i a l'*akelarre marika*.

Finalment, m'agradaria agrair a la meva família pel seu suport i el seu afecte. Gracies per donar-me la oportunitat de complir els meus somnis. En especial agrair al meu *abuelo*, per la seva empenta, per estar sempre allà, per animar-me durant tot el procés acadèmic, interessant-se pels meus somnis i pel futur que m'esperaria un cop acabada la universitat. A ell, a l'escriptor novell més vell, a ganyia, que malauradament no ha pogut arribar al final d'aquesta etapa, a qui sempre estaré agraït.

APPENDIX

List of publications included in this Thesis (Supervisor's report)

All three Studies presented in this thesis have been published in the following journals:

Gonzalez-Farre B*, **Ramis-Zaldivar JE***, Salmeron-Villalobos J, Balagué O, Celis V, Verdu J, Nadeu F, Sábado C, Ferrández A, Garrido M, Garcia-Bragado F, de la Maya MD, Vagace JM, Panizo CM, Astigarraga I, Andrés M, Jaffe ES, Campo E, Salaverria I. Burkitt-like lymphoma with 11q aberration: A germinal center derived lymphoma genetically unrelated to Burkitt lymphoma. Haematologica 2019 Sep;104(9):1822-1829. Impact factor (IF): 7.116.

*These authors contributed equally to this work.

Joan Enric has contributed in all phases of the study including the mutational and copy number analysis, gene expression analysis by qPCR, in addition to bioinformatic and statistical analysis. He has also contributed in the writing process of the manuscript.

Schmidt J*, **Ramis-Zaldivar JE***, Nadeu F, Gonzalez-Farre B, Navarro A, Egan C, Montes-Mojarro IA, Marafioti T, Cabeçadas J, van der Walt J, Dojcinov S, Rosenwald A, Ott G, Bonzheim I, Fend F, Campo E, Jaffe ES, Salaverria I, Quintanilla-Martinez L. Mutations of MAP2K1 are frequent in pediatric-type follicular lymphoma and result in ERK pathway activation. Blood. 2017 Jul 20;130(3):323-327. IF: 15.132.

*These authors contributed equally to this work.

Joan Enric has contributed in the mutational analysis and review the bibliography for specific mutations for comparisons. He has also contributed to the design and preparation of the figures.

Ramis-Zaldivar JE*, Gonzalez-Farre B*, Balague O, Celis V, Nadeu F, Salmerón-Villalobos J, Andrés M, Martin-Guerrero I, Garrido G, Gaafar A, Suñol M, Bárcena C, Garcia-Bragado F, Andión M, Azorín D, Astigarraga I, Sagaseta de Ilurdoz M, Sábado C, Gallego S, Verdú-Amorós J, Fernandez-Delgado R, Perez V, Tapia G, Mozos A, Torrent M, Solano-Páez P, Rivas- Delgado A, Dlouhy I, Clot G, Enjuanes A, Lopez-Guillermo A, Galera P, Oberley M, Maguire A,

Ramsower C, Rimsza LM, Quintanilla-Martinez L, Jaffe ES,Campo E, Salaverria I. Distinct molecular profile of IRF4-rearranged large B-cell lymphoma. Blood, 2020:135(4):274–286. IF: 17.543.

*These authors contributed equally to this work.

Joan Enric has contributed in all phases of the study including the mutational, copy number and gene expression analysis in addition to bioinformatic and statistical analysis. He has also contributed in the writing process of the manuscript.

SALAVERRIA FRIGOLA ITZIAR - 47711254P

Firmado digitalmente por SALAVERRIA FRIGOLA ITZIAR - 47711254P
Fecha: 2021.05.07 12:08:09 +02'00'

Dr. Itziar Salaverria Frigola

Doctoral advisor

List of publications not included in this thesis

First author publications

Nann D*, **Ramis-Zaldivar JE***, Müller I, Gonzalez-Farre B, Schmidt J, Egan C, Salmeron-Villalobos J, Clot G, Mattern S, Otto F, Mankel B, Colomer D, Balagué O, Szablewski V, Lome-Maldonado C, Leoncini L, Dojcinov S, Chott A, Copie-Bergman C, Bonzheim I, Fens F, Jaffe ES, Campo E, Salaverria I, Quintanilla-Martinez L. Follicular lymphoma t(14;18)-negative is genetically a heterogeneous disease. Blood Adv 2020;4(22):5652–5665. IF: 2.226. *These authors contributed equally to this work.

Ramis-Zaldivar JE*, Gonzalez-Farre B*, Nicolae A, Pack S, Clot G, Nadeu F, Mottok A, Horn H, Song JY, Fu K, Wright G, Gascoyne RD, Chan WC, Scott DW, Feldman AL, Valera A, Enjuanes A, Braziel RM, Smeland EB, Staudt LM, Rosenwald A, Rimsza LM, Ott G, Jaffe ES, Salaverria S, Campo E for the Leukemia and Lymphoma Molecular Profiling Project (LLMPP). MAP-kinase and JAK-STAT pathways dysregulation in plasmablastic lymphoma. Haematologica, 2021, Online ahead of print. *These authors contributed equally to this work.

Co-author publications

Schmidt J, Gong S, Marafioti T,Mankel B, Gonzalez-Farre B, Balagué O, Mozos A, Cabeçadas J, van der Walt J, Hoehn D, Rosenwald A, Ott G, Dojcinov S, Egan C, Nadeu F, **Ramis-Zaldívar JE**, Clot G, Bárcena C, Pérez-Alonso V, Endris V,Penzel R, Lome-Maldonado C, Bonzheim I, Fend F, Campo E, Jaffe ES, Salaverria I, Quintanilla-Martinez L. Genome-wide analysis of pediatrictype follicular lymphoma reveals low genetic complexity and recurrent alterations of TNFRSF14 gene. Blood. 2016 Aug 25;128(8):1101-11. IF=13.164 Decil1.

Schmidt J, **Ramis-Zaldivar JE**, Bonzheim I, Steinhilber J, Müller I, Haake A, Yu SC, Raffeld M, Fend F, Salaverria I, Siebert R, Jaffe ES, Quintanilla-Martinez L. CREBBP gene mutations are frequently detected in in situ follicular neoplasia. Blood. 2018 Dec 20;132(25):2687-2690. IF=15.132 Decil 1.

Presentations in scientific events

Oral presentations

Ramis-Zaldivar JE, Gonzalez-Farre B, Balague O, Celis V, Nadeu F, Salmerón-Villalobos J, Andrés M, Martin-Guerrero I, Garrido G, Gaafar A, Suñol M, Bárcena C, Garcia-Bragado F, Andión M, Azorín D, Astigarraga I, Sagaseta de Ilurdoz M, Sábado C, Gallego S, Verdú-Amorós J, Fernandez-Delgado R, Perez V, Tapia G, Mozos A, Torrent M, Solano-Páez P, Rivas- Delgado A, Dlouhy I, Clot G, Enjuanes A, Lopez-Guillermo A, Galera P, Oberley M, Maguire A, Ramsower C, Rimsza LM, Quintanilla-Martinez L, Jaffe ES,Campo E, Salaverria I. IRF4-rearranged Large B-cell lymphoma (LBCL) has a genomic profile distinct to other LBCL in children and young adults. II Encuentro de Jóvenes Investigadores CIBERONC. 27/11/2019 Madrid, Spain.

Poster presentations

Ramis-Zaldivar JE, Gonzalez-Farre B, Balague O, Celis V, Nadeu F, Andres M, Martin-Guerrero I, Garrido M, Gaafar A, Sunyol M, Barcena C, Garcia-Bragado F, Andion M, Azorin D, Astigarraga I, Sagaseta de Ilurdoz M, Sabado C, Gallego S, Verdu-Amoros J, Fernandez-Delgado R, Tapia G, Rivas-Delgado A, Dlouhy I, Salmeron-Villalobos J, Clot G, Enjuanes A, Lopez- Guillermo A, Pallavi G, Oberley MJ, Quintanilla-Martinez L, Jaffe ES, and Campo E, Salaverria, I. Large B-Cell Lymphomas in Pediatric and Young Adults Display Clinically Relevant Molecular Features Distinguishable from Adult Counterpart. ASH 2018 – 60th American Society of Hematology Annual Meeting and Exposition, 1-4 Dec 2018. San Diego, CA, US.

Ramis-Zaldivar JE, Salaverria I, Gonzalez-Farre B, Pack S, Nicolae A, Clot G, Mottok A, Horn H, Rimsza LM, Staudt L, Rosenwald A, Ott G, Scott DW, Jaffe ES, Campo E. Genome-wide analysis of plasmablastic lymphoma. EMBL Cancer Genomics Conference that will be held the 4- 6th November 2019 in Heidelberg, Germany.

Stay in foreign laboratories

CIBERONC Internship 2019 (ONCF01A). Stay in the Department of Biochemistry and molecular biology, University of Oviedo, Spain, in the group of Prof. Xose S. During this stay I learnt bioinformatic sequencing data analysis using Mate-Pair technology that allows the detection of structural variants and identification of complex genomic alterations.
(18-22/03/2019).

CIBERONC Internship 2020 (ONCF01A). Stay in the Institute of Human Genetics, University of Ulm, Germany, in the group of Prof. Reiner Siebert. Reiner's lab technical expertise ranges from conventional genetic techniques to up-to-date genome-wide profiling techniques and epigenetics. During this stay I learnt bioinformatic pipeline for methylation analysis.
(27/09/2020-19/12/20).